The Spatial Analysis and Speciation of Uranium and Thorium Series Radionuclides in the Soil of the Cronamuck Valley, County Donegal, Ireland.

Mark Dowdall

Institute of Technology, Sligo

This project is submitted in fulfillment of the National Council for Educational Awards requirements for the award of Doctor of Philosophy by research and thesis.

Project Supervisor: John O'Dea

Submitted to the National Council for Educational Awards, April, 2000.

The Spatial Analysis and Speciation of Uranium and Thorium Series Radionuclides in the Soil of the Cronamuck Valley, Co. Donegal, Ireland.

Mark Dowdall

ABSTRACT.

This thesis details the findings of a study into the spatial distribution and speciation of ^{238}U, ^{226}Ra and ^{228}Ra in the soils of the Cronamuck valley, County Donegal. The region lies on the north-eastern edge of the Barnesmore granite and has been the subject of uranium prospecting efforts in the past. The results of the project provide information on the practicability of geostatistical techniques as a means of estimating the spatial distribution of natural radionuclides and provide insight into the behaviour of these nuclides and their modes of occurrence and enrichment in an upland bog environment.

The results of the geostatistical survey conducted on the area indicate that the primary control over the levels of the studied nuclides in the soil of the valley is the underlying geology. Isopleth maps of nuclide levels in the valley indicate a predominance of elevated nuclide levels in the samples drawn from the granite region, statistical analysis of the data indicating that levels of the nuclides in samples drawn from the granite are greater than levels drawn from the non-granite region by up to a factor of 4.6 for ^{238}U and 4.9 for ^{226}Ra. Redistribution of the nuclides occurs via drainage systems within the valley, this process being responsible for transport of nuclides away from the granite region resulting in enrichment of nuclides in soils not underlain by the granite. Distribution of the nuclides within the valley is erratic, the effect of drainage flows on the nuclides resulting in localized enriched areas within the valley.

Speciation of the nuclides within one of the enriched areas encountered in the study indicates that enrichment is as a result of saturation of the soil with drainage water containing trace amounts of radionuclides. ^{238}U is primarily held within the labile fractions (exchangeable cations + easily oxidisable organics + amorphous iron oxides) of the soil, ^{226}Ra being associated with the non-labile fractions, most probably the resistant organic material. ^{228}Ra displays a significant occurrence in both the labile and non-labile fractions. The ability of the soil to retain uranium appears to be affected largely by the redox status of the soil, samples drawn from oxidizing environments tending to have little or no

uranium in the easily oxidisable and amorphous iron oxide fractions. This loss of uranium from oxidised soil samples is responsible for the elevated $^{226}Ra/^{238}U$ disequilibrium encountered in the enriched areas of the valley. Analysis of the data indicates that samples displaying elevated $^{226}Ra/^{238}U$ ratios also exhibit elevated $^{228}Ra/^{238}U$ ratios indicating a loss of uranium from the samples as opposed to an enrichment of ^{226}Ra.

DECLARATION

The work reported in this thesis was carried out by Mark Dowdall during the period September 1996 to June 2000. Aside from the analysis conducted by PlasmaTech Ltd, the work was carried out solely by Mark Dowdall. This thesis has not previously been submitted to any other institution or awarding body for consideration for the awarding of any degree.

Signed : 

Date : 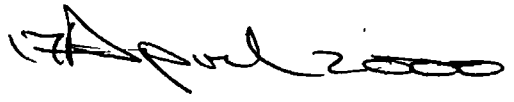

Acknowledgements.

I wish to acknowledge the following people for their support, assistance and encouragement throughout this project:

- project supervisor, John O'Dea for his support and encouragement,
- the lecturing staff of the School of Science, I.T., Sligo, Dr Barry Crocock and Dr Richard Sherlock,
- Martin Cronin, James Kelly, John Joe McGloin, Karl Willems, Ken Henry, Brendan Nestor, George, Kathleen and the canteen staff,
- Dr Paddy Fleming and Eamonn Grennan for their assistance and advice throughout the project,
- the technical staff of the School of Engineering, I.T., Sligo,
- the library staff at I.T.,Sligo,
- the lads in the lab (drink tea, play Quake, be a post grad),
- special thanks to Pat Maughan and his van and Bosco and his car,
- Gregoire Dubois,
- and especially Sarah O'Sullivan.

I would like to express my appreciation for the help proffered by the following organizations and institutions:

- the staff of the Radiological Protection Institute of Ireland,
- the staff of the Dept. of Physics, UCD,
- the staff of the North Western Cattle Breeders Association,
- the staff of the Geological Survey of Ireland,
- the sales staff of CANBERRA Industries,
- the staff of Met Eireann,

- the Garda Siochana, Ballybofey, Co. Donegal,
- the staff of Sligo Town VEC,
- the School of Science, I.T., Sligo.

I also wish to extend my sincere thanks to Mum, Dad, David and Philip for unflagging support over the last number of years. Many thanks for everything.

Table of Contents

List of Figures

List of Tables

1.0. INTRODUCTION.

1.1 General Introduction and Study Objectives

The primary objective of this study was to determine the distribution of uranium and thorium series radionuclides within the peat of the Cronamuck Valley in the Bluestack Mountains, Co. Donegal and to ascertain the chemical mode of occurrence of the radionuclides within the peat itself. The objectives also included an assessment of the performance of advanced estimation and interpolation methods in the spatial analysis of natural radionuclides and the investigation of radioactive disequilibrium in the ^{238}U decay series within areas of elevated natural radioactivity in the Cronamuck Valley.

In order to determine the spatial distribution of natural radionuclides within the valley, the methods embodied in the theory and practice of geostatistics were employed. Spatial correlation's for the radionuclides were assessed using semi-variogram analysis and this information was then used in the implementation of the point estimation process known as kriging. The final outputs were isopleth maps of radionuclide levels within the valley. The performance of the geostatistical procedure relative to other common point estimation methods for the spatial analysis of natural radionuclides was investigated for a number of parameters.

Areas of the valley exhibiting marked enrichment of radionuclides, and often concomitant radioactive disequilibrium, were investigated in detail. A wide range of chemical analyses was performed on the soil in these regions in order to determine possible controlling factors over the accumulation of radionuclides in these areas. The chemical speciation of the radionuclides in the soil was established using sequential chemical extractions. This process allowed identification of the soil phases within

which the radionuclides were incorporated. Investigation of various radionuclide ratios allowed conclusions to be drawn on the matter of radioactive disequilibrium within these regions.

An investigation of this type allows both site-specific and general conclusions to be made concerning the behaviour and fate of natural radionuclides and uranium series nuclides in particular. While the occurrence and behaviour of anthropogenic radionuclides, such as ^{137}Cs, in upland regions of Ireland has been studied in some detail, little work on natural radionuclides in such environments has been carried out in the past. The majority of work that has been conducted in Ireland has been part of uranium prospecting efforts and primarily concerned itself with the location of radionuclide enriched peat as an indicator of economically viable deposits. These surveys paid scant attention to the behaviour of the radionuclides or the processes governing their distribution, often being limited to little more than cursory analysis of the data.

Many environmental surveys rely on the collection of large amounts of data and the subsequent contouring of the variables as the final output. Little concern is given to the procedures used in the contouring process or to the accuracy of the estimates used in the process. The use of statistical techniques for the estimation of a large number of points based on a relatively small data set allows for the production of accurate isopleth maps of variables for regions where it is impossible to obtain large numbers of samples. Such methods also allow a rigid and coherent procedure to be adopted from the time of sampling to the production of final outputs and do not rely on the implementation of an estimation procedure in only the final stages of the data analysis.

Knowledge of the distribution and behaviour of natural radionuclides is important for a number of reasons alongside its intrinsic value. Uranium

series radionuclides are the precursors of radon gas, responsible for in excess of 50% of the radiation dose to the Irish population (McLaughlin, 1990). Improved knowledge of the behaviour of Ra^{226} in soils may provide for more accurate estimation of the radon production potential of soils in this country. Uranium is a heavy metal, presenting similar hazards in the environment as other heavy metal contaminants. Information about uranium in upland peat areas may provide information of relevance to the study of other heavy metals in similar environments.

Peat bogs have long been accepted as acting as uranium 'sinks' (Douglas, 1991), significant amounts of uranium accumulating in some areas over long periods of time. Disruption of such environments by agriculture, industry or afforestation may lead to releases of relatively large amounts of uranium (and its decay products) into watercourses. Knowledge of the factors controlling the occurrence and retention of uranium within these 'sinks' is desirable in order to be able to predict whether activities in or near these regions may result in uranium releases to the surrounding environment.

Previous studies on natural radionuclides in the soil of this region have been conducted as part of commercial uranium exploration efforts. Academic research efforts to date have involved the selection of, at most, one or two samples from the region as part of national surveys of radioactivity levels in soils and were limited to the determination of activity levels. This study provides an integrated assessment of the status of uranium and associated natural radionuclides in an upland peat environment, something not previously conducted in this country. It provides information on the distribution, speciation and accumulation of radionuclides within a defined region using advanced statistical and analytical procedures.

1.1.1. The Barnesmore Pluton

The Barnesmore Pluton, an isolated granite region some 52 km^2 in area, forms the Bluestack Mountain range (Grid Ref. H 022 928) in central Donegal (Fig. 1a). The pluton consists of three granite types, which are similar in mineral composition but differ in their grain size and modal composition.

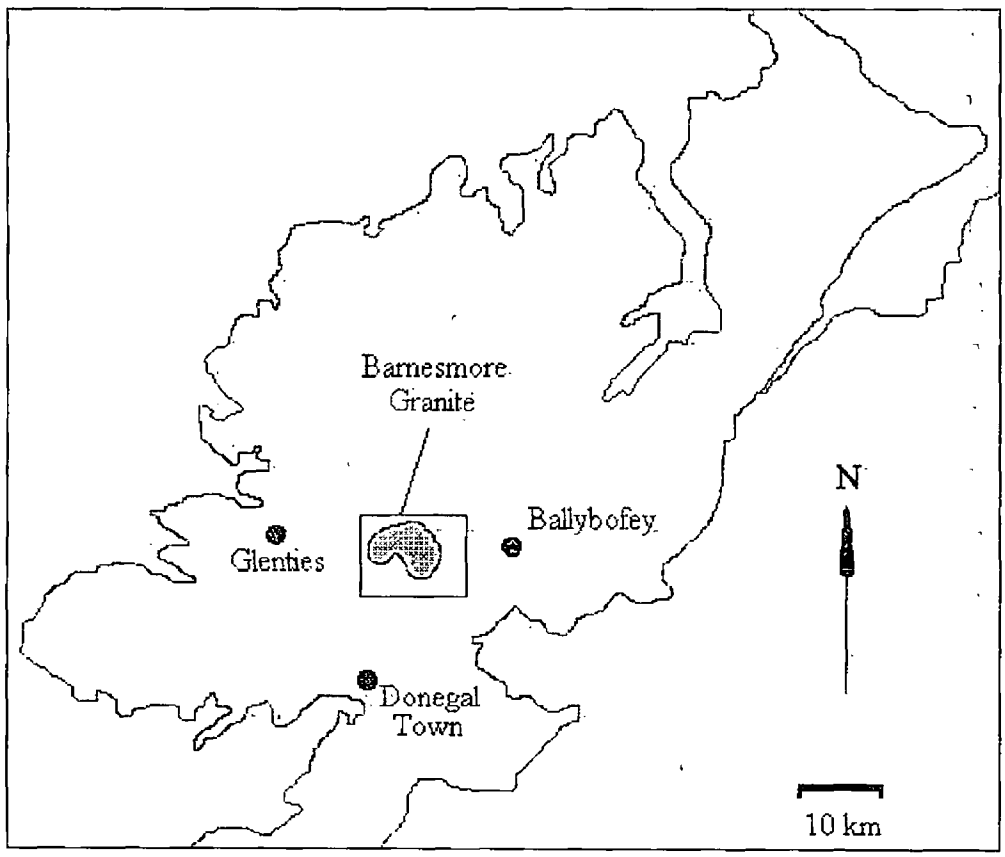

Figure 1a. Location of the Barnesmore Granite, County Donegal.

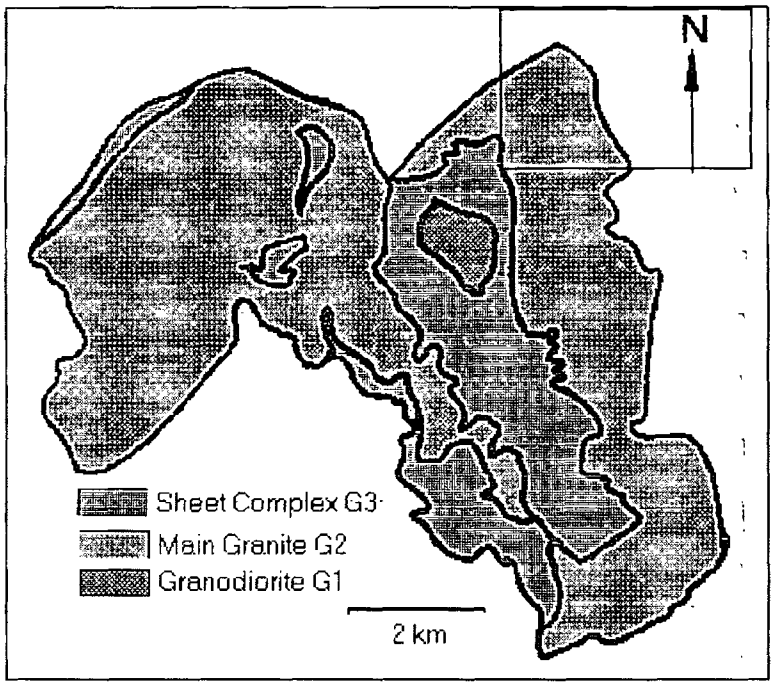

Figure 1b. Schematic of the Barnesmore Pluton. Rectangle denotes Survey 1 study region.

The pluton was emplaced in Dalradian metasediments by cauldron subsidence (Walker and Leedal, 1954) forming an elongated dome stretching in a NW - SE direction and maintaining sharp contact with the country rocks. The main granite body (G2) consists of leucocratic adamellite with a small region of granodiorite (G1) existing within the main granite. Both the G1 and G2 granites are cut by the Sheet Complex (G3) which may be subdivided into two components, G3a, an even grained leucocratic granite, and G3b, a prophyritic aplogranite (Fig.1b.).

1.1.2. Uranium Occurrence in the Bluestack Mts.

Information on the occurrence of uranium and other radioelements in the Bluestack Mountains is largely derived from two sources, academic research and from the reports of the mineral exploration companies who

conducted uranium exploration in the region during the 1970's. EEC funded exploration for uranium began in 1976 concentrating on the Caledonian plutons of Leinster, Connemara and Donegal. As this project is concerned with the Barnesmore region, only the literature pertaining to this area will be reviewed. Exploration in the Bluestack Mountains was conducted by Irish Base Metals in association with Tara Prospecting Ltd., final reports being submitted to the government in 1979. A number of techniques were employed in the prospecting programme including alpha track ("Track-Etch") detectors, ground radiometric surveys (both gross count and gamma spectrometry), stream sediment sampling, soil trenching and a range of geophysical and geochemical techniques. The period of prospecting in the Barnesmore region indicated:

> "*the presence of high background uranium content in the Barnesmore Granites,.. the definite and widespread enrichments found in weathered material and peat, the presence of secondary uranium minerals (autinite), prove that uranium is present in the area and that it is extremely mobile*" (Irish Base Metals, 1979).

Many of the techniques used at the time (portable gamma spectrometry, alpha track detectors) do not provide quantitative values of the uranium levels in the area, however the chemical analyses on rock, peat and sediment samples do provide an indication of uranium levels in the region. It should be noted that the objective of the work was the location of economically viable uranium deposits which implies that reported values are for regions where high levels of uranium were expected or had been indicated by radiometric surveys etc. The levels reported therefore are not representative of the background situation within the Barnesmore region in general.

Three of the main drainage systems in the region (Cronamuck, Barnes and Corabber Rivers) provided sediment uranium values up to 45 ppm, (Irish Base Metal Ltd., 1978), indicative of a high background uranium content within the general locality. Reported peat and rock values are more specific to small radioactive anomalies in the area. The highest reported value in rock was 279 ppm, the average value for an unreported number of rock samples being 40 ppm (Irish Base Metal Ltd., 1978). The maximum reported value for peat was 7600 ppm at a small location near Browns Hill in the southern reaches of the mountain range (Irish Base Metals Ltd., 1978).

While the reported quantities of uranium in samples taken as part of the prospecting effort are of little use in ascertaining the background uranium content of the Barnesmore region, a number of useful facts are provided in the reports. The first is the location of a number of peat anomalies within the Browns Hill (7600 ppm U/kg peat) and Cronamuck Valley regions. No uranium values are given for the Cronamuck anomalies (location of the anomalies having been indicated by the use of a portable ratemeter) but the report specifies that they are unsupported in the underlying rock (Irish Base Metals Ltd., 1978). The second is that these anomalies tend to be regions of less than 30 m x 30 m and that they tend to be grouped in clusters. No locations for these anomalous regions within the valley are detailed. These two facts indicate that uranium within the region would appear to be relatively mobile, as high levels within the peat are not associated with high levels in the underlying rock and that some areas within the general region are undergoing a uranium enrichment process, as evidenced by the small areas of extremely high uranium content, e.g. Browns Hill.

The prospecting reports of the 1970's have little to offer in establishing the average uranium levels in the Barnesmore region

but do provide useful information about how the uranium may be distributed in the region (small localised, often unrelated, enrichments in both rock and peat). Academic research on the occurrence of radioelements in the area is more objective, even though much of it appears to have been conducted in conjunction with the prospecting effort.

O'Connor *et al* (1983) reported the Barnesmore Pluton as exhibiting the highest average uranium and thorium content (8.1 ppm and 25.1 ppm respectively) of all the Irish Newer Caledonian Granites, with a relatively high potassium level of 4.1%. Uranium in the Barnesmore pluton occurs as the secondary mineral autinite, located largely within the central G3a granite (O'Connor, 1981) with no evidence of the mineral uraninite in the granites. Data on the radioelement content of the surrounding metasediments is scarce, O'Connor and Long (1985) reporting average uranium and thorium contents of 1.8 ppm and 12.0 ppm respectively for similar Dalradian lithologies in the Donegal region.

Evidence of the elevated natural radioactivity of the region is also provided by nation-wide radiometric surveys that have been conducted in the past. McAuley and Moran (1988) reported ^{40}K soil activities of 450-600 Bq/kg and ^{226}Ra soil activities of 60-100 Bq/kg for the general Barnesmore region (national averages of 350 Bq/kg and 60 Bq/kg respectively). It is worth noting that the ^{226}Ra surveys adopted a scheme with a sampling density of 1/10 km^2 and it is therefore improbable that the survey would have encountered one of the small anomalous regions reported in the prospecting surveys of the 1970's.

1.2. Peat, Organic soils and Humus

Although a large number of soil classification systems are in common usage, this project does not concern itself with the finer points of what constitutes "peat". For the purpose of this study, peat is an organic soil containing large amounts of carbon, produced in an environment where the supply of organic matter exceeds the rate of decomposition (Cruickshank, 1972). The distinction between "peat" and "organic soil" as a description of a particular soil type is unclear as many researchers use the term interchangeably and many countries adopt their own particular classification systems. Cruickshank (1972) and Farnham and Finney (1965) refer to peat (including a variety of peat types) as a sub-set of organic soils and distinguish between peat types using botanical components and the chemical nature of the soil, and it is this system that is used throughout this study.

Humus, a constituent of peat, is the total of the organic compounds in soil exclusive of undecayed plant material, partially decayed products and the soil biomass. Humus may be sub-divided into further constituent components which are classified according to their solubility in various reagents, most commonly, alkali and acidic solutions (Table 1.). Both humic and fulvic acids play a large part in the chemistry of peat and organic soils, the chemical behaviour of both these substances being controlled to a large extent by phenolic hydroxyl and carboxyl groups (Sanchez *et al*, 1988).

Dissociation of H^+ on the carboxyl group at pH values greater than 3 and similar dissociation of the hydroxyl group at pH 9 tends to give humic material a high negative charge (Tan, 1992). This proton donation by constituents of humic molecules allows for the interaction of the humic molecules with metal cations by a number of mechanisms (Fig.3.).At low pH values, cation exchange mechanisms tend to

predominate, the emphasis shifting to chelation mechanisms as the pH value increases.

Fraction	Alkali Solution (0.1 M NaOH)	Acid Solution (0.1 M HCl)
Humic acid	Soluble	Insoluble
Fulvic acid	Soluble	Soluble
Humin	Insoluble	Insoluble

Table 1. Classification of humic substances (Tan, 1992).

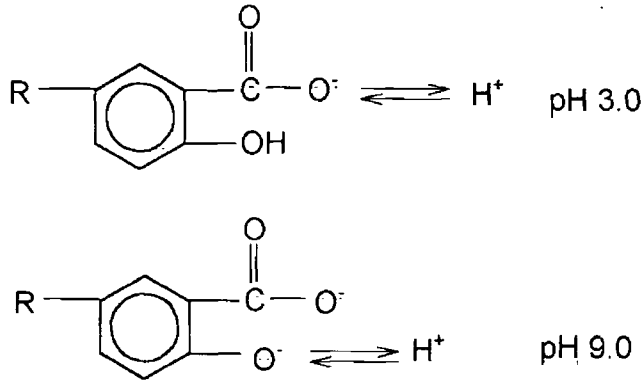

Figure 2. Proton donation by humic constituent groups at pH 3 and pH 9 (after Tan, 1992).

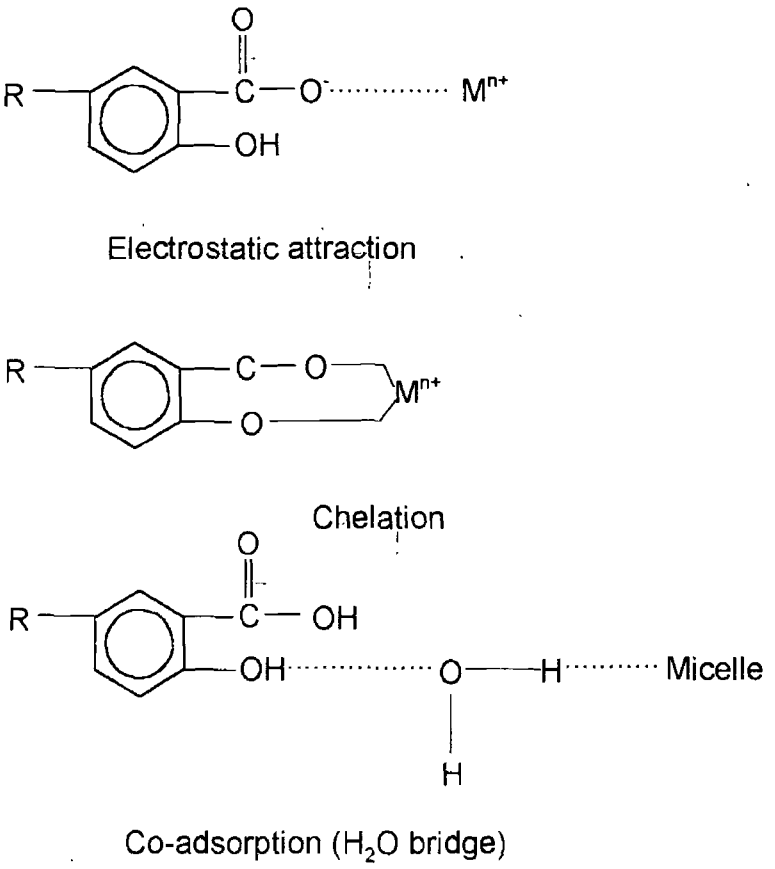

Figure 3. Chemical interaction of humic molecules with metal cations (after Tan, 1992).

1.2.1. Metal Chemistry of Peat and Organic soils.

While a complete review of the literature pertaining to organic soils and peat is beyond the scope of this project, a brief summary of the structure of peat and the processes controlling metal interactions with peat is presented in this section. Perhaps the component of peat that has been the subject of most research into metal – peat interactions is the humic acid fraction. Humic acids occur in all soils and comprise a major fraction of peat. Initially studied by Archard (1786), who first used alkali to extract humic acids, they are usually described as the portion of

the organic matter of the soil which is extracted with a 0.5 M NaOH aqueous solution and later precipitated as a brown substance upon reduction of the pH to 1 (Szalay, 1958). A more current definition is provided by Aiken (1985):

> *"a general category of naturally occurring, biogenic, heterogeneous organic substances that can generally be characterised as being yellow to black in colour, of high molecular weight and refractory".*

The portion of organic matter that is not precipitated out of solution upon pH reduction is termed fulvic acid, humin being the material that is insoluble in either acid or alkali. Although the subject of much work, the precise structure and characterisation of humic acid has still not been achieved. A number of structures have been proposed, a typical example of these structures being detailed in Fig.4. Organic material in soil is negatively charged at pH values greater than about 3. This negative charge is primarily due to the deprotonation of carboxylic and phenolic groups within the humic acid. This contribution to the cation exchange capacities of peats and organic soils has been recognised as a major mode of interaction between humic acids and metals (Schnitzer, 1986). The contribution of humic acid material to the enrichment of metals within peat has been recognised by many authors, Sholkovitz and Copeland (1981) and Lee and Jonasson (1983) studying the transport of metals in soils, Pauli (1975), Boyle (1977), Idiz *et al* (1986) and Kerndorff and Schnitzer (1980) reporting on the enrichment of metals in peat bogs by humic acids. These authors all conclude that the humic acid component of peat is a major factor in both the accumulation and transport of metals within bogs. Rashid (1974) observed preferential adsorption of Cu to humic acids in the presence of Co, Mn, Ni and Zn, the peat moss used in his experiments exhibiting an adsorption capacity of 1500 mg metal/kg humic acid.

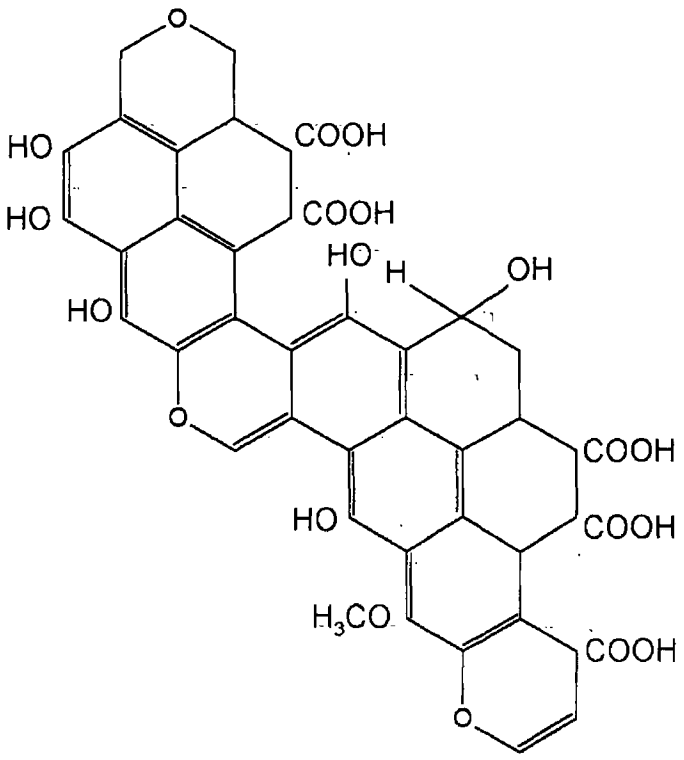

Figure 4. Proposed structure of humic acid molecules according to Fuchs (see Kononova, 1966).

Complexation has also been proposed as a process contributing to the retention of heavy metals by humic acids. Complexation or chelation occurs if two or more functional groups within the humic acid structure co-ordinate a metal ion forming a ring structure. Models developed by Leenheer *et al.* (1989) and Stevenson (1982) indicate possible chelation involving carboxyl and salicylate groups, as well as sites containing nitrogen and sulphur. In addition to playing a major part in the retention of metals within peat, complexation with humic acids also provides a means of distribution of metals. Humic acids may form soluble complexes with metals, this process being highlighted by Zielinski *et al* (1988) and Smith *et al* (1990) as a means of metal transport in surface waters.

The role of metal oxides has also been the subject of investigation with respect to metal retention. Mn(III), Fe(III), Pb(IV) and Co(III) oxides are stable in oxygenated systems under neutral pH conditions. Oxides of these metals, primarily iron and manganese, are found as soil particle coatings or suspended particles within many soils. Where iron bearing waters meet oxidised surface soil layers, the formation of iron and manganese oxides may be sufficient to cause the formation of deposits of bog iron (iron pan) as characterised by Newbould (1960). The main forms of iron oxides in peats are the minerals, goethite and lepidocrotite. Such metal oxides may also be responsible for metal enrichment in bogs given the ion adsorption capabilities of such materials. Adsorption can occur due to the acid – base nature of the surface hydroxyl groups formed on the chemisorption of water molecules . Tamura *et al* (1996) characterised adsorption of metals to iron oxides as an ion exchange process caused by the protonation and deprotonation of surface hydroxyl groups. Schwertmann and Taylor (1977) estimated that the adsorption capacity of iron oxides was between 30 and 100 µmol/g. They defined two modes of adsorption to such oxides, "non-specific" (electrostatic adsorption) and "specific" (covalent-type ion bonding), the latter being responsible for the adsorption of heavy metal cations such as Pb. Ho and Miller (1985) investigated the relationship between the adsorption of certain metals by iron oxides and organic matter, concluding that low levels of organic matter could enhance metal adsorption on the oxides, the enhancement being dependent on humic acid concentration and the pH of the solution.

The mobility of metals in peat and organic soil is dependent on a number of factors including pH, temperature and chemical composition. The most important physical parameter controlling relocation of metals in peat is water movement within the peat itself. Knight (1972) and Rycroft *et al* (1975) calculated that there was little mass distribution of inorganic compounds below the top 50 cm of peat due to the low

hydraulic conductivity of peat. This finding is in contrast to the opinions of Kochenov (1965) who asserts that groundwater infiltration of a bog may actively transport metals within the peat beds, irrespective of the nature of water flow within a bog,

1.3. Chemistry of Uranium in the Surficial Environment.

Uranium exists in four valency states, U^{3+},U^{4+},U^{5+},and U^{6+}, the tetra and hexavalent states being predominant in nature. The hexavalent state is dominant in oxidising environments such as surficial materials and rivers. It is the variable valency of uranium that largely governs its chemistry in the surficial environment. As this study is mainly concerned with the distribution and behaviour of uranium in peat, this review will concentrate on the behaviour and chemistry of uranium in rivers, peat and organic soils.

1.3.1. Chemistry of Uranium in Rivers

Surface waters typically contain 0.01 to 5 ppb uranium (Rogers and Adams,1969) although values as high as 600 ppb have been reported (Garner,1972). Palmer and Edmond (1993) calculated a global average for uranium in river water, arriving at a value of 0.18 ppb. Lopatkina (1964) derived a relationship between the uranium content of river water, the uranium content of the underlying rock and the Total Dissolved Solid (TDS) content of the water:

$$U_{water}(ppb) = 0.002.U_{rock}(ppm).TDS(ppm)$$

Halbach *et al* (1980) found good agreement between the values determined for uranium in streams draining a granite region (0.42 – 0.16 ppb) and those predicted by the Lopatkina relationship. The solubility of uranium in surface waters is largely dependent on the valence

state of uranium and the chemical species present in the water. Uranium occurs in surface (fresh) waters as U^{4+} and U^{6+} (and to a much lesser extent, U^{5+}). The work of Szabo and Zapecza (1987) established correlation's between dissolved uranium content and both Eh and dissolved oxygen, confirming the fact that uranium is most soluble in the hexavalent state, dissolved uranium being usually in the form of di- and tricarbonate uranyl species. Dongarra (1984) concluded that uranium circulation in fresh water is controlled by carbonate content. Langmuir (1978) showed that uranium may also complex with fluoride, sulphate, hydroxyl and phosphate species and that in the pH range 4 to 7.5, phosphate complexes may predominate. Holbert *et al* (1995) found that high levels of uranium were associated with samples containing both high sulphate and high carbonate levels. Zielinski *et al* (1988) calculated that in the drainage system of a uranium rich organic sediment, carbonate and phosphate complexes of uranium were the predominant inorganic uranyl species. Dialysis experiments reported by Zielinski (1988) indicated that at least some uranium was associated with macromolecular organic particles. The association of uranium with carbonate in river water is supported by Doi *et al* (1975) who found a relationship between uranium content and carbonate content in Japanese springs and streams. Longworth *et al* (1989) studied the drainage of a uranium rich organic soil, establishing that almost all uranium in the drainage system was in true solution (defined by the author as existing as particles with diameters less than 2 nm). Smith *et al* (1990), studying the same site as Longworth, concluded that complexation by organic materials was the dominant mode of occurrence of uranium in the waters, the complexing agents being low molecular weight fulvic acids.

There appears to be general consensus in the literature on the mode of occurrence of uranium in surficial waters. The majority of researchers concur that uranium occurs predominantly in conjunction with the

inorganic species carbonate and phosphate and as organic complexes with humic and fulvic acids. A smaller number of researchers conclude that the redox conditions of the waters have some bearing on the dissolved uranium content.

1.3.2. Chemistry of Uranium in Peat

The behaviour of uranium in various soil types has been well documented in the literature from about 1950. Less information exists on the chemistry and behaviour of uranium in peat and organic soils. Kochenov *et al.*(1965) outlined a series of features of the occurrence of uranium in peat beds overlying uranium rich areas:

- the distribution of uranium within the beds is irregular, dropping to background levels between areas of enrichment, which only constitute 5 to 10% of the total bed
- the uranium is concentrated in the lower parts of the bed, decreasing to background towards the surface
- iron behaves exactly like uranium within the peat profile
- uranium enrichments are not restricted to any botanical type of peat
- areas of uranium enrichment lie on the bottom of valleys and gullies and are usually fed by streams or ground waters.

Although this paper appears to suggest a relationship between iron and uranium, at least in terms of their behaviour, no evidence is presented to support this. Many of Kochenov's assertions are supported by Wilson (1984) who also concludes that uranium distribution within peat bogs is always extremely heterogenous, high uranium contents usually being associated with radioactive springs occurring in uranium enriched granite regions.

While such generalisations are useful, they do not provide information on the mode of enrichment of the peat beyond the fact that the uranium appears to be introduced to the beds by circulating water. Szalay (1964) concluded that the insoluble (in 0.5M NaOH) humic acid fraction of peat was mainly responsible for the enrichment of uranium in peat by a cation exchange process. Although this argument has been supported by Titaeva (1967), Doi *et al.* (1975) found that peat whose humic acid component had been removed tended to adsorb more uranium from solution than peat whose humic acids remained intact. Idiz *et al.* (1986) concurs with Szalay, finding that uranium is the only metal whose enrichment in peat bogs is controlled by the organic component. Halbach *et al.* (1980) investigated the role of humic and fulvic acids in the mobilisation and fixation of uranium in a peat bog and concluded that uranium is primarily removed from the granite bedrock as a uranyl fulvate complex but is fixed in the peat as a uranyl humate complex. Hansen and Stout (1968) postulated that the strength with which uranium binds to organic material in soil is dependent on the degree of humification exhibited by the organic material.

While the majority of work in this area appears to confirm the association between uranium and the humic acid component of peat, little work has been completed on the mode of interaction between uranium and the humic component. A number of processes have been proposed to account for the fixation of uranium by organic matter and humic acid. Idiz *et al* (1986) suggests a combination of adsorption, cation exchange and reduction. Goldhaber *et al.* (1987) characterised the reduction of the uranyl ion (UO_2^{2+}) by hydrogen sulphide (a typical reducing agent found in the anaerobic environment of a peat bog) as a slow process and hypothesised that the process may be catalysed by adsorption of the uranyl ion onto mineral surfaces. The findings of Disnar (1981), and Nash *et al.* (1981) suggest that at environmental temperatures and without significant hydrogen

sulphide generation, uranium is fixed by rapid ion exchange and complexation with the acidic functional groups of humic acid. Zielinski and Meier (1988) found that uranium bound to humic acids could only be displaced by highly acidic solutions or solutions concentrated in CO_3^{2-} and that uranium is firmly fixed to humic acid in a non - exchangeable manner.

A significant number of researchers conclude that, at least in some soils, amorphous iron oxides are the major component responsible for uranium enrichment. Lowson *et al* (1986) reported that up to 80% of the uranium in a soil derived from granite bedrock was associated with this fraction. Megumi (1979), using ammonium oxalate as the extracting agent, found that up to 50% of uranium in soil was associated with amorphous iron oxides, no trend in the proportion being observed with sample depth. Starik *et al* (1958) studied the adsorption of uranium onto ferric hydroxides and concluded that maximum adsorption occurred at pH 5, reduced adsorption being exhibited at pH values above and below 5. Ames and Dhanpat (1978) conclude that Eh and pH are the factors controlling uranium accumulation in soil and peat, Eh and pH being the dominant processes in the control of the behaviour of manganese and iron in such environments. Bearing in mind this fact, it is not unreasonable to assume that the effect of Eh and pH on uranium adsorption is indicative of it's being adsorbed to iron and manganese oxides within the soil. The majority of researchers conclude that little uranium is held as exchangeable cations, Lowson *et al* (1986) finding less than 1%, Megumi (1979) observing values less than 0.8%. This conclusion appears to contradict Szalays' findings (that uranium is primarily bound by cation exchange processes) although the contradiction may be resolved by bearing in mind that although uranium is bound by cation exchange it may not be exchangeable once bound in this manner. In an earlier paper, Megumi and Mamuro (1977) hypothesised that the enrichment or depletion of radionuclides

(including uranium) in soil is affected by the oxides of manganese and iron. No indication is given of whether the "oxides" referred to are amorphous iron/manganese oxides or bog iron. Their assertion however that the effect of these oxides is to reduce uranium to the tetravalent state (from the mobile hexavalent state) would appear to point to amorphous iron/manganese oxides. An association between uranium and iron oxides is also indicated by Yakobenchuk (1968) who observed a correlation between uranium levels and oxides of iron and aluminium.

The capacity of peat and humic acid for uranium adsorption has been investigated by a number of researchers. Szalay (1958) reports capacities of up to 3% (w/w), Armands (1967) arriving at a geochemical enrichment factor (G.E.F.) of 10,000, in agreement with Szalay's (1964) proposed figure of 10,000, the G.E.F. being defined as:

$$G.E.F. = [UO_2^{2+}]_{peat} / [UO_2^{2+}]_{water}$$

Lopatkina (1967) argues that the G.E.F. calculated by Szalay was arrived at under laboratory conditions and that in nature, the G.E.F. can vary from 500 to 50,000 as the dissolved total salt content varies from 10 to 900 ppm. Horrath (1960) calculated enrichment factors of 200 - 350 for peat, these values differing significantly from other researchers findings. Read *et al* (1993) investigated the capacity of peat for uranium adsorption and concluded that, at saturation, peat could adsorb up to 16% (w/w) uranium, Lopatkina (1967) arriving at a similar value.

The mobility of uranium within peat has been investigated by a number of researchers. Burns *et al* (1991), studying radionuclide migration in soils in America, concluded that leaching is the main mechanism of migration for uranium. Subsurface throughflow is also indicated as a migration process on gradients. It is worth noting however that ^{214}Bi, the daughter of ^{222}Rn, was used to determine uranium levels in this study.

Given the possible loss of radon from the soil, and the probable disequilibrium between ^{226}Ra and ^{238}U, the use of this isotope may not have provided an accurate picture of the behaviour of uranium in this instance. Dyck (1978) observed radium soil anomalies directly over uranium deposits in southern Saskatchewan, but the associated uranium anomalies occurred downhill of the deposit, in the valley floor. Although not stated in the report, this may provide further evidence of the downhill subsurface migration of uranium, at least at the site investigated by Dyck. Sheppard (1980) concurs with Burns with respect to subsurface flow and notes the possibility of uranium migration via particle movements in well drained, well weathered soil. Halbach *et al* (1980) identified acidic, oxidising surface water as the agent responsible for uranium mobilisation in peat overlying a granite bedrock. Landstrom and Sundblad (1986) concluded that the leaching of surrounding soils and subsequent inflow (the nature of the inflow, subsurface or surface, is not detailed) to small, swampy depressions in a Swedish bog was the source of elevated uranium in the depressions. The fact that uranium is only considered mobile in an oxidising environment is highlighted by the work of Sheppard and Thibault (1988) on the migration of radionuclides in mires. Uranium appeared to be immobile relative to a number of radionuclides, the reducing nature of the soil being cited as the reason.

Although a significant number of papers on the occurrence of uranium in peat are to be found in the literature, a general consensus on the controlling factors of uranium enrichment in peat does not seem to be prevalent. Although the association of uranium with the humic acid fraction of peat appears to be generally accepted, a significant number of researchers have reported different findings. The majority of these researchers highlight amorphous soil iron oxides as the factor that would appear to be controlling uranium levels within peat. The disparity between the findings of the researchers indicates that there is most probably a high level of site specificity in relation to the mechanisms

controlling uranium accumulation in peat and organic soils. A problem with laboratory studies of the adsorption of uranium to peat and humic acid is the exclusion of a broad range of parameters prevailing in natural systems, from the studies. Field based research may therefore provide a better indication of the mode of interaction. All researchers agree however that uranium is essentially immobile in a reducing environment but mobile under oxidising conditions. There is also agreement on the migration mechanism of uranium within peat, water flow being the agent responsible.

1.4. Chemistry of Radium in the Surficial Environment

Radium, which is chemically similar to barium, has only one oxidation state, +2. Radium hydroxide ($Ra(OH)_2$) is the most soluble of all the alkaline earth hydroxides, including the hydroxides of actinium and thorium. The bicarbonate and chloride compounds of radium are all water soluble, but radium coprecipitates with barium as the sulphate or chromate. Of all the alkaline earth metals, radium shows the least tendency for complex formation, although Schubert *et al* (1950) detected 1:1 complexes of radium with citric, tartaric and succinic acids in the pH range 7.2 to 7.4.

1.4.1. Chemistry of Radium in Rivers

As some salts of radium are soluble in water, surficial waters may be enriched in radium. The radium concentration of river water typically lies in the range 10^{-10} to 10^{-11} µg/g (Koczy, 1963) although mineral springs have been shown to contain 748×10^{-6} µg/g (Gera, 1975). Szabo and Zapecza (1987) found significant correlation between ^{226}Ra and iron, manganese, bicarbonate and barium in ground and spring waters, also concluding that Eh and dissolved oxygen are important controls over

levels of the radionuclide in water. Holbert *et al* (1995) established a relationship between total dissolved solids (T.D.S.) and ^{226}Ra, also concluding that elevated uranium levels (in waters) do not occur concurrently with elevated ^{226}Ra. Michel (1990) also found a correlation between ^{226}Ra in water and T.D.S.

Little evidence exists in the literature of any significant amount of work having being completed into the occurrence of radium in surface fresh waters, the main emphasis having being on the assessment of levels and behaviour of radium in groundwater from a health physics perspective. As with uranium, Eh and pH, along with the concentration of various inorganic species such as bicarbonate, appear to be the controlling factors in relation to the concentration of radium in surface fresh waters.

1.4.2. Chemistry of Radium in Peat

Radium is present as Ra^{2+} over the normal soil pH range of 4 to 8. Although radium shows little tendency to form complexes (Schubert *et al*, 1950), Granger *et al* (1961) showed that it may be expected to replace other divalent cations in replacement reactions. Arnold and Crouse (1965) obtained a correlation between radium adsorption and cation exchange capacity, the leaching studies of Havlik *et al* (1968) supporting the view that cation exchange is an important mechanism for radium adsorption. Megumi (1979) established that, unlike uranium or thorium, radium may have a significant occurrence as an exchangeable ion. Nathwani and Phillips (1979a) showed that organic matter was the component of soil responsible for radium adsorption and that soils with a low cation exchange capacity exhibited reduced ability for adsorption. Titaeva (1967) studied the nature of radium bonding in peat and concluded that radium is largely associated with the organic residues that are insoluble in dilute NaOH, by a process involving ion exchange. A further conclusion however, is that in the presence of high soil water

calcium concentrations, the radium becomes unexchangeable. Nathwani and Phillips (1979b) concluded that in the presence of elevated Ca^{2+}, radium adsorption by soils from water was severely retarded. Greeman and Rose (1990) found that, in a soil derived from carbonate rock, up to 24% of the total radium was associated with organic soil fractions and humified matter.

Taskayev *et al* (1978) studied the speciation of ^{226}Ra in soils exhibiting high concentrations of the isotope, concluding that ^{226}Ra is firmly fixed within the soil, and that the ratio of the water soluble and exchangeable proportions varies significantly with depth. A further conclusion was that organic acids present in the soil increase the mobility of the isotope, no reason for this enhanced mobility being given in the report.

1.5. Chemistry of Thorium in the Surficial Environment

Of the six thorium isotopes found in nature, only Th^{232} is of quantitative importance, the other isotopes being relatively minor components of the three decay series. Thorium only occurs in the +4 valency state in nature. Thorium forms insoluble hydroxides, fluorides and phosphates, while soluble thorium compounds include nitrate, sulphate and chloride. Thorium also forms metal complexes with citric and oxalic acids and substances such as acetyl acetone. The amount of literature referring to thorium in the environment reflects the relative un-importance attached to this element compared to uranium and radium.

1.5.1. Chemistry of Thorium in Rivers

Thorium is found in very low concentrations in freshwaters. Kamath *et al* (1964) determined levels of 1.1 – 2.7 ppb in surface waters of a region in India. These figures are among the highest reported values for water taken from non-uraniferous regions, typical values being in the region of

0.008 to 0.9 ppb (Miyake *et al*, 1964, Dementyev and Syromyatnikov, 1965). Garner (1972) hypothesised that the low occurrence of thorium in surface waters is due to thorium being readily adsorbed by solid components in water and its being precipitated out of solution as the hydroxide. Dementyev and Syromyatnikov (1965) established that approximately 50% of thorium in groundwater exists as carbonate and phosphate complexes, the remainder being adsorbed onto particulates. Sillen and Martell (1964) calculated that thorium has very low solubility in water at pH values greater than 5, $Th(OH)_4$ being the dominant species above pH 5. Langmuir and Herman (1980), in what could possibly be regarded as one of the definitive papers on the subject, support the findings of Sillen and Martell, and also make a number of valuable points. The authors assert that at pH values from 5 – 9, thorium rarely exhibits concentrations in natural waters greater than 1 ppb due to the insolubility of its parent minerals (thorianite and monazite) and strong adsorption of thorium by natural materials. They also hypothesise that many of the relatively high values for thorium in water, reported in the literature, are due to the samples containing thorium adsorbed on particulates which have not been removed prior to analysis.

The literature contains relatively little information on the occurrence of thorium in freshwater. The majority of the studies that do exist consist of thermodynamic analyses regarding thorium species solubilities. It can be inferred however, that the concentration of thorium in the majority of freshwaters is extremely low given it's tendency to form the insoluble hydroxide and it's strong association with water borne organic matter.

1.5.2. Chemistry of Thorium in Peat

Thorium in organic soils tends to be present as insoluble oxides and hydroxides of manganese and iron (Schulz, 1965), Rancon (1973) establishing that strong humic and fulvic complexes with thorium occur

in acidic soils. This relationship between humic components of soil and thorium is supported by Hansen and Huntington (1969) but countered by Tyuryukanova and Kalugina (1971), who established that soils high in humic acids (peats and mountain podsols) had low thorium levels relative to alluvial soils. This low level of thorium in peat is ascribed to the weak assimilation of thorium in plant species that populate organic soils, the decay products of which constitute a major proportion of peat. Rancon (1973) detailed four processes governing soil-thorium interactions, (1) $Th(OH)_4$ precipitation, (2) adsorption from dilute solutions onto clay soils, (3) adsorption to organic components under acidic conditions, and (4) low adsorption under alkaline conditions due to the dissolution of humic acids. The strength of the humic-thorium association was highlighted by Bondietti (1974) using a calcium citrate solution to desorb thorium from soil. This solution desorbed 30% of thorium from montmorillonite and kaolinite but could only desorb 1% from a calcium humate material.

In direct contrast to uranium, solutional transport of thorium within soil is a relatively unimportant process. The major mode of thorium transport is by particle movement within the soil, Baranov *et al* (1964) concluding that thorium transport occurs largely in the colloidal state. Verkovskaja *et al* (1967) determined that plant cycling of thorium was not as important as for radium in the movement of the element in soil. The immobility of thorium within peat is reflected in the suggestion by Landstrom and Sundblad (1986) that $^{228}Ra/^{232}Th$ disequilibrium ratios could be used in plotting recent water flow within bogs.

1.6. Uranium Series Disequilibrium

Generally, a radioactive decay series is said to be in secular equilibrium when the activities of all daughter products equal that of the initial parent. A state of disequilibrium exists if one or more of the daughters

are removed from the decay series by a process other than radioactive decay. In the surficial environment, such processes typically involve diffusion of the gaseous members of decay series, i.e. the Rn isotopes, migration of daughter nuclides in solution and differential uptake of daughter nuclides by plants.

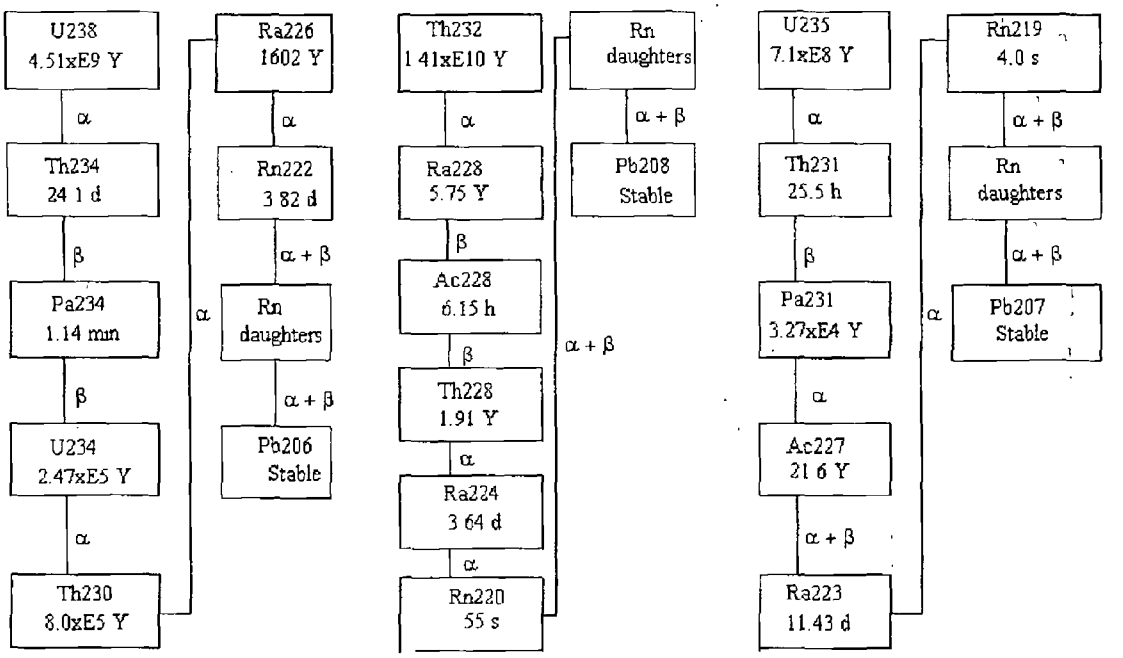

Figure.5. Decay scheme for (a) ^{238}U and (b) ^{232}Th

1.6.1. Uranium Series Disequilibrium in Soil

Four processes are generally accepted as giving rise to disequilibrium in the uranium decay series in the surficial environment:

Diffusion of Daughters. Diffusion of radon at a soil-gas interface allows escape of the gas from the decay chain, producing disequilibrium conditions in the subsequent daughters, relative to the nuclides preceding radon. Diffusion of non gaseous daughters across soil-water

boundaries may also result in disequilibrium especially if the half-life of the daughter is long and the ratio of the daughters concentration in the two phases is high.

Alpha Recoil. The high energies of the alpha particles emitted by members of the uranium decay series (4-9 MeV) results in daughters recoiling (under the Law of Conservation of Momentum) up to distances of 20 nm or more (Ivanovich and Harmon, 1992). Recoil over such distances is, in some cases, sufficient to propel a daughter nuclide out of, for example, a soil particle into a liquid phase, thus removing the daughter from the system. The process of alpha recoil has been used to explain disequilibrium between ^{234}U and ^{238}U in systems where selective leaching has not occurred (Osmond and Cowart, 1976).

Szilard-Chalmers Effect. A related phenomenon is that of the Szilard-Chalmers effect or 'vulnerability to leaching'. Alpha recoil of a daughter nuclide through a crystal lattice produces damage along the recoil path. Subsequent changes to the daughters electronic configuration, combined with the damage to the lattice can increase the susceptibility of the nuclide to leaching.

Dissolution and Precipitation. Perhaps the most important process causing disequilibrium in the uranium decay series in soil is selective leaching of daughters by percolating soil water. Under certain conditions of Eh and pH, uranium and other isotopes exhibit greater solubility than, most notably, radium and thorium. This fact leads to the removal of uranium as it is dissolved and carried away by soil water, and, conversely, enrichment of uranium as the soil water enters a region where chemical conditions favour its precipitation. $^{226}Ra/^{238}U$ disequilibrium in soil is largely due to the process of selective leaching and deposition. Uranium is mobile under oxidising conditions whereas radium, and its parent nuclide ^{230}Th, are essentially immobile in the

surficial environment. This process has been identified as causing disequilibrium in young organic uranium deposits (Zielinski *et al*, 1986, Levinson *et al*, 1984). Megumi (1979) asserted that disequilibrium in the ^{238}U decay series (prior to Rn^{222}) is due primarily to the immobility of ^{230}Th. Greeman and Rose (1990) studied radioactive disequilibrium in the ^{238}U series for a number of soils and concluded that in the surface horizons of soil, ^{226}Ra excess could be attributed to the cycling of ^{226}Ra by plants, leading to an increase in the isotope relative to ^{238}U. This view appears to be supported by Taskayev *et al* (1977) who points out that, relative to soil, radium is less strongly bound in plant tissues and soil litter and the mobility of the isotope may be increased at the soil surface due to decay of radium bearing plant material. Von Gunten *et al* (1996) observed ^{226}Ra activities a factor of 20 above the activity of ^{238}U in a karst region of Switzerland and proposed that, following continuous weathering of calcite particles, uranium was lost from the soil as the soluble carbonate complex, ^{226}Ra being retained within the soil. de Jong *et al* (1993) hypothesised that the $^{226}Ra/^{238}U$ disequilibrium in a Saskatchewan soil was probably due to the mode of deposition of the parent material rather than subsequent selective leaching of members of the series. Titaeva and Veksler (1977) discuss the possibility of ^{226}Ra excess being due to the deposition of ^{226}Ra from water onto the surface of weathered particles but offer no conclusive proof.

Ivanovich and Harmon (1992) state categorically that in soils subject to leaching, the primary cause of radioactive disequilibrium is the removal of uranium relative to thorium and immobile daughters. A second statement is that in marshy, reducing environments, radium may be more mobile than uranium causing a different pattern of disequilibrium to arise.

1.7. Summary of Relevant Literature

The majority of previous work on the occurrence of natural radionuclides in peat and organic soils falls into two categories. The first concerns itself with the general distribution of radionuclides within peat bogs (Kochenov *et al*, 1965), the second being the description of the modes of occurrence of the radionuclides within the peat in relation to the constituents of peat responsible for radionuclide retention and enrichment (Szalay, 1964). Most of the authors contributing to the former agree on the broad features of radionuclide occurrence within peat bogs, that radionuclide distribution is primarily controlled by geology and drainage patterns within the bog. Radionuclide enrichment therefore occurs in areas where drainage water collects, at the bottom of peat beds and on the floors of valleys, areas of enrichment often occurring some distance away from bedrock containing elevated levels of these nuclides. This agrees to a large extent with the notion of uranium being mobile in an oxidising surficial environment, concomitant enrichment of other nuclides, primarily ^{226}Ra, being due to ingrowth. Most authors agree on this mobility of uranium and the relative immobility of radium and thorium in the same environment. The primary processes involved in the retention of these nuclides within peat appear to be precipitation of thorium as the hydroxide and radium as the sulphate. Thorium and radium are also strongly bound by organic matter, most probably in the humic acid component of the soil.

This level of consensus is not encountered on the matter of the speciation of radionuclides within the peat itself. The arguments for the association of uranium with organic matter (specifically humic acids) and amorphous iron oxides both rely on the results of field and laboratory studies conducted over many years and in many different countries. Studies of the enrichment of peat with natural radionuclides based on laboratory work only, tend to agree that humic acids are the

primary agents for the adsorption and enrichment of radionuclides. Field based studies however, differ greatly in their findings, the association between uranium series nuclides and amorphous iron oxides being proposed, to a greater or lesser extent, as the primary agent. This conflict is probably evidence of a certain site specificity or at least a relation based on soil types or groups and reflects the difficulty in making comparisons on the behaviour of a species which is governed by a wide variety of controlling factors. The chemical nature of the relationship between natural radionuclides and humic acids is also the subject of much contention, the majority of authors proposing a range of mechanisms, such as ion-exchange, reduction and complexation as the primary means of incorporation of radionuclides onto humic acids, a substance whose nature and chemical characteristics have still to be fully investigated.

Little or no previous information exists on the specific causes of uranium series disequilibrium in organic soils or peat bogs. This arises from the nature of studies on radionuclide accumulation within peat bogs. The majority of such studies have been either conducted or funded by parties interested in the location of viable uranium deposits. The cause of radioactive disequilibrium in the uranium decay series (prior to ^{222}Rn) also remains the subject of much discussion. This is perhaps due to the number of radionuclides in the series between ^{238}U and ^{226}Ra and the number of possible mechanisms by which disequilibrium may occur between any two members of the series. Many authors investigate specific pairs of nuclides, such as ^{230}Th and ^{238}U and then attempt to apply the perceived reasons for the disequilibrium between the two studied nuclides to other pairs, such as ^{238}U and ^{226}Ra. This results in conflicts between various authors on the nature and causes of the disequilibrium. Some information may be gleaned from reports of geochemical prospectors encountering radiometric anomalies in peat areas that contain little actual uranium. Loss of uranium by unspecified

processes is invariably cited as the cause with little or no evidence of this fact being given in the reports. Although such reports rarely discuss results not directly concerned with the location of ore deposits, it is probable that at least some of these authors have evidence that uranium loss, as opposed to radium enrichment, is indeed the cause of $^{226}Ra/^{238}U$ secular disequilibrium.

2.0. GEOSTATISTICS: THEORY AND PRACTICE.

2.1. Introduction

Empirically described by Krige (1951) and theoretically grounded by Matheron (1963), geostatistical methods were initially employed in the field for which they were developed, ore reserve estimation. In the past two decades the methods have been increasingly applied to the problem of pollution assessment and the mapping of environmental variables, the surge in interest being reflected in the increase in the amount of literature on the application of geostatistics in the field of environmental monitoring.

Traditional methods of estimation and interpolation have relied on two distinct approaches, the "area of influence" method and classical statistical treatments. The former utilises both the spatial position of the known samples and the value of the variable at those points, the latter adheres to classical statistical theory by assuming the known sample values to be random observations drawn from a given population, no regard being given to the spatial location of the samples. Both methods have proven to be far from ideal for a number of reasons. The "area of influence" method, typically demonstrated in polygonal estimation, is unable to produce confidence limits or a measure of the reliability of the produced estimates. Although classical statistics are in a position to produce such values, the spatial location of the samples is ignored in the estimation procedure, an omission which was deemed undesirable by the geologists using the techniques for the purpose of reserve valuation.

2.2. Regionalised Variables.

In an attempt to produce an estimation method that incorporated both the value and position of known samples in the production of estimates and provided a measure of the estimates reliability, Matheron (1970) conceived of the concept of "Regionalised Variables". A random variable is a variable that varies in a probabilistic manner between individual samples. A regionalised variable is a random variable that varies in value according to its location within some predetermined area, i.e. an ore body, or survey region. Journel and Huybregts (1978) define the two components of a regionalised variable:

i. an observation of the variable at point w_i within the greater area w, is a realisation of a random variable $Z(w_i)$ for the point w_i. This component is random in that the set of random variables for every point within w is a random function.

ii. the random variables for two locations, w_i and w_{i+h} (separated by vector h) are not considered independent. i.e. $Z(w_i)$ and $Z(w_{i+h})$ are spatially correlated.

The description of regionalized variables provided above is a mathematical expression of the phenomena intuitively recognised by many practitioners of environmental monitoring, that samples separated by great distances are usually more dissimilar than samples separated by smaller distances.

2.3. The Intrinsic Hypothesis

Geostatistical methods involve the analysis of the spatial correlation of the variable in question and the production of

estimates for unsampled locations based on the extent and nature of the spatial correlation. The former is achieved using a technique known as semi-variogram analysis, the latter employing a procedure known as kriging. Both these methods rely on the data set being used fulfilling the intrinsic hypothesis. This hypothesis is generally satisfied if:

i. the expectation value of the difference between two points, w_i and w_{i+h}, separated by a vector h, should be zero

ii. the variance of the differences between points separated by the vector h is only a function of the magnitude of the vector.

$$Var[Z(w_{i+h}) - Z(w_i)] = 2\gamma h \qquad [1]$$

where γ is the semi-variogram value.

The initial assumption of the intrinsic hypothesis is best explained with the use of an example. A number of samples, all spatially separated by a vector h, are analysed for a variable denoted q. If the difference in the value of q exhibited by samples separated by h is only a function of h, then the distribution of the differences depends on h and hence the mean and variance of the distribution also depend on h. The mean difference, a*(h), between points (denoted w) can be established by:

$$a^*(h) = \sum[q(w) - (q(w+h)]\ 1/n \qquad [2]$$

where n is the number of points.

The term a*(h) can also be deemed the 'expected' difference between samples separated by the vector h. If this value is zero then no difference is expected between samples separated by h. In practical terms this means that in an area determined by the magnitude of h, all

samples should exhibit similar values for the variable q. If this is not true then a trend is said to exist within the area, or the expected difference between two points does not equal zero.

The second part of the intrinsic hypothesis concerns itself with the concept of "stationarity of difference". If the above example is implemented again, the variance of the distribution of the differences between samples separated by a vector h may be given by $2\gamma(h)$, also called the variogram value. This value should only be a function of the magnitude of h and not the direction or location of h within the study area.

The extent to which the fulfilment of the conditions of the intrinsic hypothesis affect the implementation of geostatistical procedures remains unclear from the examples provided in the literature. Although many researchers include a statement of the intrinsic hypothesis in their articles (McBratney and Laslett, 1993, Einax and Soldt, 1995), none give any indication of their having tested their data for fulfilment of the conditions. The presence of a trend in a data set is often given as a reason for the implementation of advanced data modifications to remove or model the trend (Flatman and Yfantis, 1984). Clarke (1979), in one of the standard texts on the subject, states that trends in a data set are not a problem insofar as they may manifest themselves at distances which are great enough that they do not pose a problem for local estimation. Clarke also states that there is no statistical test for stationarity, and that stationarity within a data set may only be assumed and not proven. Stationarity is a function of the random component of the spatial structure, not the data itself, and a test would therefore require multiple realisations of the random function, a feat not possible in practice.

2.4. The Semi-variogram

The extent and form of the spatial correlation of the data set is investigated using semi-variogram analysis. The semi-variogram is a graphical representation of how the similarity between variable values varies as a function of the distance (and direction) separating them. The *theoretical* semi-variogram is a plot of one half of the variance of the differences in variable values (y axis) as a function of the distance, or "lag", separating pairs of points (x axis), the general equation for the semi-variance being:

$$\gamma(h) = (1/2n(h)_{i=1}) - [q(w_{i+h}) - q(w_j)]^2 \qquad [3]$$

As only a limited number of pairs are available in a practical study, an *experimental* semi-variogram is plotted using the available data and a theoretical model is fitted to the resulting plot. The curve fitted to the data can be seen to consist of two distinct parts, an initial rising segment and a second, level region (Fig.6.). The point at which the curve levels off is used to calculate both the sill (y axis) and the range of correlation (x axis).

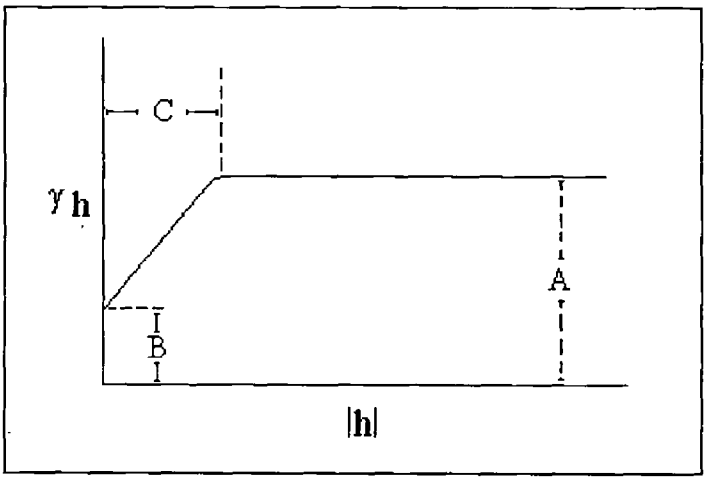

Figure 6. Semi-variogram schematic. A - sill, B - nugget, C - range of correlation.

The sill is the maximum semi-variance exhibited by the data set and the range of correlation is the lag (or separation distance) at which the sill value is reached. Pairs of points separated by a distance greater than the range of correlation are considered to be spatially uncorrelated. A sample can be taken as representative of an area defined by the range of correlation. The range of correlation provides a mathematical means of measuring the "area of influence" described in other estimation methods. The semi-variance value indicated by the sill can be divided into two components, B and A-B in Fig.6.. The "nugget effect", often denoted Co, (B in Fig.6.) represents the random variance in the data. The semi-variance, represented by A - B in Fig.6., is the structured component of the data set's variance.

The experimental semi-variogram only provides information on the data set used to construct the plot. In order to describe the entire region (and lag distances for which a semi-variogram value has not been computed), it is necessary to fit a mathematical model to the data to produce the *theoretical* semi-variogram. A number of models are frequently used to describe the theoretical semi-variogram and these are briefly described below.

The most commonly used model in geostatistics, the spherical model, is indicative of a high degree of spatial continuity. It is linear near the origin before flattening out as it approaches the sill at *a* (the range of correlation). It is described by the equation:

$$\gamma(h) = 1.5h/a - 0.5(h/a)^3 \qquad [4]$$

where a is the range and h is the lag distance.

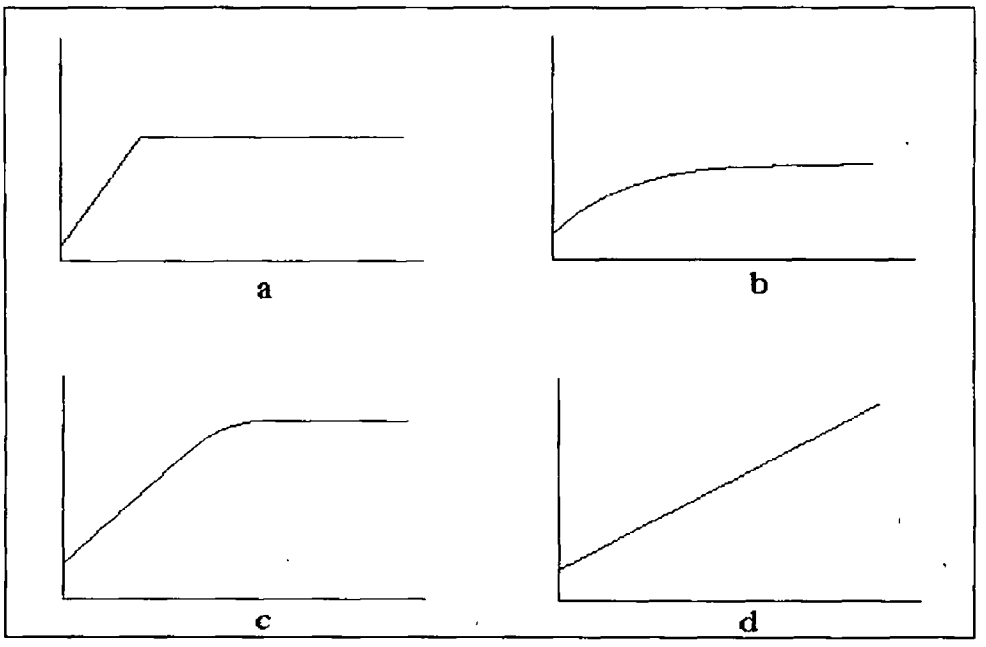

Figure 7. Theoretical semi-variogram models. (a) spherical, (b) exponential, (c) gaussian, (d) power.

The exponential model reaches the sill asymptotically, being linear near the origin, and may be described by the equation:

$$\gamma(h) = 1 - \exp(-3h/a) \qquad [5]$$

Gaussian models are used to model extremely continuous variables. Exhibiting parabolic behaviour near the origin, the gaussian model reaches the sill asymptotically, the range being accepted as the point at which the curve reaches 95% of the sill value:

$$\gamma(h) = 1 - \exp(-3h^2/a^2) \qquad [6]$$

Power models are a collection of models described by a general equation:

$$\gamma(h) = hn + Co \qquad [7]$$

where $0 < n < 2$, h is the lag distance and Co is the nugget of the semi-variogram.

In practice it is often not possible to compute semi-variances for the exact lags plotted in the semi-variogram, especially if the data has not been taken from a regular grid. The specification of a lag tolerance is therefore common practice.

A significant feature of many data sets is a state of anisotropy. A data set is said to be isotropic if the properties of the semi-variogram remain constant for all the directional variograms. A directional semi-variogram is a semi-variogram plotted for one direction only, i.e. N-S or E-W. If the range or sill of a semi-variogram model differs between directional components, then it is said to be anisotropic. If the only difference between directional semi-variograms is the length of a, the range, then the anisotropy is geometric. Zonal anisotropy occurs when the directional semi-variograms differ in relation to the value of the sill. Correction for geometric anisotropy involves incorporating the different range lengths into an ellipsoid describing the zone of influence around any sample point, as opposed to the circle of influence exhibited by points in an isotropic data set. Zonal anisotropies cannot be removed in this way and the different semi-variogram structures for the various directions must be accounted for in any subsequent estimation procedures.

A feature of many semi-variograms is a parabolic ascension of the semi-variogram at some point, an example of this being shown in Fig.8. Clarke (1979) demonstrates the use of this feature in the identification of trends within a data set and concludes that as long as the trend does not occur near the range of correlation then it may safely be ignored. This view is supported by the work of Royle and Hosgit (1974), who cite an example of a sand and gravel deposit which displayed a parabolic

upward curve, this feature being used as proof of the existence of a trend within the data. These workers also conclude that unless the parabolic nature of the semi-variogram occurs before or near the range of correlation it poses no difficulty to further stages in the geostatistical process.

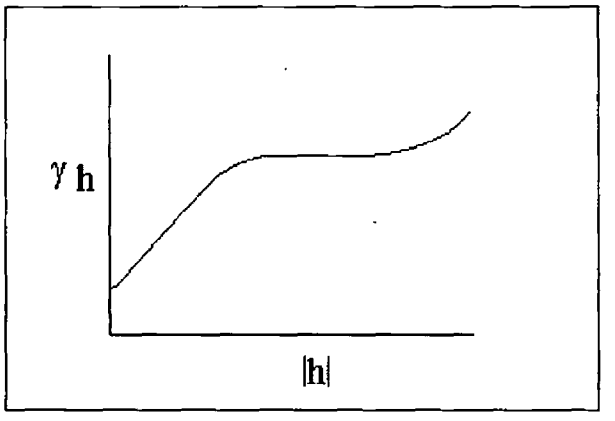

Figure 8. Gaussian semi-variogram with evidence of trend.

2.4.1. Semi-variogram Analysis: Lognormal Data Sets

The treatment of lognormal data sets in the construction and modelling of semi-variograms has been the subject of much discussion. Gilbert and Simpson (1983) and Litaor (1995) both recommend the logarithmic transformation of lognormal distributions in order to better approximate a normal distribution, both presenting un-substantiated evidence that geostatistical procedures perform better on normally distributed data. McBratney and Laslett (1993) hypothesise that the nugget (the random component of the spatial correlation) may be over emphasised in semi-variograms of lognormal data due to the high values at the upper end of the distribution being confused with 'random noise' in the semi-variogram structure.

2.5. Geostatistical Estimation: Kriging

The estimation method known as kriging employs a weighted moving average interpolation procedure. Weights are assigned to known samples, the assignation of weights being governed by the information in the semi-variogram. Generally the closest neighbouring samples are attributed the greatest weights although in a data set exhibiting geometric anisotropy, a sample a distance away from an unknown point may be attributed a heavier weighting than a nearer sample depending on the ranges of influence in the two directions. Kriging may either produce estimates for points in space (punctual) or for three dimensional volumes (block kriging). Block kriging is usually implemented in the estimation of ore bodies or similar phenomena, punctual kriging being used in environmental studies. The function for point kriging is:

$$z^*(x_o) = \sum_{i=1}^{n} \lambda_j z(x_j) \qquad [8]$$

$z^*(x_o)$ is the estimate value at the unknown location x_o, λ_j being the weight assigned to the known sample z at (x_j). The weights are assigned according to the following equation, subject to a number of constraints.

$$\sum_{j=1}^{n} \lambda_i \gamma(x_i, x_j) + \mu = \gamma(x_j, x_0) \quad i = 1, 2, \ldots\ldots, n. \qquad [9]$$

(x_i, x_j) being the distance separating points x_i and x_j, (x_i, x_o) being the distance between the unknown point x_o and the known point x_i, μ is a Lagrange multiplier. A distortion free distribution of weights is obtained by using the following constraint:

$$\sum_{i=1}^{n} \lambda_i = 1 \qquad [10]$$

One of the most often cited advantages of kriging as an estimation method is the production of a measure of the error associated with the estimates produced by the kriging process. The production of this indicator of the estimate reliability is achieved as demonstrated by the following example. A point *x*, for which we wish to estimate the value of the variable q, is surrounded by many other points for whom the value of q is known. A semi-variogram for the data set which contains these points has been calculated and a theoretical model has been fitted. When the value of q at *x* is estimated an error is incurred:

$$\text{error} = q_x - q_x^* \qquad [11]$$

where q_x is the actual value of the variable q at x and q_x^* is the estimate of the value of the variable q at *x*. If the estimating procedure is unbiased (i.e. no trend present) then repeated estimations of q_x^* will have an average error of 0. The spread, or standard deviation, of these errors gives an indication of the reliability of the estimating procedure for the point *x*. For the purpose of this example, the estimation error variance will be denoted 'e*var'. The variance of the errors can be calculated (theoretically) as the mean squared deviation from the mean error. This is equal to:

$$\frac{(\text{error} - \text{mean error})^2}{n}$$

n being the number of estimations performed. However, as the estimating procedure is unbiased, the mean error will be equal to 0, the variance of the errors reduces to:

$$\frac{(q_x - q_x^*)^2}{n} \qquad [12]$$

As the value n represents the number of samples (whose values of q are known) used to estimate q_x^*, the semi-variogram value will be known

for each of the samples that constitute the set n, as the distance that separates x from each of the samples is already known. As the semi-variogram value is half the variance of the differences in the variable q exhibited by pairs of samples separated by a distance h, multiplication of the semi-variogram value by 2 will give a measure of the reliability associated with an estimate made based on a sample a distance h away from the unknown point.

The discussion of geostatistical theory presented in the previous section has, by necessity, maintained a relatively low level of mathematics. More detailed presentation of the mathematical foundation of geostatistics and the associated procedures may be found in Journel and Huybregts (1978), David (1977) and Krige (1951).

2.6. Sampling Design for Geostatistical Surveys

The design of sampling grids for geostatistical surveys has received some attention in the literature. Wang and Qi (1998), using artificially created sample sets, ascertained that a regular grid system exhibited the best estimation performance. McBratney and Laslett (1993) recommend a random approach to sampling when the data displays a short range of correlation, nearest neighbour sites close to the unknown having strong spatial correlation. Flatman *et al* (1988) describes a sampling plan involving transects along the major axes with a regular grid at the junction of the axes. Geostatistical procedures appear well suited to the spatial analysis of soil properties and constituents for a number of reasons. Many soil properties, including radionuclide levels, are controlled by the underlying geology. Such parameters, in contrast with those such as ^{137}Cs soil levels (governed primarily by meteorological variables), are more likely to be spatially correlated, nearby samples being more similar than samples separated by large distances.

Gilbert and Simpson (1983) investigated the application of geostatistical procedures for the spatial analysis of fallout patterns around nuclear test sites in the U.S. Badr *et al* (1996) utilised semi-variogram analysis to confirm geological control over soil gas radon concentrations, fitting exponential models to raw semi-variograms. Litaor (1995) analysed the spatial distribution of $^{239+240}Pu$ and ^{241}Am around the Rocky Flats installation in Colorado, adopting a semi-variogram analysis and point kriging for estimation, gaussian models being used to describe the spatial continuity. Geostatistical analysis has previously been used to determine the distribution of uranium, albeit only within an ore body. Akin and Bianconi (1984) assessed uranium mineralisation within a surficial deposit in Australia. The uranium showed a strong degree of spatial correlation, although the spherical models applied to the semi-variograms incorporated a large nugget effect due to a random component in the uranium's spatial structure. Geostatistical methods were adopted by Einax and Soldt (1994) in the investigation of heavy metal contamination of soils, McBratney and Laslett (1993) describing some geostatistical approaches to a similar problem. Geostatistical procedures have also been applied to the analysis of a number of other environmental parameters including soil pH (Yost *et al*, 1982), conductivity (Russo and Bressler, 1981), sodium levels (Burgess and Webster, 1980) and sand content (Vauclin *et al*, 1982).

Srivastava and Isaaks (1989) established that geostatistical methods performed better than other methods of estimation for a number of parameters and hypothesised that this was due to the implementation of a customised statistical measure of distance rather than a geometrical description. Litaor (1995) observed, in comparing isopleth maps produced by geostatistics with those produced by a least squares method, that the kriging method eliminated some features visible in the other maps. He ascribed the differences to the smoothing effect of the process, kriging typically overestimating low values and underestimating high

ones. The assessment of the performance of kriging in relation to other methods has been routinely performed in the mining industry. Barnes (1977) compared geostatistics to a polygonal and inverse distance procedures for ore evaluation, the geostatistical method performing favourably. Knudsen *et al* (1978) contrasted geostatistics with more conventional estimation methods, kriging outperforming the other methods over the chosen parameters. McBratney and Laslett (1993) point out that the implementation of geostatistics is often justified on the basis that the values in a data set are more similar the closer they are in space. Their argument is that other estimation procedures can highlight and use this feature and that an empirical comparison of geostatistics in relation to other methods has not been carried out in an environmental setting.

Although geostatistical procedures appear to be gaining acceptance in the field of environmental monitoring, its only application to natural radionuclides appears to have been within the mining industry itself. There is little or no indication in the available literature of its having being applied to the monitoring of natural radionuclides in the environment although it has been employed in the assessment of contamination by anthropogenic radionuclides. While geostatistical methods appear to offer a number of significant advantages over more conventional estimation techniques and seem to be well suited to the analysis of the distribution of natural radionuclides in soil, a number of points are worth considering. The application of geostatistics remains relatively new in the field of environmental monitoring and have not been implemented long enough to have gained wide acceptance. Geostatistical methods are quite general in relation to scale, examples in the literature have ranged from centimeters to kilometers but it should be realised that as the spacing between samples increases, the advantages of treating a variable as regionalised become less and geostatistical results begin to approach those of classical statistics. A large number of unresolved issues appear to exist in the field. There remains no true

measure of the goodness of fit of any theoretical model applied to the raw semi-variogram, the most appropriate model often being chosen on the basis of trial and error. The assumption that the applied model describes spatial variability over the full region must always be made. Disagreement appears to exist on the correct treatment of log normally distributed variables and data sets exhibiting trends. The assumptions of the intrinsic hypothesis cannot be verified in any meaningful way for any data set.

Despite these caveats, the implementation of a geostatistical procedure, after a meaningful and thorough examination of a data set, can offer advantages over other estimation procedures. At the very least, the use of such methods allows for a more in-depth analysis of a surveys' results than would be provided through the blind use of some of the more conventional methods. The computational requirements of geostatistics and the lengthy analysis involved, in combination with the problems listed above may serve to deter researchers in the environmental field from the adoption of such methods. Possible evidence for this is the large amount of published material in the statistical and mathematical journals and the relative lack of material in the earth science and environmental area. When geostatistics are used, the implementation often appears to suffer due to either a lack of exploratory analysis of the data or via the use of commercial software with little regard for the quality of the final outputs.

3.0. METHODS

3.1. Site Selection and Description (Survey 1)

The Cronamuck Valley lies on the north eastern periphery of the Barnesmore pluton, between Cronamuck Mountain and Clogher Hill, running in a NE – SW direction for approximately 5 km. The site was chosen for a number of reasons. The peat of the Cronamuck Valley had previously been shown to exhibit elevated levels of natural radionuclides (Irish Base Metals, 1979), as had the underlying geology (O'Connor, 1983). The geology of the area has been well defined and the granite of the pluton maintains sharp contact with the surrounding country rocks. The site is relatively accessible by foot during the summer months and is sparsely populated. Little agriculture is conducted in the region, large areas of the valley remaining un-modified by man. The main modification is the recent planting of conifer plantations, with associated drainage schemes, in some parts of the valley. The soil in the valley is a typical upland peat, depth being less than 1m on the sides of the valley, deepening to up to 2m on the valley floor. Soils to the west of the survey region are better drained, being sandy towards the base of the soil. While there is still no agreed method of classifying organic soils (Cruickshank,1972), the method of Farnham and Finney (1965) has been adopted throughout this study. Based on this classification, the peat of the valley floor is an oligotrophic mountain peat. Naturally occurring vegetation in the valley consists largely of heath plants (*Calluna* and *Erica* spp) and bog sedges (*Eriophorum* spp).

The main drainage systems within the valley are the Cronamuck River and Clogher Burn stream, both running in a northern direction along the valley floor and joining with the Owendoo River, flowing from the west, at the north eastern end of the valley (Fig.9.). Both the Owendoo and Cronamuck rivers are relatively wide (5 m) shallow, fast flowing rivers.

Clogher Burn is approximately 1 m wide, varying in depth (0.5 - 1.5 m) and flow along its length. Along the deeper sections, the stream appears almost stagnant, the flow becoming turbulent as the bed change from deep silt to rock. Precipitation within the valley is heavy, average annual rainfall being 1800 mm (Met Eireann, 1999). Where the waterways reach the lowest parts of the valley, flooding of the soils is present throughout much of the year. A number of small streams are also present within the valley, the majority of which flow into Clogher Burn at various points. Large amounts of rock outcrop are present within the valley, predominantly along the sides of the valley and lessening towards the valley floor.

3.2. Study Methodology

In order to fulfil some of the objectives of the study, a two stage approach was implemented. The initial stage, termed Survey 1, served to study the spatial distribution of the radionuclides within the valley. A series of samples of peat from within the valley were taken and analysed for uranium and thorium series radionuclides. The chosen radionuclides were ^{238}U, ^{226}Ra and ^{228}Ra. The samples were also analysed for ^{40}K. Other radionuclides such as ^{234}Th and ^{235}U were analysed for but only in so far as they were necessary for the determination of the primary four. ^{238}U and ^{226}Ra were selected as representative of the ^{238}U decay series, ^{228}Ra being chosen as an indicator for the ^{232}Th series. The behaviour of ^{235}U is unlikely to deviate significantly from that of ^{238}U.

Although radium behaves slightly differently to thorium, the adoption of ^{228}Ra as an indicator for the ^{232}Th series seems reasonable given the short half-life of ^{228}Ra relative to the time spans involved in pedogenic processes. In certain areas, behaviour of ^{230}Th was inferred from the behaviour of ^{228}Ra as the two isotopes of thorium (^{232}Th and ^{230}Th) do not behave differently in relation to their chemistries.

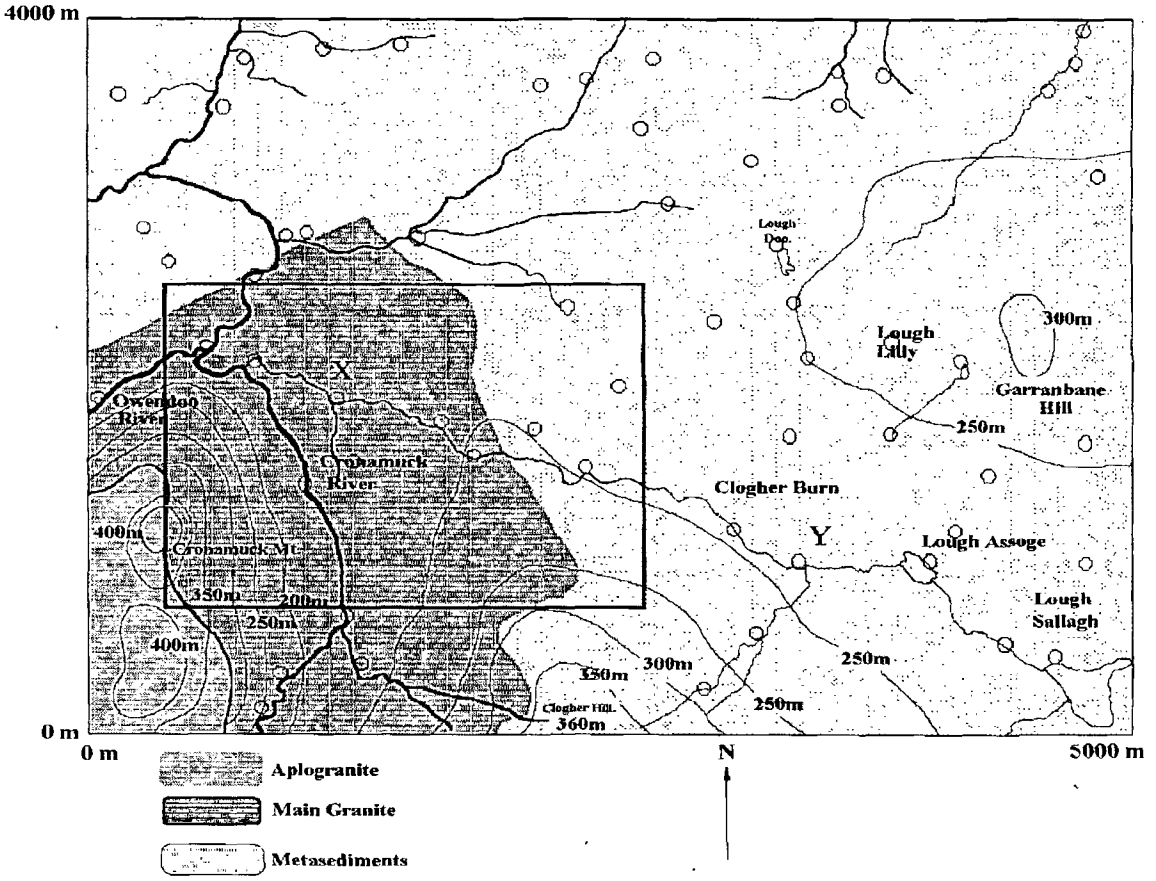

Figure 9. Map of the Cronamuck Valley, Co. Donegal. Open circles denote the sampling locations of Survey 1. Rectangle denotes location of Survey 2 but does not represent the actual size of the survey area. X and Y indicate locations of water saturated depressions at the confluences of Clogher Burn with two un-named streams.

The results from Survey 1 were analysed according to a geostatistical procedure. This method was adopted for a number of reasons. The size of the data set was limited by the relatively long analysis time required for samples containing low levels of radionuclides. The valley also remains inaccessible for much of the year, and given the logistics of moving large samples of peat from the area, an approach that would yield the maximum amount of information for a relatively small data set was needed. For the reasons outlined in Section 2.5, geostatistics were

deemed suitable for this study given the limitations detailed above. A statistical comparison was made between the geostatistical estimation procedure and a number of conventional estimation procedures in order to investigate the performance of the geostatistical analysis in describing the distribution of the radionuclides. Once isopleth maps of the radionuclide levels within the valley had been obtained, the second stage of the project was implemented.

The second stage of the project, termed Survey 2, was focused on areas of elevated radioactivity highlighted by the results of Survey 1. In order to ascertain the chemical form of radionuclides within these areas, and possible reasons for their enrichment, an in-depth analysis of a number of samples from within the chosen areas was carried out. The analytical sequence consisted of both chemical and radiochemical analyses, necessary to fulfil the objectives of the study.

A broad range of chemical parameters of the soil were analysed in order to determine possible reasons for, or controls of, the enrichment of radionuclides within these areas. Parameters were chosen on the basis of the findings of previous research cited in the literature, and included iron and manganese levels (total and soluble) within the soil, redox status of the soils, humic acid content, total organic content and cation exchange capacity. Many of these parameters have previously been identified, or proposed, as controlling factors on the accumulation and behaviour of natural radionuclides within soil.

All samples were analysed for total levels of the selected radionuclides, the levels of the radionuclides in various fractions of the peat being analysed using sequential chemical extraction with subsequent radiochemical analysis. The fractions of the peat chosen for study were exchangeable cations, easily oxidisable organic matter (which includes humic acids) and amorphous iron oxides, radionuclides found in these

fractions being deemed labile (capable of moving, or having moved in the past). The three fractions chosen represent the fractions most commonly reported in the literature as being responsible for the enrichment of radionuclides within peat.

A number of depth cores were taken from within the enriched areas in order to determine the vertical distribution of radionuclides and possible vertical movement of the radionuclides within the peat. The cores were differentiated according to depth as opposed to horizon, as horizon development within the peat was either poor or non ascertainable. The depth cores were analysed in the same manner as the discrete samples. Samples of vegetation and the underlying rock were also taken and analysed for radionuclide content.

The drainage systems around the areas of enrichment were sampled and analysed for a number of parameters. Chemical factors that either control radionuclide content in surface waters or that act as indicators of possible radionuclide content were analysed. These include the redox status of the water, total dissolved solids, metal content and radionuclide content. The purpose of this stage of the project was to determine whether or not waterborne radionuclides may be responsible for the elevated radionuclide levels in the region studied as part of Survey 2.

A number of activity ratios were also studied in both Surveys 1 and 2. The ratios $^{226}Ra/^{228}Ra$, $^{228}Ra/^{238}U$ and $^{226}Ra/^{238}U$ were chosen for a number of reasons. The study of the $^{226}Ra/^{238}U$ ratio allows for assessment of the state of secular disequilibrium in the ^{238}U series. Adopting ^{228}Ra as an indicator for ^{232}Th (and assuming ^{232}Th immobility) allows decisions to be made on whether variations in the $^{226}Ra/^{238}U$ ratio are due to either ^{238}U enhancement or depletion or ^{226}Ra enhancement or depletion.

3.3. Sampling Rationale

The sampling plans for the two surveys differed due to the different objectives of each survey. The plan for Survey 1 involved taking samples to describe spatial patterns within an area of 20 km^2. The second involved taking samples from an area of less than 2500 m^2 in order to describe chemical and radiochemical conditions. The sampling plan for Survey 1 involved the identification of 60 sites (Fig.9., co-ordinates provided in Table i, Appendix 1) within a 4 x 5 km rectangle encompassing the Cronamuck Valley. The bottom left hand corner of this rectangle was assigned the easting – northing co-ordinate of 0,0. These sites were chosen as being readily identifiable on a small scale (six inch) map using location markers such as stream confluences, etc. Circles with diameters of 300 m were inscribed around each site and a sample was selected from within the circle in the following manner. Two random numbers were generated on a calculator to describe a direction and distance from the circle centre from which the sample was being taken. The estimated error in the co-ordinates for any point was +/- 20 m in any direction. Sites that were flooded, hazardous or occurred over rock outcrop or water were reselected via a second set of random numbers. Although regular sampling grids are common in geostatistical surveys a grid system was not adopted for a number of reasons. The nature of the terrain in the valley meant that for any realistic grid of approximately 60 – 80 samples, up to 20% of the samples could not be taken from the points dictated by the grid due to their falling on rock outcrop or water. The exact location of points on a grid would also have required the use of a theodolite which proved extremely difficult from a logistical point of view.

Samples of soil were selected from the base of the peat bed for a number of reasons. Geostatistical analysis requires that all samples are taken from the same "support" or matrix in relation to a possible contaminant

source. This means that if studying, for example, the distribution of surface contamination from a stack, all samples must be taken from the surface or from an equal depth below the surface. To describe the spatial distribution of radionuclides in peat, the samples selected must only vary in relation to their position within the region and not in their relation to the contaminant source, in this case, the bedrock. Given the variable depth of the bog, this meant selecting all samples from just above the rock-soil interface. Furthermore, plants have been shown to enrich radium in the surface layers of soil (Greeman and Rose, 1990), therefore samples of soils from the surface may not always be representative of the soil column or of conditions pertaining throughout the peat. Establishing the 'surface' of the peat in the region also proved difficult due to the varying depth of the organic mat lying on the top of the peat in the region.

A region of elevated radioactivity (location X, Fig.9.) was selected for the location of Survey 2, based on the results of Survey 1. The sampling plan for Survey 2 differed in that more detailed information was required from the samples taken. Two sites were selected at random within the region (Fig.10.). Pits were excavated to the underlying rock and samples taken at incremental depths of 15 cm from the walls of the pits. A number of other sampling sites were selected within the region and samples were taken from the soil-rock interface. Two further pits were excavated at sites calculated to be outside the elevated region and sections were taken in the same manner as before. Samples of rock were taken from the base of a number of pits, this being achieved by removing the first inch of rock with a geological hammer and then taking a sample from the fresh material underneath. The first centimetre was removed as in all cases it was heavily weathered and cracked and may not have been representative of the rock itself.

Water from the drainage system of the valley was sampled at random along lengths of the rivers and streams that constitute the drainage system of the chosen region. Samples were selected from both upstream and downstream of the enriched area, and also from a river (the Owendoo river) well removed from the area. Figure 11. indicates the locations from which samples of river and stream water were taken.

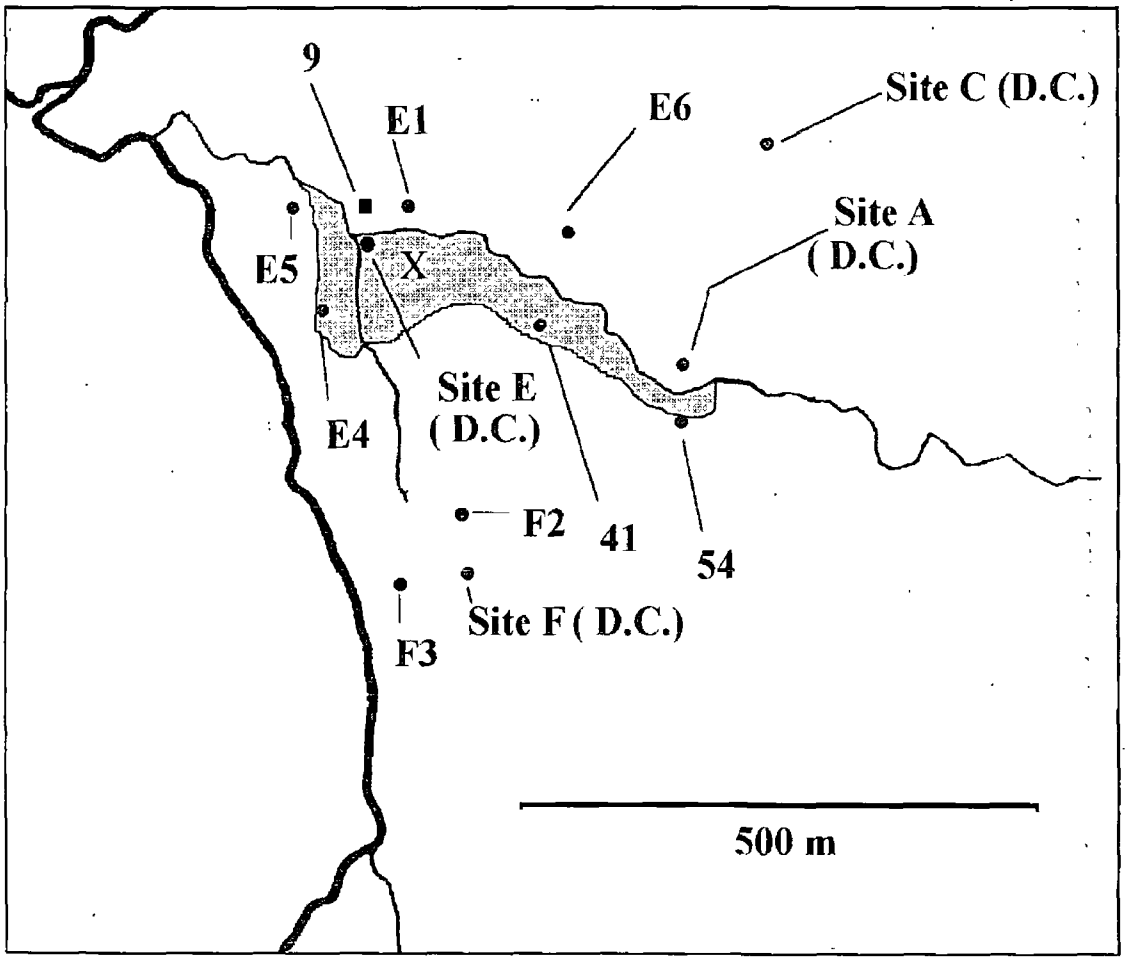

Figure 10. Location of sampling points of Survey 2. D.C. denotes depth sections, shaded area denotes water saturated depression at location X. Sample locations 9, 41 and 54 were drawn from Survey 1 but included in Survey 2 due to their location.

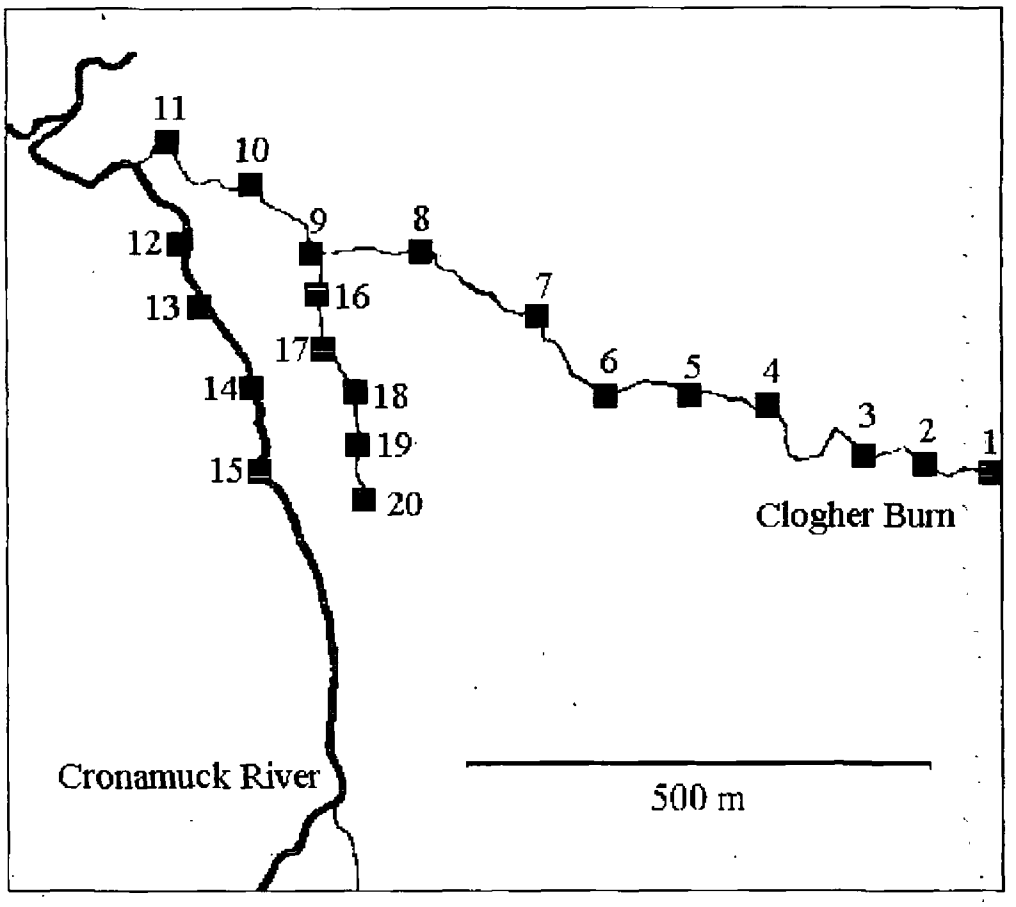

Figure 11. Location of surface water sampling sites.

3.4. Sample Preparation

3.4.1. Soil

Soil samples consisted of 10–15 kg of wet peat. Large stones and twigs were removed before placing the samples in polyethylene bags. The inclusion of fresh vegetation in the samples was avoided where practicable. The bags were partially evacuated and sealed to reduce loss of moisture before being transported to the laboratory. Once in the laboratory, the samples were placed on aluminium foil covered trays, weighed, and transferred to a fan assisted oven. The gross samples were dried at 110^0 C for 48 hours. Once dried to constant mass, the samples were reweighed to establish moisture content. Where possible, soils were

dissaggregated with a rubber stopper before being sieved through a 2 mm stainless steel mesh. In some cases the dried peat formed hard nuggets which were resistant to dissaggregation. These were ground using a stainless steel food blender before sieving. The powdered dried soil was then packed into 1l Marinelli re-entrant beakers for gamma analysis.

The samples of Survey 2 were treated slightly differently from those of Survey 1 in that once the radiometric analysis was complete, the contents of the Marinelli beakers were riffled and a portion of approximately 150 g was removed. This portion was ground to a fine powder in a steel mill grinder, riffled again, and 100 g of this material was taken for the sequential chemical extractions. A further 10 g of this material was used in the chemical analyses.

3.4.2. Rock

Rock samples consisted of 3–4 kg of rock in each case. The rock was washed in distilled water and scrubbed with a plastic brush to remove any adhering detritus. The samples were then crushed to less than 2 mm using a stainless steel hammer and thick polyethylene sheeting. Crushed samples were then packed in Marinelli beakers for gamma analysis.

3.4.3. Water

Water samples were collected in acid washed (10% AnalaR HNO_3 for three days) 1 l plastic bottles. Each bottle was rinsed with the river water before the bottle was filled. On return to the laboratory, the samples were filtered (0.45 μm) and split into two portions. The first was acidified with concentrated HNO_3 and stored, the second was left unacidified and stored.

3.4.4. Vegetation

Samples of vegetation were washed in distilled water and then placed on 2 mm wire mesh. Distilled water was then sprayed over the sample for a period of 2 hours in order to remove adhering soil particles. The samples were then placed on aluminium foil trays and dried at 101^0C for 48 hours. Once dried, the vegetation was then ground to less than 2 mm using a stainless steel food blender.

3.5. Analytical Methods

3.5.1. Radiometric Analysis

The primary radioanalytical technique employed throughout the project was high resolution gamma ray spectrometry. The system employed consisted of a high purity germanium detector coupled with an 8 K multi- channel analyser. The analysis package consisted of the GENIE–PC software suite.

3.5.1.1. Detector Calibration

Given the fact that a broad range of sample matrices were to be analysed throughout the course of the project, the detection system was calibrated for a number of different sample matrix densities in order to eliminate the possibility of self absorption errors between samples and standards. This was achieved using the methods outlined by Nemeth and Parsa (1992). A range of artificial calibration sample matrices were created from varying proportions of sawdust and sand, the range of densities being from 0.5 g/cm^3 to 1.2 g/cm^3. The components of the calibration samples were chosen to reflect the organic and inorganic constituents of the samples likely to be analysed through the course of the project.

The calibration solution consisted of a traceable mixed radionuclide standard solution obtained from the French Commissariat A L'Energie Atomique (Ref. No. ELMA60-9MLO1, Appendix 4). The solution contained known activities of 10 radionuclides emitting gamma radiation in the energy range 59.5 keV to 1836.0 keV. This solution was diluted to 1:100 using new, calibrated, Grade A volumetric glassware, the diluent being 1M HCl (AnalaR grade with ultra pure water). Each ml of the dilution contained a total activity of 8.91 kBq +/- 4%.

Three 1 l volumes of each density matrix were prepared. 100 g of the material was removed from each 1 l volume and placed in an acid washed porcelain crucible. 1 ml of the standard dilution was added to each 100 g portion using a calibrated pipette. The crucibles and contents were then dried at 90^0C for 6 hours. The contents of the crucibles were then homogenised by grinding of the contents (within the crucibles) with a pestle. The contents of the crucibles were then returned to their respective 1 l volumes, each volume being homogenised using a 2 mm aperture sieve. The matrices were then packed into 1 l Marinelli re-entrant beakers. All practicable precautions were taken to avoid loss of material in the preparation and packing of the standards and cross contamination of standard matrices.

Each standard matrix was counted for a period long enough to ensure that the total count in the smallest peak was greater than 10,000 counts after background correction (negligible in all cases). The average efficiency of the three standards at each density was taken as the counting efficiency. In no case did the S.D. of the efficiency for the three standards for each density vary by more than 5% (1σ). The procedure was also repeated for an aqueous matrix to allow for analysis of liquids.

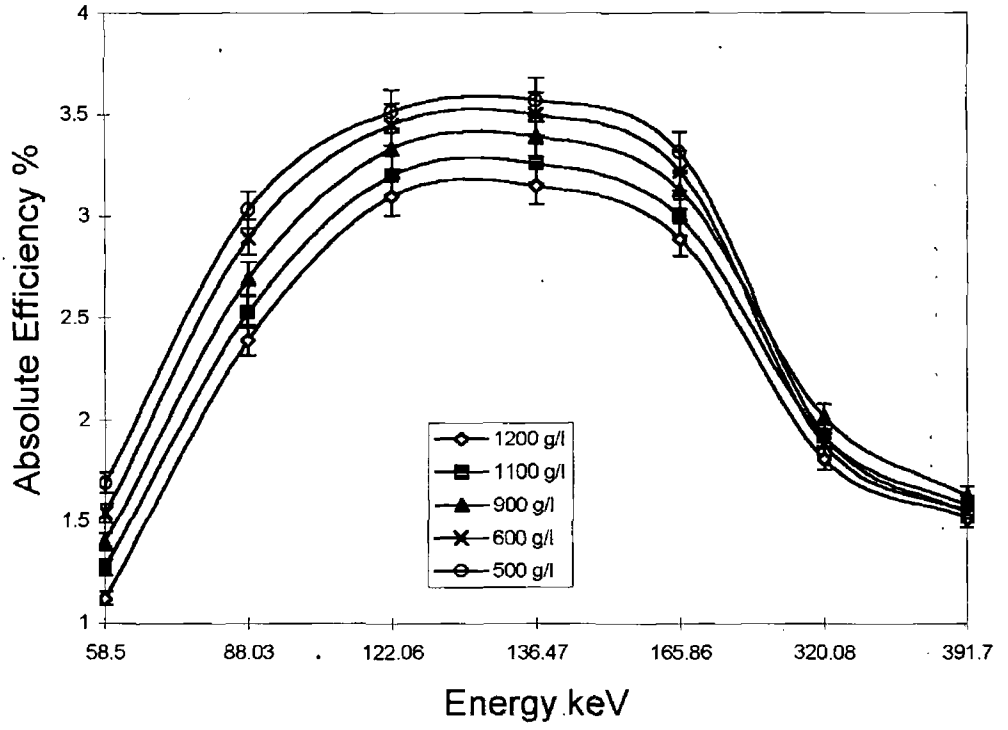

Figure 12. Variation in counting efficiency (%) as a function of energy (keV) for a number of matrix densities.

Efficiency and energy calibrations were checked via analysis of IAEA Reference Material 152 (contaminated milk powder, Appendix 4.) and periodically throughout the course of the project using aliquots of ^{226}Ra standard solution R9/50/151 (Appendix 4.) which had been hermetically sealed for 60 days to allow for radon ingrowth to occur. Results were typically within 5% of the certified value. Results of the calibration procedure for a number of different matrix densities are detailed in Fig.12 as a plot of detector efficiency (%) against energy over the range 58 keV to 391 keV. The effect of matrix density on efficiency is greatest at gamma energies of less than approximately 300 keV, variations in efficiency due to varying matrix density diminishing at energies higher than 300 keV.

3.5.1.2. Isotope Analysis

Analysis of the radionuclides of the uranium and thorium series was achieved via the emissions of a number of the daughters of the progenitors of both series.

3.5.1.2.1. ^{238}U Analysis

Quantification of ^{238}U is complicated by the fact that ^{238}U itself has only a weak emission at 49.5 keV (< 0.07% emission probability). The direct determination of ^{238}U in environmental samples is therefore impracticable by gamma ray spectrometry. A number of daughter nuclides however have sufficiently strong gamma emissions which may be utilised to determine ^{238}U activity, these being ^{226}Ra, ^{234}Th and ^{234m}Pa. ^{235}U, whose isotopic abundance is constant in the vast majority of environmental samples, may also be used to infer ^{238}U activities. There are problems associated with each daughter however, which further complicates the procedure. The emissions of ^{235}U and ^{226}Ra at 185.7 keV and 186.1 keV respectively cannot be resolved by conventional gamma ray spectrometers. In samples of high activity (ca. 1000 Bq/kg), the ^{235}U contribution to the joint peak at 186 keV may be assessed via it's emissions at 163 keV and 205 keV. This is not practicable with the activities exhibited by the majority of environmental samples. The ^{226}Ra contribution may be determined by hermetically sealing the sample container for a period sufficient to ensure secular equilibrium between ^{226}Ra and its daughters, ^{214}Pb and ^{214}Bi (> 30 days) and utilising their strong gamma emissions.

Alternatively, the immediate ^{238}U daughter, ^{234}Th, may be used via it's emissions at 63 keV and the doublet peak at 92 keV. ^{234}Th, with a half life of less than 30 days, is generally accepted to be in secular

equilibrium with it's parent, ^{238}U, in soil samples (Miller and Loosemore, 1971). Problems arise due to the fact that samples which contain high levels of thorium may produce thorium (K) X-rays in the 92 keV region and that the 63 keV peak also includes contributions from ^{231}Th (emission probability 0.023%) and ^{232}Th (emission probability < 0.255%). Given that ^{235}U (of which ^{231}Th is a daughter) levels in environmental samples are usually low and the low emission probability, the ^{231}Th contribution at 63 keV may safely be ignored.

The use of the ^{234m} Pa peak at 1001 keV has received some attention as a means of quantifying ^{238}U. Sutton *et al* (1993) could not find equilibrium between Pa^{234m} and ^{238}U in silt samples. Their work identifies inconsistencies between data published (at the time of their paper's publication) on the emission probabilities of this isotope and conclude that its emission probability is closer to 0.91% as opposed to the previously accepted value of approx. 0.589%. A more recent piece of work by Yucel *et al* (1998) investigated the use of this peak and concluded that it provides quantitative measures of ^{238}U activities for count periods of less than 14 hours. The quoted probability in this case was 0.835%.

The procedure adopted in this project was to quantify the ^{238}U activity of the samples via the ^{234}Th emissions. This was decided on for a number of reasons. Given the controversy surrounding the 1001 keV peak of ^{234m} Pa, the fact that ^{235}U activities in the samples were relatively low (indicating a low ^{231}Th contribution at 63 keV), logistical problems surrounding sample storage (to allow radon equilibration) and the low thorium levels in the samples, the ^{234}Th method was deemed most suitable. The method was tested for a number of samples (phosphate fertilisers and a uraniferous soil from Finland) displaying moderate to high ^{238}U and ^{232}Th activities and assured $^{234}Th/^{238}U$ equilibrium. ^{235}U activities in these samples were sufficient to allow for quantification via

the 205 keV peak. In all cases the activity of ^{238}U determined via the ^{234}Th peaks agreed (within counting error) with the activity of ^{238}U determined via the ^{235}U peak (utilising a $^{238}U/^{235}U$ activity ratio of 21.4).

3.5.1.2.2. ^{226}Ra Analysis

Once the ^{238}U activity of the sample had been determined, the ^{235}U activity was determined using the activity ratio given above. The ^{235}U contribution to the 186 keV peak was determined using the following relationship:

$$^{235}U \text{ Counts} = (A^{235}U)\, C_T\, R_U\, Eff_{186}\, W$$

where $A^{235}U$ is the activity of ^{235}U (Bq), C_T is the count time in seconds, R_U is the emission probability of ^{235}U at 185.7 keV and W is the sample mass in kg. The ^{235}U contribution was then subtracted from the peak area and the ^{226}Ra activity was determined.

In the case of the liquid samples from the sequential chemical extraction procedure, a different procedure was used. Samples were sealed in the Marinelli beakers for in excess of 40 days to allow for radon equilibration. The ^{226}Ra activity was then determined via the emissions of ^{214}Pb and ^{214}Bi at 352 keV and 609 keV respectively. In a manner similar to the ^{226}Ra determination in solid samples, the ^{235}U activity was determined, and hence, the ^{238}U activity.

The ability of the sealed Marinelli beakers to retain radon gas was assessed using a traceable ^{226}Ra standard solution (Radioactive Reference Solution No. R9/50/151 from Amersham Intl. Plc., Appendix 4.). An aliquot of this solution containing 9 Bq of ^{226}Ra was placed in 600 ml of the extraction solution, this being repeated three times for

each of the three extracting agents (9 solutions in all). The solutions were de-gassed using an ultrasonic bath for 1 hr and then made up to 1 l with ultrapure water before sealing in the Marinelli beakers. The beakers were sealed with thick PVC electrical insulation tape.

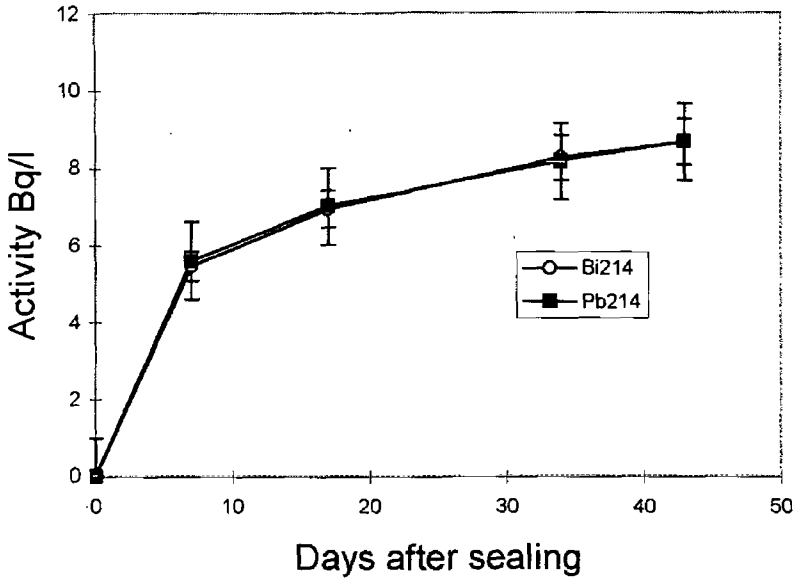

Figure 13. Plot of ^{214}Pb and ^{214}Bi activity (Bq) against time.

The activity of ^{214}Pb and ^{214}Bi was measured at various times over a 40 day period, the average activity of the three standards for each extraction solution being plotted against time to investigate if secular equilibrium was attained. As can be seen from Fig.13, radioactive equilibrium (90%) was achieved under the conditions employed in a period less than 40 days.

3.5.1.2.3. ^{232}Th Analysis

^{232}Th does not possess a gamma emission allowing for direct determination by gamma ray spectrometry. The most common means of

assessing ^{232}Th levels in samples is via one of its daughter nuclides. The nuclides most commonly reported for this purpose in the literature are ^{212}Pb at 239 keV (Zikovsky and Blagoeva, 1994), ^{208}Tl at 583 keV and 2615 keV (Baeza *et al*, 1994) and ^{228}Ac at 911 keV, 968 keV (Malanca *et al*, 1996). ^{228}Ac is always in secular equilibrium with it's parent ^{228}Ra (due to the ^{228}Ac half-life of 6.13 hours) and, given the ^{228}Ra half-life of 6.7 yrs and its relative immobility in the surficial environment, it seems reasonable to assume equilibrium between ^{232}Th and ^{228}Ac. Throughout this project, ^{232}Th activities were assessed using the ^{228}Ac peaks at 911 keV and 968 keV. The ^{212}Pb peak was deemed unsuitable due to the interference from ^{214}Pb and the ^{208}Tl peak at 2615 keV was unobservable for technical reasons.

3.5.1.2.4. ^{40}K Analysis

Measurement of this radionuclide by gamma ray spectrometry is relatively straightforward given that ^{40}K possesses a strong, well separated peak, at 1460 keV, by which it was determined.

3.5.1.3. Nuclear Data

The nuclear data used throughout this study (emission probabilities, half lives, gamma energies) was taken from a number of sources, tabulated in Table II.

3.5.1.4. Counting

Samples were counted for a period sufficient to ensure a 2σ counting error of less than 10% (15% for ^{226}Ra) after correction for laboratory background. Typical count times varied from 1 day to 1 week. Nuclides were identified using a library driven search routine. Once the spectra

had been obtained, the appropriate detector calibration (based on matrix density and constitution) was used for quantitative analysis. Repeated (6 times) analyses of one sample yielded a repeatability of better than 9%.

Nuclide	Energy (keV)	Intensity (%)	Source Reference.	Half-life
^{234}Th	63.2	4.80	Adsley *et al*, 1998	24.10 days
	92.3/92.8(D)	5.58		
^{235}U	185.7	57.20	Ruellan *et al*,1996	7.038E+8 yrs
	205.3	5.01		
^{226}Ra	186.2	3.59	Karmalitsyn *et al*, 1996	1600 yrs
^{214}Pb	241.9	7.43	Shizuma *et al*, 1992	26.8 m
	295.2	19.30		
	351.9	37.60		
^{214}Bi	609.3	46.10	Shizuma *et al*, 1992	19.9 m
^{228}Ac	911.2	25.80		6.15 hrs
	968.9	15.80	Arpesella *et al*, 1996	
^{40}K	1460.8	11.00	El-Daoushy and Garcia-Tenorio,	1.277E+9 yrs
^{137}Cs	661.6	85.10	1995.	30.07 yrs
			Arpesella *et al*, 1996	

Table II. Selected gamma ray emissions (keV), emission intensities (%), latest reference sources and half-lives of studied radionuclides. m = minutes, hrs = hours and yrs = years.

3.5.1.5. In-situ Gamma Measurements

A number of measurements of gamma radiation levels in the field were taken as part of Survey 2. These measurements were made using a 3x3 inch NaI scintillation crystal connected to an ELECTRA ratemeter from NE Technologies Ltd.

3.5.1.5.1. Detector Calibration

The ELECTRA is a single channel ratemeter employed typically as a contamination meter which provides no information as to the gamma energy range being detected. As the instrument was required to delineate localised differences in gamma flux due to uranium series radionuclides, it was therefore necessary to establish some means of preventing radiation from other radionuclides, primarily the higher energy ^{40}K and ^{208}Tl emissions, from being detected. This was achieved via manipulation of the applied detector voltage (HV) and the upper level discriminator (ULD) in the following manner.

Two sources, ^{40}K and ^{60}Co, were suspended over the detector crystal at a distance of approximately 100 mm. The HV value was noted and the ULD was reduced to its lowest value and the count rate recorded. Counts were allowed to accumulate until approximately 10,000 had been recorded to reduce the statistical error to an acceptable level. The ULD was then increased by 0.1 V and the count rate noted again. This procedure was repeated until the maximum ULD (3.0 V) was reached. The 1st differential of the count rate was then plotted against the ULD to obtain a gamma spectrum (Fig.14a.). The ULD value corresponding to each of the three photopeaks was then recorded. This entire procedure was repeated for a variety of HV settings. The variation in the ULD setting required to "record" events from the two radionuclides as a function of applied HV is shown in Fig.14b.

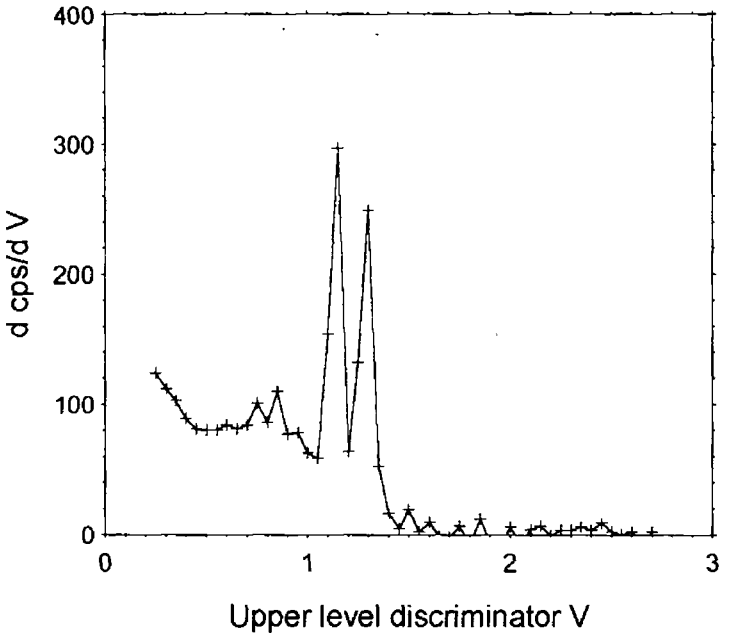

Figure 14a. ^{60}Co spectrum obtained using procedure outlined in Section 3.5.4.1

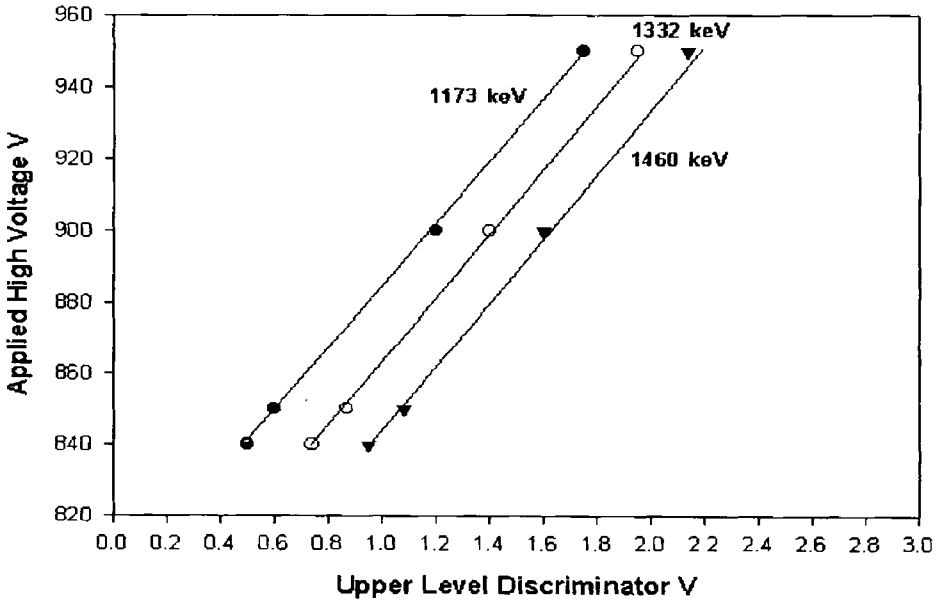

Figure 14b. Plot of applied high voltage against upper level discriminator (ULD) obtained during energy calibration of the ELECTRA ratemeter.

Using the information contained in Fig.14b. allowed settings to be made to both parameters that prevented the ratemeter recording counts at energies higher or lower than the energy bracket of interest. In this case, the energy bracket was between 100 keV and 700 keV which encompasses the strong emissions of ^{235}U and the majority of ^{238}U daughters while avoiding interference from K^{40} (but not ^{40}K Compton events). As no attempt was being made to quantify radionuclide levels using the instrument, it was not calibrated for such measurements.

3.5.1.5.2. Field Measurements

The detector housing was mounted within a polypropylene frame such that the detector face was elevated 15 cm from the ground. This distance was chosen as the gamma energies being measured were of relatively low energy and would therefore undergo significant attenuation over greater distances, even in air. A secondary reason was that local readings were required, the reading obtained being intended to represent a region of less than 10 m in diameter. Given the undulating topography of the area, it was considered possible that, at a higher elevation, the detector may have picked up on lateral emissions coming from hillocks etc. adjacent to the area where the reading was being taken from. Count times were typically 15-20 minutes long resulting in total counts of between 5000 and 10,000.

3.5.2. Chemical Analysis

3.5.2.1. pH

The pH value of the soil was measured in situ. A small depression was made in the peat and allowed to fill slightly with soil water. A calibrated portable pH electrode and temperature probe were then inserted into the hole and left to equilibrate for 600 s before the reading was taken. In very dry samples, some distilled water was added to the hole to improve

electrical conductivity. For water samples, the probe and temperature probe were left to equilibrate for a period of 60 s before being read.

3.5.2.2. Eh

Eh measurements, related to the redox potential of the soil, were also made in situ. A hole was made in the peat and a portable redox probe was then inserted into the hole. The probe was left for 600 s to equilibrate before reading. For water samples, the probe was left to equilibrate for 180 s before the reading was recorded.

3.5.2.3. Moisture Content

On receipt into the laboratory, the weighed sample of soil (approx. 10 – 15 kg) was dried at 110^0C for 48 hrs or to constant mass. When cool, the sample was reweighed, loss in mass being the moisture content.

3.5.2.4. Organic Matter

Organic matter was determined via loss on ignition for 4 hrs. A known mass of powdered soil (approx. 5 g) was placed in a fired (900^0 C for 12 hrs), pre-weighed crucible and heated at 500^0 C for 4 hrs. The crucible was then cooled in a dessicator and weighed. The loss of mass on ignition was taken as the amount of organic matter present in the sample,

3.5.2.5. Cation Exchange Capacity

Cation exchange capacity was measured using an adaptation of the sodium saturation method (Chapman, 1965). 4.0 – 6.0 g of dried powdered soil were placed in a round bottomed polyethylene centrifuge tube. 33 ml of a 1.0 N NaOAc solution (pH 7.5) were added and shaken

on a rotary shaker for 5 min to remove adsorbed cations. The suspension was then centrifuged at 10 k rpm for 10 min, the supernatant being discarded. This procedure was performed three times. Three 33 ml aliquots of propan-2-ol were then used to rinse the soil, following the same centrifuge procedure as before. Finally, three 33 ml aliquots of 1.0 M NH_3OAc were used to desorb the adsorbed sodium. The supernatants in this final stage were filtered through a 0.45μm filter before being combined and made up to 100 ml in a volumetric flask. The sodium content of the supernatant was determined using flame photometry. The amount of sodium adsorbed per gram of peat was then used to determine the cation exchange capacity of the samples in meq/100 g.

In order to estimate the reproducibility of the procedure, one homogenised sample of soil was subdivided into three portions, each portion being analysed as above. The standard deviation of the results was less than 10%.

3.5.2.6. Humic Acid Content

The humic acid content of the samples was determined via extraction with 0.5 M NaOH (Stevenson, 1965). An accurately weighed amount (1.0–2.0 g) of dried powdered soil was placed in a 50 ml polyethylene centrifuge tube to which was added 40 ml of 0.5 M NaOH solution. The suspension was shaken for 1 hr before being centrifuged at 10 k rpm for 10 min. The supernatant was discarded and the solid material was resuspended in fresh 0.5 M NaOH before being shaken for 1 hr and centrifuged as before. This process was repeated until the supernatant ran clear four successive times. The solid material was then resuspended in distilled water and centrifuged as above. The solids were then transferred to a fired, preweighed crucible and dried at 110^0C for 24 hrs. Once dry, the samples were weighed, the humic acid content being the loss in sample mass, expressed as percent (w/w). The procedure was

repeated on three replicate samples, reproducibility being better than 12%. Subtraction of the humic acid percentage from the total organic matter percentage provided a value for the non-humic content of the samples.

3.5.2.7. Total Iron, Manganese, Calcium and Potassium

Weighed amounts of dried, powdered sample (approx. 1 g) were leached with 5 ml of 3:1 $HCl:HNO_3$ for 1 hr at 90^0C before being filtered through a glass fibre pre-filter, then through a 0.45 μm filter. The leachates were transferred to 100 ml volumetric flasks and made up to volume with distilled water. The iron, manganese and calcium contents of the leachates were measured using atomic absorption spectrometry, potassium being measured by flame photometry.

3.5.2.8. Soluble Iron, Manganese, Calcium and Potassium Content

A known amount of dried powdered soil (approx. 10 g) was placed in a beaker with 50 ml of distilled water and shaken for 1 hr. The suspension was then filtered through a glass fibre pre-filter before being filtered through a 0.45 μm filter. The solutions were then added to 100 ml volumetric flasks and brought up to volume with distilled water.

3.5.3. Sequential Extractions

The chemical reagents used to extract the various fractions of the peat were those adopted by Greeman (1990), the solid/liquid ratios being those of Bunzl *et al* (1995). These methods offer a number of advantages over those such as Rose *et al* (1977) by using reagents that are more specific than those of earlier workers. Hence, $MgCl_2$ replaces NH_4OAc for the extraction of exchangeable cations, and NaOCl replaces the more

aggressive hydrogen peroxide for the extraction of easily oxidisable organic matter. No distinction was made between manganese and iron oxides in the selection of sodium dithionite as the extracting agent. All reagents were adjusted to pH 5 +/- 0.5 as this approximates the actual pH of the soil samples.

3.5.3.1. Sequential Chemical Extractions - Methods

The following procedures were used for the sequential chemical extractions of the soil. All practicable means were taken to ensure that no cross contamination occurred between samples and that no sample was lost at any point in the procedure.

3.5.3.1.1. Exchangeable Cations

100g of powdered, dried soil was placed in an acid washed (10% HNO_3 for 4 days) 1 l polyethylene bottle. 600 ml of 1 M $MgCl_2$ was added and the bottle was shaken on a shaker table for 2 hrs, at room temperature, before being let stand for 30 min. The supernatant was filtered (Whatman No.6), the solids being washed with 300 ml of distilled water and refiltered. The washings were added to the initial filtrate and filtered through a 0.45 µm filter. The solution was stabilised with 1 ml of concentrated HNO_3 and made up to 1 l with extracting agent before being prepared for gamma analysis. The solid residue was then returned to the plastic bottle for the next extraction.

3.5.3.1.2. Easily Oxidisable Organic Matter

To the solid residue from the previous stage were added 600 ml of an aqueous 5% NaOCl solution. The bottle was shaken for 2 hrs then let stand for 30 minutes. It was necessary to periodically vent off gaseous chlorine produced in the reaction and no attempt was made to reduce the

significant amount of heat generated in the bottles by the oxidation of the organic matter. The supernatant was poured into 50 ml centrifuge tubes and centrifuged at 10 k rpm for 5 min. The supernatant liquid was stored, the solids being returned to the bottle and washed with 300 ml of distilled water. The solids were kept suspended and the mixture was then centrifuged again at 10 k rpm for 5 min. The supernatants were bulked, and brought to 1 l with extracting solution before being prepared for gamma analysis.

3.5.3.1.3. Extractable Iron (and Manganese) Oxides

The solid residue of the previous stage was mixed with 600 ml of extracting solution consisting of 50 g sodium dithionite per litre of a 0.3 M sodium citrate/0.2 M sodium bicarbonate buffer. The mixture was maintained at 80^0 C for 1 hour in a water bath. It was necessary to release hydrogen sulphide gas at various stages in the extraction. Once complete, the suspension was allowed stand for 30 min, the supernatant was centrifuged at 10 k rpm for 5 min, the solids being washed with 300 ml of distilled water before being centrifuged again. The supernatants were bulked, and filtered through a 0.45µm filter. The extracts were then brought to 1 l with extracting solution before being prepared for gamma analysis.

A blank was prepared for each extraction, consisting of the appropriate volume of extracting solution without any soil. The blanks were treated in exactly the same manner as the samples. Reproducibility was estimated by conducting the extractions on four aliquots of an homogenised soil sample. The RSD for each extraction over the four samples was better than 18%.

3.5.4. Chemical Analysis - Water

3.5.4.1. pH and Eh

Measurements of pH, Eh and conductivity were conducted in the field using calibrated portable probes, an equilibration time of greater than 60 s being allowed before a reading was taken.

3.5.4.2. Total Dissolved Solids

A 50 ml aliquot of filtered (0.45 µm) unacidified sample was placed in a weighed, acid washed and fired 100 ml porcelain evaporation dish. The sample was then placed on a steam bath until the liquid was completely evaporated and the dish was then dried at 80^0C. Upon cooling to room temperature in a dessicator the dish was reweighed and the dissolved solid load of the sample calculated. All samples were analysed in triplicate, the average of the three results being reported.

3.5.4.3. Metal Analysis

Analysis of the water samples for total iron and uranium was conducted by PlasmaTech Ltd, Business Innovation Centre, Ballinode, Sligo using Inductively Coupled Plasma Mass Spectrometry (Varian PlasmaQuad). Operational conditions were as follows:

Rf power: Forward - 1.4 kW
Reflected - 4 W
Gas control: Auxiliary - 0.55 l/min
Coolant - 12.75 l/min
Nebuliser - 0.911 l/min

Spray chamber: Double bypass, water cooled Scott-type

Ion sampling: Nickel 1.0 mm orifice sampling cone, nickel 0.75 mm orifice skimmer cone.

Vacuum conditions: Expansion - $2.7 . 10^{0}$ mbar, intermediate $-0x10^{-4}$ mbar, analyser - $3.7 . 10^{-6}$ mbar.

Sample flow: 1 ml/min.

Torch: Conventional ICP-AES.

Nebuliser: Meinhard.

The instrument was calibrated with NIST traceable reference standards and quality control was conducted using a traceable riverine water reference solution (SLRS-2, National Research Council Canada). Analysis of this solution under the analytical conditions employed for this project yielded results within 5% of the stated value with a precision of better than 10%.

3.6. Geostatistical Analysis

The data set from Survey 1 was entered into a matrix consisting of easting and northing co-ordinates (m), (Table i, Appendix 1) and activities of the samples for the radionuclides ^{238}U, ^{226}Ra, ^{228}Ra and ^{40}K.

3.6.1. Semi-Variogram Analysis

Semi-variogram analysis and theoretical model fitting was performed using Variowin Ver.2.2 (Pannatier, 1996) and GEO-EAS (Englund and Sparks, 1988), some analysis being conducted using GEOSTATISTICAL TOOLBOX (Froideuaux, 1990). Although the gross features of semi-variograms can be determined relatively easily, fine tuning of the range and sill parameters was conducted using a cross validation procedure in conjunction with simple point kriging. Cross validation involves the elimination of a known sample point from the matrix and the estimation

of that point using the kriging conditions and semi-variogram model chosen. The process is repeated until all samples have been estimated. The comparison of the estimates with the actual values allows assessment of the performance of the kriging procedure (and the semi-variogram parameters). Between 10 and 20 models were tried for each semi-variogram (omni- and directional), the models differing in range and sill value, the model producing the lowest average error and the smoothest error map being selected. An omni-directional semi-variogram was constructed for each radionuclide as well as four directional semi-variograms for each radionuclide to assess the degree of anisotropy present.

3.6.2. Kriging

Ordinary block kriging of the data was performed using GEO-EAS. Areas of 250 x 250 m were established, 16 estimated points lying in each block, resulting in a grid of 320 estimates. A search radius of 1200 m was implemented around each point to be estimated, a minimum of 3 known points being required in each search radius (maximum 14) before estimation would take place. The search conditions employed were based on the results of an extensive series of cross validation analyses. Once the kriging process was finished, the estimates were contoured using the GEO-EAS contouring sub-program. Where the natural logarithms of data were used in the kriging process, back transformation was achieved using the equations provided by Litaor (1995).

4.0. RESULTS and DISCUSSION

4.1. Spatial Distribution of Radionuclides

One of the primary objectives of the project was to establish how natural radionuclides were distributed within the soil of the Cronamuck Valley. This section discusses the results of Survey 1 which was conducted in order to ascertain how natural radionuclides are distributed within the valley via the implementation of a geostatistical procedure.

4.1.1. Survey 1: Preliminary Investigations

The data set from Survey 1 consisted of spatial co-ordinates and specific activities of ^{238}U, ^{226}Ra, ^{228}Ra and ^{40}K for 60 samples drawn from the survey region. Summary statistics for each of the radionuclides are presented in Table III, raw data being presented in Table i., Appendix 1. All of the radionuclides distributions are influenced by the presence of small numbers of samples exhibiting high levels of radionuclides causing the frequency distributions for the radionuclides to skew to the left (Fig.15a.). Only ^{40}K passes the Kolmogorov – Smirnov test for normality ($p = 0.574$), with ^{228}Ra passing the test ($p = 0.073$) only after removal of the largest three values from the data set, reflecting the underlying normal distribution of the ^{228}Ra data set. Construction of probability plots for the four radionuclides indicated lognormal distributions for ^{238}U, ^{226}Ra and ^{228}Ra (Fig.15b.). The probability plot for ^{40}K supported the normal distribution indicated by the initial statistical analysis of the data. If two or more distributions are identical then quantile-quantile plots of the distributions will produce a straight line (Srivastava and Isaaks, 1989). In order to investigate the relationship between the distributions of the three radionuclides, the data set for each radionuclide was ranked in ascending order and both ^{226}Ra and ^{228}Ra were plotted against ^{238}U (Fig.16.).

	^{238}U	^{226}Ra	^{228}Ra	^{40}K	$^{226}Ra/^{238}U$
N	60	60	60	60	60
Mean	79.3	104.7	35.8	526.4	1.70
Std. Dev.	149.9	125.5	25.1	278.1	1.02
Skew.	3.78	1.50	1.93	-0.06	0.85
Min.	2.7	4.0	3.0	8.0	0.47
25% tile	20.0	24.5	22.6	354.3	1.21
Median	29.5	47.7	30.5	551.3	1.47
75% tile	87.9	111.3	39.0	697.0	2.11
Max.	788.0	479.0	135.0	1088.0	5.54

Table III. Summary statistics of sample activities and $^{226}Ra/^{238}U$ activity ratios of samples taken in Survey 1. Activities in Bq/kg.

The ^{228}Ra and ^{238}U distributions remain relatively similar at the lower end of each distribution although the distribution of ^{226}Ra differs significantly from ^{238}U across the entire range of values. Significant differences between the ^{228}Ra and ^{238}U distributions are however obvious at the higher end. Such a plot for a normal distribution should yield a straight line and this fact serves to demonstrate that the deviation from normality in the ^{226}Ra and ^{228}Ra sets is primarily caused by the high values in the sets. As this project is concerned mainly with the three radionuclides ^{226}Ra, ^{228}Ra and ^{238}U, the degree of correlation between these radionuclides was tested using Spearmans rho correlation for non–normal distributions. Each of the radionuclides exhibited strong correlation with each other (Table IV.).

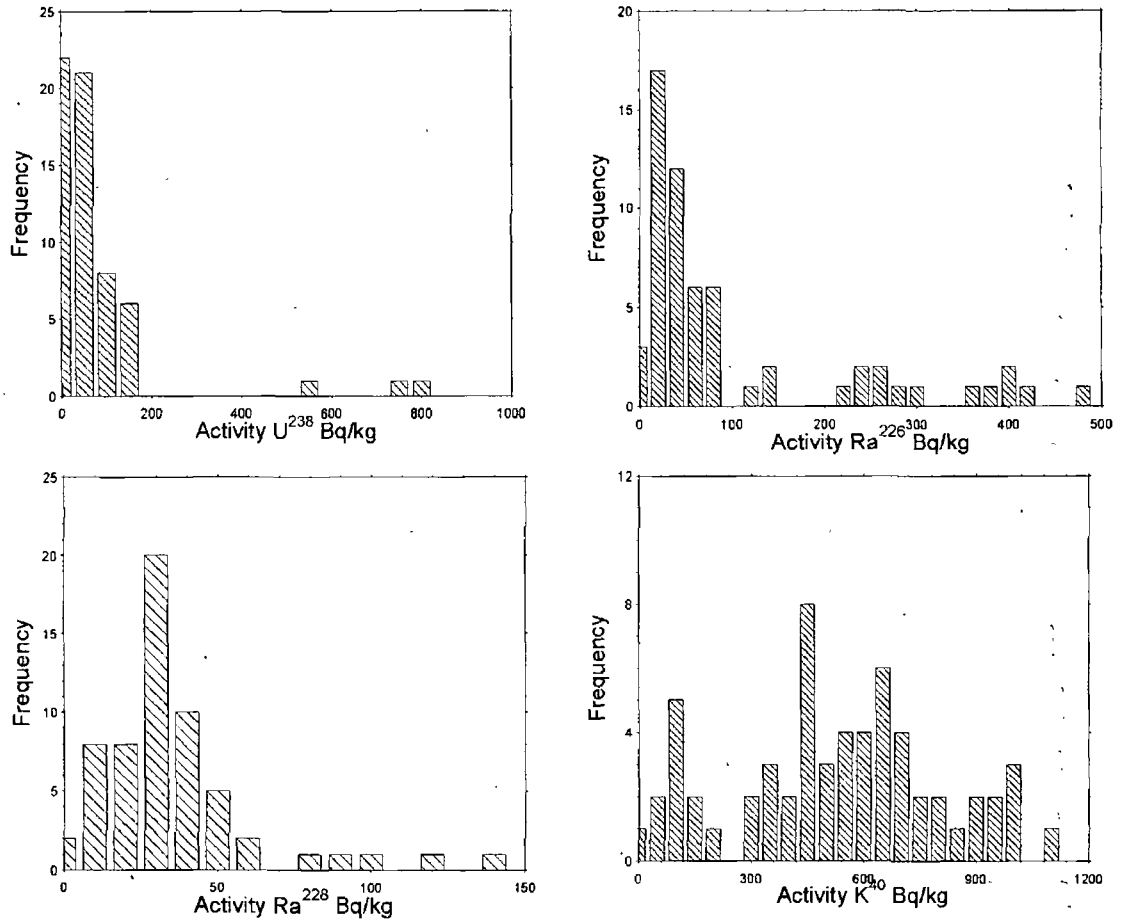

Figure 15a. Histograms of the distributions of ^{238}U, ^{226}Ra, ^{228}Ra and ^{40}K for the 60 samples of Survey 1.

To investigate whether the radionuclide content of samples extracted from the part of the valley underlain by the granite differed from the radionuclide content of samples drawn from the metasediment area of the valley, the Survey 1 data set was split into two groups, the groups being designated on-pluton and off-pluton for convenience. Summary statistics for the two groups are presented in Tables Va and Vb, raw data for both sets is presented in Table i, Appendix 1.

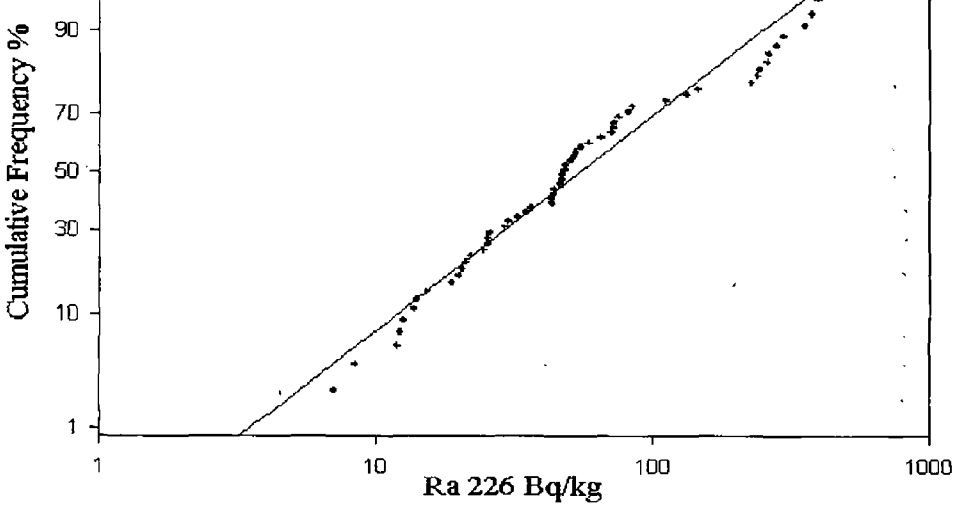

(i)

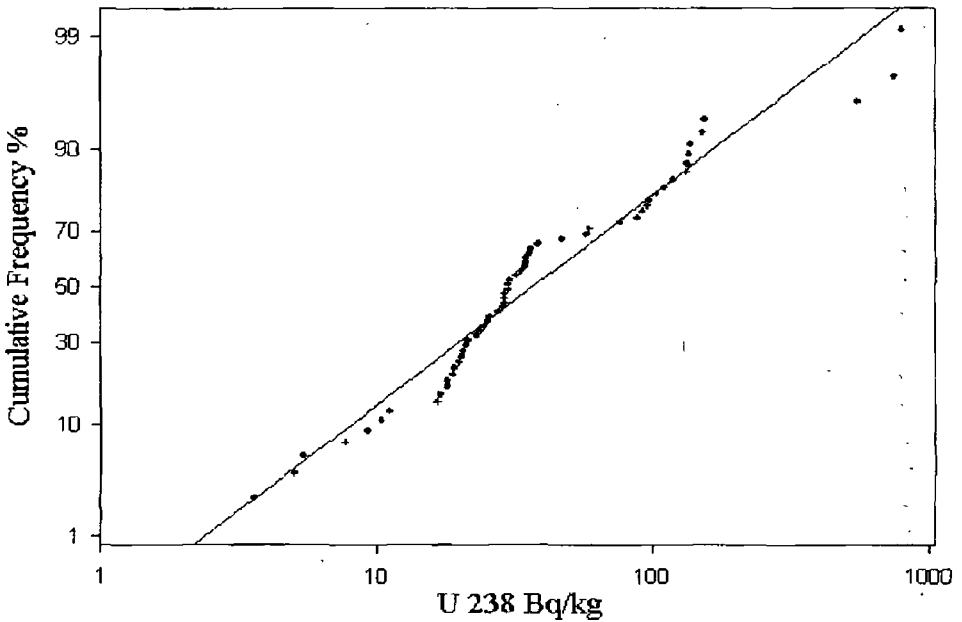
Cumulative Frequency %
99
90
70
50
30
10
1
1
10
100
1000
U 238 Bq/kg


99

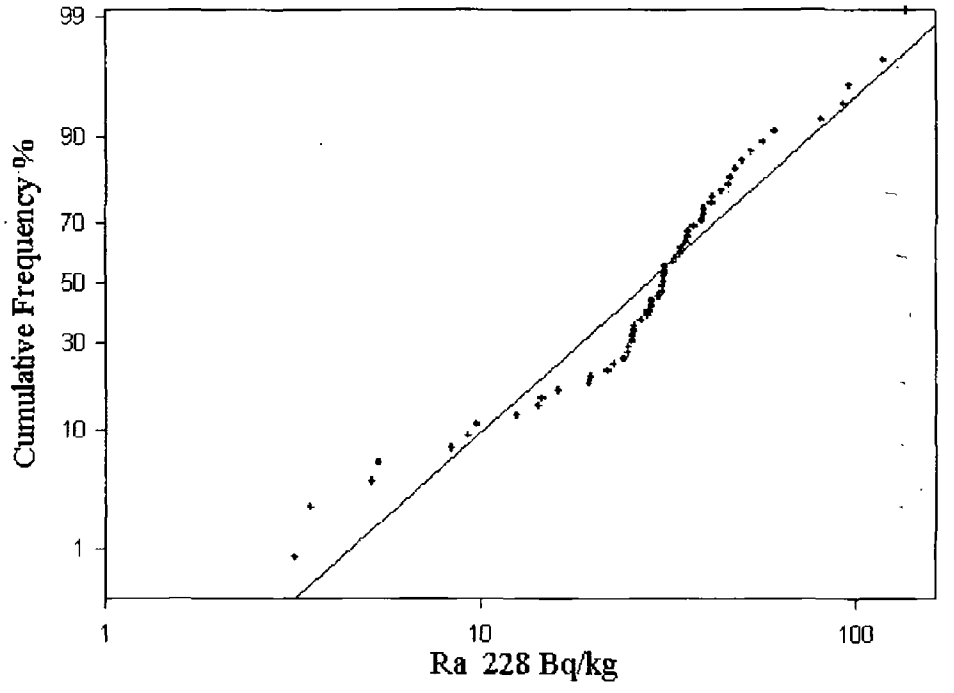

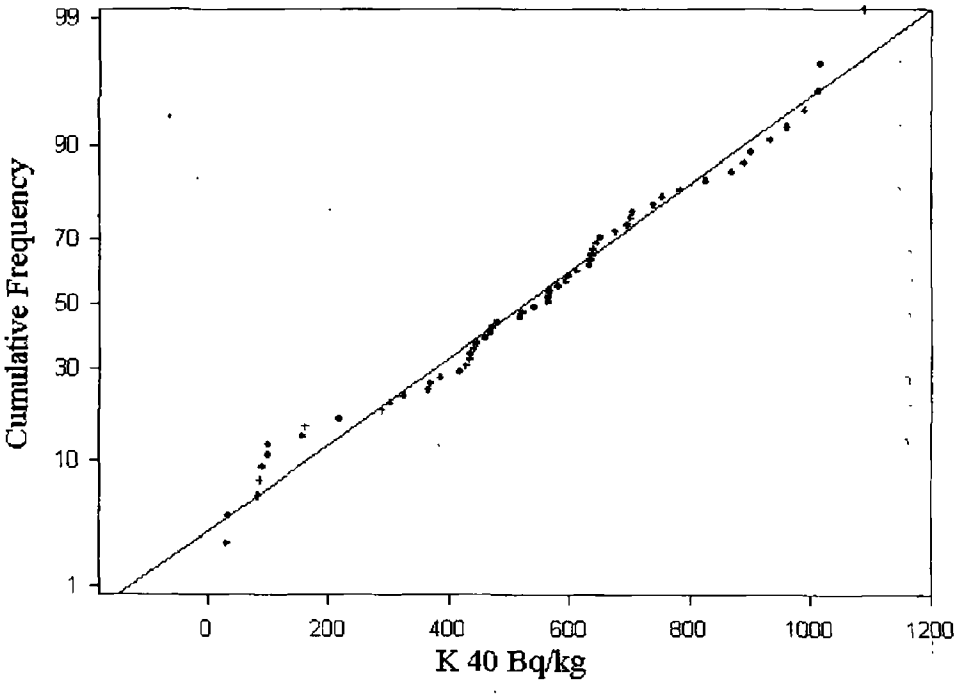

(ii)

Figure 15b. Probability plots of, (i) ^{238}U, ^{226}Ra and (ii). ^{228}Ra and ^{40}K. Note log scaling of x-axis for ^{238}U, ^{226}Ra and ^{228}Ra.

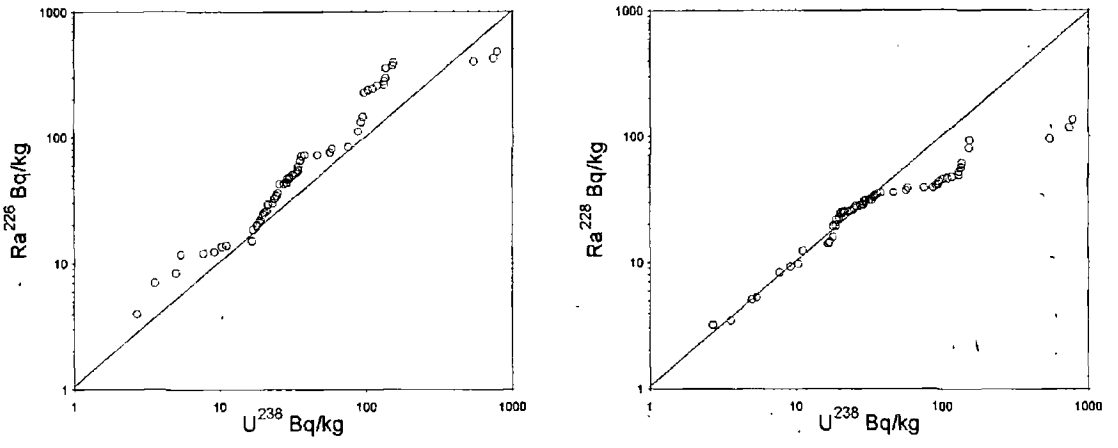

Figure 16. Plot of ^{226}Ra and ^{228}Ra against ^{238}U, all activities ranked in ascending order. Note logarithmic scaling. Values in Bq/kg.

		^{238}U	^{226}Ra	^{228}Ra
^{238}U	Correlation Coefficient	1.000	0.858*	0.804*
	Significance (2 tailed)	.	0.000	0.000
	N	60	60	60
^{226}Ra	Correlation Coefficient	0.858*	1.000	0.735*
	Significance (2 tailed)	0.000	.	0.000
	N	60	60	60
^{228}Ra	Correlation Coefficient	0.804*	0.735*	1.000
	Significance (2 tailed)	0.000	0.000	.
	N	60	60	60

Table IV. Correlation matrix for ^{238}U, ^{226}Ra and ^{228}Ra activities for the data set of Survey 1. * denotes significance at the 0.05 (2 tailed) level.

The average U^{238} value for the on-pluton set is 4.6 times the average for the off-pluton set, the magnitude being approximately the same for Ra^{226} (4.92). Average Ra^{228} levels for the on-pluton set are only greater than the off-pluton set by a factor of 1.37. Both minimum and maximum

values remain higher for the on-pluton set for ^{238}U, ^{226}Ra and ^{228}Ra while the maximum values for ^{40}K are comparable.

	^{238}U	^{226}Ra	^{228}Ra	^{40}K	$^{226}Ra/^{238}U$
N	14	14	14	14	14
Mean	199.7	268.8	44.42	704.2	2.1
Std. Dev.	234.6	124.9	24.5	267.9	1.1
Min.	33.0	48.5	22.6	162.0	0.5
Med.	125.3	260.0	37.8	788.4	2.1
Max.	788.1	479.0	117.3	1015.1	5.5

Table Va. Summary statistics for the on-pluton data set. Activities in Bq/kg.

	^{238}U	^{226}Ra	^{228}Ra	^{40}K	$^{226}Ra/^{238}U$
N	46	46	46	46	46
Mean	42.7	54.5	32.3	472.5	1.5
Std. Dev.	79.5	69.0	24.3	254.5	0.6
Min.	2.7	4.0	3.2	8.1	0.5
Med.	25.3	39.7	28.3	519.1	1.4
Max.	546.0	393.0	135.0	1088.1	3.4

Table Vb. Summary statistics for the off-pluton data set. Activities in Bq/kg.

The off-pluton set is affected strongly by a small number of elevated ^{238}U values, 95% of the data remaining below 58.7 Bq/kg, the maximum value being 546.0 Bq/kg. The same is also true for the ^{226}Ra data, the 95% tile being only 21% of the maximum value for the data set. The ^{226}Ra values for the on-pluton data exhibit this feature to a lesser extent as the maximum value is only 13% greater than the 95% tile value. The ^{238}U values for this data set (on-pluton) are affected by elevated levels,

80% of the samples containing less than 152 Bq/kg, the maximum value being 788 Bq/kg (5.18 times the 80% tile). ^{228}Ra statistics are similarly affected by a small number of elevated levels in both data sets. The maximum ^{228}Ra level is 3.27 times the 80% tile in the off-pluton set and 2.55 times the 80% tile for the on-pluton set. To test whether the two sets of data are significantly different with respect to radionuclide activities, a Mann-Whitney test for non-normal distributions was implemented. The results of this test indicate that a significant difference exists between the activities exhibited in peat samples taken from the granite region (on-pluton set) and those taken from the metasediment region (off-pluton set). ^{238}U ($p < 0.001$), ^{226}Ra ($p < 0.001$), ^{228}Ra ($p = 0.03$) and ^{40}K ($p = 0.01$) activities are all higher in samples drawn from the granite region. The ratio ^{226}Ra/^{238}U was not significantly different ($p = 0.063$).

Construction of scatterplots for the data sets (Figs. 17-20) allows preliminary investigation of how the radionuclides are distributed throughout the survey area. A cursory inspection indicates the clustered presence of elevated ^{238}U, ^{226}Ra and ^{228}Ra values in the south-western corner of the survey region which corresponds to soils underlain by the granite. The high values for the radionuclides in the non-granite region which heavily influenced the statistics for the off-pluton data set are visible in the south-eastern region of the valley. Also visible, beside the highest ^{238}U values, are a series of much lower values indicating a sharp decline in ^{238}U levels over a relatively small distance. The scatterplot for ^{40}K indicates a broader spread of values, high values occurring throughout the sampled region.

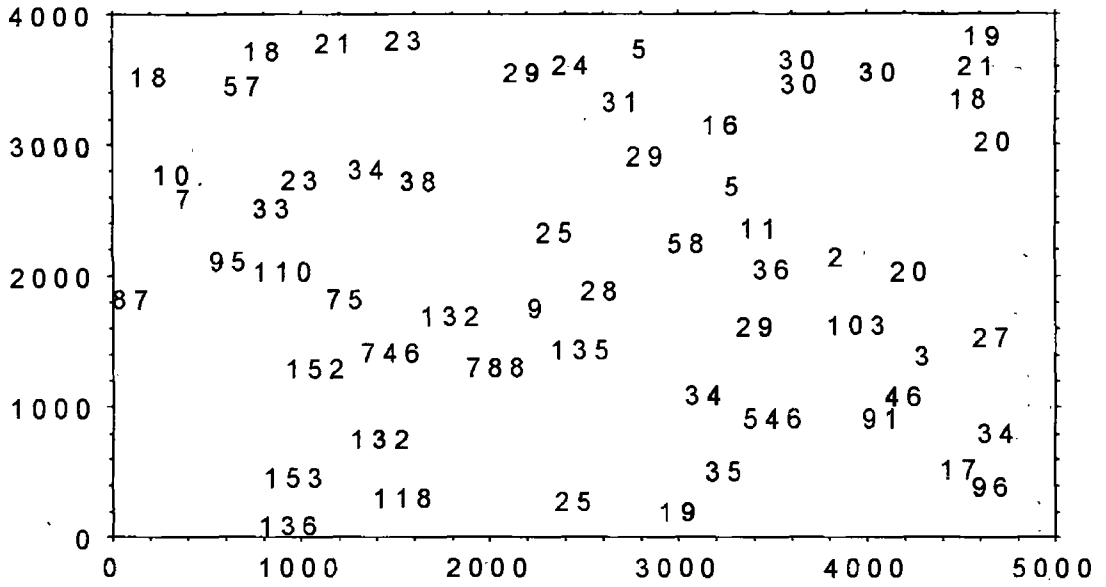

Figure 17. Scatterplot of ^{238}U values for the 60 samples of Survey 1. Values in Bq/kg. Axes units – m. Note that sample values have been rounded down to nearest whole number for clarity.

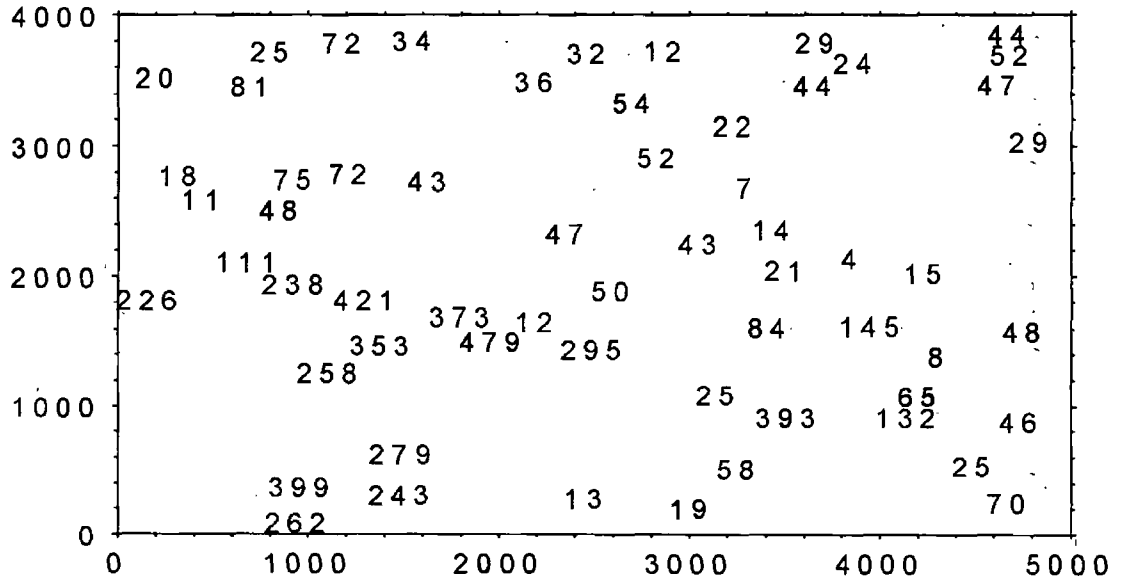

Figure 18. Scatterplot of ^{226}Ra values for the 60 samples of Survey 1. Values in Bq/kg. Axes units – m. Note that sample values have been rounded down to nearest whole number for clarity.

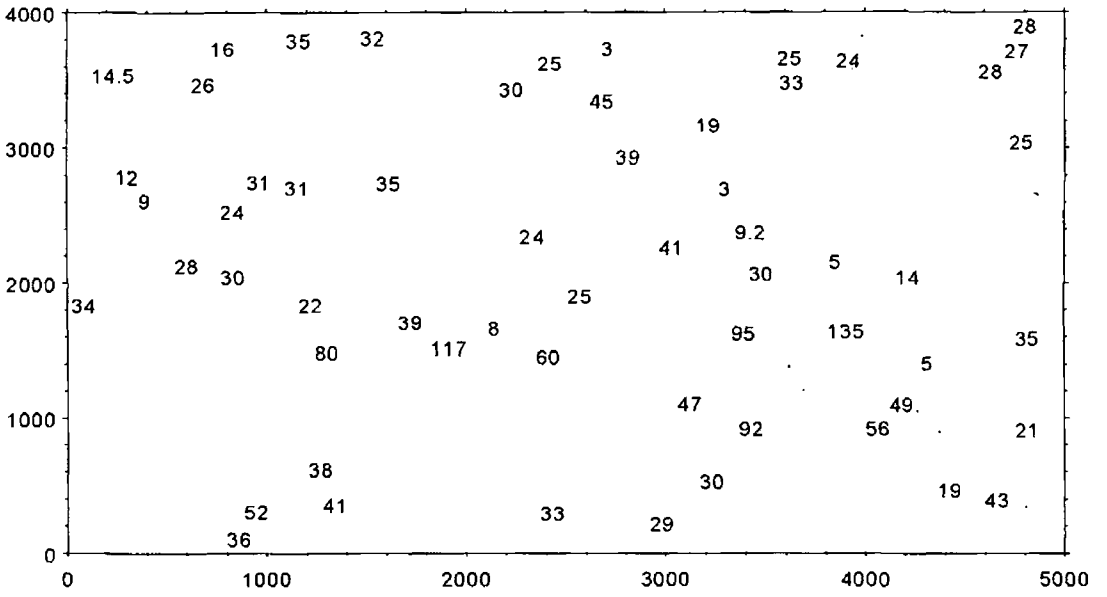

Figure 19. Scatterplot of ^{228}Ra values for the 60 samples of Survey 1. Values in Bq/kg. Axes units – m. Note that sample values have been rounded down to nearest whole number for clarity.

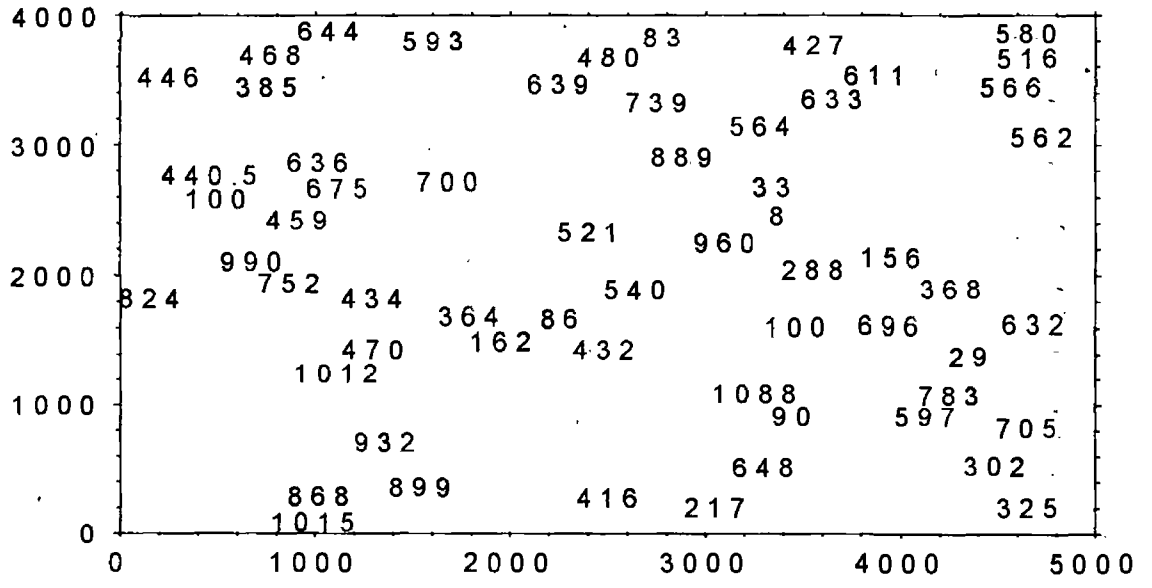

Figure 20. Scatterplot of ^{40}K values for the 60 samples of Survey 1. Values in Bq/kg. Axes units – m. Note that sample values have been rounded down to nearest whole number for clarity.

In order to investigate whether the average radionuclide levels and the variability between samples remains constant throughout the Survey 1 region, a technique based on the principle of 'moving windows' was used. Moving windows involves the setting up of smaller sub-regions throughout the greater survey area and determining summary statistics for the samples located within each sub-region. Analysis of the results of such an exercise allows determination of whether trends exist within the samples region in relation to variability between samples and average radionuclide levels. The existence of trend within a data set has important implications with respect to the Intrinsic Hypothesis as outlined in Section 2.2.

As the number of samples used in this study was relatively small, it was realised that large windows would be required thereby reducing the total number of windows obtained. It was therefore decided that overlapping windows would be used in order to provide a realistic number of windows, each containing approximately 10 individual samples. The window size chosen was 2000 m by 2000 m and this window was moved through the greater survey region as follows. The initial window was placed in the bottom left corner of the survey region (Window 1) and summary statistics for the samples contained within that window were calculated. The window was moved 500 m to the right (Window 2) and summary statistics were calculated. The window was then moved another 500 m to the right and so on until the right hand limit of the survey region was reached. It was then returned to the left hand side but to a position 500 m more northerly than Window 1. This process was repeated until all the area had been covered resulting in the production of summary statistics for a total of 35 windows. Once all the windows had been obtained, summary statistics for ^{238}U, ^{226}Ra, ^{228}Ra, ^{40}K and $^{226}Ra/^{238}U$ were calculated. Tabulated results are provided in Tables VIa through VId , raw data is presented as Table ii, Appendix 1.

29.76 29.7	36.06 27.03	28.22 13.58	25.42 14.49	24.09 14.41	23.28 15.51	18.82 10.90
128.93 213.17	134.17 222.29	124.10 224.97	88.25 203.85	29.44 26.67	30.98 28.57	27.20 28.62
128.93 213.17	134.24 211.95	222.68 554.84	97.21 202.93	39.08 39.08	31.46 27.33	29.10 28.57
257.78 288.92	218.35 275.18	222.55 291.76	143.85 240 78	79.37 150.91	71.01 134.55	75.75 144.49
252.37 272.59	217.08 261.35	196.93 271.43	162.12 259.05	96.59 162.92	86.89 155.28	76.15 144.28

Table VIa. Summary moving window statistics for ^{238}U. All values in Bq/kg. Upper figure denotes average value, lower figure denotes standard deviation.

53.44 67.24	61.85 61.19	42.14 15.47	31.80 15.14	29.21 15.81	25.96 16.27	25.62 16.45
187.51 169.40	186.64 174.41	166.16 179 55	92.63 144.22	42.41 38.61	41.73 42.05	38.97 44.22
187.51 169.40	195.67 169.49	188.62 178.73	110.50 153.03	61.65 79.96	41.20 40.01	39.75 43.60
304.29 112.90	260.65 150.44	256.85 165.82	145.84 171.29	87.33 123.77	72.35 98.53	78.82 104.62
329.44 87.27	282.47 145.45	233.18 168.46	164.05 181.23	109.80 131.87	91.64 109.42	82.03 102.83

Table VIb. Summary moving window statistics for ^{226}Ra. All values in Bq/kg. Upper figure denotes average value, lower figure denotes standard deviation.

22.95 9.83	27.27 6.20	30.21 10.88	25.35 12.92	23.43 12.76	21.95 13.80	19.69 10.88
34.85 28.04	35.90 28.82	39.45 27.95	37.36 31.86	36.32 38.02	37.98 41.09	37.34 43.29
34.85 28.04	37.94 28.38	41.71 28.60	41.14 31.99	40.38 38 24	38.48 38.55	39.12 42.02
48.51 30.70	45.07 30.87	46.26 32.33	47.76 34.13	39.16 30.12	43.74 37.61	46.99 39.28
50.83 27.79	48.00 28.27	45.14 29.23	52.55 34.51	55.67 39.77	53.20 39.11	47.08 38.97

Table VIc. Summary moving window statistics for ^{228}Ra. All values in Bq/kg. Upper figure denotes average value, lower figure denotes standard deviation.

517.01 183.60	564.47 113.09	614.37 238.90	491.79 306.98	461.91 294.53	435.08 313.40	368.08 238.89
566.96 295.93	549.68 298.82	572.99 306 63	417.93 31.23	421.36 328.80	418.69 336.70	340.96 260.32
566.96 295.93	539.92 286.71	307.69 1.95	441.10 358.91	446.32 372.95	457.10 390.01	380.40 366.67
660.28 309.22	559.92 320.50	495.72 291.42	407.03 340.64	410.18 355.85	443.85 345.60	416.95 343.55
698.30 309.06	591.22 334.41	497.45 303.09	377.04 304.30	431.73 325.13	463.04 339.17	461.88 339.70

Table VId. Summary moving window statistics for ^{40}K. All values in Bq/kg. Upper figure denotes average value, lower figure denotes standard deviation.

Examination of the results of the moving window analysis highlights the trend in the data that was initially suggested by the scatterplots of the data. Average ^{238}U, ^{226}Ra and ^{228}Ra values all increase steadily on

moving from the north-eastern corner of the survey region (underlain by metasediments) to the south-western corner (underlain by granite). The trend is not as visible for the ^{40}K values. While an analysis such as this does highlight trends within the greater survey region, the presence of elevated values in the centre of the region, as indicated by the scatterplots of the data, is not evident due to the smoothing effect of the averaging process. The highest standard deviations for both ^{238}U and ^{226}Ra occur in the central area of the survey region, this fact being indicative of the close juxtaposition of samples containing elevated radionuclide activities and samples containing much lower activities.

Standard deviations of the radionuclide levels for the samples contained within each window also increase in a similar manner to the average levels. This feature indicates a certain proportionality between the average radionuclide levels and the variability of the levels. In order to investigate this proportionality further, plots were constructed of the window average against the window standard deviation for each of the four radionuclides (Fig.21.-24). An analysis of such plots allows determination of the extent of this proportionality if it exists and provides further information on the nature of the distribution of the radionuclides.

The proportionality between the window radionuclide averages and standard deviations indicated by the moving window analysis is strongly upheld by the results of the average – standard deviation plots. The effect is strongest for ^{238}U and virtually non existent for ^{40}K. ^{226}Ra exhibits a strong but non linear relationship between the two parameters. Srivastava and Isaaks (1989) attribute a proportional effect to the data being log normally distributed which is indeed the fact in this case.

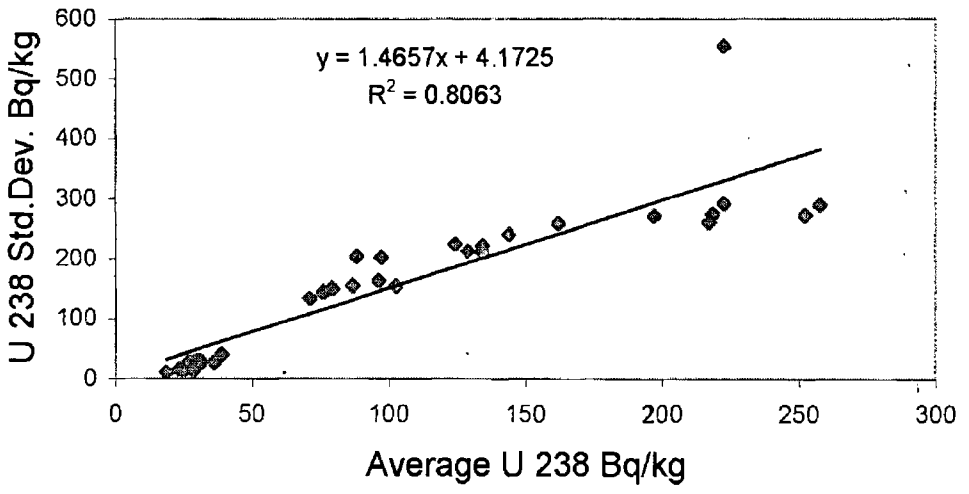

Figure 21. Plot of ^{238}U window average against ^{238}U window standard deviation. Units in Bq/kg.

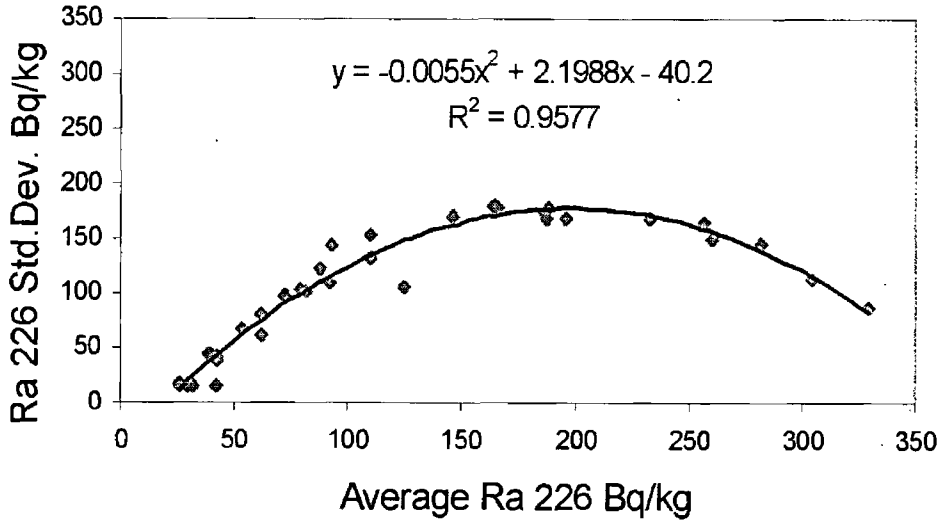

Figure 22. Plot of ^{226}Ra window average against ^{226}Ra window standard deviation. Units in Bq/kg.

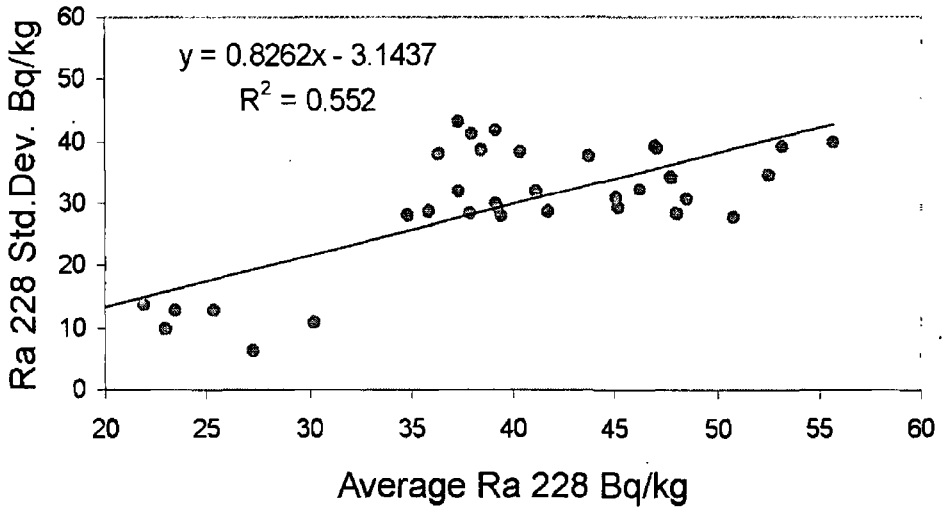

Figure 23. Plot of ^{228}Ra window average against ^{228}Ra window standard deviation. Units in Bq/kg.

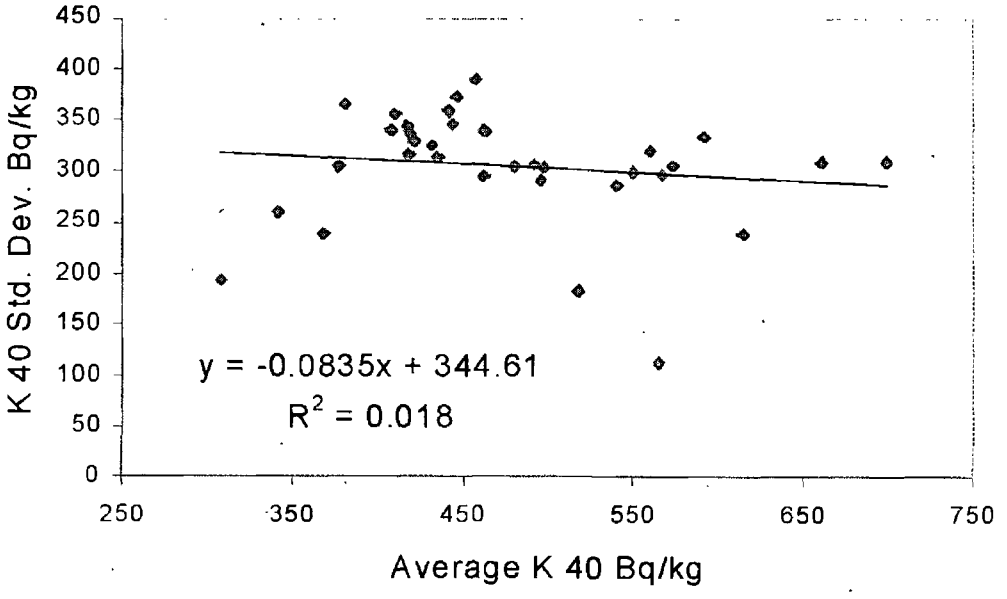

Figure 24. Plot of ^{40}K window average against ^{40}K window standard deviation. Units in Bq/kg.

4.1.1.1. Summary

The previous analysis of the Survey 1 data set serves a number of purposes. Knowledge of the features of the data set allows an assessment of what problems are likely to be encountered in further stages of the analysis and also predicts problems that may arise in the implementation of any point estimation process. Two features in particular are of concern, the presence of a trend for three of the radionuclides and the close juxtaposition of samples exhibiting contrasting levels. How, and to what extent, these features affect subsequent procedures implemented on the data set, in this case, geostatistical operations, cannot be predicted until at least the preliminary stages of such analyses have been carried out.

In relation to the distribution of the radionuclides within the valley, an initial examination of the data set indicates that a statistically significant difference exists between levels of the radionuclides (^{238}U, ^{226}Ra and ^{228}Ra in peat underlain by granite and that underlain by the metasediments. The average U^{238} level over the granite is 4.6 times the level over the metasediments, the values for ^{226}Ra being 4.9 and 1.37 for ^{228}Ra. The difference is also apparent in the scatterplots of the data, high values tending to cluster towards the south-western portion of the surveyed area. Examination of the off-pluton data sets indicates that transport of radionuclides off the pluton may be occurring, the data set being strongly effected by the presence of a small number of samples drawn from the metasediment area exhibiting high radionuclide levels.

4.1.2. Survey 1: Semi-variogram Analysis

The primary tool in any geostatistical study is analysis of the spatial continuity of the data using a semi-variogram. Such an analysis involves separating the data set into pairs of samples each separated by a certain distance or lag. Half the variance of the difference in the variable values exhibited by the pairs of samples separated by that lag is then plotted against the lag increment to form a raw semi-variogram. A model is then fitted to the raw semi-variogram in order to describe the spatial continuity over the whole survey region.

Two potential problems are indicated by the initial analysis of the Survey 1 data set. The first is the fact that the majority of the radionuclides approximate log normal distributions, the second being the trend in the data set for a number of the radionuclides, indicated by the moving window analysis. Some researchers (Rendu, 1979, Litaor, 1995) suggest that log normal distributions should be transformed to normal distributions before semi-variogram analysis, whilst this is refuted by others (Clarke, 1979) who indicate that the data should only be transformed if the log normal data set does not provide a smooth semi-variogram. The presence of a trend may also affect the semi-variogram by imposing a parabolic curve on the raw semi-variogram. The final computed omni-directional semi-variograms, with fitted models, are shown in Fig.'s 25 - 28, details of fitted models are displayed in Table VII. Depiction's of the directional semi-variograms may be found in Appendix 2.

The raw semi-variograms were constructed and theoretical models fitted using the Variowin (Pannatier, 1996) software package. Semi-variograms were only plotted up to a lag distance that corresponded to approximately half the maximum lag distance present in the data set.

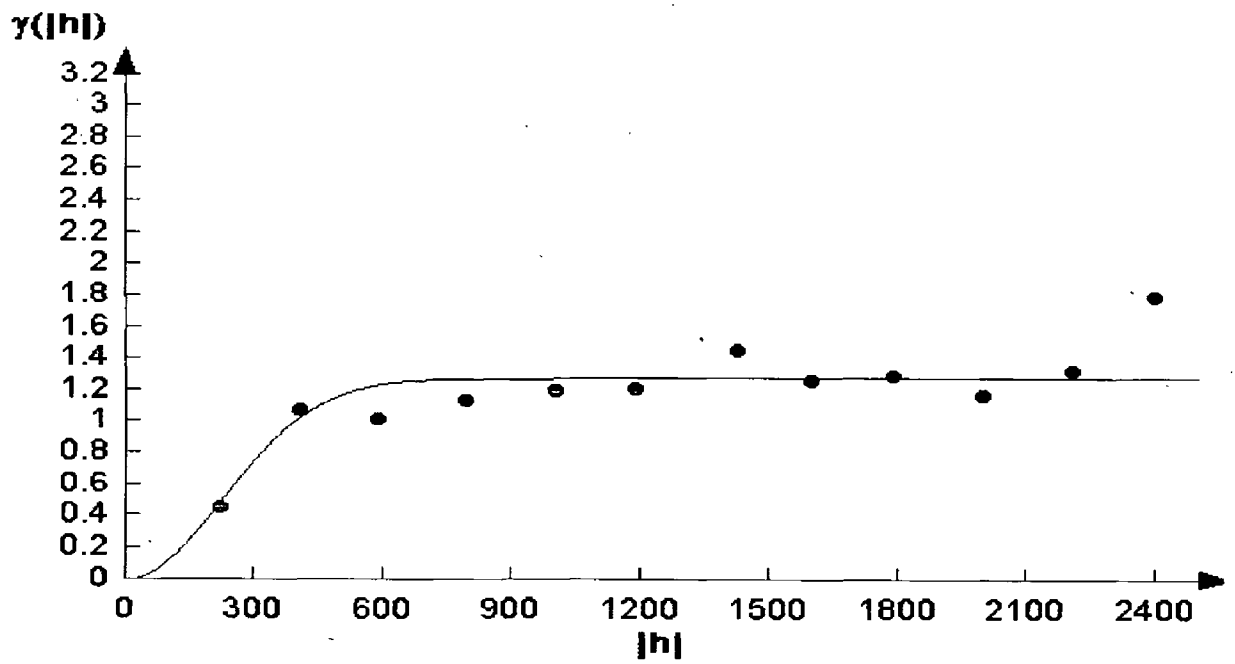

Figure 25. Omni-directional semi-variogram for ln ^{238}U. X axis units - m, y axis units - (ln Bq/kg)^2.

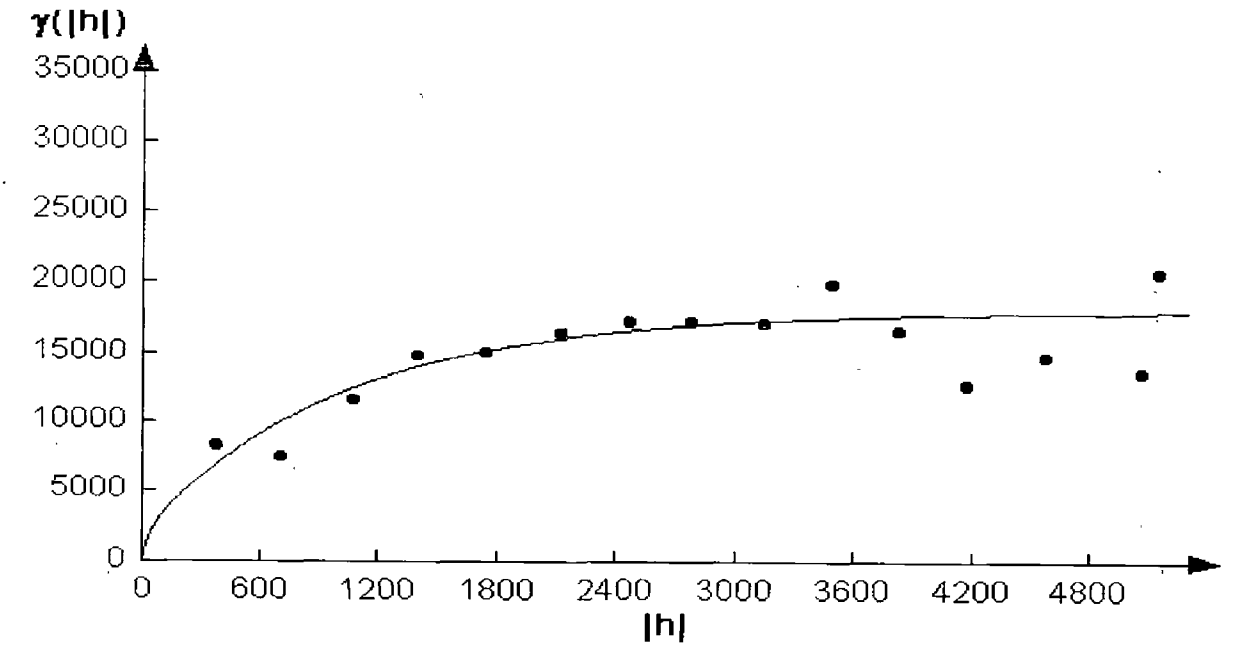

Figure 26. Omni-directional semi-variogram for ^{226}Ra. X axis units - m, y axis units - (Bq/kg)^2.

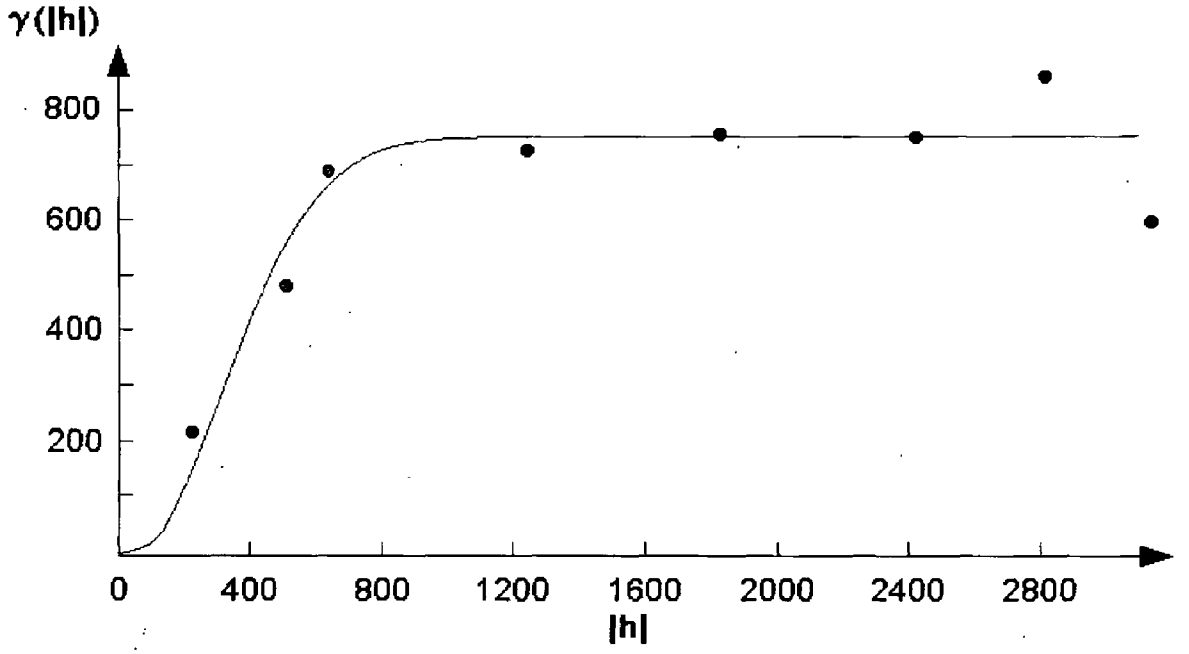

Figure 27. Omni-directional semi-variogram for ^{228}Ra. X axis units - m, y axis units - $(Bq/kg)^2$.

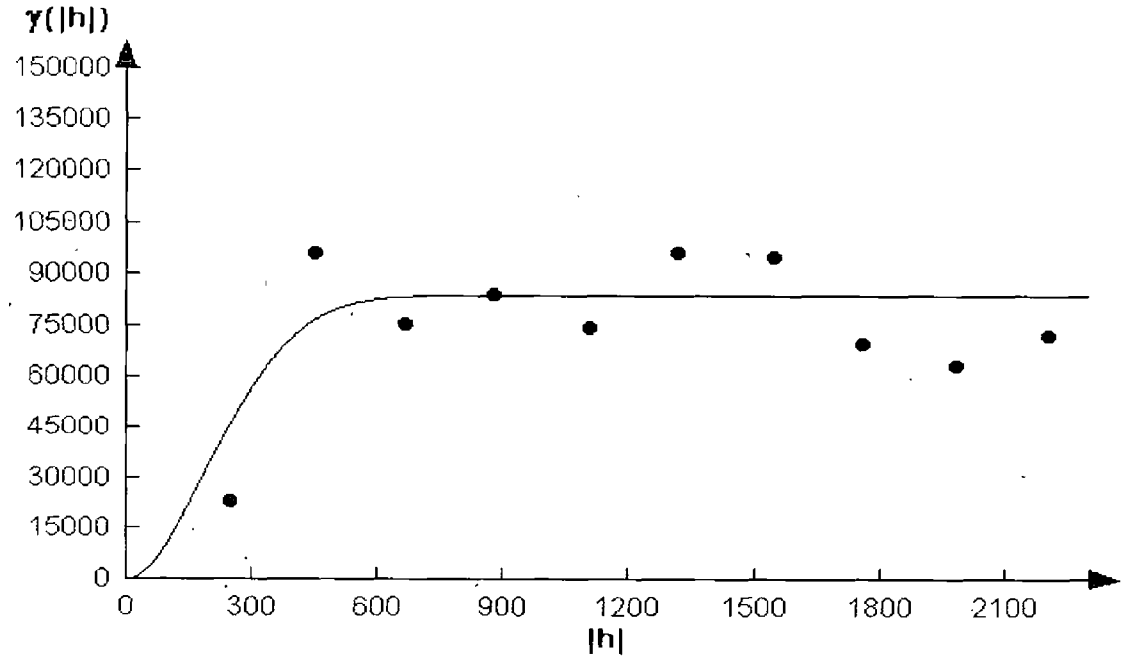

Figure 28. Omni-directional semi-variogram for ^{40}K . X axis units - m, y axis units - $(Bq/kg)^2$.

	ln ^{238}U	^{226}Ra	^{228}Ra	^{40}K
Model	Gaussian	Exponential	Gaussian	Gaussian
Sill Value	1.15	18000	750	83000
Nugget	0.0	0.0	0.0	0.0
Range m	600	3000	700	750
N – S m	650	3000	400	600
E – W m	700	3000	1000	1100

Table VII. Theoretical models fitted to semi-variograms of radionuclides of Survey 1.

This procedure was followed as the number of pairs contributing to the semi-variance decreased with increasing lag distance, resulting in reduced reliability at greater lag distances. In order to investigate the finer detail of the semi-variograms, h-scatterplots were employed to deduce which samples contributed most to the semi-variance at each lag distance and to locate any aberrant pairs that may have had an disproportionate effect on the semi-variance value for each lag. The technique of h-scatterplots involves the plotting of the value of a variable at location w_i against the value of the same variable at a location w_{i+h}, separated from w_I by the vector h. Such plots allow the investigation of which pairs of samples are contributing most to the semi-variance value exhibited in the semi-variogram for the lag distance that corresponds to h. All semi-variograms, both omni-directional and directional for all radionuclides, were analysed in this fashion to determine how representative the raw semi-variograms were of the spatial structure. Model fitting was accomplished using a least squares procedure. On average, ten possible models were calculated for each semi-variogram and each model was tested using a cross validation procedure that is described in detail in Section 3.5.1. A smooth semi-variogram could not be obtained for the un-transformed ^{238}U data set so

the variable was transformed using the natural logarithm of the data to produce a much smoother semi-variogram.

All the radionuclides exhibit strong spatial correlation, the range of correlation varying among the radionuclides. Over the distances for which the semi-variograms were plotted there is no evidence of trend except in the ^{238}U semi-variogram where the beginning of an ascension may be observed at the greater lag distances. This feature is only evident in the E-W and NE-SW directional semi-variograms for this radionuclide (Fig. i., Appendix 3.) highlighting the presence of the trend that was indicated for these directions in the moving window analysis. No evidence of the trend in the ^{226}Ra values is provided in the directional semi-variograms. Three of the four radionuclides, ^{238}U, ^{40}K and ^{228}Ra display geometric anisotropy in their spatial structures.

The features of the semi-variograms of most interest are the relatively long ranges of correlation and the lack of "nugget effect" or a random component to the spatial structure of the radionuclides. The significant variation in the range of correlation in the N-S and E-W directions for ^{40}K and ^{228}Ra is indicative of maximum spatial correlation in the direction with the longest range, in this case E-W. This seems surprising given that the orientation of the pluton relative to the survey area would suggest maximum continuity in the N-S direction. However in light of the fact that the initial statistical analysis suggests transport of radionuclides off the pluton, this may not be so depending on the direction and extent of the radionuclide movement. An inspection of the moving window data (Table VI) for ^{228}Ra seems to indicate a more gradual reduction in values on moving off the pluton in an E-W direction than in a N-W direction, especially in the southern part of the surveyed region.

4.1.2.1. Summary

The semi-variogram analysis of the radionuclides indicates a level of suitability in relation to geostatistical estimation procedures. All of the radionuclides exhibit a high degree of spatial correlation without nugget effect, the trend present in the data set not manifesting itself at lag distances less than the range of correlation. Although geometric anisotropy is present for some of the radionuclides, no zonal anisotropy was encountered. The length of the range of correlations for the radionuclides is significant as it allows for more accurate estimation of points. The range of correlation governs the magnitude of the search radius (the area around a point to be estimated within which points whose variable values are known must be located to be included in the estimation procedure) and therefore the number of sample points to be used in estimating the unknown point. The number of samples contributes to the accuracy, a larger number being preferable. The large search radius also allows a reduction in the number of points that are not provided with an estimate value as a result of not having any known sample points within the search radius. Although the effect of the trend in the data does not impinge on the semi-variogram structure until after the range of correlation (and is therefore unlikely to affect estimation), the problem of closely spaced samples of varying activity remains unaffected as a neighbouring sample will always exert more weight on a point to be estimated than a more distant sample, irrespective of the number of samples used in the estimation.

4.1.3. Estimation: Kriging

In order to obtain as accurate a picture as possible of the spatial distribution of the radionuclides within the valley and given the limited data set, the geostatistical estimation procedure known as kriging was implemented.

4.1.3.1. Cross Validation Analysis

Once semi-variograms had been constructed and theoretical models fitted to the data, the estimation process known as kriging was initiated. In order to optimise the estimation process, a cross-validation procedure was adopted. Cross-validation analysis involves the eliminating of single known data points from the data set and estimation of the variables value at the samples location. The data point is then replaced and the procedure is repeated until all sample locations have been estimated. Comparison of the true data set with that provided by the estimation process allows for the investigation of how the estimation procedure performs throughout the entire data set.

An initial exploration of how the process performed across the data set is provided via the use of bubble plots, the size of the bubbles providing an indication of the absolute error in the estimate at that data point (Fig. 29 - 32). For three of the four plots, ^{238}U, ^{228}Ra and ^{40}K, poor estimation performance is encountered along the contact of the pluton with the metasediments, indicated by the preponderance of the largest errors in this region. This poor performance is undoubtedly caused by the high variability in soil radionuclide activities, as indicated by the moving window statistics, over the contact of the two lithologies.

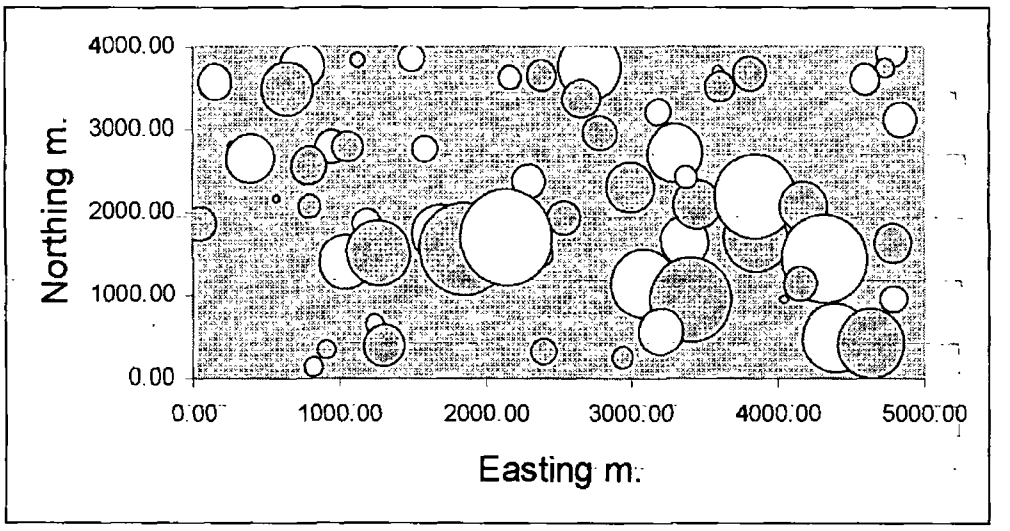

Figure 29. Bubble plot of the ^{238}U estimation error in the 60 samples of Survey 1 using a cross validation analysis of the kriging procedure. Dark circles denote over-estimation, light circles denote under-estimation.

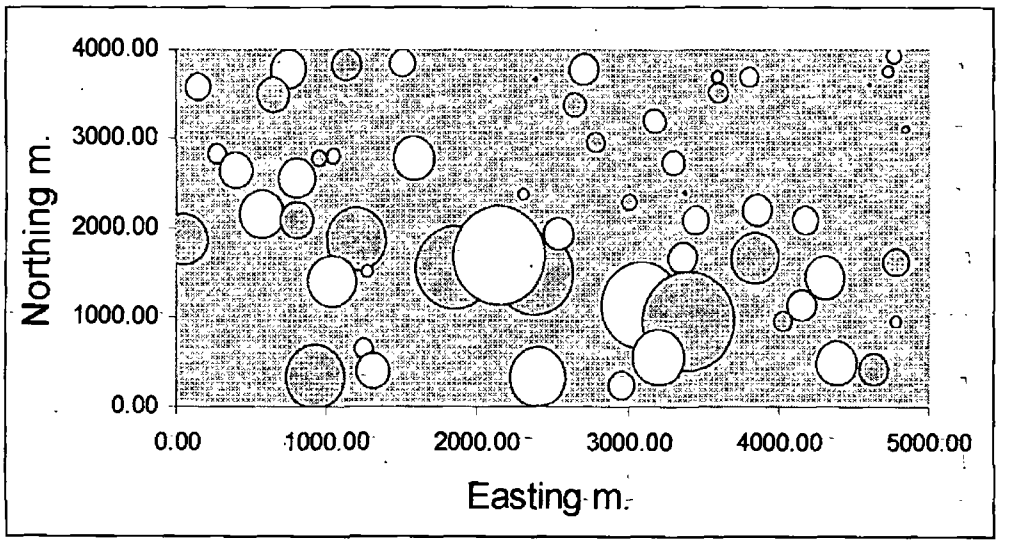

Figure 30. Bubble plot of the ^{226}Ra estimation error in the 60 samples of Survey 1 using a cross validation analysis of the kriging procedure. Dark circles denote over-estimation, light circles denote under-estimation.

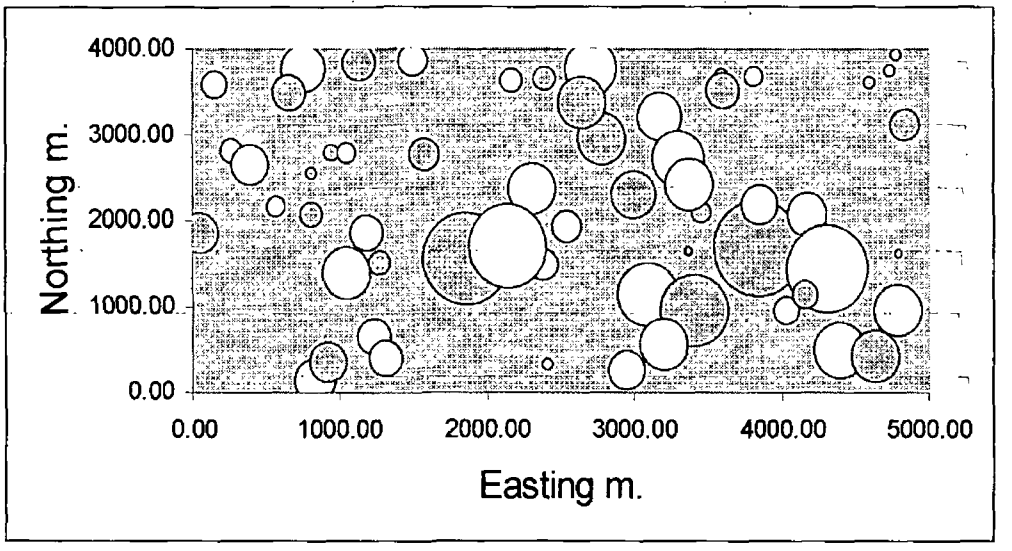

Figure 31. Bubble plot of the ^{228}Ra estimation error in the 60 samples of Survey 1 using a cross validation analysis of the kriging procedure. Dark circles denote over-estimation, light circles denote under-estimation.

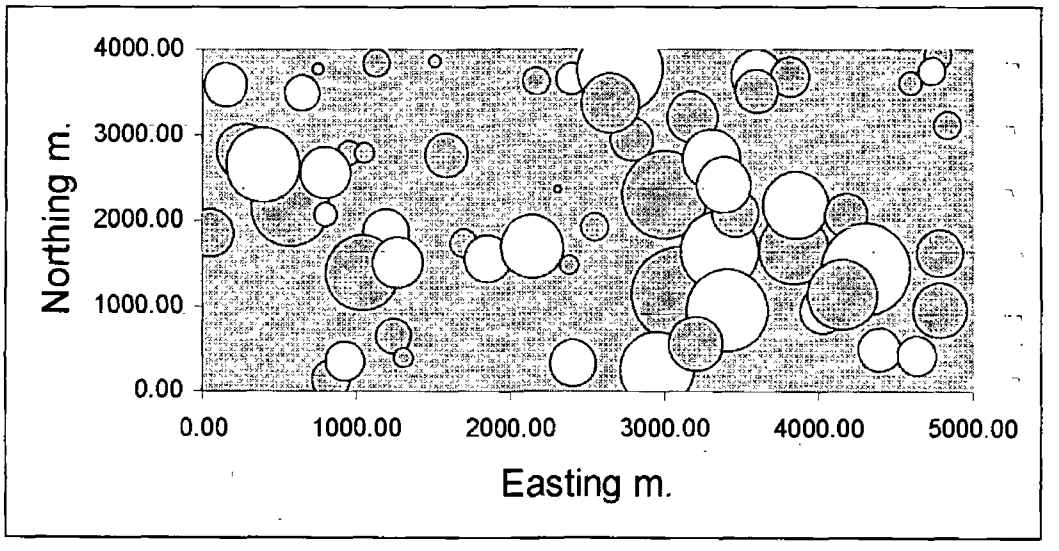

Figure 32. Bubble plot of the ^{40}K estimation error in the 60 samples of Survey 1 using a cross validation analysis of the kriging procedure. Dark circles denote over-estimation, light circles denote under-estimation.

The poor performance of the estimation procedure for the samples exhibiting the highest radionuclide activities is also demonstrated by plots of estimation errors against radionuclide values (Fig.33-34). These plots indicate the smoothing effect of the kriging process, high values being consistently underestimated and low values being overestimated. The poor estimation for certain areas, indicated by the bubble plots for the cross validation procedure, is also evident in the contour maps of the kriging standard deviations for the region (Fig.35-38.).

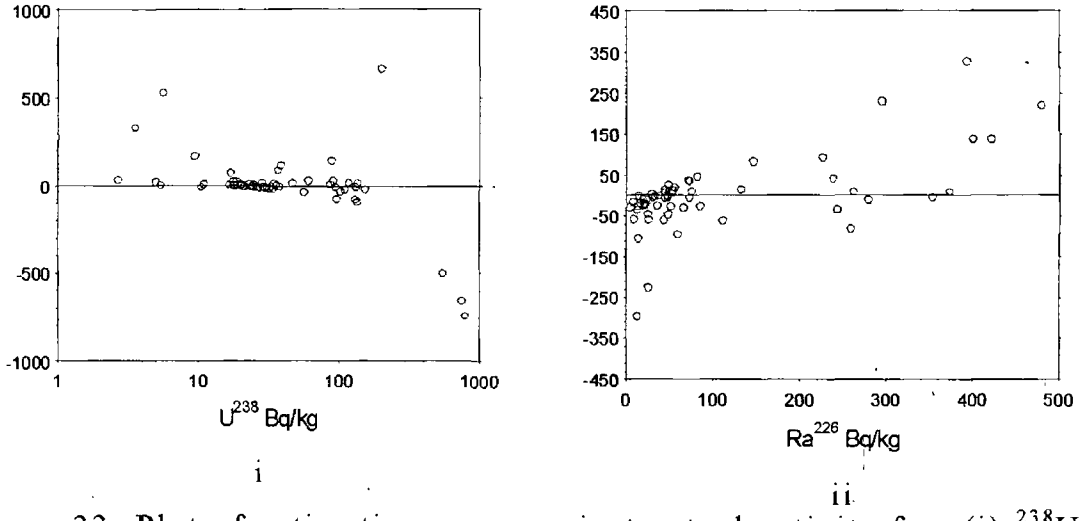

i ii

Figure 33. Plot of estimation error against actual activity for (i) ^{238}U and (ii) ^{226}Ra. Note semi-log scale of (i). Values in Bq/kg.

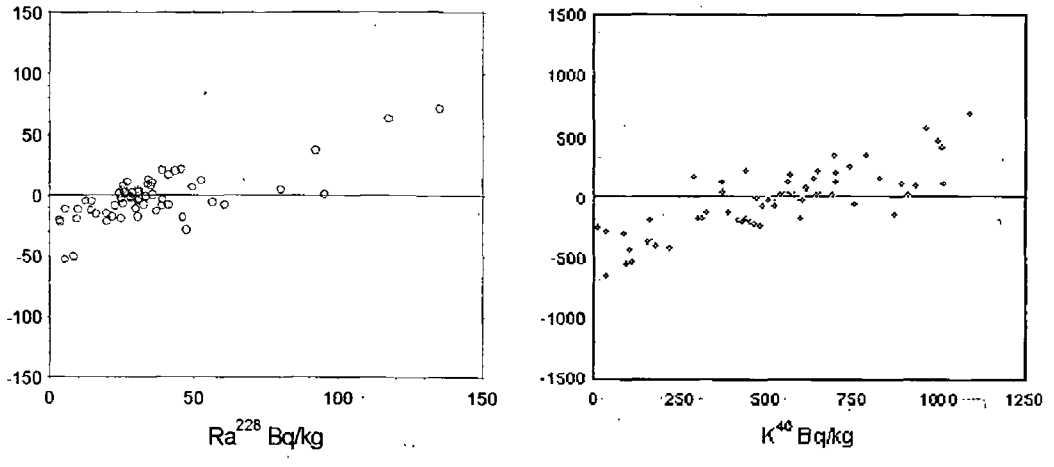

(i) (ii)

Figure 34. Plot of estimation error against actual activity for (iii) ^{226}Ra and (iv) ^{40}K. Values in Bq/kg.

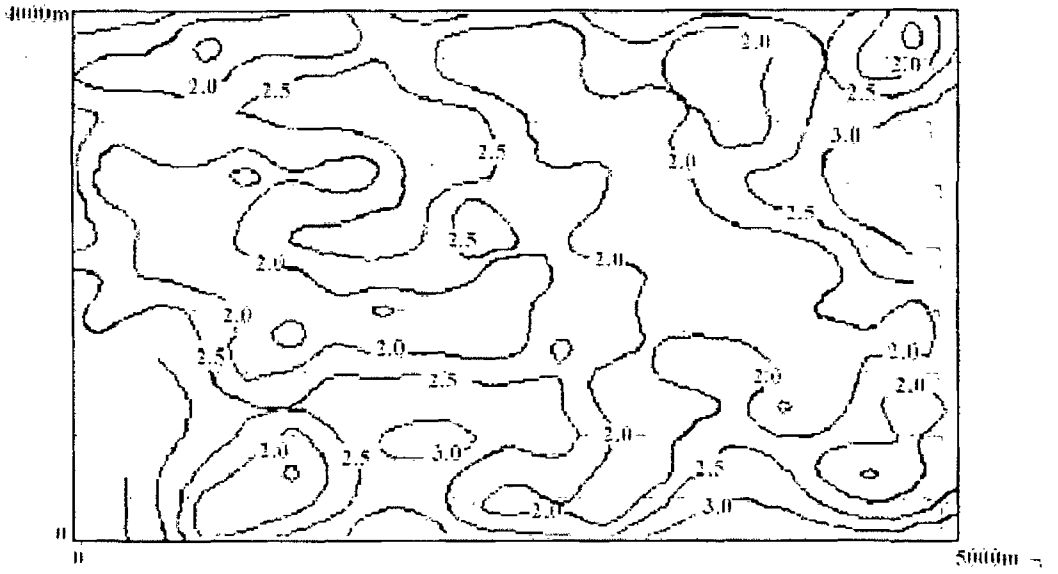

Figure 35. Contour plot of the standard deviations of the kriged estimates for ln-^{238}U.

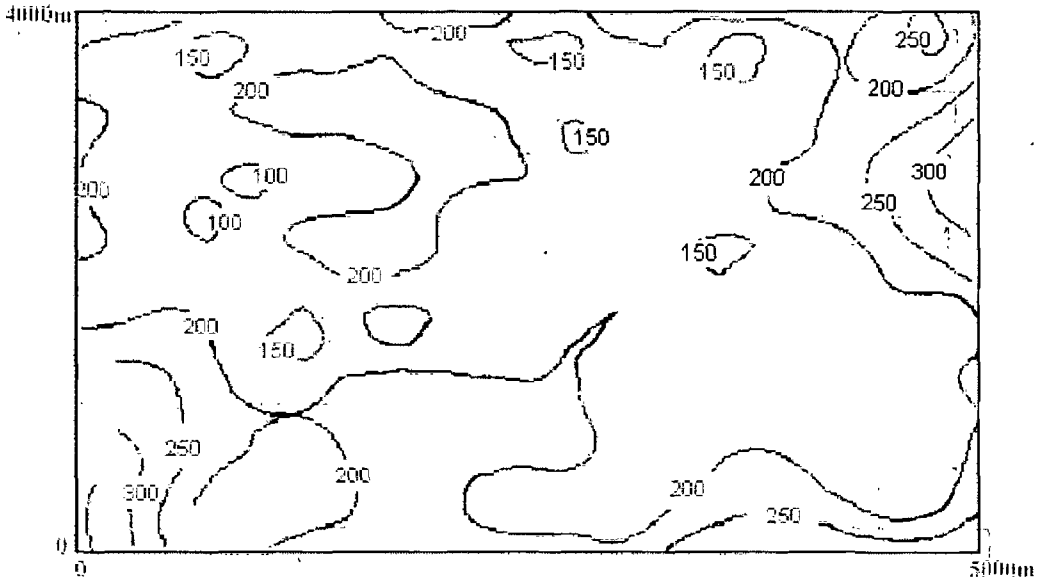

Figure 36. Contour plot of the standard deviations of the kriged estimates for ^{226}Ra.

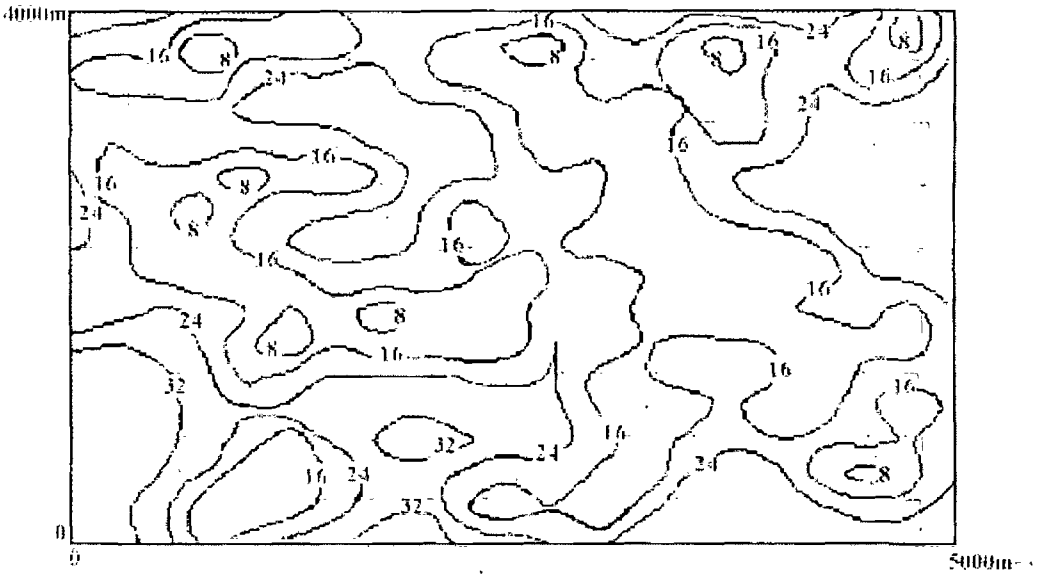

Figure 37. Contour plot of the standard deviations of the kriged estimates for ^{228}Ra.

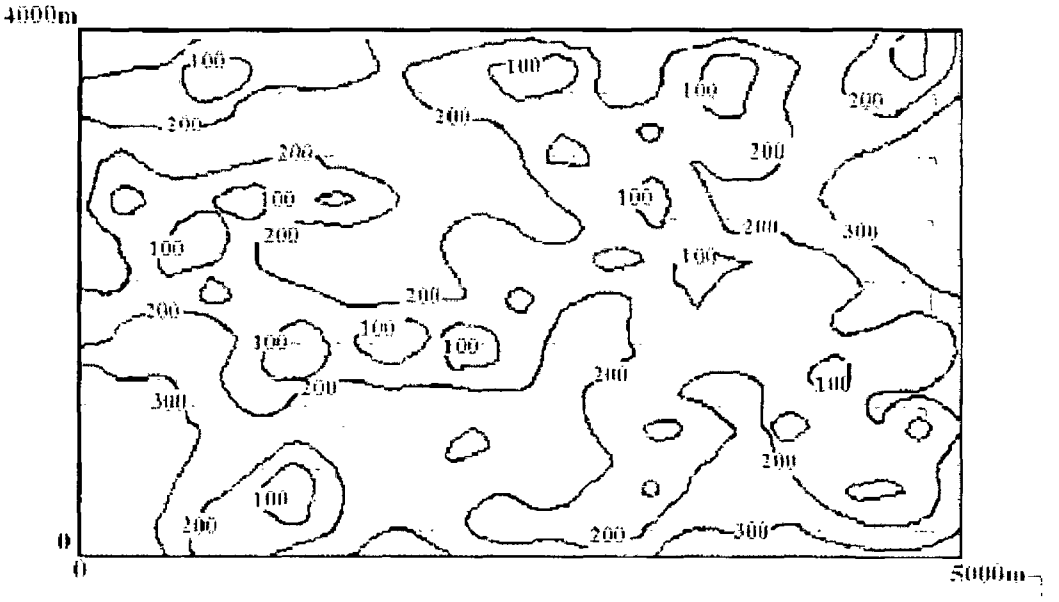

Figure 38. Contour plot of the standard deviations of the kriged estimates for ^{40}K.

The highest kriging standard deviations occur in locations exhibiting high radionuclide specific activities as indicated in the cross validation

analysis. This feature is due to a combination of factors that include a low sampling density in the south eastern corner of the study region and the occurrence of high radionuclide activities in close proximity with areas exhibiting lower activities.

4.1.3.2. Comparison of Point Estimation Procedures

A comparison of the performance of kriging and more conventional point estimation procedures (triangulation, polygonal and inverse distance squared) was made in order to examine the possible benefits of geostatistical estimation. The results of this comparison are presented and discussed in Appendix 5 as the published paper:

Dowdall, M. and O'Dea, J. Comparison of Point Estimation Techniques in the Spatial Analysis of Radium-226, Radium-228 and Potassium-40 in Soil.
Environmental Monitoring and Assessment **59**. 1999. pp. 191 - 209.

4.1.3.3. Summary

The comparison of the geostatistical procedure with more conventional estimation methods highlights a number of points. Kriging outperforms triangulation, inverse distance squared and a polygonal method in relation to the reproduction of the sample values and the distribution of the estimation errors. Kriging also provides estimates with the lowest mean error. However, the method does not perform as well as the polygonal procedure in relation to replicating the statistical distribution of the data set. This feature is a direct result of the smoothing of the kriging process which results in conditional bias, or over and under-estimation for samples whose radionuclide levels are low or high

respectively. This bias is also evident in the bubble plots of the cross validation procedure, the highest estimation errors occurring in association with samples at either end of the sets distribution. The problem of bias is exacerbated by the nature of the data set in relation to the close positioning of low and high samples.

Whether or not the kriging process offers significant advantages over the other, more traditional, methods depends largely on what is required from the procedure. In this instance, a general appraisal of the distribution of radionuclides within the valley was desired, with the identification of enriched areas. Of lesser concern was the actual activity of the samples in these areas. However, although kriging performed well within the context and objectives of this study, the results of the previous analysis indicate that in a situation involving, for example, estimation to assess compliance with regulatory controls, kriging may not be the most suitable procedure to use.

4.1.4. Distribution of Radionuclides within the Cronamuck Valley

Contour maps of the specific activities of the radionuclides were constructed using the estimate grids provided by the kriging process. These maps are presented in Fig. 39-42.

A number of features are evident from the contour maps of the four radionuclides activities. The elevated radionuclide activities over the granite portion of the study region are clearly delineated for all the radionuclides except K^{40} whose values are more evenly distributed. The contour plots indicate a sharp reduction in ^{238}U, ^{226}Ra and ^{228}Ra activities over a relatively short distance corresponding to the contact of the granite with the country rocks at location X.

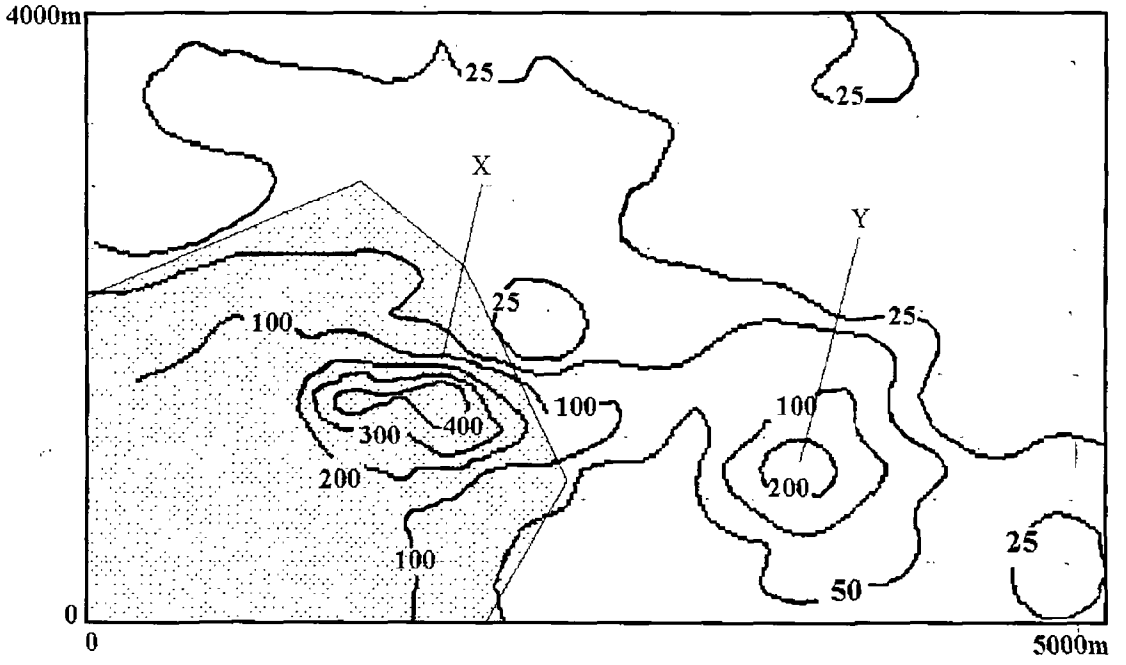

Figure 39. Contour map of ^{238}U activity estimates. Contour values in Bq/kg. Shaded area denotes granite region. X and Y indicate locations of water saturated depressions.

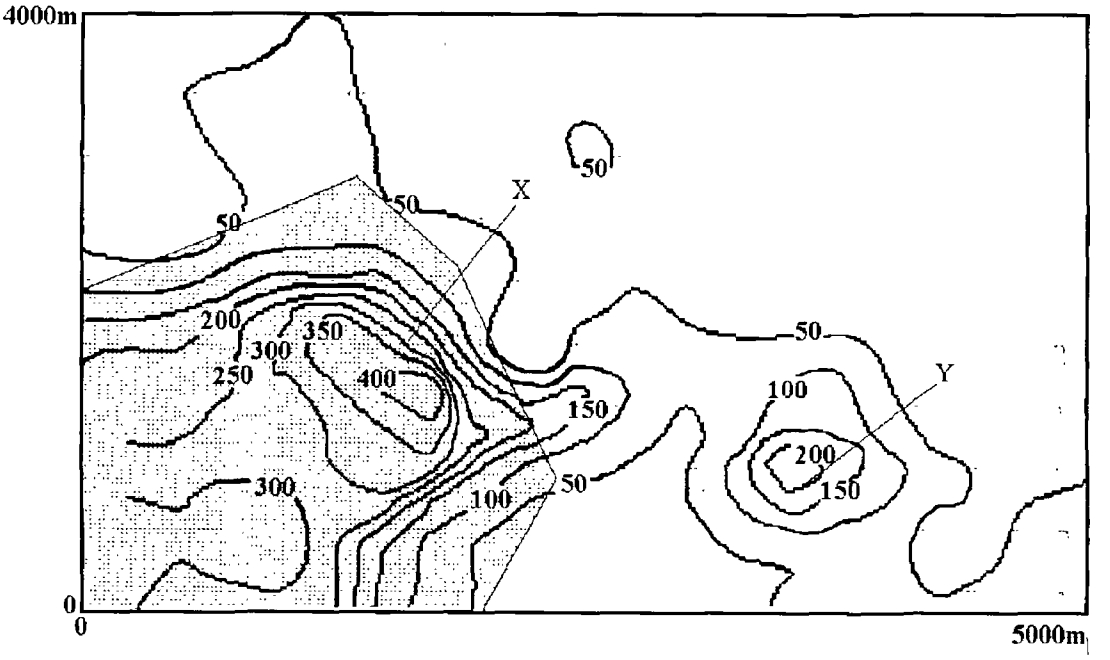

Figure 40. Contour map of ^{226}Ra activity estimates. Contour values in Bq/kg. Shaded area denotes granite region. X and Y indicate locations of water saturated depressions.

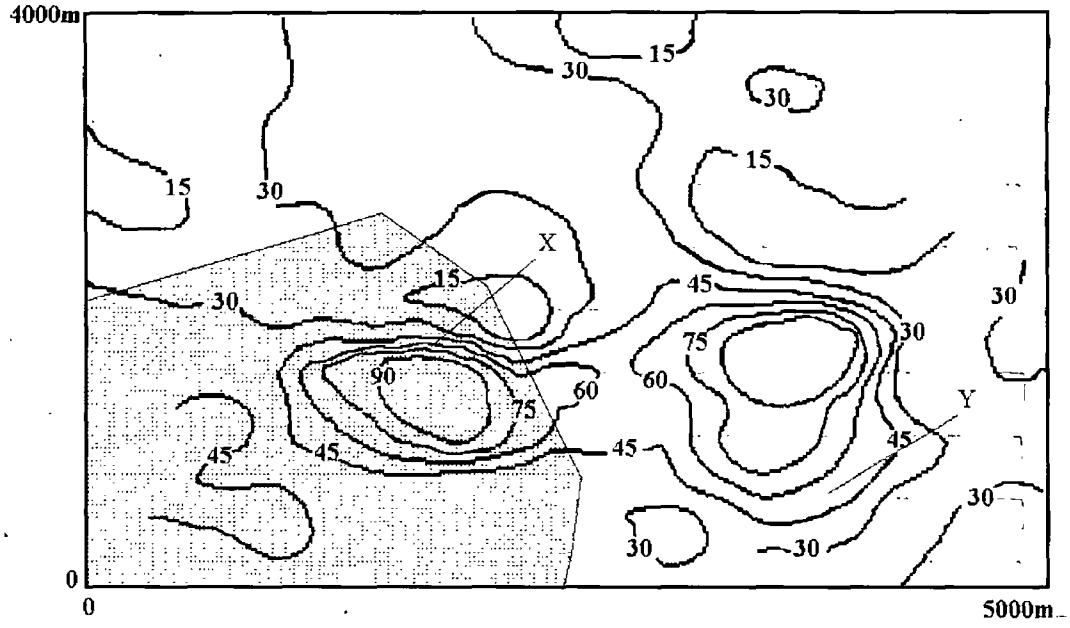

Figure 41. Contour map of ^{228}Ra activity estimates. Contour values in Bq/kg. Shaded area denotes granite region. X and Y indicate locations of water saturated depressions.

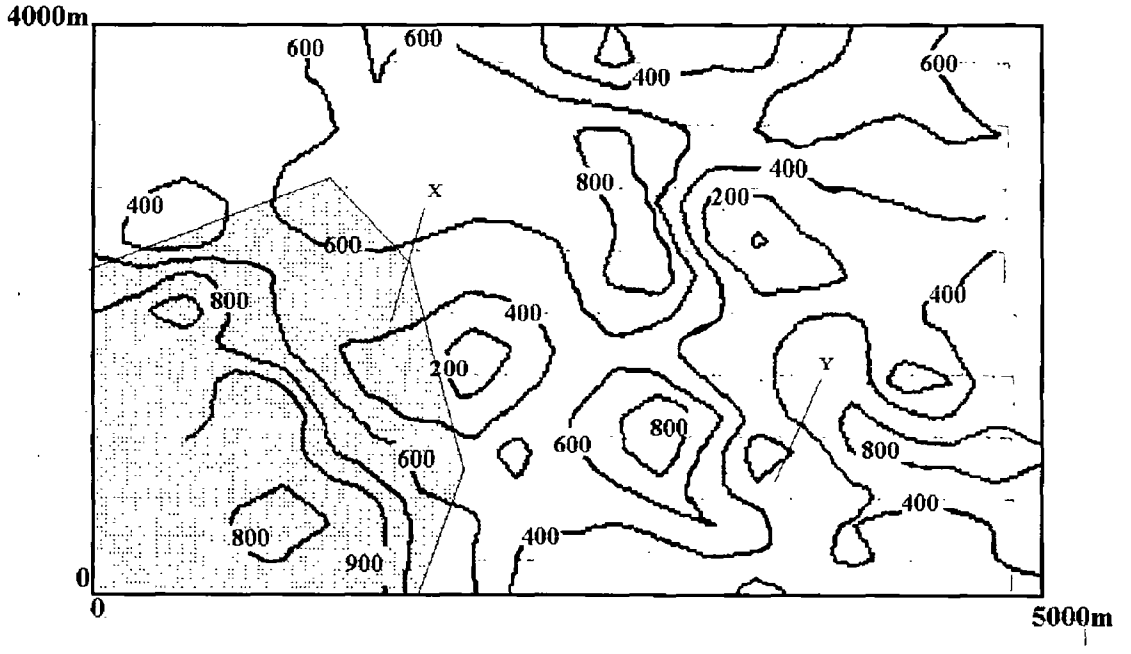

Figure 42. Contour map of ^{40}K activity estimates. Contour values in Bq/kg. Shaded area denotes granite region. X and Y indicate locations of water saturated depressions.

^{238}U activities decrease from 400 Bq/kg to 25 Bq/kg over a distance of less than 500 m across the contact at location X. ^{226}Ra follows a similar decrease (400 to 50 Bq/kg) and ^{228}Ra activities exhibit a reduction from 90 Bq/kg to 15 Bq/kg. This drop in radionuclide activity on crossing the granite – metasediment contact is most evident for the two radium isotopes which exhibit a tighter contour pattern than ^{238}U, perhaps reflecting the suggested immobility of radium in the surficial environment (Shepperd, 1980).

A second area of elevated activity within the valley, indicated by the contour maps, occurs at location Y, this area lying some distance away from the granite but being upstream of location X. Radionuclide levels at this location are not are not as high as for location X however location Y does display the same contour pattern as X, a rapid reduction in radionuclide activities occurring towards the north eastern corner of the location. Both location X and location Y occur at points on the Clogher Burn stream. This stream runs along the valley bottom (between X and Y) and the contour maps of ^{238}U, ^{226}Ra and ^{228}Ra all exhibit a band of elevated radioactivity between X and Y that appears to coincide with the course of the Clogher Burn. As both X and Y occur in water logged depressions along the course of this stream, and the stream runs along the bottom of the valley, it appears logical to suggest that distribution of natural radionuclides within, and transport away from, the peat overlying the granite region is governed largely by water drainage. On a larger scale however, it is apparent from the contour maps that the underlying geology controls the levels of uranium and thorium series radionuclides in the peat of the Cronamuck valley.

Taking values of 8.1 ppm and 25.1 ppm as the average levels of uranium and thorium respectively in the Barnesmore granite (O'Connor *et al*, 1983) and using mass to activity conversion factors of 12.2 Bq/mg and

4.1 Bq/mg for ^{238}U and ^{232}Th (Eisenbud, 1987), it is possible to estimate the level to which the peat overlying each of the two lithologies is enriched relative to the underlying rock. The soil lying on the granite lithology is enriched by a factor of 2 for ^{238}U but the soil remains depleted (or un-enriched) in ^{232}Th with less than half the activity of the rock being present in the peat (based on ^{228}Ra activities). Employing values of 1.8 ppm and 12.0 ppm for the uranium and thorium levels in the metasediments (O'Connor and Lang, 1985) produces enrichment factors for uranium and thorium of 1.9 and 0.6 for the peat overlying the metasediments, these figures being calculated on the assumption that ^{228}Ra is in equilibrium with ^{232}Th. Using the above mass to activity conversion and the rock radionuclide levels reported by O'Connor (1983) and O'Connor and Lang (1985), indicates an approximate equality in the activities of ^{238}U and ^{232}Th for the granite rock and a $^{232}Th/^{238}U$ activity ratio of approximately 2 for the metasediments. Neither of these ratios are upheld in the overlying soil. Calculating ^{232}Th / ^{238}U activity ratios for the soil of the two regions yields values of 0.22 for the granite and 0.75 for the non-granite. The disparity between the values for the granite lithology and its overlying soil suggests either loss of thorium relative to uranium, enrichment of uranium in the soil or a significant disequilibrium between ^{228}Ra and ^{232}Th. The latter seems unlikely given the relatively short half-life of ^{228}Ra and adopting the generally accepted concept of thorium being immobile in such environments, it would appear that the basal layers of peat in the Cronamuck Valley are enriched in uranium.

The results of Survey 1 support the findings of the uranium prospectors who initially surveyed the valley in the 1970's in that radionuclide enrichment within the valley is localised, and given that there is some evidence that enrichment is a result of the transport and deposition of radionuclides by water, it would appear unlikely that enriched areas of

peat are supported by elevated radionuclide levels in the rock underlying the areas of enrichment. The findings of the prospectors (Irish Base Metals, 1978), that there is a high background activity within the valley and that uranium is mobile within the soil, are also echoed by the current conclusions. The Survey 1 results are also supportive of the work of a number of researchers in this field. Kochenov (1965) indicated a number of features of uranium enrichment in peat, two of which are completely upheld by the results of this survey, primarily the irregular distribution of uranium within the peat and the association of uranium enriched areas with areas with gullies and depressions in the valley. Wilson's (1984) conclusion that uranium enrichment in peat is associated with uranium bearing waters also appears to be confirmed by the findings of Survey 1. The previously mentioned apparent immobility of radium and thorium echoes the findings of many researchers including Sheppard (1980) and Taskayev *et al* (1978) as detailed in Section 1.3.1..

4.1.4.1. Summary

The disparity in radionuclide levels in peat overlying the granite and peat overlying the metasediments initially demonstrated in Section 4.1. is made highlighted by the isopleth maps. However, although the fact that the part of the valley underlain by granite exhibits higher levels of the studied radionuclides, the transport of radionuclides, indicated by the off-pluton data set (Section 4.1.1.), from the granite region to the metasediments is indicated by the maps. The cause of this transport is made clear by the fact that highest radionuclide levels in the valley occur at the lowest points of the valley, typically in the water saturated depressions that are encountered along the course of the Clogher Burn. As location Y lies at the foot of a slope and is fed by water draining the granite, it is reasonable to assume that transport of radionuclides off the pluton is via drainage water flowing off the granite. Location X also lies

at the foot of a slope and is also fed by waters draining the granite, supporting the opinion that although lithology appears to govern peat radionuclide levels on a large scale, some small scale redistribution of the radionuclides within the valley occurs as a result of the flow of water draining the peat. The findings of this project, with respect to the distribution of the radionuclides, is largely supported by the findings previously reported in the literature, particularly Kochenov's (1965) studies of radionuclide occurrence in peat bogs.

4.2. Radionuclide Accumulation in the Cronamuck Valley

One of the most obvious features of the spatial distribution of radionuclides within the Cronamuck Valley is the localised accumulation of uranium and thorium series radionuclides in certain areas of the valley. In order to further delineate one of these locations and to ascertain the reasons for these accumulations, a second survey, Survey 2, was implemented.

The aim of this survey was an investigation of the speciation of the radionuclides within one of the two regions of anomalous radioactivity identified in Survey 1 (locations X and Y, Fig.9) and the identification of possible controlling factors on radionuclide enrichment within the peat itself. The approach adopted involved the use of a portable gamma ray spectrometer to investigate the spatial extent of the radionuclide enrichment within one of these regions, chemical and radiometric analysis of the peat and drainage system both within and outside the chosen area of accumulation and radiometric analysis of the underlying lithology. This section outlines the results of these investigations and presents conclusions on the form and behaviour of the radionuclides within one of the enriched areas (location X) and on the

nature, and possible reasons for, $^{226}Ra/^{238}U$ disequilibrium within the area.

The location of the sampling sites of Survey 2 are detailed in Fig. 10. A total of four depth cores were taken (Sites A, C, E and F) as well as six other discrete samples (E1, E4, E5, E6, F2 and F3), taken using the same procedure as for Survey 1 samples. Sites A and E were located within the area of enrichment termed location X. Sites C and F, lying outside the area were taken for comparative purposes, Site F lying on the granite but outside the depression at X, Site C lying neither in the depression or on the granite. The set of samples used for analysis also incorporated three samples taken from the area as part of Survey 1 (sample's 9, 41 and 54).

4.2.1. Portable Gamma Ray Spectrometry

A portable NaI gamma ray spectrometer was employed to make a series of field measurements around the radiometric anomaly chosen for Survey 2. The instrument was calibrated as described in section 3.4.2.1. and 30 readings were taken (raw data tabulated in Table xiii., Appendix 1). The data was contoured and the results are displayed in Fig. 43. A number of difficulties were encountered in the exercise, primarily the effect of outcrop on the readings and the variation in count rate depending on the depth and saturation of the overburden. To counter these effects, some effort was made to ensure that readings were taken over sites with the same overburden depth and some distance (approx. 20 m) away from outcrop.

As can be seen from Fig. 43., the highest readings were centred on the confluence of Clogher Burn and the unnamed stream flowing from the south. This area is at the lowest part of the water saturated depression

(and also the lowest part of the Cronamuck valley) found at this location. Readings drop away rapidly on moving north away from the depression but the drop is less pronounced as one follows the general shape of the depression, which runs in a NW - SE direction along the course of Clogher Burn.

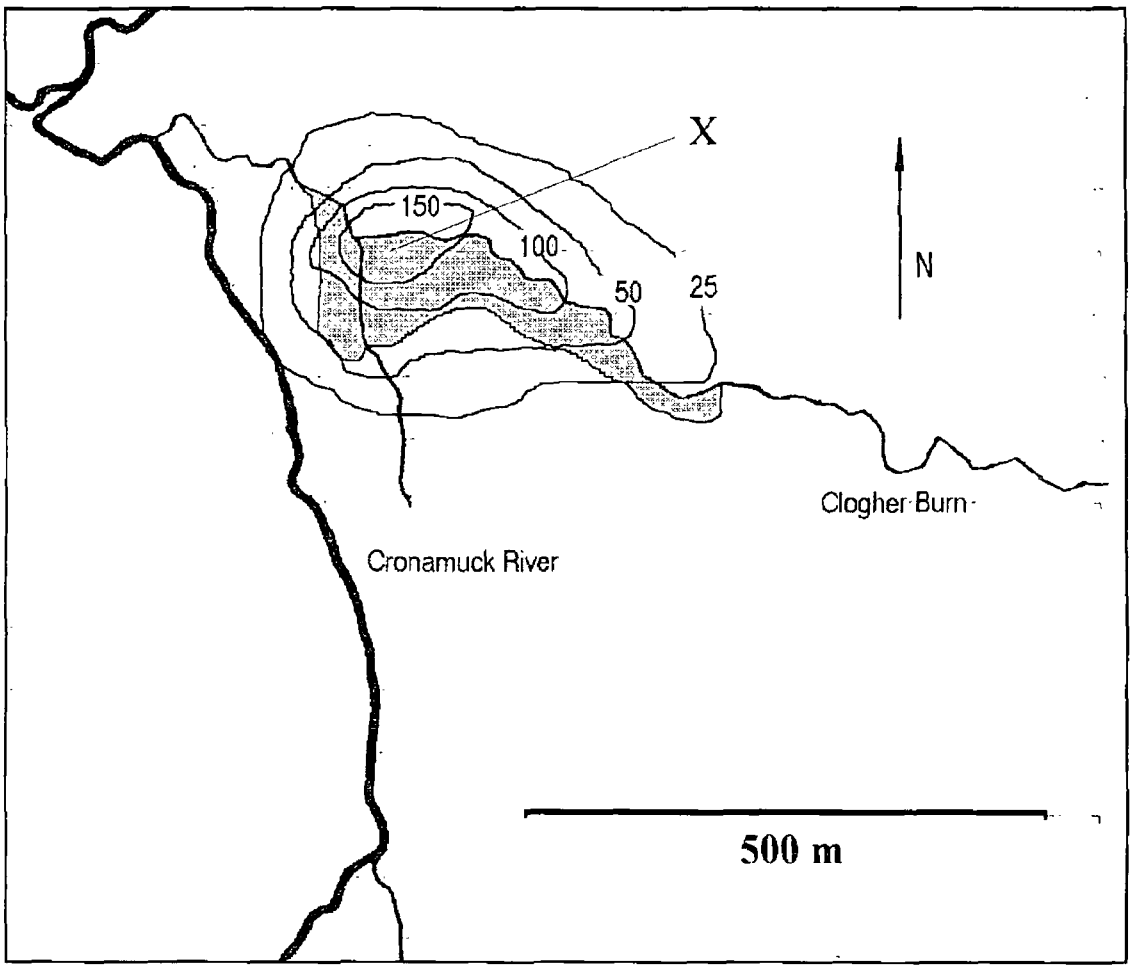

Figure 43. Isopleth map of gamma spectrometer readings over radiometric anomaly X studied in Survey 2. Contours in counts per second. Shaded area denotes extent of water saturated depression.

The portable spectrometer readings agree broadly with the findings of Survey 1 and confirm that this area of elevated radioactivity, highlighted

in Survey 1, is associated with the saturated depression. It should be noted that the other area of elevated radioactivity in the valley is also located within a heavily saturated depression at the confluence of a second stream and Clogher Burn, an observation that supports the previous suggestion that radionuclide accumulation within the valley may be due to radionuclide transport by water.

4.2.2. Drainage system analysis

A series of 20 water samples were taken from the drainage system associated with the location under study. A series of chemical analyses were performed on these samples which were also analysed by ICP-MS for uranium. The purpose of this exercise was to ascertain the chemical condition of the drainage system and to identify a possible influx of uranium into the area. Raw data is provided in Table xii., Appendix. 1. Summary statistics for chemical parameters studied are provided in Table VIII., uranium results are contained in Fig.44.

	pH	Eh mV	Conductivity $\mu S\ cm^{-1}$	T.D.S. ppm	Fe ppm
N	15	20	17	18	19
Average	6.44	110.05	68.76	101.78	0.15
Std.	0.83	40.80	20.25	93.79	0.16
Min	4.30	33.00	20.20	40.00	0.01
25th	6.21	74.75	62.10	58.50	0.01
Median	6.62	115.50	68.10	85.00	0.05
75th	7.05	149.00	84.00	109.50	0.23
Max	7.21	160.00	104.00	462.00	0.51

Table VIII. Summary statistics for the chemical properties of the water samples taken during Survey 2.

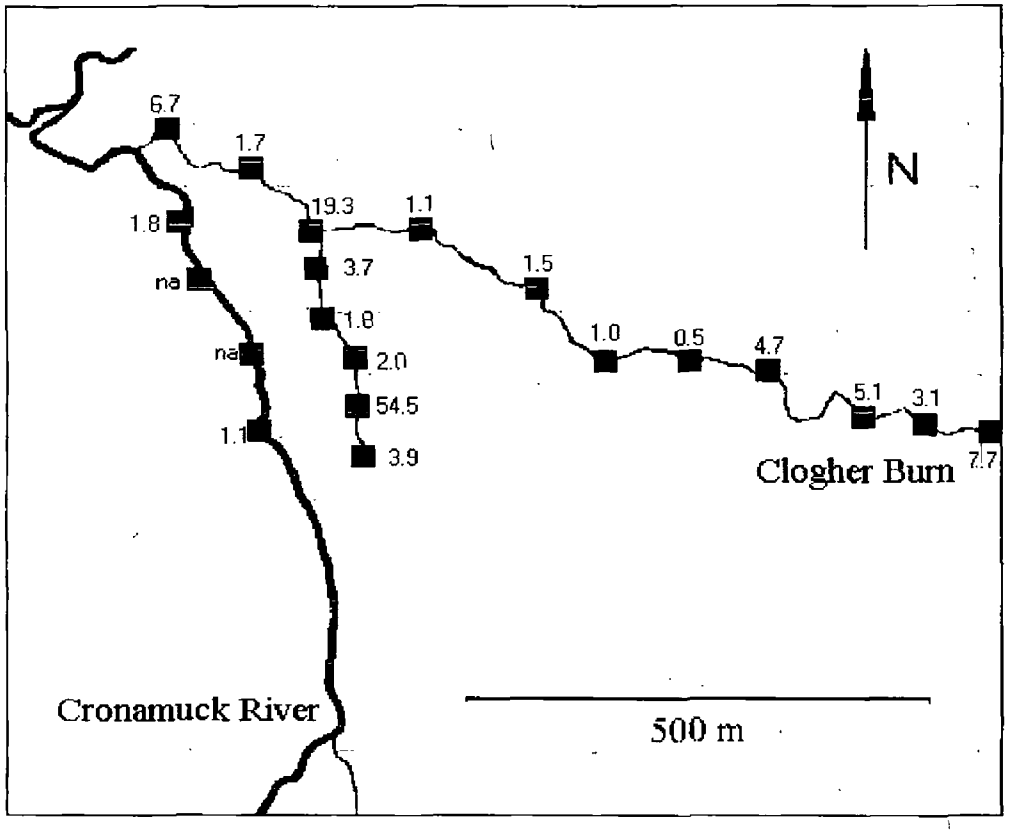

Figure 44. Drainage system uranium levels. Values in ppb.

As national values for uranium in fresh water were unavailable, it was not possible to ascertain how the levels encountered in this study compare with an average national value. Figures obtained by the prospectors of the 1970's (Irish Base Metals, 1979) for uranium levels in stream water draining a different part of the valley indicate levels in the range 0.01 - 0.5 ppb, which are substantially lower than values obtained in this study. Without details of the analytical method, sampling technique etc., meaningful comparison is impossible. The values obtained in this study are in broad agreement with the range of 0.01 to 5.0 ppb quoted by Rogers and Adams (1969) as typical surface water levels but largely exceed the global average of 0.18 ppb calculated by Palmer and Edmond (1993). The high value of 54.5 ppb could not be explained (bracketed as it is by values an order of magnitude lower) and was assumed to be erroneous on the basis of the results of a Q-test (Q >

0.30, N = 18). The value of 19.3 ppb occurs at the junction of the unnamed stream and Clogher Burn, at a point where the highest levels of uranium are encountered in the peat. It is therefore possible that the water at this location exhibits high levels of uranium due to contact with enriched peat. Given the data to hand, it is impossible to deduce a likely cause for the elevated level (19.3 ppb) at this site although it is possible to conclude that the drainage system flowing along the bottom of the valley does contain appreciable amounts of uranium. It is possible therefore that the Clogher Burn and its associated streams may provide a source of uranium and other radionuclides to the depressions at X and Y, which, in conjunction with chemical conditions favourable to uranium retention occurring at X and Y, may give rise to the levels of enrichment observed at the sites during the course of Survey's 1 and 2.

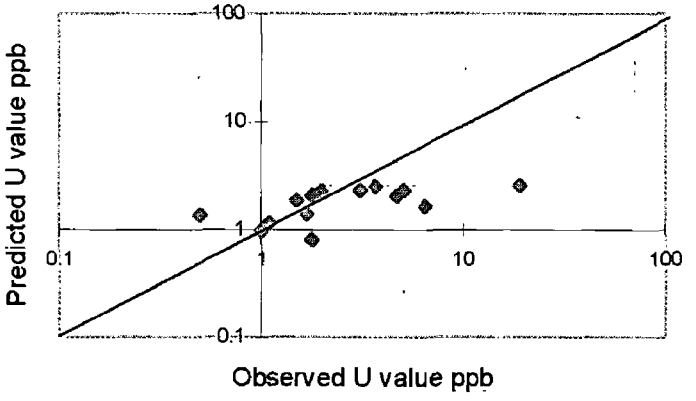

Figure 45. Observed uranium levels against uranium levels predicted by Lopatkina relationship.

Adopting an average uranium content of 12.9 ppm for the eight rock samples taken from within the study area (Table XV) a comparison was made between the observed values and those predicted by Lopatkina's (1964) formula for uranium levels in fresh waters (see Section 1.3.1.). As can be seen from Fig.45., there is relatively good agreement between the observed and predicted values for low levels of uranium although the

relationship degenerates at higher values. The only significant correlation (0.01 level) exhibited by the data exists between the level of total dissolved solids and uranium levels in the samples.

4.2.3. Chemical and Radiological Properties of Depth Profiles

4.2.3.1. Sites A and E

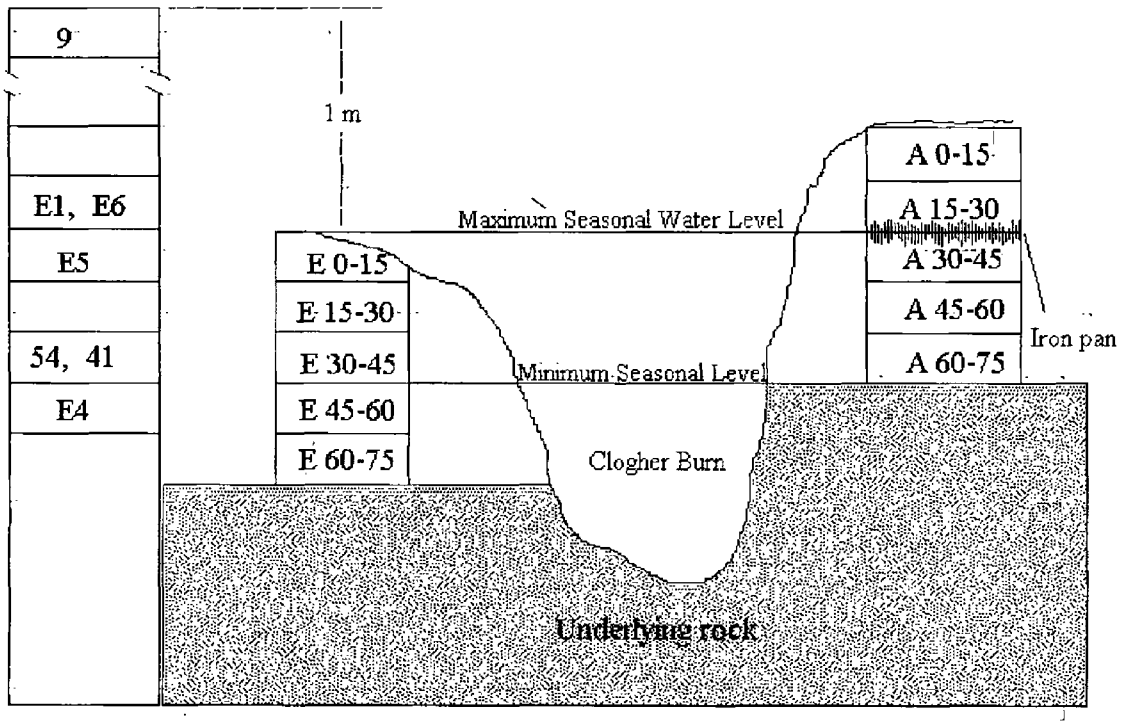

Figure 46. Vertical positions of Sites A, E and individual samples relative to the Clogher Burn.

Sites A and E both lie within the saturated depression that coincides with one of the two areas of radionuclide enrichment delineated by the results of Survey 1 (location X) and the survey conducted using the portable gamma ray spectrometer. Results of the radiometric and chemical analyses conducted on these profiles may serve to provide information on the enrichment of radionuclides within the area and may highlight possible controls on the accumulation and behaviour of radionuclides within the valley in general.

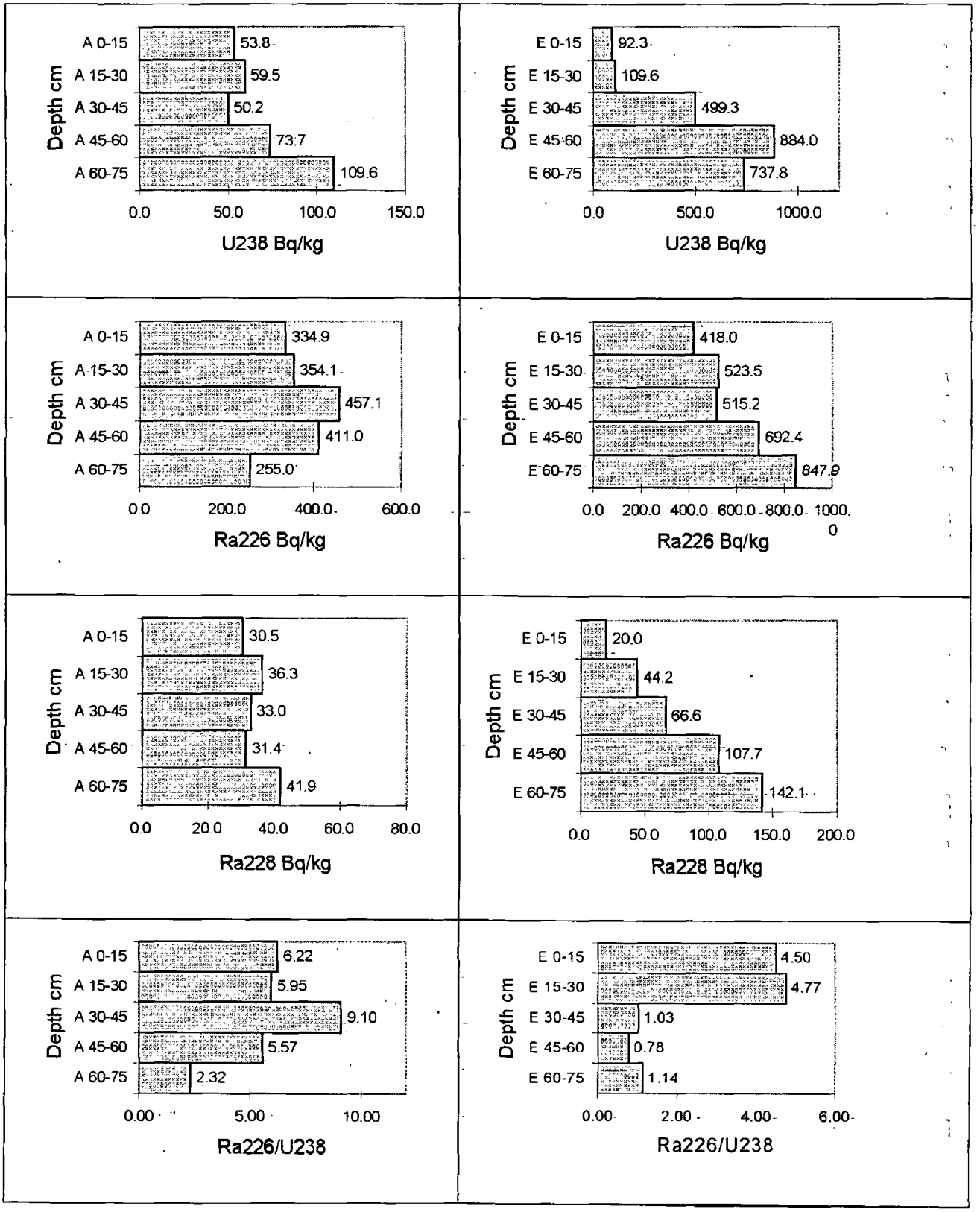

Figure 47. Radiometric properties of profiles taken from Sites A and E.

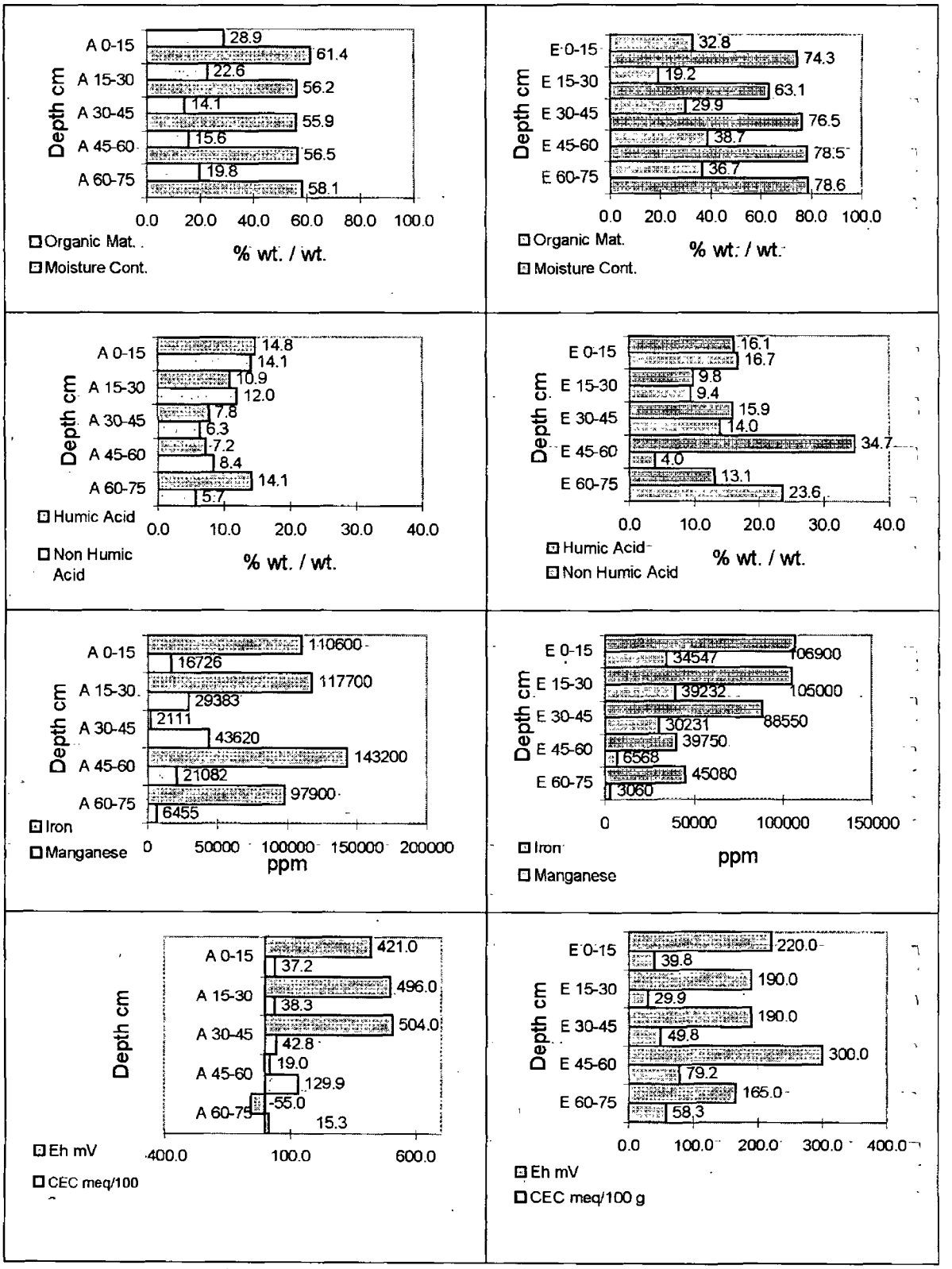

Figure 48. Chemical properties of profiles taken from Sites A and E.

^{238}U activities throughout the soil profile at Site A differ considerably from those at Site E. All layers in the profile exhibit lower activities for this radionuclide. The difference between the activities in the upper and lower layers is less marked than for Site E. Both ^{226}Ra and ^{228}Ra activities remain relatively constant throughout the profile, maximum activities for these nuclides being exhibited in the 30-45 cm layer as opposed to the bottom layers for Site E. The activities of both these nuclides remain lower than for Site E. The $^{226}Ra/^{238}U$ ratio is greater than unity at all depths at Site A. A large excess of ^{226}Ra is evident in the upper layers of Site A, the maximum ratio being associated with the 30-45 cm layer.

The three radionuclides, ^{238}U, ^{226}Ra and ^{228}Ra all exhibit a marked increase with depth at Site E, the increase being most for ^{238}U. ^{226}Ra increases by only a factor of 2 over the entire profile whereas ^{238}U levels increase steadily on going down the profile, the bottom layer containing 7 times the amount of ^{238}U as the top layer (Fig.47.). The most prominent feature of the radiometric profile at this site is the marked reduction in U^{238} activities on going from the 30-45 cm layer to the surface which is not accompanied by an associated reduction in ^{226}Ra activities. ^{228}Ra activities throughout the profile display a similar pattern to those of ^{226}Ra. The $^{226}Ra/^{238}U$ ratios throughout the peat profile vary from approximately unity at the lower depths to greater than four in the upper levels of the profile. ^{228}Ra levels increase steadily on going down the profile, as do the levels of this radionuclide at Site A.

The chemical properties of the soil profile at A, (Fig.48.), provide insight into what factors may control the accumulation of radionuclides within localised areas of elevated radioactivity. The marked transition from a reducing environment to an oxidising one at the 30-45 cm layer

(as indicated by the relevant Eh values) coincides with the layer exhibiting the highest $^{226}Ra/^{238}U$ ratio for the soil profile at Site A. This interface was evident in the field as a concreted crust of iron oxide some 2 - 3 cm thick. The presence of this crust is not indicated in the results obtained for iron levels at that depth as solid lumps of the material were removed prior to analysis of the sample. The difference in the redox state across this crust is obvious from the change in Eh values (a measure of redox potential) on moving down the profile. Immediately above the iron pan, the Eh value is 504 mV (very oxidising), this value changing to one of 19 mV (very reducing) just below the pan. Cruickshank (1972) notes that soils beneath such pans tend to be extremely reducing due to the inability of air to penetrate the pan to the lower soil depths. Maximum ^{226}Ra values are encountered in this layer in direct contrast to the ^{238}U values which are at their lowest at this depth.

The presence of this crust can be explained as follows. The bank of the Clogher Burn at which site A is located is some 30-40 cm higher than the bank on which Site E is located (Fig. 46.). Iron pan (a hard layer of ferric oxide) forms when groundwater carrying dissolved iron in the reduced state meets an oxidising environment (such as near the surface of the soil) and the iron is precipitated out as the oxide (Cruickshank, 1972). Studying the results of the chemical analysis of the drainage system (Table xiii., Appendix 1.) it can be seen that the water of Clogher Burn, prior to reaching the area of enrichment, is relatively reducing, with Eh values less than 100 mV. This may be attributed to the depth of the stream (approx. 0.75-1.25 m) and its sluggish flow at this point. The redox state of the stream gradually becomes more oxidising as the stream reaches the area of enrichment, as the water becomes shallower, more turbulent and hence more aerated. This process is reflected in the dissolved iron values, the amount of dissolved iron gradually decreasing

as the redox state of the water becomes more oxidising, promoting the precipitation of the dissolved iron load. This precipitation of iron forms iron pan which gradually builds up to form a visible layer.

The difference between Sites A and E, with respect to redox states at various depths and the behaviour of iron in the profile, is related to the vertical positioning of the soil profiles relative to the stream water level. The upper levels of Site A are never saturated with water and hence remain relatively oxidising throughout the year. It is at the point of maximum seasonal ascension of the stream that the iron pan is located, at the interface between the saturated lower depths, which are reducing in nature, and the oxidising upper layers.

This situation is not present at Site E, as no level of this profile is ever completely unsaturated throughout the year. While an iron pan at Site E has not formed, levels of iron are at a maximum at a depth that corresponds approximately with the depth at which the iron pan occurs at Site A. This may be due to precipitation of iron from the stream water as it is exposed to the relatively oxidising upper layers of Site E but a pan may not have formed, as the upper levels of Site E do not have such a distinct interface between oxidising and reducing conditions (due to seasonal saturation of the upper layers) as does Site A.

The position of Site A relative to the Clogher Burn stream is reflected in the moisture levels of the profile (Fig.46. and Fig.48.). Site A exhibits moisture levels typically in the range 50 - 60%, while Site E, due to its lower level in relation to the stream, has moisture levels in excess of 75% (Fig.48.). Organic material levels at Site A are lower than for Site E at all levels except for the 15 - 30 cm level, probably indicative of the more oxidising conditions pertaining at Site A than at Site E, where

organic matter levels are almost all above 30%. The amount of organic material present at Site's A and E are low relative to typical organic matter levels for soil in the valley. Soil samples taken from outside the depression exhibit levels of > 90%, Site's A and E containing less organic material due to the greater amounts of iron and manganese present, layer 30 - 45 cm of Site A containing an estimated 30 -40% iron. Mineral material is also present in greater amounts at these two sites due to the presence of sand that has been carried downstream settling out in the relatively still waters of the depression.

The total iron and manganese content of the soil at Site E increases towards the top of the soil column, possibly due to the deposition of these metals when the water level in Clogher Burn is periodically lower. The higher iron and manganese levels at the surface of the profile are indicative of a more oxidising environment although this is not reflected in either the Eh or moisture levels. It should be noted that at the time of sampling (March-April) the soil column was uniformly saturated due to the level of the Clogher Burn watercourse. The Eh value of 300 mV recorded for the 45 - 60 cm level is assumed to be erroneous given the fairly uniform reduction in Eh values on going down the profile and the fact that there is no logical explanation for an oxidising layer to be preceded and succeeded by more reducing layers. It is likely that the observed saturation level is not prevalent throughout the year and that the surface of the soil column experiences a fluctuation in redox conditions over the course of a year, becoming more oxidising during the summer months. The lack of a distinct iron pan or crust, usually found at the interface of an oxidising layer with more reducing conditions underneath, would appear to support the hypothesis that the surface layers at Site E undergo fluctuations in redox conditions. The pH of the soil remains constant throughout the profile. The layer of peat at a depth of 45 – 60 cm exhibits the largest amount of humic acid, however the

bottom layer has a low content of this material, assumed to be due to the relatively large amount of inorganic detritus present at the rock – soil interface. The cation exchange capacity of these two layers reflects the relative amounts of humic acid present, the bottom layer having a capacity that is much lower than the preceding layer which displays the highest capacity of any layer in the profile.

The previous discussion highlights a number of pertinent facts about how the radionuclides are dispersed throughout the profiles taken at A and E. Both profiles differ markedly in relation to the occurrence of ^{238}U, Site A exhibiting levels of this nuclide up to an order of magnitude lower than those at Site E, while ^{226}Ra and ^{228}Ra levels are comparable at most depths of the profile. In most cases the highest levels of nuclides are found at the lower levels of the profiles. There appears to be some relationship between the iron pan found at Site A and how the nuclides are distributed within that profile. The highest levels of ^{226}Ra at Site A correspond with iron pan as does a marked rise in the $^{226}Ra/^{238}U$ ratio. Given the fact that the predominant difference between Sites A and E is the position of the profiles relative to the Clogher Burn and that this difference produces different moisture levels and redox conditions within the peat, it may be possible that the radiological differences between the two profiles exist as a result of their positions relative to the Clogher Burn. By inference, it is also possible to conclude that the elevated radionuclide levels within the depression are due to the influx of water bearing trace amounts of the radionuclides (confirmed for ^{238}U during the drainage system analysis). If Clogher Burn is viewed as the major source of radionuclides within the depression then the profile at Site A may exhibit lower levels of radionuclides because it was either never enriched (due to its position relative to the water) or was enriched and then subsequently depleted due to some change in soil conditions.

4.2.3.2. Sites C and F

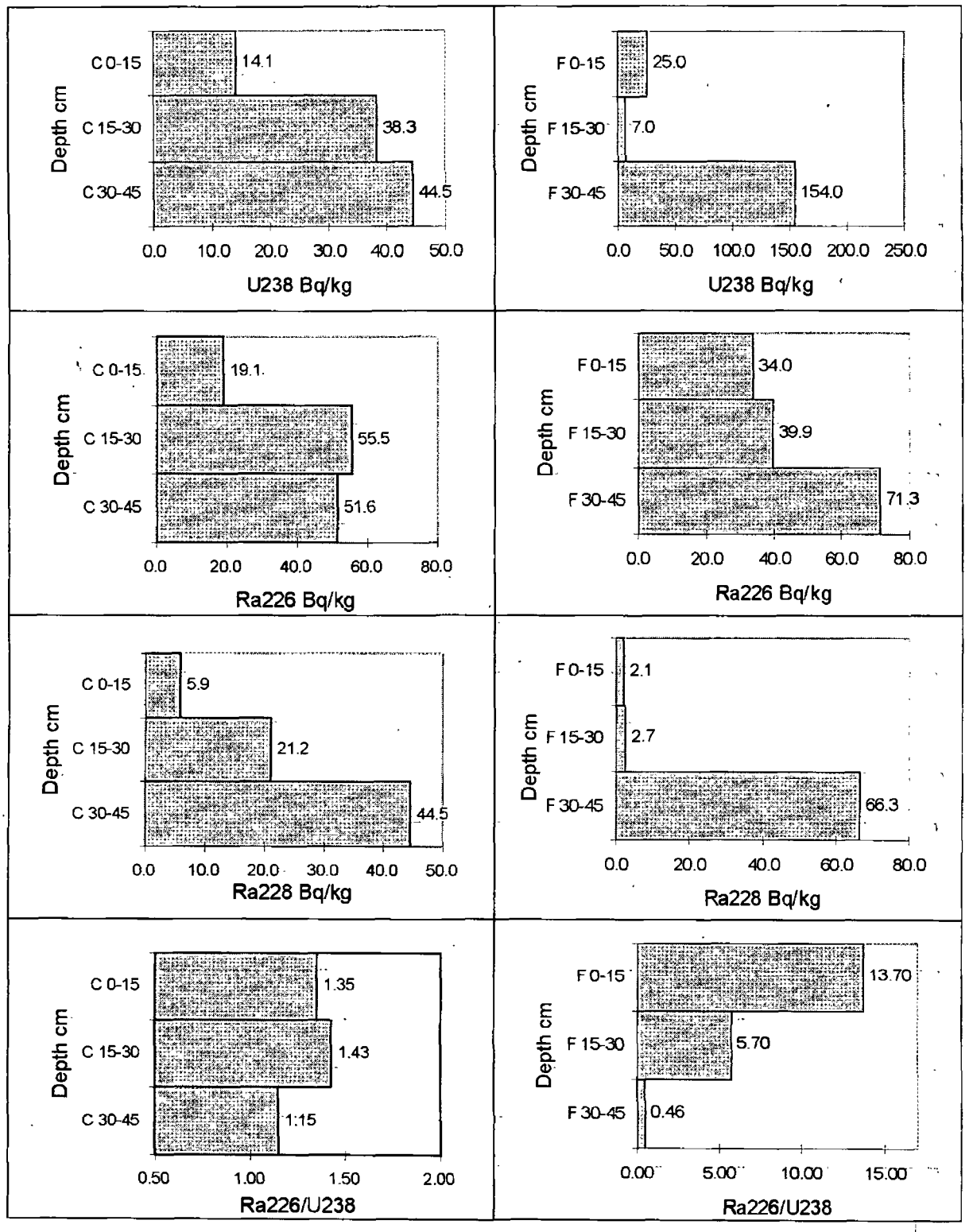

Figure 49. Radiometric properties of profiles taken from Sites C and F.

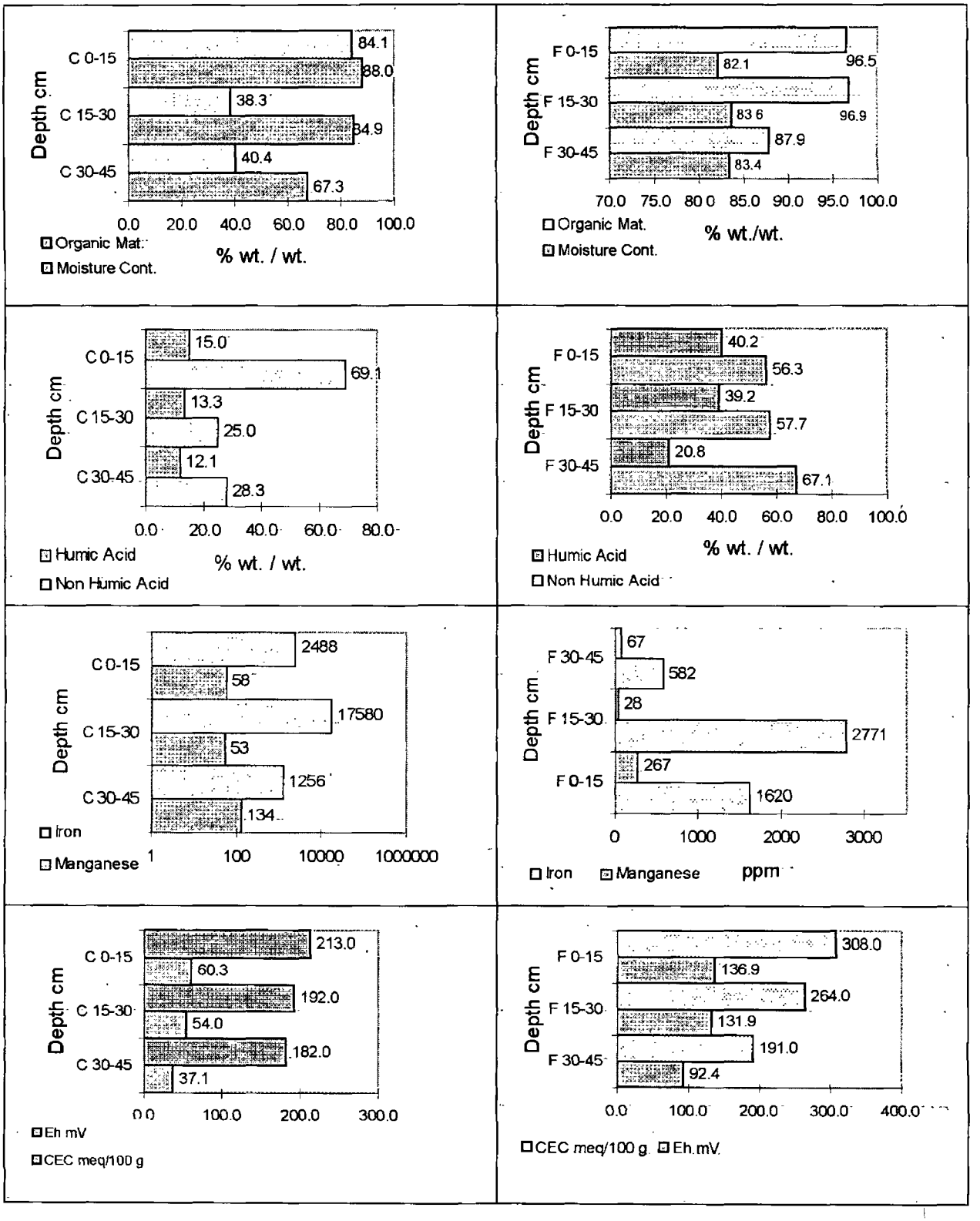

Figure 50. Chemical properties of profiles taken from Sites C and F.

The predominant feature of the profile taken at C is the lower activities of all three radionuclides relative to the previous three profiles (Figs. 49 and 47.). This fact is due to a combination of the profile having being taken from an area underlain by metasediments as opposed to granite and its not being exposed to the same volume of water as Site's A and E. The profile at C is similar to that of F in that all the radionuclides activities increase towards the bottom of the profile (Fig.50.). Profile C differs from the others however due to the fact that the $^{226}Ra/^{238}U$ ratio is relatively constant throughout the profile, remaining close to unity at all depths. Radionuclide levels at Site C are extremely low relative to those samples taken from within the depression. The obvious conclusion to be drawn is that Site C is not exposed to the same influx of radionuclides as are E and A, namely Clogher Burn and the unnamed stream flowing from the south. Also, as Site C lies on a south facing aspect overlying metasediments, percolating soil water is unlikely to bear the same level of radionuclides as water draining the granite area thereby removing another source of enrichment. Site F, located outside the localised area of enrichment, exhibits a markedly different radiological profile to Site's E and A (Fig.54.), but similar to Site C. Elevated activities are only found in the basal layers of the profile at Site F, the activity of ^{238}U being up to six times greater in the bottom layer than in the top. This feature is not as evident for ^{226}Ra for which the difference is much less distinct. The ^{226}Ra levels in the surface layers of Site F are unsupported by ^{238}U, the $^{226}Ra/^{238}U$ ratio being over 13 times higher at the surface than throughout the body of the peat.

Site C's position relative to the depression is clear from the low levels of iron and manganese present when compared to samples drawn from within the depression, samples from Site C being lower by up to a factor of 10 (Fig.49.) An interesting observation that may be made is that the amount of humic acid material (well decayed organic material) present in

each layer is only 0.2 - 0.5 times the amount of non humic organic material present (Table xiii., Appendix 1.), this situation seeming to indicate a relatively young soil or lack of decay of organic material due to reducing conditions, the second situstion (lack of decay) appearing unlikely given that Eh values at the site approach 200 mV. The low iron and manganese content of the profile at Site F reflects the fact that the site lies outside the area from which the E and A profiles were taken. The profile at F also exhibits greater levels of organic matter although the humic acid content remains comparable with the other sites (Fig.50.). The relatively high moisture content is reflected in the reducing nature of the soil but the pH remains constant throughout the profile.

The depth distribution of ^{238}U appears to be related to the redox status of the samples. The 0-15 cm and 15-30 cm layers of both the A and E profiles exhibit lower uranium levels than the deeper layers. Uranium levels are lowest for the upper layers of profile A which has a typical moisture level of approximately 50% compared with moisture levels of 80% for the profile at E. The effect of the water level of Clogher Burn is clearly displayed in the profile at A which exhibits iron pan formation at the 30-45 cm layer and whose radiological properties differ considerably on going across this boundary. ^{226}Ra levels (for the A profile) are at their highest at this depth while uranium levels are, conversely, at their lowest. The profile at E, which does not display such a marked difference in radiological properties (or Eh value) with depth, remains saturated for most of the year due to the bank from which it was drawn being some 30 cm lower than the bank at which A was located. Radionuclide levels at Site E all increase with depth, the lowest activities occurring within the upper layers of the profile. It must be assumed that the upper layers of the E profile are not saturated for all of the year and therefore undergo periods where the Eh value increases as

the soil becomes more oxidising. Such a process would explain the lack of ^{238}U in the upper layers of Site E.

While the results of the analysis of peat profiles provide evidence that radionuclide enrichment is due to infiltration of the peat with uranium bearing stream water, the results do not indicate the mode of occurrence of the radionuclides within the peat. In order to investigate possible relationships between the radionuclides and the chemical properties of the peat, a statistical analysis of the data using Spearmans correlation for non-parametric data was implemented to highlight possible correlation's. Detailed correlation matrices for the twenty five samples taken in Survey 2 (including profile samples) are provided in Appendix 3. All the radionuclides exhibit significant (99% level) positive correlation's with each other. U^{238} is not correlated with organic material, humic acid content, non humic content, cation exchange capacity or iron/manganese levels. ^{226}Ra exhibits significant negative correlation with the amount of non humic acid material ($r = -0.691$) and a weaker (significant at 95% level) correlation with the amount of organic material present ($r = -0.402$). This correlation is not evident for ^{228}Ra indicating some difference in the behaviour of the two radium isotopes, most probably due to the difference in their half-lives and the differing behaviour of their parent radionuclides.

Despite the strong opinions voiced in the literature by Szalay (1964), Idiz *et al* (1986) and Halbach *et al* (1980) among others regarding the positive association of uranium with organic matter and humic acids, there is no evidence of this in the correlation analysis of the data. It should be noted however that the inclusion of samples from Sites E and C may have prejudiced the analysis given that these sites have not undergone the same level of enrichment as Sites E and A. A repeat analysis of the data set, omitting samples from C and F, did not produce

evidence of any correlation either. Neither is it possible to discount the views of Lowson et al (1986) and Megumi (1979) regarding the association of uranium with amorphous iron oxides based on the lack of correlation between uranium (or any of the other radionuclides) and iron levels in the peat samples. However, as Site A contained a large proportion of iron in a solid concreted form, all five depth samples from Site A were removed and a plot of ^{226}Ra against iron level was constructed. As no other site bore evidence of iron in this form, it is assumed that the majority of iron in the remaining samples was amorphous and therefore some evidence should be present if a relationship exists between ^{226}Ra and amorphous iron. Figure 51 appears to suggest higher ^{226}Ra levels in soil samples that contain higher levels of amorphous iron. Little or no relationship is observed for a similar plot involving ^{238}U levels (Fig. 51.). No relationship could be observed for ^{228}Ra. Although no mention of the relationship between solid forms of soil iron and radionuclides is made in the literature, pieces of the solid iron oxide layer were subjected to radiometric analysis (Table VIII.). It can be seen from Table VIII. that relatively little ^{228}Ra is found associated with the solid iron oxides although it would appear that significant amounts of ^{226}Ra and ^{238}U may be associated with this material.

Two points however should be borne in mind. The first is that the analysis of the material indicated a 10-15% content of organic material, most probably as inclusions within the solid material as the surface had been cleansed prior to radiometric analysis. A proportion of the radionuclide content of the concreted iron material may therefore have been associated with these organic matter inclusions. The second point is that amorphous forms of iron may have been associated with the material, the subsequent results including the radionuclides in this

material. Therefore it may be possible that the radiological results for this material may be slightly elevated.

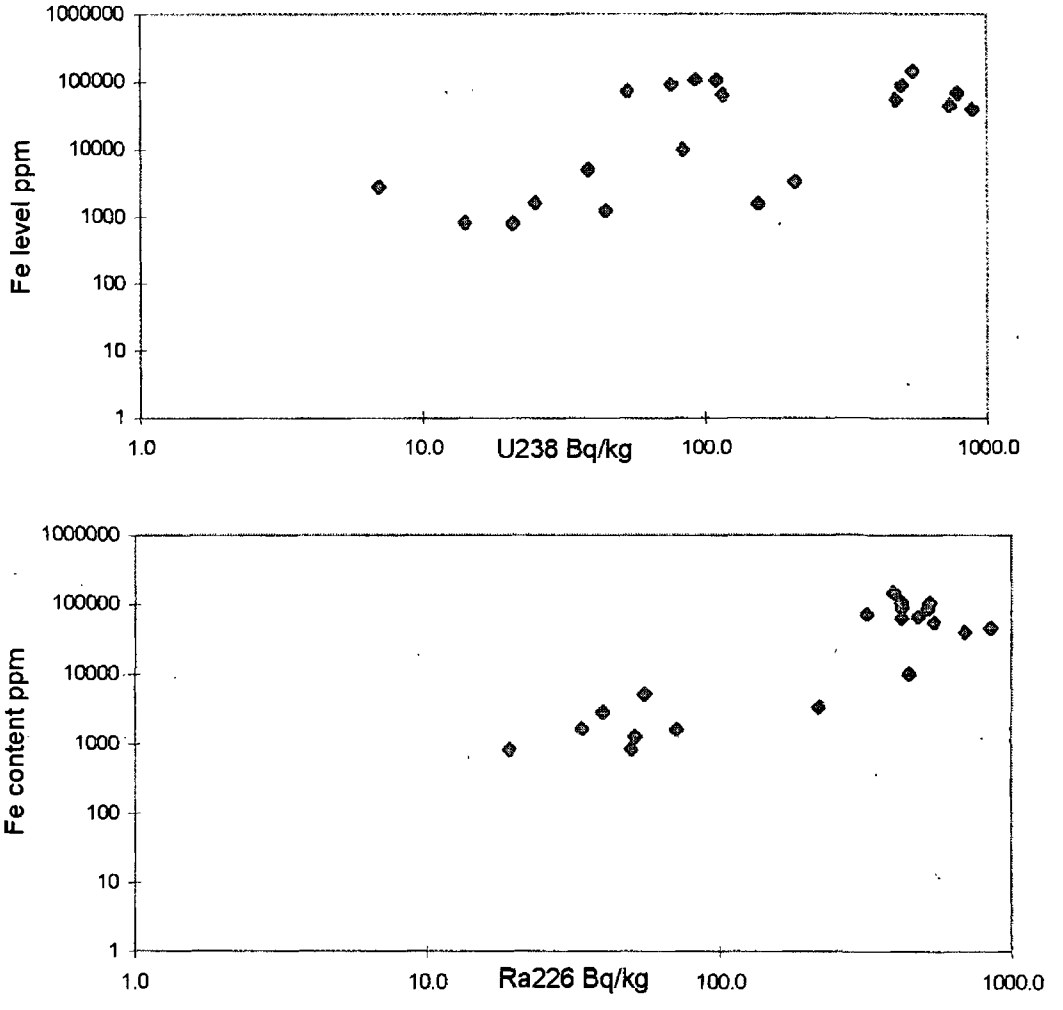

Figure 51. Plots of ^{238}U and ^{226}Ra against iron levels after removal of Site A samples from the data set. Note log axes.

Sample	^{238}U Bq/kg	^{226}Ra Bq/kg	^{228}Ra Bq/kg
1	125.2	248.26	6.9
2	140.5	220.6	10.1
3	110.8	185.1	8.9

Table IX. Radionuclide levels in solid iron oxide removed from Site A.

Although many authors (Sheppard, 1980) report on the immobility of thorium in the surficial environment, there is some evidence from the depth profiles that enrichment of soil with ^{232}Th has occurred although the level of enrichment is less than for ^{238}U. If levels of ^{232}Th (inferred from ^{228}Ra levels) in the depression are compared with levels at Site F, this site being outside the depression but overlying the granite, it may be seen that the basal layer of Site E has 2.1 times as much ^{232}Th as the corresponding layer of site F (Table vii., Appendix 1.), the same layer of Site E having 10.1 times as much ^{226}Ra and 4.8 times as much ^{238}U. Although the peat within the depression appears to be enriched in ^{232}Th comparison of these ratios indicates that, of the three radionuclides, the level of enrichment is lowest for ^{232}Th. As enrichment implies a movement of nuclides from one location to another, it would appear that ^{232}Th is the least mobile of the radionuclides based on the results of this study.

A number of the features exhibited by the peat profiles are supported in the literature. The occurrence of the highest radionuclide levels in the basal layers of profile F (which is assumed to be representative of conditions pertaining in the peat overlying the granite in general) is in agreement with the findings of Kochenov (1965), Wilson (1984), and Greeman and Rose (1990). Kochenov (1965) hypothesises that uranium

enrichments occur in areas (gullies and valleys) fed by stream waters, in accordance with the findings of this project, this view also being upheld by Landstrom and Sundblad (1986). The occurrence of uranium enrichment in these areas would also go some way towards explaining the localised uranium enrichments found in the valley during the prospecting of the 1970's (Irish Base Metals, 1978). The production of localised enrichments by such a process also explains why many of the enriched areas found by the prospectors were found to be unsupported in the underlying rock.

4.2.3.3. Summary

With respect to the occurrence of elevated radionuclide levels within the depression originally identified as location X, the previous sections indicated that an influx of water (Clogher Burn and an unnamed drainage stream), bearing trace amounts of radionuclides, has resulted in peat found within the depression exhibiting elevated levels. This conclusion is supported by a number of facts. Both Sites C and F were taken from outside the depression, neither site exhibiting the same level of enrichment as those taken from within. The ^{238}U content of the peat sections at Site A appear to suggest that the occurrence of this nuclide in the peat is related to the samples position relative to the water level in Clogher Burn. Site E, whose lower depths remain saturated permanently exhibit the highest levels of ^{238}U, the upper levels of Site A, which are rarely saturated, exhibit the lowest. The upper levels of Site E and the lowest sections of Site A, which undergo comparable saturation, have comparable ^{238}U levels. The redox state of the peat also seems to exert some control over the levels of ^{238}U. The upper layers of both Sites A and E are more oxidising than the lower levels and exhibit the greatest depletion of ^{238}U. This fact conforms to the accepted notion that ^{238}U is most mobile in an oxidising environment, the U^{6+} state being more

soluble than the U^{4+} state. Combining this fact with the results of the previous analyses leads to the conclusion that radionuclide enrichment in the water saturated depressions of the Cronamuck valley is via an influx of water bearing at least amounts of radionuclides into a region where the prevalent chemical conditions are conducive to the retention and accumulation of these radionuclides.

Although the previous section has highlighted the probable reasons for the elevated radionuclide levels within the depression, no information has yet been provided in relation to the mode of association between the radionuclides and the soil constituents. In order to investigate the relationship between the soil and the radionuclides a selective extraction procedure was employed, the results of which are detailed in the following section.

4.2.4. Radionuclide speciation

With a view to obtaining a greater insight into the chemical parameters influencing radionuclide accumulation within the enriched areas of the valley, and to determine the mode of occurrence of the radionuclides, a sequential chemical extraction of the peat was conducted. As only the peat of the enriched area was of interest in this regard, the profiles taken at C and F were not included in this analysis, reducing the total number of samples in this data set from twenty-five to seventeen.

4.2.4.1. Sites A and E

Results of the speciation analysis at Site A indicate that ^{238}U is bound primarily in the amorphous iron oxide fraction of the upper layers of Site A (Fig.52). The amount of ^{238}U incorporated in this layer remains relatively constant throughout the profile, as does the amount occurring

as exchangeable cations, a minor proportion of the total level. The most obvious feature of the profile is the change in the amount of ^{238}U occurring in the easily oxidisable organic matter on traversing the iron pan at 30 - 45 cm.

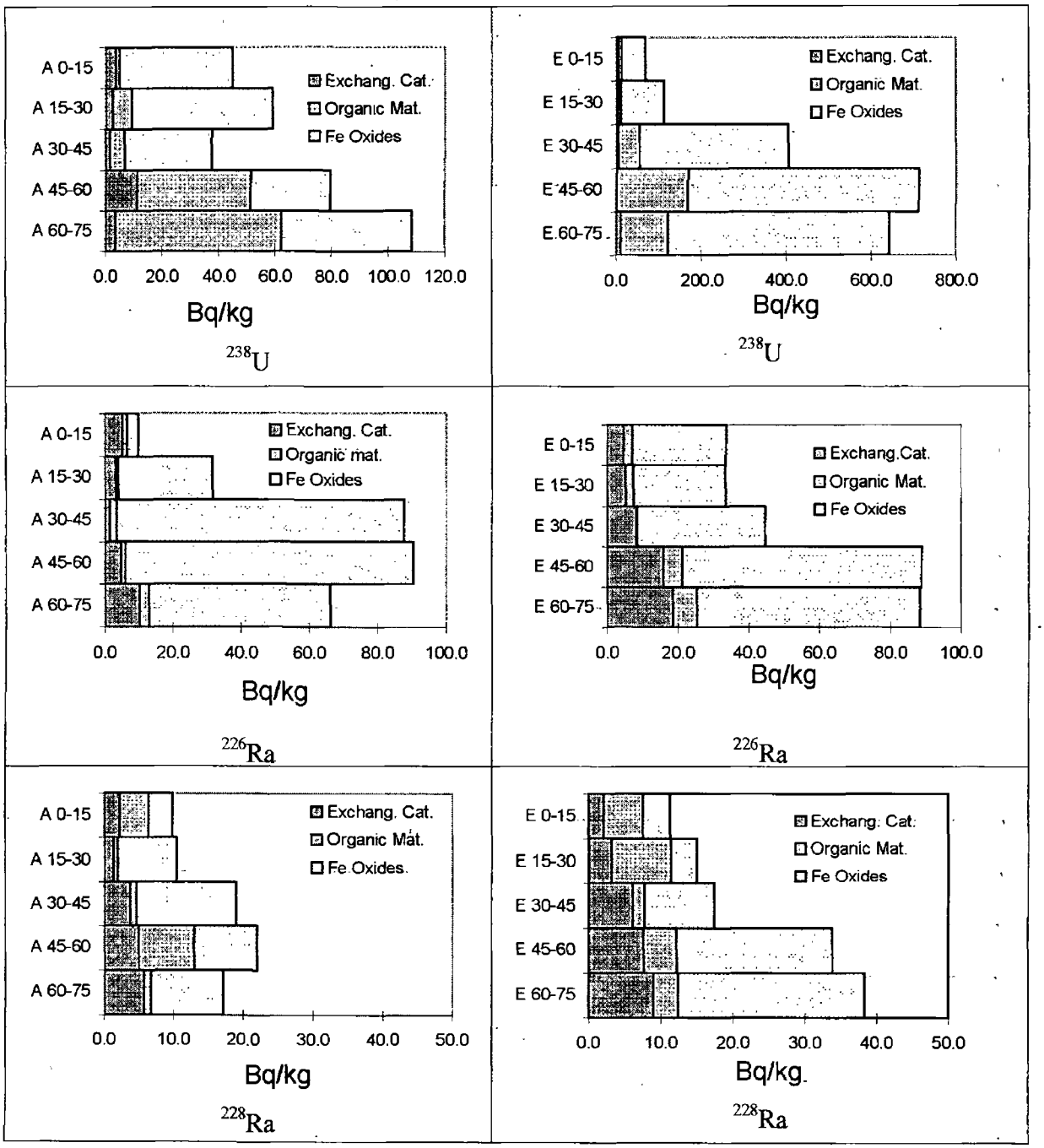

Figure 52. Speciation of ^{238}U, ^{226}Ra and ^{228}Ra at Sites A and E.

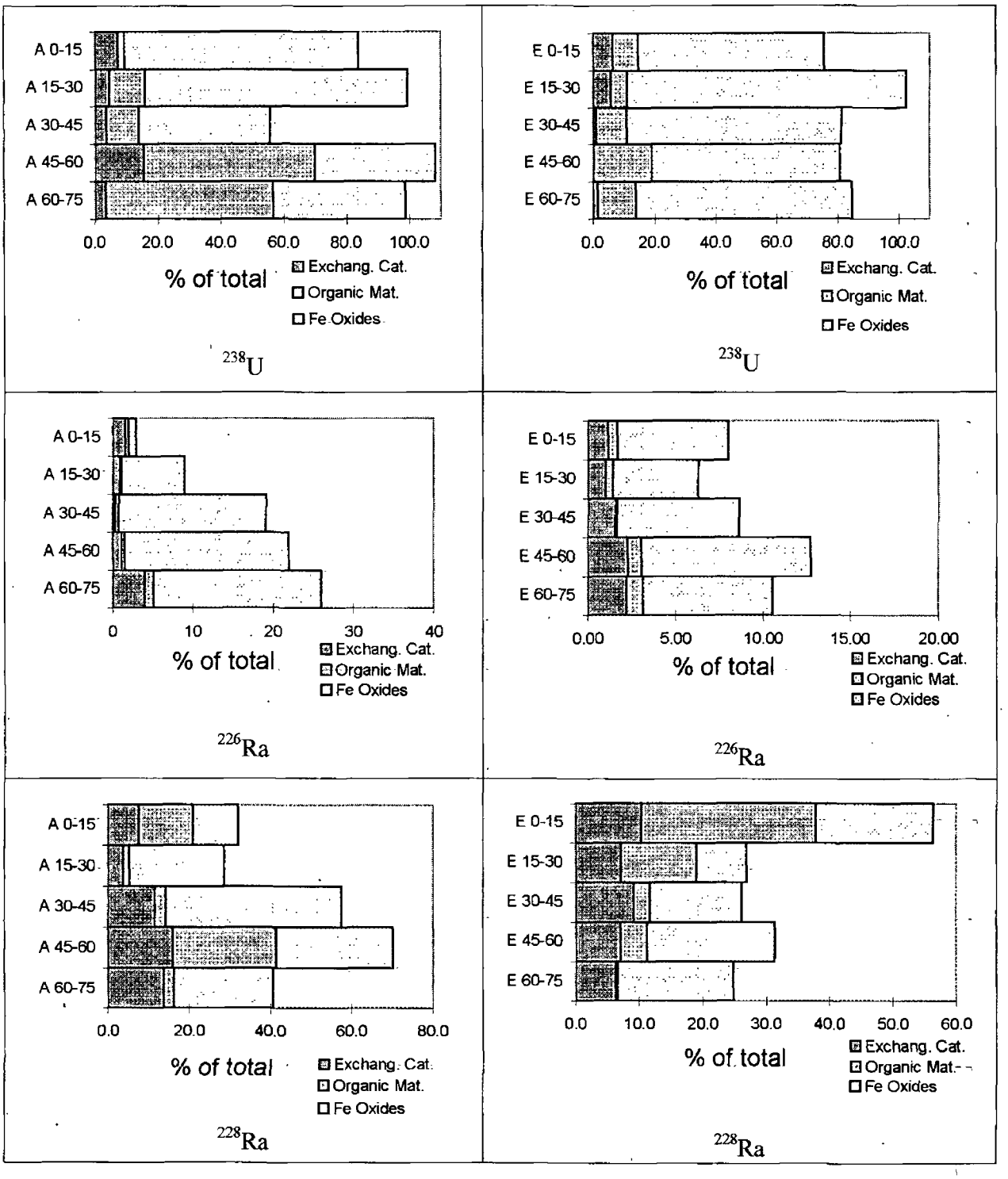

Figure 53. ^{238}U, ^{226}Ra and ^{228}Ra contents of individual fractions expressed as a percentage of total sample activity.

Up to 50% of the total ^{238}U in the soil at the lower depths of Site A occurs in the easily oxidisable organic fraction, this percentage dropping to less than 10% in the upper three layers. This finding is indicative of a loss of uranium from this fraction within the upper layers of the soil, above the iron pan, at Site A. No layer of the profile from Site A exhibits the same proportion of ^{238}U associated with this fraction as the layers at site E (Fig.53.) which are all greater than 60% . This loss of uranium from the easily oxidisable fraction in the upper layers of Site A is supportive of the views of Idiz *et al* (1986), Goldhaber et al (1987) and Ames and Dhanpat (1978) who all highlight redox processes as a factor governing the ability of humic acid/organic material to retain uranium. As the upper layers of Site A are more oxidising due to their lower saturation level, it would appear that the lower levels of uranium in these layers is due to either a loss of uranium via oxidation and loss in solution or a reduction in the ability of this fraction to retain uranium under oxidising conditions.

^{226}Ra also displays predominance in the iron oxide fraction at Site A, little or no ^{226}Ra occurring in the other two fractions analysed (Fig.52.) However, unlike ^{238}U, a smaller proportion of the total ^{226}Ra is bound in the labile fractions (i.e. exchangeable cations + amorphous iron oxides + easily oxidisable organic matter). This fact supports the views of Titaeva (1967) who ascertained that radium is associated with organic residues that are insoluble (i.e. non-humified) in NaOH. As the hypochlorite extraction does not remove the more resistant organic residues (Kogel-Knaber and Hatcher, 1989), it would appear that a significant proportion of the ^{226}Ra present at the site is present in that form. The lack of ^{226}Ra in the labile fractions is not unexpected given the immobility of radium in such environments (Burns *et al*, 1991) and indeed, the proportion of the total ^{226}Ra bound in the labile fractions at Site A is in approximate agreement with the proportions calculated by Greeman and Rose (1990).

^{228}Ra also features strongly in the amorphous iron oxide fraction but does appear to have a stronger association with organic material than ^{226}Ra although a significant proportion occurs with iron oxides (Fig.53.).

^{238}U occurrence at Site E is also predominantly within the amorphous iron oxides although the amount in this fraction does vary with depth by up to a factor of 4 (Fig.52.). In a similar pattern to Site A, the lowest occurrence in the organic fraction is associated with the upper layers of the profile, the amount increasing significantly with depth. Converting the values to percentages of total activity does however, display a different pattern to that exhibited at Site A (Fig.53). In contrast to Site A, the increase in the proportion of U^{238} occurring in the easily oxidised organic matter with depth is not as pronounced. The top two layers of Site E which display the lowest ^{238}U content appear to follow the same approximate distribution of the nuclide among the three fractions as the deeper three layers which contain the most ^{238}U. This is presumably due to the fact that the upper levels of Site E are never as oxidising as the same levels of Site A and hence uranium loss is not as severe as for Site A.

^{226}Ra levels in each fraction at Site E increase steadily on going down the profile (Fig.52.), the highest levels occurring in the amorphous iron oxide fraction. The proportion of this nuclide bound in the iron oxide fraction is less at Site E than at Site A, the proportion never exceeding 13% of the total present in the sample. The proportion of the total ^{226}Ra present at Site E in the labile fractions is greater than the proportion present at Site A in the same fractions by more than a factor of two at all levels of the profile.

4.2.4.2. Individual Samples

A number of individual samples were also subjected to speciation analysis for comparative purposes. The radiological properties are presented in Table X., the speciation data being presented in Tables XI - XII. Chemical data for the samples is presented in Table xii., Appendix.1.

Sample	^{238}U Bq/kg	^{226}Ra Bq/kg	^{228}Ra Bq/kg
E1	53.1	320.4	18.6
E4	476.0	540.0	123.5
E5	115.3	421.6	38.8
E6	83.6	444.8	32.2
9	75.9	421.5	22.6
41	546.2	393.0	30.4
54	788.0	479.0	117.3

Table X. Radionuclide activities for individual samples of Survey 2.

Sample	^{238}U Ex.Cation	^{238}U Eas.Org.	^{238}U Fe Oxides
E1	2.0 (3.8)	19.9 (37.6)	31.0 (58.3)
E4	10.6 (2.2)	114.0 (23.9)	320.0 (67.2)
E5	17.5 (15.2)	54.0 (46.8)	40.1 (34.7)
E6	3.5 (4.2)	4.1 (4.8)	1.1 (1.3)
9	7.5 (10.0)	36.6 (48.2)	21.1 (27.8)
41	8.2 (1.5)	74.9 (13.8)	283.0 (51.8)
54	17.0 (2.2)	85.9 (10.9)	451.2 (57.2)

Table XI. ^{238}U speciation for individual samples of Survey 2. Values in brackets denote percentage of total ^{238}U activity.

Sample	^{226}Ra Ex.Cation	^{226}Ra Eas.Org.	^{226}Ra Fe Oxides
E1	1.6 (0.5)	2.5 (0.8)	76.0 (23.7)
E4	23.8 (4.4)	11.6 (2.1)	3.9 (0.7)
E5	37.5 (8.9)	9.6 (2.3)	17.7 (4.2)
E6	2.9 (0.6)	1.1 (0.3)	2.2 (0.5)
9	1.1 (0.3)	1.2 (0.3)	13.0 (3.1)
41	14.0 (3.5)	1.4 (0.4)	19.0 (4.8)
54	8.0 (1.6)	2.4 (0.5)	31.5 (6.6)

Table XII. ^{226}Ra speciation for individual samples of Survey 2. Values in brackets denote percentage of total ^{226}Ra activity.

Sample	^{228}Ra Ex.Cation	^{228}Ra Eas.Org.	^{228}Ra Fe Oxides
E1	4.7 (25.1)	2.1 (11.1)	9.7 (52.3)
E4	14.2 (11.5)	4.1 (3.3)	8.1 (6.6)
E5	3.9 (10.8)	3.8 (9.9)	2.3 (6.0)
E6	4.7 (14.5)	1.7 (5.2)	2.8 (8.6)
9	4.7 (20.6)	0.5 (2.2)	2.2 (10.1)
41	8.6 (28.4)	6.1 (20.1)	8.7 (28.6)
54	4.1 (3.5)	2.4 (0.5)	14.9 (12.7)

Table XIII. ^{228}Ra speciation for individual samples of Survey 2. Values in brackets denote percentage of total ^{228}Ra activity.

A number of facts present themselves on examination of the results for the individual samples. Four of the samples (E4, E5, 41 and 54) lie within the waterlogged depression marked in Fig.10. These samples contain relatively large amounts of U^{238} in the easily oxidisable organic fraction compared to the three samples lying outside the depression, although the proportions of this nuclide existing in this fraction are greater for these samples. The samples lying within the depression all contain greater amounts of ^{238}U in the amorphous iron oxide fraction than samples outside, ^{226}Ra values being comparable. Investigation of

how the radionuclides are distributed among the three fractions depending on how the samples are positioned relative to the water level of Clogher Burn also provides some insight into how the radionuclides behave within the soil. Samples E1, E6, E5 and 9 are positioned above the maximum level of water in Clogher Burn and are rarely saturated. Samples 54, 41 and E4 are regularly saturated, being positioned lower down in the depression (Fig.46). The former four contain, on average, 30.5% of the total ^{238}U content of the sample in the amorphous iron oxide fraction compared to an average of 58.7% for the latter three which remain more saturated (60.3% average moisture as opposed to 80.2%). Although ^{226}Ra levels are comparable between the two groups (470 Bq/kg and 402 Bq/kg), there is a disparity between the levels of ^{238}U exhibited. The saturated group contains an average ^{238}U level of 603.4 Bq/kg with the unsaturated group containing 82 Bq/kg ^{238}U on average.

In an attempt to explain the pattern of occurrence observed in the depth profiles at sites A and E and the individual samples, correlation between the levels of each radionuclide in each fraction and the studied chemical parameters was sought. As the occurrence of the radionuclides in the exchangeable cation fraction proved slight in most cases, this fraction was not included in the analysis. Detailed correlation matrices are provided in Tables xix - xxvii., Appendix.3.

^{226}Ra levels in the easily oxidisable organic fraction display significant (p = 0.01 level) correlation's with ^{226}Ra as an exchangeable cation indicating that easily removed ^{226}Ra (and hence very mobile) is due to its presence in the easily oxidisable organic fraction. Assuming that the ^{226}Ra present as an exchangeable cation is derived totally from the ^{226}Ra present in the aforementioned organic fraction indicates that, on average, 71% of the total ^{226}Ra bound in the easily oxidisable organic matrix

(easily oxidisable + exchangeable) is mobile. This implies that ^{226}Ra is not firmly bound in the easily oxidisable material and its immobility in soil must therefore be due to the predominance of its occurrence in the amorphous iron oxide fraction, a fact supported by the findings of the speciation analysis. This may be contrasted with the fact that exchangeable ^{238}U constitutes only 23%, on average, of the easily oxidisable + exchangeable, indicating strong binding of ^{238}U with easily oxidisable organic material. ^{228}Ra occurrence as an exchangeable cation constitutes, on average, 76% of total occurrence in the two fractions, a figure that is comparable to the ^{226}Ra value. Assuming ^{228}Ra to be an indicator for ^{232}Th implies that thorium bound to easily oxidisable material is relatively easily removed and hence mobile. ^{226}Ra levels in the amorphous iron oxide fraction are negatively correlated with humic acid levels indicating a possible role for humic acid in the occurrence of radium in the amorphous iron oxide fraction.

The role of organic material in the binding of uranium in peat is reflected in a positive correlation between ^{238}U levels in the easily oxidisable organic fraction and total ^{238}U levels. As ^{238}U levels in this fraction are positively correlated with the levels existing in the amorphous iron oxide fraction there may be an equilibrium (chemical) existing between levels of this nuclide in these two fractions. ^{238}U levels in the organic fraction are positively correlated with moisture levels in the soil. The predominant effect of moisture levels in the soil is to affect the redox condition of the soil, greater saturation producing a more reducing soil. No correlation however is observed between ^{238}U in any fraction and Eh value. In a reducing environment uranium is considered immobile (Sheppard, 1980) and this view is supported by the results of this analysis, samples with lower moisture levels having lower ^{238}U levels relative to samples exhibiting greater degrees of saturation. It is possible to conclude, however, that the samples with the lesser

degree of saturation and the lower ^{238}U content may be thus due to their not being exposed to the same volumes of uranium bearing water as the samples with greater saturation and corresponding higher uranium content. This seems improbable given the fact that samples exhibiting the lower levels of labile ^{238}U tend to contain relatively high levels of ^{226}Ra, some proportion of which, it must be presumed, came about via ingrowth from an initial concentration of ^{238}U. The conclusion is drawn therefore, that the samples taken from the depression, which contain the lower amounts of labile ^{238}U, must at some point have contained greater amounts of ^{238}U in these fractions, a large proportion of which has been lost via some change in the condition of the soil. The change most likely to have precipitated such a loss is a change from reducing conditions to oxidising conditions via a lessening in the degree of saturation of the soil.

4.2.4.3. Summary

In relation to the mode of occurrence of radionuclides within the studied depression, a significant finding is the fact that the total amount of uranium occurring in the depression is associated with the labile soil fractions. This is supportive of the previous findings of this study and is consistent with the conclusion that elevated uranium levels at the site are due to transport of the nuclide via the drainage system. The samples that display the greatest levels of apparent uranium loss all exhibit low levels of this nuclide in the easily oxidisable organic fraction. Consideration of this fact in light of the conclusions of the preceding Sections lends weight to the notion that redox status exerts a control over the association of, at least, uranium with humic acids and decayed organic matter. While much of the literature supports the concept of redox status controlling uranium retention on iron oxides, the effect of redox on the accumulation of uranium by organic matter has been studied

less frequently. The results of this study suggest that uranium retention by such material may be affected to a large extent by the prevailing redox status of the soil or peat. ^{226}Ra and ^{228}Ra have a much lower occurrence in the labile fractions of the soil and exhibit a certain level of disparity in their mode of occurrence, most probably due to their relative positions in their decay chains in relation to their nearest thorium parent and the differences in their half-lives. As radium exhibits a low level of solubility, it is likely that much of the radium within the depression arises via ingrowth from, primarily, uranium.

4.3. $^{226}Ra/^{238}U$ Secular Disequilibrium

An obvious feature of both Surveys 1 and 2 was the anomalous $^{226}Ra/^{238}U$ disequilibrium exhibited by samples lying within the enriched areas. The level of disequilibrium of the samples taken in Survey 2 is anomalous both in terms of the magnitudes of the ratios exhibited by the samples and in the varying levels of disequilibrium found at different depths within individual profiles and at different locations within the studied area. The disequilibrium condition within the area at location X is summarised below (Fig.54), the diagram indicating a large disparity between ratios for samples separated by relatively small distance. An initial examination indicates that samples lying outside the depression tend to have large excesses of ^{226}Ra relative to ^{238}U and that depth profiles tend to exhibit broadly varying ratios at different depths. The obvious questions therefore relate to whether the disequilibrium conditions observed are due to ^{226}Ra enrichment relative to ^{238}U or ^{238}U depletion relative to ^{226}Ra and why the enrichment/depletion occurs.

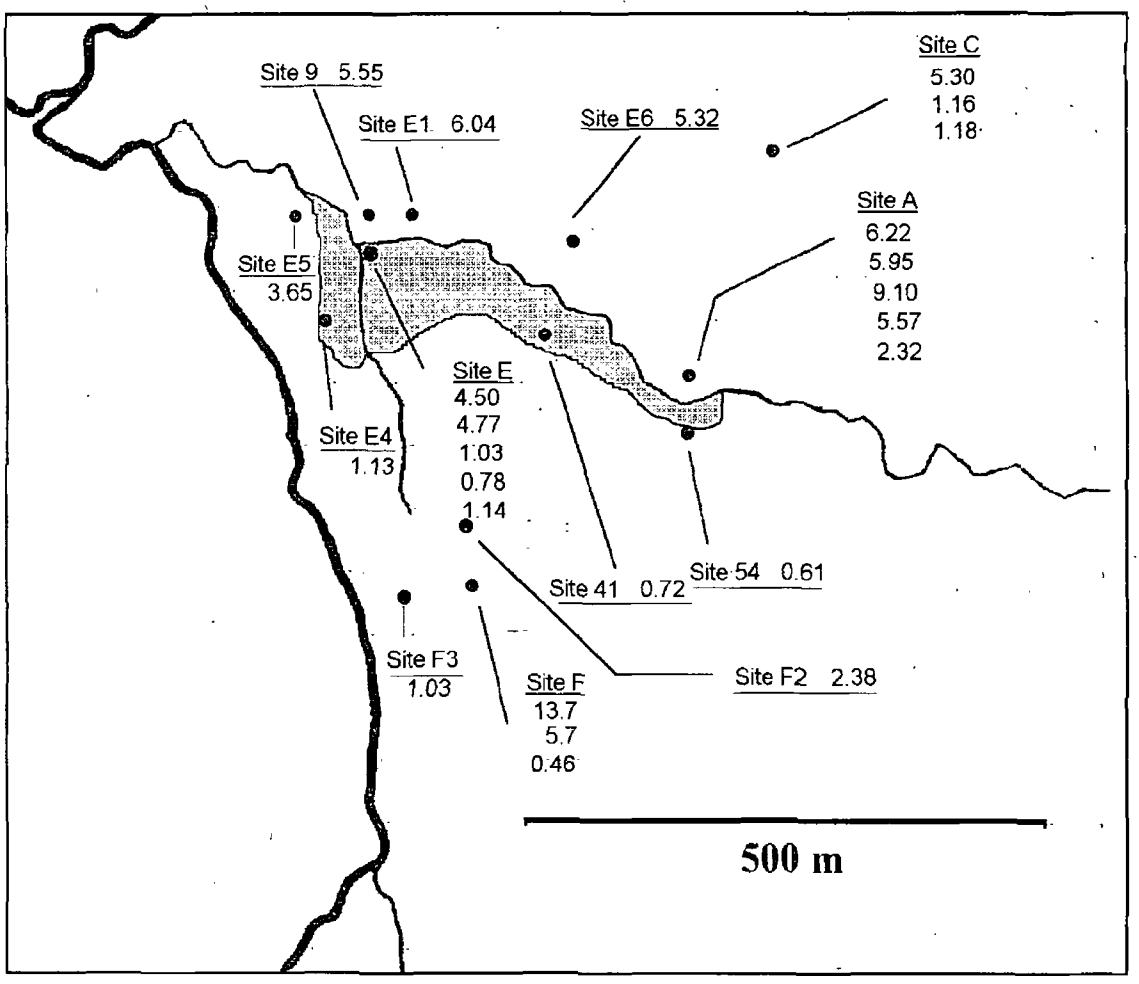

Figure 54. $^{226}Ra/^{238}U$ ratios for samples taken as part of Survey 2.

4.3.1. Radiometric Analysis

For the purpose of this investigation, the data set from Survey 2 was divided on the basis of whether or not a samples $^{226}Ra/^{238}U$ ratio was above or below the average $^{226}Ra/^{238}U$ ratio (1.71) for the entire valley. Such a division produced the following two sets of figures.

ABOVE 1.71		BELOW 1.71	
Sample	$^{226}Ra/^{238}U$	Sample	$^{226}Ra/^{238}U$
E 0-15	4.50	E 30-45	1.03
E 15-30	4.77	E 45-60	0.78
A 0-15	6.22	E 60-75	1.14
A 15-30	5.95	E 4	1.13
A 30-45	9.10	54	0.61
A 45-60	5.57	41	0.72
A 60-75	2.32	F 30-45	0.46
E 1	6.04	C 0-15	1.35
E 5	3.65	C 15-30	1.43
E6	5.32	C 30-45	1.15
9	5.55	F 3	1.05
F 0-15	13.70		
F 15-30	5.70		
F 2	2.38		

Table XIV . Survey 2 data set split on basis of sample's $^{226}Ra/^{238}U$ ratio relative to the Survey 1 $^{226}Ra/^{238}U$ average of 1.71.

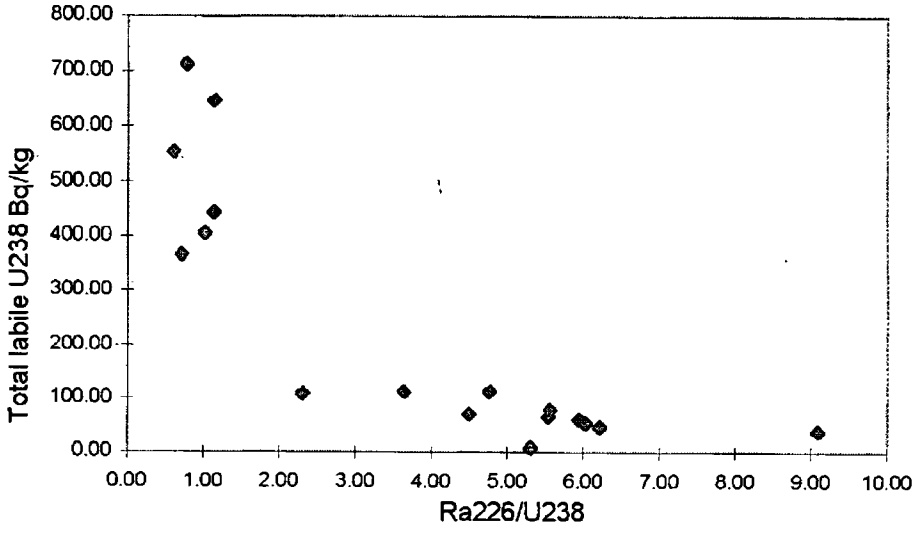

Figure 55. Plot of total labile ^{238}U (Bq/kg) against $^{226}Ra/^{238}U$

Assuming that uranium loss or enrichment would occur from within the labile fractions (exchangeable cations + amorphous iron oxides + easily

oxidisable organics), evidence was sought from within these fractions by plotting a graph of total labile ^{238}U against the $^{226}Ra/^{238}U$ ratio. Figure 55 provides some evidence for a relationship between the level of ^{238}U in the labile fractions of the soil and the disequilibrium condition of the sample. This graph does not however indicate whether enrichment or depletion of ^{238}U (relative to ^{226}Ra) has occurred, only that the level of ^{238}U in the labile fractions has a bearing on the $^{226}Ra/^{238}U$ ratio. As radium and thorium are assumed to be immobile in the surficial environment, some evidence for which has been provided by this study, then comparison of the $^{228}Ra/^{238}U$ ratio (adopting ^{228}Ra as an indicator of ^{232}Th) provides an indicator of whether or not ^{238}U has been enriched or depleted. A plot of $^{228}Ra/^{238}U$ against $^{226}Ra/^{238}U$ (Fig.56.) indicates that as the amount of ^{238}U present relative to ^{226}Ra decreases then a corresponding drop is evident in the amount of ^{238}U present relative to ^{228}Ra, and therefore, ^{232}Th. This point forces the conclusion that an increase in the $^{226}Ra/^{238}U$ ratio is caused by a loss of ^{238}U rather than a gain of ^{226}Ra.

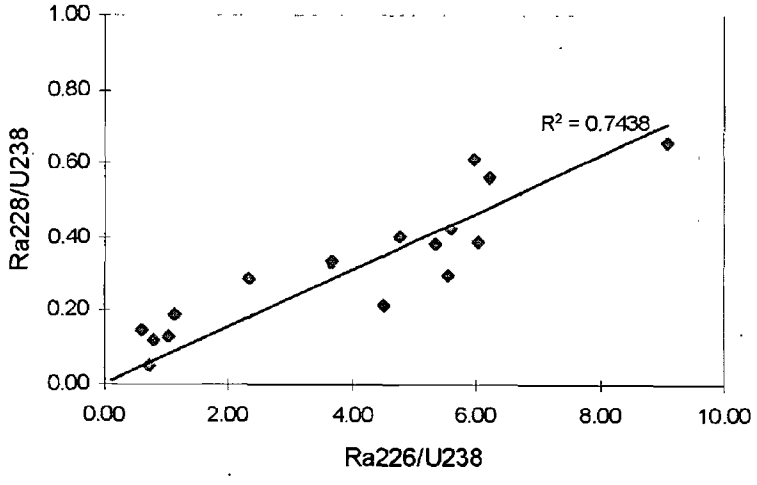

Figure 56. Plot of $^{226}Ra/^{238}U$ against $^{228}Ra/^{238}U$.

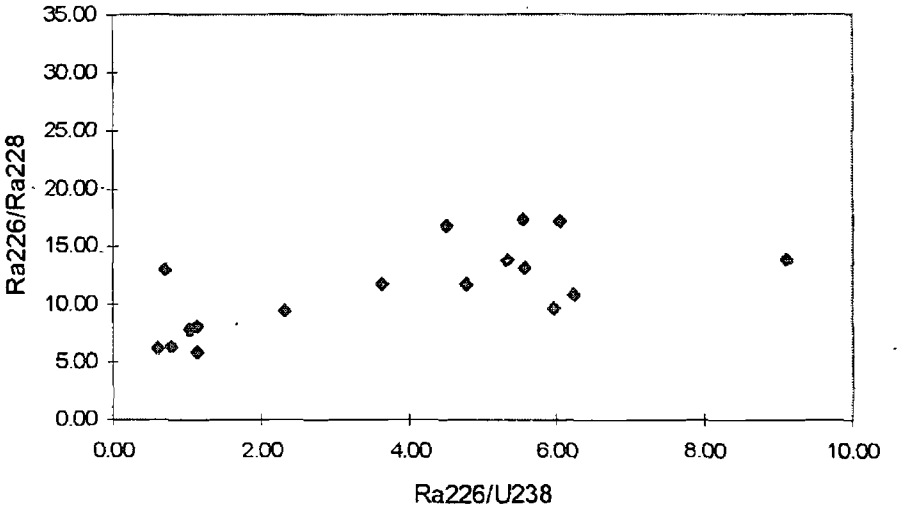

Figure 57. Plot of $^{226}Ra/^{228}Ra$ against $^{226}Ra/^{238}U$.

This conclusion is supported by the relationship between ^{226}Ra and ^{228}Ra at various $^{226}Ra/^{238}U$ ratios (Fig.57.). The amount of ^{226}Ra present in the soil compared to the amount of ^{228}Ra remains relatively constant irrespective of the $^{226}Ra/^{238}U$ ratio, a condition that would not exist were varying $^{226}Ra/^{238}U$ ratios due to influx or loss of ^{226}Ra. In order to ascertain from which of the labile fractions uranium is lost, plots of ^{238}U levels in both the amorphous iron oxides and easily oxidisable fractions were constructed (Fig.58).

Elevated $^{226}Ra/^{238}U$ ratios appear to be related to loss of uranium from both the easily oxidisable organic material and amorphous iron oxides. Although it appears that elevated $^{226}Ra/^{238}U$ ratios are due to loss of ^{238}U from the labile fractions of the soil, it is worth considering again if the disequilibrium state is due to an influx of ^{226}Ra to the soil (most probably via drainage water as discussed in section 4.1.5. Assuming such

an influx has occurred, it would be expected that the labile fractions of soils exhibiting high $^{226}Ra/^{238}U$ should contain high ^{226}Ra levels.

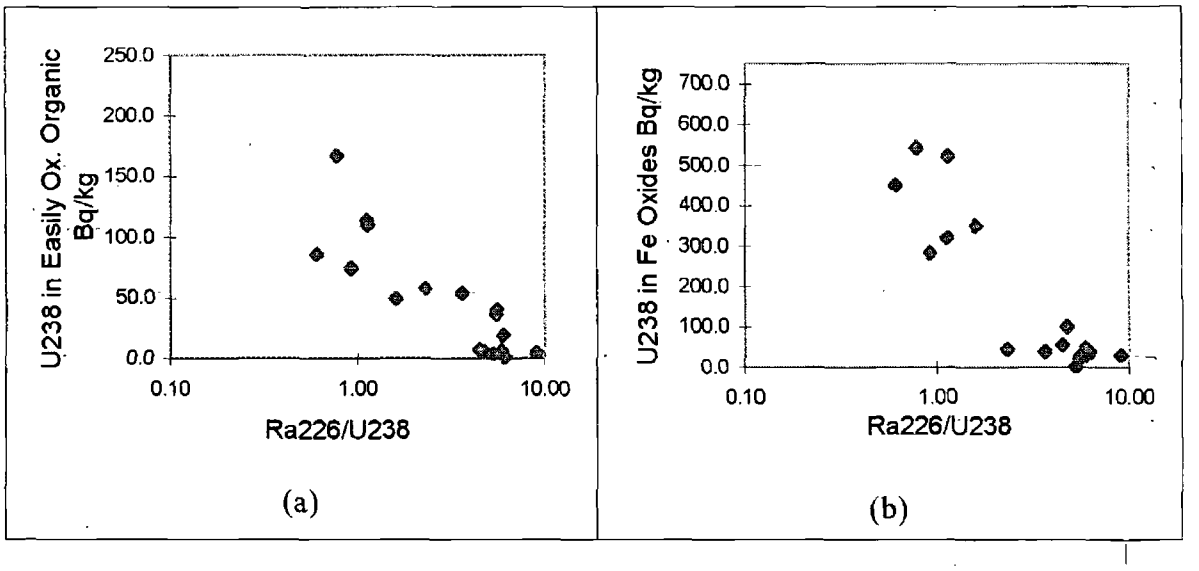

Figure 58. Plots of ^{238}U in (a) easily oxidisable organic fraction and (b) iron oxides fraction against $^{226}Ra/^{238}U$. Note log scale.

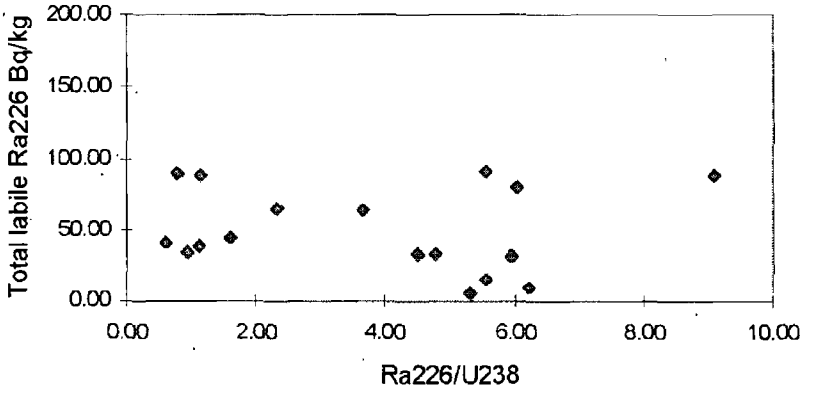

Figure 59. Plot of total labile ^{226}Ra against $^{226}Ra/^{238}U$.

Figure 59. provides no evidence of elevated labile ^{226}Ra at higher $^{226}Ra/^{238}U$ ratios. Greeman and Rose (1992) hypothesise that elevated ^{226}Ra relative to ^{238}U may be due to selective cycling of ^{226}Ra by plants at the soil surface. A series of measurements of the radionuclide content of plants growing at the site were made in order to investigate whether or not this may be so. Four individual samples were taken from Site A

and four were taken from Site E, results being displayed in Table XV. There is no evidence of ^{226}Ra enrichment by vegetation at the sites, samples displaying ^{226}Ra activities greater than those of ^{238}U approaching the average soil ratio for the valley. Samples drawn from Site E, whose surface layers exhibit excessive ^{226}Ra relative to ^{238}U, display preferential uptake of uranium which would seem to discount the theory that selective uptake of ^{226}Ra may account for elevated $^{226}Ra/^{238}U$ ratios.

Sample	^{238}U Bq/kg	^{226}Ra Bq/kg	^{228} Ra Bq/kg	$^{226}Ra/^{238}U$
1 A	124.0	201.6	84.6	1.63
2 A	132.1	188.3	79.5	1.43
3 A	140.3	175.6	81.0	1.25
4 A	110.5	198.7	75.8	1.80
1 E	462.2	271.3	192.4	0.58
2 E	390.5	241.8	175.9	0.62
3 E	420.1	220.3	180.0	0.52
4 E	378.9	205.7	160.2	0.54

Table XV. Radionuclide activities for vegetation sample drawn from Sites A and E.

Although radiometric analysis of vegetation from the sites does not indicate preferential uptake of ^{226}Ra to such an extent that would account for observed excess, two further points should be taken into account. The average lifespan of vegetation at the sites is undoubtedly short relative to the age of the soil, therefore small excesses of ^{226}Ra in plant tissues could feasibly result, over a time period corresponding to many life cycles, in ^{226}Ra excess as observed in the soil samples. This point is supported by the fact that, on average, 89.5% of the total ^{226}Ra

resides in non labile fractions. Assuming that the non-labile fractions contain resistant or non-humified organic material + rock residues ("float") + mineral residues (concreted manganese and iron oxides), then estimation of the amount of ^{226}Ra in the non-humified organic residue may be made using the ^{226}Ra contents of these materials and their relative proportions per unit mass of soil. On average, 75% of the total ^{226}Ra per unit soil mass is associated with the resistant organic fraction, compared to negligible amounts of ^{238}U, although there is no apparent relationship between the amount of ^{226}Ra in this fraction and the observed disequilibrium (Fig.60.). The fact that little or no ^{238}U resides in this fraction cannot be explained by the results of this study and is a point worthy of further investigation.

A second mechanism that may account for excessive ^{226}Ra is preferential leaching of ^{226}Ra from the underlying lithology during soil formation processes. Such a process should lead to observable depletion of ^{226}Ra relative to ^{238}U in the rock, however a series of sample from the area show no evidence of this, $^{226}Ra/^{238}U$ ratios being close to unity (Table. XVI).

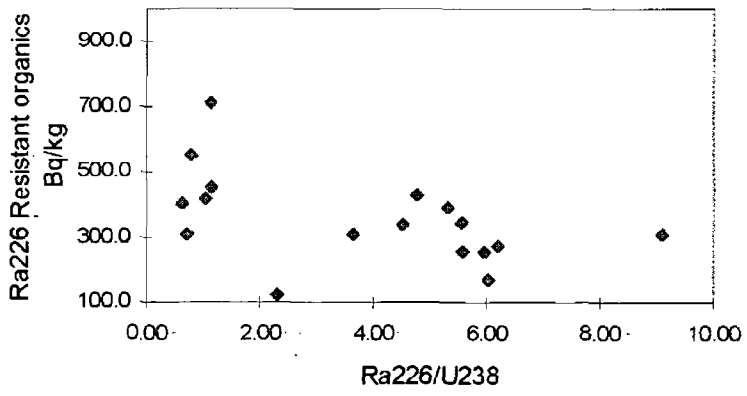

Figure 60. Plot of ^{226}Ra in the resistant organic fraction against $^{226}Ra/^{238}U$ disequilibrium.

Sample	^{238}U Bq/kg	^{226}Ra Bq/kg	^{228}Ra Bq/kg	^{226}Ra/^{238}U
1 A	134.6	145.4	86.1	1.08
2 A	168.0	150.6	98.2	0.89
3 A	157.4	132.9	79.2	0.84
4 A	146.2	128.7	74.6	0.88
1 E	143.2	164.5	98.6	1.15
2 E	174.1	152.9	106.7	0.88
3 E	156.2	148.9	101.0	0.95
4 E	159.8	127.0	96.2	0.79

Table XVI. Radionuclide content of rock samples from Sites A and E.

In order to further investigate whether or not the observed disequilibrium ratios were due to ^{238}U depletion or ^{226}Ra enrichment, the two sample groups (Table XIV.) were analysed for significant differences in their radiological characteristics using a Mann-Whitney Rank Sum test for non-normally distributed groups. Significant differences were detected between the two groups for a number of variables. ^{238}U (p = 0.023), ^{228}Ra (p = 0.011), ^{226}Ra/^{238}U (p = <0.001) and ^{226}Ra/^{228}Ra (p = <0.001) were all significantly different between the two groups. No significant difference was observed for ^{226}Ra (p = 0.603) or ^{228}Ra/^{238}U (p = 0.147). While the differences between the two groups in relation to ^{238}U and ^{226}Ra/^{238}U were expected, the result in relation to ^{226}Ra/^{228}Ra and ^{228}Ra were not and remain unexplained at this point. Supporting the theory that loss of ^{238}U has occurred from samples exhibiting elevated ^{226}Ra/^{238}U ratios is the fact that a significant difference (p< 0.001) exists between the two groups in relation to the amount of labile ^{238}U present in the samples, samples with ratios below 1.71 containing, on average, 521 Bq/kg of labile ^{238}U and samples with ratios above 1.71 containing only an average of 68.2 Bq/kg. The argument that the observed elevated ^{226}Ra/^{238}U ratios are due to loss of

^{238}U from the labile fractions is supported by the strong differences exhibited by the two groups in relation to ^{238}U levels in the easily oxidisable fractions and amorphous iron oxides (p = 0.002 and 0.001 respectively). No difference exists between ^{226}Ra levels in either of these fractions.

The previous discussion has sought to explain the observed disequilibrium ratios of the samples from Survey 2 in relation to the mode of occurrence of the radionuclides and their distribution between the different fractions of the soil. The evidence so far presented appears to suggest a loss of ^{238}U relative to ^{226}Ra as explanation for elevated $^{226}Ra/^{238}U$ ratios in the samples. This does not account for the ratios exhibited by some samples which remain significantly below the average for the valley. In order to provide some explanation as to why ^{238}U is depleted in some samples and enriched in others (samples being separated by relatively small distances), a detailed examination of the chemical conditions pertaining to the samples is necessary.

4.3.2. Chemical Analysis

Examination of the conditions pertaining at the site and a knowledge of the chemical behaviour of the radionuclides in question allows for conclusions to be drawn about the likely processes that have resulted in the disequilibrium conditions observed. This discussion will concern itself with how chemical conditions may have a bearing on the disequilibrium observed, a detailed description of the chemical properties of the samples having being provided in Section 4.2.3 . Raw data for the chemical properties of all the samples of Survey 2 may be found in Appendix 1.

Having divided the data set of Survey 2 on the basis of $^{226}Ra/^{238}U$ disequilibrium relative to the average value for the valley of 1.71 (calculated from the data set of Survey 1), an analysis of the data pertaining to chemical conditions was conducted. On the basis of a Mann-Whitney test, the only chemical parameter that is significantly different between the two groups is moisture content. Samples whose ratios lie below 1.71 value contain an average of 80.1% moisture, samples whose ratios are above 1.71 containing an average of 65.5% moisture. While this difference does not seem great, the situation may be clarified by removing samples from Site F (which does not lie strictly within the enriched area) which reduces the average moisture content of samples with ratios above 1.71, to 60%. The moisture content of samples whose ratio is below 1.71 is therefore, on average, some 33% greater than for samples with ratios above 1.71. This difference in moisture content, most probably related to the positions of the samples relative to the Clogher Burn stream and its associated depressions (see Fig.54.), raises two possibilities. The first is that loss of uranium from the elevated $^{226}Ra/^{238}U$ samples has occurred for some reason related to the moisture level of the soil, or secondly, that enrichment of these samples with uranium never took place. The second hypothesis assumes that initial enrichment of the samples with uranium took place via saturation of the soil with uranium bearing stream water.

The second hypothesis, that enrichment of the soil never occurred due to the positioning of the soil relative to the stream , seems unlikely for a number of reasons. ^{226}Ra is considered immobile in the surficial environment and is unlikely to have reached the levels displayed in the soil by any other means than ingrowth from ^{238}U. There is no evidence of enrichment of ^{226}Ra in the soil via preferential leaching of the nuclide from the underlying rock, nor is there any real evidence for the enrichment of the nuclide via plant cycling (see section 4.3.1.). It is also

unlikely that the samples whose ratios are above 1.71 always contained the same amount of moisture that they do now, the depth of the soil having increased over time.

The initial hypothesis, that samples previously enriched with uranium, via saturation with uranium bearing stream water, underwent a subsequent loss of uranium, seems more likely. The previous discussion has indicated that statistical evidence points to a loss of uranium from the labile fractions of the soil. The most obvious situation that would result in such a loss is a change in either the source of uranium to the soil and/or a change in the chemical conditions of the soil affecting the ability of the soil to retain uranium. The most significant impact on soil uranium chemistry that a drop in the water content of the soil would have is a change in the redox status, a reduction in water content increasing the oxidative nature of the soil.

The scenario of loss of uranium from previously enriched peat resulting in elevated $^{226}Ra/^{238}U$ ratios is well supported in the literature. The loss of uranium from organic material via oxidation has been previously reported as causing $^{226}Ra/^{238}U$ disequilibrium in peat bogs by Zielinski *et al*, (1986) and Levinson *et al* (1984). The categorical statements of Ivanovich and Harmon (1992), that secular disequilibrium arises as a result of loss of uranium relative to immobile daughter nuclides, is well supported by the results of this study. Other proposed processes resulting in elevated $^{226}Ra/^{238}U$ ratios (plant enrichment, deposition etc.) are not in accordance with the results of this project.

4.3.3. Summary

Based on the results obtained in this study, the most likely cause for anomalous $^{226}Ra/^{238}U$ disequilibrium appears to be loss of ^{238}U. Samples

whose Ra/U^{226} average remains close to or less than the average value for the soils of the valley display appreciable levels of ^{238}U in the labile fractions whereas those exhibiting elevated ratios typically display a lack of ^{238}U in these fractions. The concept that ratios are elevated due to loss of ^{238}U is supported by the fact that $^{226}Ra/^{238}U$ ratios are highest in the more oxidising surface layers of the profiles where loss of uranium, as the more soluble hexavalent U^{6+}, is most likely. Uranium lost in this manner from the upper layers is unlikely to be replenished as the these levels only undergo periodic saturation with the water that is the most likely source of the uranium in the depression.

The loss of uranium is supported by the fact that a comparison of $^{226}Ra/U^{226}$ ratios with the ratio $^{228}Ra/^{228}U$ indicates a loss of uranium, relative to the immobile ^{232}Th, has occurred in samples displaying elevated $^{226}Ra/^{238}U$ ratios. Evidence provided by the previous discussion is supported by the results of the speciation analysis which indicate that conditions pertaining in the upper layers of the profiles within the depression are conducive to the loss of uranium via oxidation to the hexavalent state and subsequent loss in solution. The hypothesis that elevated ratios are as a result of the peat not being enriched by uranium in the first place are not supported by the evidence yielded by this study. The most obvious problem with such a theory is the presence of significant amounts of ^{226}Ra in layers with high ratios. Given the relative immobility of ^{226}Ra, it appears that much of the radium present in these layers must have arisen via ingrowth from an initial level of uranium. As the peat of the upper layers of the profile must have, at some point in the past, been at a lower level than it is at present and would therefore have been in a similar position to the lower levels of Site E, i.e. undergoing uranium enrichment as a result of continuous saturation with uranium bearing water in a reducing environment.

6.0 CONCLUSIONS

The results of this project may be subdivided into two distinct groups, those pertaining to the distribution of the radionuclides within the valley and those relating to the mode of occurrence of the radionuclides within the areas of enrichment within the valley.

The distribution of uranium and thorium series radionuclides within the valley is largely governed by the underlying lithology, average ^{238}U soil levels are greater than the levels in soils underlain by metasediments by a factor of 4.6 within the granite region, average ^{226}Ra levels are greater by a factor of 4.9 and ^{228}Ra (^{232}Th) by a factor of 1.3. Statistical analysis confirms that a significant difference exists between soil radionuclide levels in the granite region and soil radionuclide levels in the region underlain by the metasediments. As no correlation is observed between any soil property likely to exert an effect on soil radionuclide levels and any of the radionuclide activities, it must be assumed that geology is the controlling factor governing the level of these radionuclides in the soil of the Cronamuck Valley. This assertion is fully supported by the results of a detailed geostatistical analysis, the final outcome of which was the production of isopleth maps of radionuclide levels within the valley. These maps highlight the strong level of control exerted by the underlying geology and serve to demonstrate the relative immobility of radium and thorium relative to uranium in this environment. The maps also support the findings of previous studies into the occurrence of natural radionuclides in this locality and the results concur with other research done into the occurrence of uranium and thorium series radionuclides in peat.

On a smaller scale, it may be seen that water flow and drainage patterns within the valley exert a level of control over the radionuclides

distribution. Evidence is provided by the regions of elevated radioactivity at the deepest parts of the valley, and by the occurrence of the highest levels in areas associated with water saturated depressions. The major sources of water to these depressions appears to be small drainage streams draining the granite region of the valley. Transport by water is responsible for the one enriched region not lying on the granite that was encountered in this study. This conclusion was based on examination of the contour maps in relation to the topographical features of the valley and the likely drainage patterns.

The results of the geostatistical survey indicate that soil levels of natural radionuclides are amenable to this form of analysis, a high degree of spatial correlation having being exhibited by all the radionuclides studied. Geostatistical procedures applied to the problem of spatial analysis of natural radionuclides offer significant advantages over more traditional estimation procedures, results obtained in this study indicating that the estimation procedure known as kriging significantly out-performs a number of other estimation procedures over a wide variety of parameters that may be used to test estimation effectiveness. The smoothing effect of the kriging process tends to produce low estimates for high values and *vice versa*. This feature may tend to limit the usefulness of the technique as a means of identifying areas of elevated radioactivity on a larger scale or during surveys designed to ensure compliance with regulatory controls, but on the scale of the project whose results are reported here, the technique does exhibit advantages in relation to the reliability of the ultimate output. Many of the problems associated with the implementation of geostatistical procedures may be avoided by examination of the data prior to actually carrying out the estimation.

Further work suggested by the results of Survey 1 centres on the redistribution of radionuclides within the peat via water flow. The movement of uranium and thorium series radionuclides as a result of water flow within peat has not been covered in any depth in the literature. The results of this project suggest that drainage of water flowing off the granite region may result in transport of radionuclides away from the granite region, causing enrichment of peat underlain by a lithology not usually associated with high soil radionuclide levels. The processes involved in this transport are worthy of further study given the fact that prediction of indoor radon levels is often reliant on identifying lithologies that characteristically exhibit high levels of uranium. This study has shown that water transport of radionuclides may cause soil overlying a non-uraniferous rock type to become enriched in the radionuclides that ultimately give rise to indoor radon.

Geostatistical processes, combined with surveys of radionuclide levels, may provide some insight into the nature of water movements within peat bog areas. This study has shown that enrichment of radionuclides is associated with water flow patterns in the peat and it may be possible to map water flow using uranium series radionuclides as an indicator of flow patterns.

Based on the results of the study, it is reasonable to suggest that the redox condition of the soil exerts a strong influence over the accumulation of uranium and thorium series radionuclides. The association of areas exhibiting the highest levels of radionuclides encountered in the study are associated with heavily saturated areas of soil with correspondingly low Eh values, indicating the reducing conditions under which uranium is least mobile. The results of the speciation analysis indicate that in the oxidising upper layers of the soil, uranium is lost from the labile fractions which contain high levels of

uranium in the lower, more reducing bottom layers. It is this loss of uranium from the labile fractions that gives rise to the elevated $^{226}Ra/^{238}U$ ratios observed in the samples. ^{226}Ra is not associated with the labile fractions of the soil, appearing to reside in the undecayed plant material. ^{228}Ra, and by inference, ^{232}Th levels are evenly divided between labile and non-labile fractions. The study confirms the widely accepted immobility of radium isotopes in the surficial environment.

The behaviour of ^{226}Ra in relation to the processes governing its distribution between different soil phases remains unclear. The disparity of its behaviour relative to ^{238}U is worthy of further investigation. The precise location of ^{226}Ra within the soil fractions has not been identified by this study and work remains to be done on the mode of occurrence of this radionuclide in organic soils. Further work is also required with respect to the mode of transport of ^{226}Ra from the labile phases of the soil (with which its parent, ^{238}U, is associated) to the non-labile fractions where it is found in greatest quantities. The behaviour of nuclides intermediate in the decay chain between ^{238}U and ^{226}Ra, such as ^{230}Th, also warrants further attention, as it may be the behaviour of these nuclides that ultimately determines the location of ^{226}Ra within the soil. Although the effect of redox conditions on the occurrence of ^{238}U has been well demonstrated by this study, the results at hand yield no insight into the precise mechanisms involved in the association of uranium with either organic material or amorphous iron oxides.

This study highlights the localised occurrence of areas of elevated radioactivity in the peat overlying the studied part of the Barnesmore granite. The results also indicate the vulnerability of these areas with respect to changes in the redox conditions and the ability of the peat to retain the accumulated radionuclides. Of concern is the potential release of the accumulated radionuclides as a result of redox changes brought

about via the activities of the forestry companies currently involved in the afforestation of many upland bogs. The effect of bog drainage on uranium sinks in upland Irish bogs has not been assessed previously in this country and requires investigation for a number of reasons. This study only investigated a small portion of the Barnesmore granite and it is probable that there are a large number of enriched areas of peat (possibly exhibiting a much greater level of enrichment) within the greater granite region. It is therefore probable that a significant amount of uranium (and associated daughters) are vulnerable to release from the peat via changes in redox conditions as a result of drainage and aeration of the peat. The ultimate destinations for such nuclides once released are the numerous water courses draining the Barnesmore region. Given the predominance of private water supply schemes in the area, it is feasible that the radiological quality of such water supplies may be degraded should a large scale release of radionuclides occur. Of secondary concern is the use by the local population of peat drawn from these areas as a source of domestic fuel. Further work should therefore concern itself with an assessment of the radiological risk posed to the local population by possible releases of radionuclides from the "sinks" described in this study and by the abstraction of peat from these areas for domestic uses.

REFERENCES.

Adsley, Backhouse, J. S., Nichols, A. L. and Toole, J. ^{238}U Decay Chain.: Resolution of Observed Anomalies in the Measured Secular Equilibrium between Th^{234} and Daughter Pa^{234m}. *Appl. Radiat. Isot.* **49**. 1998. pp. 1337.

Aiken, G.R. Isolation and Concentration Techniques for Aquatic Humic Substances. in *Humic Substances in Soil, Sediment and Water: Geochemistry, Isolation and Characterisation*. (Aiken, G.R., McKnight, D.M., Wershaw, R.L. and MacCarthy, P. Eds.) Wiley-Interscience, New York. 1985. pp. 363. – 385.

Akin, H. and Bianconi, F. A Geostatistical Evaluation of the Napperby Surficial Uranium Deposit, Northern Territory, Australia. in *Surficial Uranium Deposits, I.A.E.A. Technical Document No.322*. Vienna. 1984. pp. 197 - 200.

Ames, L.L. and Dhanpat, R. Radionuclide Interactions with Soil and Rock Media Volume I. Processes Influencing Radionuclide Mobility and Retention, Element Chemistry and Geochemistry, Conclusions and Evaluation. *U.S.E.P.A. Rep. No. PB292460*. 1978. pp. 3-228 – 3-239.

Archard, F.K. Chemische Untersuchung des Torfs. Crells. Ann. **2**. 1786. pp. 391 – 403.

Armands, G. Geochemical Prospecting of a Uraniferous Bog, at Masugnysbyn, Northern Sweden. in *Geochemical Prospecting in Fennoscandia*. Kvalheim, A. (Ed.). Interscience, N.Y. 1967. pp. 127 – 154.

Arnold, W.D., Crouse, D.J. Radium Removal from Uranium Mill Effluents with Inorganic Ion Exchangers. *I&EC Process Design and Development*. **4**. 1965. pp. 335 - 337.

Arpesella, C., Bellotti, E., Miramonti, L. and Sverzellatti, P. P. Gamma Ray Activity of Neodymium Samples. *Nucl. Instrum. Methods. Phys. Res.* **A372**, pp. 415. 1996.

Badr, I., Oliver, M. A. and Durrani, S.A. Statistical Evidence of the Geological Control Over Radon Soil Gas Concentrations and its Implications for Mapping Radon Potential. *Radiat. Prot. Dosim.*, **63**. 1996. pp. 281 – 291.

Baeza, A., DelRio, M., Miro, C. and Paniagua, J. Natural Radionuclide Distribution in Soils of Caceres (Spain): Dosimetry Implications. *J. Environ. Radioactivity*. **23**. 1994. pp. 19 – 37.

Baranov, V.I., Morosova, N.G., Kunasheva, K. G. and Grigorev, G. I. Geochemistry of some Natural Radioactive Elements in Soil. *Sov. Soil. Sci.* **8**. 1964. pp. 733.

Barnes, M. P. Mineral Inventory Versus Production Planning Case Study – Sacaton Mine, Arizona. Proc. 14th International APCOM Symp. Pennsylvania. 1977. pp. 932 – 949.

Bondietti, E.A. Adsorption of Pu (IV) and Th (IV) by Soil Colloids. *Agronomy Abstracts*. 1974. pp. 242 – 245.

Boyle, R. Cuperiferous in the Sackville Area, New Brunswick, Canada. *J. Geochem Explor.* **8**. 977. pp. 495 – 527.

Burgess, T.M. and Webster, R. Optimal Interpolation and Isarithmic Mapping of Soil Properties. II. The Variogram and Punctual Kriging. *J. Soil. Sci.* **31**. 1980. pp. 315 – 331.

Bunzl, K., Kretner, R., Schramel, P., Szeles, M. and Winkler, R. Speciation of ^{238}U, ^{226}Ra, ^{210}Pb, ^{228}Ra and Stable Pb in the Soil Near an Exhaust Ventilating Shaft of a Uranium Mine. *Geoderma*. **67**. 1995. pp. 45 – 53.

Burns, S.F., Thompson, R.H., Beck, J.N. and Meriwether, J.R. Thorium, Uranium and Cesium-137 in a Soil Catena near Dubach, Louisiana, USA. *Radiochimica Acta*. **52/52**. 1991. pp. 241 – 247.

Chapman, H. D. Cation -Exchange Capacity in *Methods of Soil Analysis Part II* (C. A. Black, Ed.). American Society of Agronomy Inc. 1965. pp. 899 - 900.

Clarke, I. *Practical Geostatistics*. Applied Science Publishers. England. 1979. pp. 3 – 50.

Cruickshank, , J. G. *Soil Geography*. David and Charles (Holdings) Ltd., England. 1972. pp. 185 – 197.

David, M. *Geostatistical Ore Reserve Estimation*. Elsevier Scientific Publishing Company, Amsterdam, Oxford, New York. 1977. pp. 1 –364.

deJong, E., Acton, D.F. and Kozak, L.M. Naturally Occurring Gamma-emitting Isotopes, Radon Release and Properties of Parent Materials of Saskatchewan Soils. *Canadian Journal of Soil Science*. **74**. 1993. pp. 47-53

Dementyev, V. S. and Syromyatnikov, N. G. Mode of Thorium Isotopes in Groundwaters. *Geochem. Intl.* **2**. 1965. pp. 141 - 147.

Disnar, J. R. Etude Experimentale de la Fixation de Metaux par un Materiau Sedimentaire Actual D'origine Algaire - II. Fixation *in vitro* de UO_2^{2+},Cu^{2+},Ni^{2+},Zn^{2+},Pb^{2+},Co^{2+},Mn^{2+}, ainsi que de VO_3^-,MoO_4^{2-} et GeO_3^{2-}. *Geochim.Cosmochim.Acta*. **45**. 1981. pp. 363 - 379.

Doi, K., Hirono ,S. and Sakamaki, Y. Uranium Mineralization by Ground Water in Sedimentary Rocks, Japan. *Econ. Geol.* **70**. 1975.pp. 628 - 646.

Dongarra, G. Geochemical Behaviour of Uranium in the Supergene Environment in *Uranium Geochemistry, Mineralogy, Geology, Exploration and Resources*, The Institution of Mining and Metallurgy, London. 1984. pp. 18-24.

Douglas, E. Wetlands: uranium sinks or sources – implications. U.S. Geological Survey, MS 939, Denver, CO, 80225-0046. *Geological Society of America – Abstracts with program*. 1991. pp. 112.

Dyck, W. The Mobility of Uranium and its Decay Products in Temperate Surficial Environments. in. *Short Course on Uranium Deposits, their Mineralogy and Origin*. (Kimberley, M. M. Eds.). Mineral Association of Canada. 1978. pp. 57-98.

Einax, J. and Soldt, U. Geostatistical Investigations of Polluted Soils. *Fresenius J. Anal. Chem*. 351. 1995. Pp. 48 – 53.

Eisenbud, M. *Environmental Radioactivity: From Natural, Industrial and Military Sources*. Academic Press inc., London. 1987. pp. 420 – 421.

El-Daoushy, F. and Garcia-Tenorio, R. Well Ge and Semi-Planar Ge (HP) Detectors for Low Level Gamma-Spectrometry. *Nucl. Instrum. Methods Phys. Res.* **A356,376**. 1995.

Englund, E. and Sparks, A. GEO-EAS: *Geostatistical Environmental Assessment Software. Users Guide*. USEPA Rep. 6004-88/033. 1988. USEPA. Las Vegas, Nevada.

Farnham, R. S. and Finney, H. R. Classification and Properties of Organic Soils. *Advances in Agronomy*. **17**. 1965. pp. 115 – 162.

Flatman, G. T. and Yfantis, A. A. Geostatistical Strategy for Soil Sampling: The Survey and the Census. *Environmental Monitoring and Assessment*. **4**. 1984. pp. 335 – 349.

Flatman, G. T., Englund, E. J. and Yfantis, A. A. Geostatistical Approaches to the Design of Sampling Regimes in *Principles of Environmental Sampling* (Keith, L. H. Ed.)American Chemical Society. 1988. pp. 73 – 84.

Froideauax, R. *Geostatistical Toolbox Primer. Version 1.3*. FSS International.1990. 10, Chemin de Drize. 1256 Troinex, Switzerland.

Garner, R.J. *Transfer of Radioactive Materials from the Terrestrial Environment to Animals and Man*. CRC Press, Chemical Rubber Co., Cleveland, Ohio. 1972.

Gera, F. Geochemical Behaviour of long-lived Radioactive Wastes. Oak Ridge National Laboratories Report. ORNL-TM-4481.1975.

Gilbert, R.O. and Simpson, C. S. Kriging for Estimating Spatial Patterns of Contaminants: Potential and Problems. *Environmental Monitoring and Assessment*. **5**. 1985. pp. 113 – 135.

Goldhaber, M.B., Hemingway, B.S., Monagheghi, A., Reynolds, R.L. and Nothrup, H.R. Origin of Coffinite in Sedimentary Rocks by a Sequential Adsorption Mechanism. *Bull. Mineral*. **110**. 1987. pp.131 - 144.

Granger, H. C., Santos, E.S., Dean, B.G. and Moore, F.B. Sandstone Type Uranium Deposits at Ambrosia Lake, New Mexico - an Interim Report. *Econ. Geol*. **56/7**. 1961. pp. 1179 - 1209.

Greeman, D.J., Rose, A.W. Form and Behaviour of Radium, Uranium and Thorium in Central Pennsylvania Soils Derived from Dolomite. *Geophysical Research Letters*. **17/6**. 1990. pp. 833 - 836.

Halbach, P., VonBorstel, D. and Gundermann, K-D. The Uptake of Uranium by Organic Substances in a Peat Bog Environment on a Granitic Bedrock. *Chemical Geology*. **29**. 1980. pp. 117 - 138.

Hansen, R.O. and Huntington, G. L. Thorium Movements in Morainal Soils of the High Sierra, California. 1969. *Soil Science*. **108**. pp. 257 - 265.

Hansen , R. O. and Stout, P. R. Isotopic Distribution of Uranium and Thorium in Soils. *Soil Science*. **105**. 1968. pp. 44 - 48.

Havlik, B., Grafova, J. and Nycova, B. Radium-226 Liberation from Uranium Ore Processing Mill Waste Solids and Uranium Rocks into

Surface Streams I. The Effect of Different pH of Surface Waters. *Health Physics*. **14**. 1968. pp. 417 - 419.

Ho, C. H. and Miller, N. H. Effect of Humic Acid in Uranium Uptake by Hematite Particles. *J. Coll. Int. Sci.* **106**. 1985. pp. 281 – 288.

Holbert, K.E., Stewart, B. D. and Eshragi, P. Measurement of Radioactivity in Arizona Groundwater using Improved Analytical Techniques for Samples with High Dissolved Solids. *Health Physics*. **68/2**. 1995. pp. 185 – 194.

Horrath, E. Investigations of Uranium Adsorption to Peat in Natural Waters containing U-Traces. Magyar Todomanyos Akd. Atommag Kutato Intezete, Kozlemenyek. 1960. pp. 177 – 183.

Idiz, E.F., Carlisle, D. and Kaplan, I.R. Interaction between Organic Matter and Trace Metals in a Uranium Rich Bog, Kern County, California, USA. *Applied Geochemistry*. **1**. 1986. pp. 573 - 590.

Irish Base Metals Ltd/Tara Prospecting Ltd. Final Report on Research into the Occurrence of Radioactive Raw Materials in Ireland. 1979. pp. 33-34.

Irish Base Metals Ltd/Tara Prospecting Ltd. Interim Report on Research into the Occurrence of Radioactive Raw Materials in Ireland. 1978. pp. 35 - 38.

Ivanovich, M., Harmon, R.S. *Uranium Series Disequilibrium: Applications to Earth, Marine and Environmental Sciences*. Clarendon Press, Oxford. 1992.

Journel, A.G., Huybregts, Ch., J. *Mining Geostatistics*. Academia Press, London and New York. 1. 1978.

Kamath, P. R., Khan, A. A., Rao, S. R., Pillai, T. N., Barker, M. L. and Ganapathy, S. Environmental Natural Radioactivity Measurements at Trombay Establishment. in *The Natural Radiation Environment*. (Adams, J. A. S. and Lowder, W. M. Eds.)Univ. Chicago Press. 1964. pp. 957 – 978.

Karmalitsyn, N. I., Sepman, S. V. and Kharitonov, I. A. The Standardisation of Ra^{226} Radionuclide Solutions. *Nucl. Instrum. Methods Phys. Res.* **A369**. 1996. pp. 411.

Kerndorff, H. and Schnitzer, M. Sorption of Metals on Humic Acid. *Geochim. Cosmochim. Acta*. **44**. 1080. pp. 1701 – 1708.

Kochenov, A. V., Zinev'yev, V. V. and Lovaleva, S. A. Some Features of the Accumulation of Uranium in Peat Bogs. *Geokhimiya*. **1**. 1965. pp 97 - 103.

Knight, A. H., Boggie, R. and Shepherd, H. The Effect of Ground Water Level on Water Movement in Peat: a Study using Tritiated Water. *J. Appl. Ecology*. **9**. 1972. pp. 633 – 642.

Knudsen, H. P., Kim, Y. C. and Mueller, E. A Comparative Study of the Geostatistical Ore Reserve Estimation Method over the Conventional Methods. *Min. Engng*. **30/1**. 1978. pp. 54 – 58.

Koczy, F. F. The Natural Radioactive Series in Organic Material in Radioecology, Proc. of the 1st National Symposium, Colorado, Sept.

1961. Schultz, V., Klement, A. W. (eds.). Reinhold, New York. 1963. pp. 611 - 613.

Kogel-Knaber, I. and Hatcher, P. G. Characterisation of alkyl-carbon in forest soils by CPMAS ^{13}C NMR spectroscopy and dipolar dephasing. *The Science of the Total Environment*. **81/82**. 1989. pp. 169 - 177.

Kononova, M.M. *Soil organic matter*. Pergamon Press Inc. New York. 1966.

Krige, D.G. A Statistical Approach to some basic Mine Valuation Problems in the Witwatersrand. *Journal of the Chemical, Metallurgical and Mining Society of South Africa*. **52**. 1951. pp. 116.

Landstrom, O. and Sundblad, B. Migration of Thorium, Uranium, Radium and Cs-137 in Till Soils and their Uptake in Organic Matter and Peat. Studsvik Energiteknik AB. 1986. SKB – TR – 86 - 24.

Langmuir, D. Uranium Solution-Mineral Equilibria at Low Temperatures with Applications to Sedimentary Ore Deposits. *Geochim. Cosmochim .Acta*. **42**. 1978. pp. 547-569.

Langmuir, D. and Herman, J. S. The Mobility of Thorium in Natural Waters at Low Temperatures. *Geochimica et Cosmochimica Acta*. **44**. 1980. pp. 1753 – 1766.

Lee, J. and Jonasson, I. Contribution of Organic Complexation to Ni, Co, and Cu Speciation in Surface Waters; Implications for Geochemical Surveys. *J. Geochem. Explor*. **18**. 1983. pp. 25 – 48.

Leenheer, J.A., McKnight, D.M., Thurman, E.M. and MacCarthy, P. Structural Components and Proposed Structural Models of Fulvic Acid from the Suwanee River. in *Humic Substances in the Suwanee River, Georgia: Interactions, Properties and Proposed Structures*. (Averett, R. C., Leenheer, J.A., McKnight, D.M. and Thorn, K.A. Eds.). U.S. Geol. Surv. Rep. 87-557. 1989. pp. 205 – 229.

Levinson, A. A., Bland, C. J. and Dean, J. R. Uranium Series Disequilibrium in Young Surficial Uranium Deposits in Southern British Columbia. *Can. J. Earth. Sci.* **21**. 1984. pp. 559 – 566.

Litaor, M.I. Spatial Analysis of Plutonium-239 + 240 and Americium-241 in Soils around Rocky Flats, Colorado. *J. Environ. Qual.* **24**. 1995. Pp. 506 – 516.

Longworth, G., Ivanovich, M. and Wilkins, M. A. Uranium Series Disequilibrium Studies at the Broubster Analogue Site. UK Dep. Environ. London. Rep. No. DOE/RW/89.104. 1989.

Lopatkina, A. P. Characteristics of Migration of Uranium in the Natural Waters of Humid Regions and Their Use in the Determination of the Geochemical Background for Uranium. *Geochem. Intl.* **Nos.4-6**. 1964. pp. 788-795.

Lopatkina, A. P. Conditions of Accumulation of Uranium in Peat. *Geokhimiya*. **6**. 1967. pp. 708 – 719.

Lowson, R.T., Short, S.A., Davey, B.G. and Gray, D.J. ^{234}U / ^{238}U and ^{230}Th / ^{234}U Activity Ratios in Mineral Phases of a Lateritic Weathered Zone . *Geochim. Cosmochim. Acta*. **50**. 1986. pp. 1697 – 1702.

McAuley, I.R., Marsh, D. ^{226}Ra Concentrations in Soil in the Republic of Ireland. *Rad. Prot. Dosim.* **45**. 1992. pp. 265-267.

McAuley, I.R., Moran, D. Natural Radioactivity in Soil in the Republic of Ireland. *Rad. Prot. Dosim.* **24**. 1988. pp. 47 -49.

McBratney, A. B. and Laslett, G. M. Sampling Schemes for Contaminated Soil in *Integrated Soil and Sediment Research: A Basis for Proper Protection*. Eijsackers, H.J.P. and Hamers, T. (Eds.) Kluwer Academic Publishers, Netherlands. 1993. pp. 435 – 459.

McLaughlin, J. P. Indoor Radon: sources, health effects and control. *Technology Ireland*. **22**. 1990. pp. 27 – 30.

Malanca, A., Gaidolfi, L., Pessina, V. and Dallara, G. Distribution of Ra^{226}, Th^{232} and K^{40} in Soils of Rio Grande do Norte (Brazil). *J. Environ. Radioactivity*. **30**. 1996. pp. 55 – 67.

Matheron, G.F. *La Theorie des Variables Regionalisees et ses Applications*. Fascicule 5,. Les Cahiers du Centre de Morphologie Mathematique de Fontainbleau, Ecole Superieure des Mines des Paris. 1970.

Megumi, K. and Mamuro, T. Concentrations of Uranium Series Nuclides in Soil Particles in Relation to Their Size. *Hoken Butsuri*. **12/3**. 1977. pp. 181 - 189.

Megumi, K. Radioactive Disequilibrium of Uranium and Actinium series Nuclides in Soil. *J. Geophys. Res.* **84**. 1979. pp. 3677 - 3682.

Met Eireann. Public Information Service. 1999.

Michel, J. Relationship of Radium and Radon with Geological Formations. in *Radon, Radium and Uranium in Drinking Water*. Cothern, C.R., Rebers, P.A. (Eds.). Lewis Publishers, Chelsea, M. I. 1990. pp. 83 – 95.

Miller, J.M. and Loosemore, W.R. Instrumental techniques for uranium prospecting. in *Uranium Prospecting Handbook*. Bowie, S.H.U., Davis, M. and Ostle, D. (Eds.). The Institution of Mining and Metallurgy. Proceedings of a NATO sponsored Advanced Study Institute on methods of prospecting for uranium minerals. London. 1971. pp. 135 – 148.

Miyake, Y., Sugimura and Tsubota, H. Content of Uranium, Radium and Thorium in River Waters in Japan. in *The Natural Radiation Environment*. (Adams, J. A. S. and Lowder, W. M.). Univ. Chicago Press. 1964. pp. 219 – 225.

Nash, K., Fried ,S., Friedman, A.M. and Sullivan, J.C. Redox Behaviour, Complexing and Adsorption of Hexavalent Actinides by Humic Acid and Selected Clays. *Environ. Sci. Tech.* **15**. 1981. pp. 834 - 837.

Nathwani, J.S., Phillips, C.R. Adsorption of ^{226}Ra by Soils (I). *Chemosphere*. **5**. 1979a. pp. 293 - 299.

Nathwani, J.S., Phillips, C.R. Adsorption of ^{226}Ra by Soils in the Presence of Ca^{2+} Ions: Specific Adsorption II. *Chemosphere*. **5**. 1979b. pp. 293 - 299.

Nemeth, W. K. and Parsa, B. Density Correction of Gamma Ray Detection Efficiency in Environmental Samples. *Radioactivity and Radiochemistry*. **3(3)**. 1992. pp. 32 – 39.

Newbould, P.J. The Ecology of Cranesmoor, a New Forest Valley Bog. *J. Ecol.* **48**. 1960. pp. 361 – 383.

O'Connor ,P.J., Long, C.B. and Hennessy, J. Radioelement Geochemistry of Irish Newer Caledonian Granites. *Geol. Surv. Ire. Bull.* **3**. 1983. pp. 125 – 140.

O'Connor, P.J. Radioelement geochemistry of Irish granites. *Mineral. Mag.* **44**. 1981. pp. 485 - 495.

O'Connor, P.J., Long, C.B. Radioelement Abundance Data for Some Dalradian Rocks from Co.Donegal, Ireland. *Mineralogical Magazine*. **49**. 1985. pp. 643 - 648.

Osmond, J.K., Cowart, J.B. *Atomic Energy Review*. **14**. 1976. pp. 621.

Palmer, M.R. and Edmond, J.M. Uranium in River Water. *Geochimica et Cosmochimica Acta*. **57**. 1993. Pp. 4947 – 4955.

Pannatier, Y. Variowin 2.2. *Software for Spatial Data Analysis in 2D*. Springer Verlag. New York. 1996.

Pauli, F.W. Heavy Metal Humates and their Behaviour Against Hydrogen Sulphides. *Soil. Sci.* **119**. 1975. pp. 98 – 105.

Rancon, D. The Behaviour in Underground Environments of Uranium and Thorium Discharged by the Nuclear Industry. in *Environmental Behaviour of Radionuclides Released by the Nuclear Industry*. IAEA-SM-172/55. 1973. pp. 333 - 346.

Rashid, M. A. Adsorption of Metals on Sedimentary and Peat Humic Acids. *Chemical Geology*. **13.** 1974. pp. 115 – 123.

Rendu, J-M. M. Normal and Lognormal Estimation. *Mathematical Geology*. **11/4.** 1979. pp. 407 - 421.

Rogers, J.J. W., Adams, J.A.S. Uranium. in *Handbook of Geochemistry*. K.H. Wedepohl (Ed.) Springer-Verlag,Berlin.Vol.II/2 1970.

Rose, A. W., Schmiermund, R. L. and Mahar, D. L. Geochemical Dispersion of Uranium Near Prospects in Pennsylvania, U.S. Dept. of Energy Rep. No. GJBX-59(77). 1977. pp. 87.

Royle, A. G. and Hosgit, E. Local Estimation of Sand and Gravel Reserves by Geostatistical Methods. *Transactions of the Institute of Mining and Metallurgy*. Vol. **83**. 1974. pp. A53 – A62.

Ruellan, H., Lepy, M. C., Etcheverry, M., Plagnard, J. and Morel, J. A New Spectra Code Applied to the Analysis of U^{235} and U^{238} in the 60 to 200 keV Energy Range. *Nucl. Instrum. Methods Phys. Res.* **A369**. 1996. pp. 651.

Russo, D. and Bresler, E. Soil Hydraulic Properties as Stochastic Processes: I. An Analysis of Field Spatial Variability. *Soil. Sci. Soc. Am. J.* **45**. 1981. pp. 682 – 687.

Rycroft, D. W., Williams, D. J. A. and Ingram, H. A. P. The Transmission of Water Through Peat. II. Field Experiments. *J. Ecol.* **63**. 1975. pp. 557 – 568.

Sanchez, A. L., Schell, W. R. and Thomas, E. D. Interactions of ^{57}Co, ^{85}Sr and ^{137}Cs with peat under acidic precipitation conditions. *Health Physics*. **54/3**. 1988. pp. 317 - 322.

Schubert, A.J., Russell, E.R. and Myers, L.S. Dissociation Constants of Radium-Inorganic Acid Complexes Measured by Ion Exchange. *J. Biol. Chem*. **185**. 1950. pp. 387 - 398.

Schnitzer, M. Reactions of Humic Substances with Metals and Minerals. in *Mineral Exploration: Biological Systems and Organic Matter*. (Carlisle, D., Berry, W.L., Kaplan, I.R. and Watterson, J. Eds.). 1986. Rubey Vol. 5. Prentice-Hall, New Jersey.

Schulz, R.K. Soil Chemistry of Radionuclides. *Health Physics*. **11**. 1965. pp. 1317 - 1324.

Schwertmann, U. and Taylor, R. M. Iron Oxides. in *Minerals in Soil Environments*. (Dixon, J. B., Weed, S. B., Kittrick, J. A., Milford, M. H. and White, J. L. Eds.). Soil Sci. Soc. Am. 1977. pp. 145 – 180.

Sheppard, M. I. The Environmental Behaviour of Uranium and Thorium. Atomic Energy of Canada Ltd. 1980. AECL – 6795.

Sheppard, M. I. The Environmental Behaviour of Radium. Atomic Energy of Canada Ltd. 1980. AECL-6796. pp. 5 - 10.

Sheppard, M. I. And Thibault, D. H. Migration of Technetium, Iodine, Neptunium and Uranium in the Peat of Two Minerotrophic Mires. *J. Environ. Quality*. **17**. 1988. pp. 644 – 653.

Shizuma, K., Fukami, K., Iwatani, K. and Hasai, H. Low Background Shielding of Ge Detectors for the Measurement of Residual ^{152}Eu Radioactivity Induced by Neutrons from the Hiroshima Atomic Bomb. *Nucl. Instrum. Methods. Phys. Res.* **B66**. 1992. pp. 459.

Sholkovitz, E.R. and Copeland, D. The Coagulation, Solubility and Adsorption Properties of FE, Mn, Cu, Ni, Cd, Co and Humic Acid in River Water. *Geochim. Cosmochim. Acta*. **45**. 1981. pp. 181 – 189.

Sillen, I. G., Martell, A.E. Stability Constants of Metal-Ion Complexes. Special Publication. 17. 1964. The Chemical Society, London

Smith, B., Stuart, M. E., Vickers, B. P. and Peachey, D. The Characterisation of Organics from the Natural Analogue Site at Broubster, Caithness, Scotland. Br. Geol. Surv. Keyworth. Rep. No. WE/89/33. 1990. pp. 42.

Srivastava, R. M. and Isaaks, E. H. *Applied Geostatistics*. Oxford University Press, New York. 1989. pp. 319 - 350

Starik, I. Ye., Starik, F. Ye. And Apollonova, A.N. Adsorption of Traces of Uranium on Iron Hydroxide and its Desorption by the Carbonate Method. *Zh. Neorgan. Khimmi*. 1958.

Stevenson, F.J. *Humus Chemistry: Genesis, Composition, Reactions*. Wiley-Interscience. New York. 1982. pp. 443.

Stevenson, F.J. Gross chemical fractionation of organic matter. in *Methods of Soil Analysis Part II* (C. A. Black, Ed.). American Society of Agronomy Inc. 1965. pp. 1409 – 1421.

Sutton, G. A., Napier, S. T., John, M. and Taylor, A. Uranium –238 Decay Chain Data. *The Science of the Total Environment*. **130/131**. 1993. pp. 393 – 401.

Szabo, Z. and Zapecza, O.S. Relation Between Natural Radionuclide Activities and Chemical Constituents in Ground Water of the Newark Basin, New Jersey. in *Radon, Radium, and Other Radioactivity in Ground Water: Hydrogeologic Impact and Application to Indoor Airborne Contamination*. Graves, B. (Ed) Proceedings of the NWWA Conference, April 7-9, 1987. Somerset, N.J.

Szalay, A. The Significance of Humus in the Geochemical Enrichment of Uranium. in *Peaceful Uses of Atomic Energy: Survey of Raw Materials Resources. 2*. United Nations, Geneva. 1958. pp. 182 – 186.

Szalay, A. Cation Exchange Properties of Humic Acids and their Importance in the Geochemical Enrichment of UO_2^{++} and other Cations. *Geochim. Cosmochim. Acta*. **28**. 1964. pp. 1605 - 1614.

Tamuta, H., Katayama, N and Furuichi, R. Modelling of Ion Exchange Reactions on Metal Oxides with the Frumkin Isotherm. 1. Acid – Base and Charge Characteristics of MnO_2, TiO_2, Fe_3O_4 and Al_2O^3 Surfaces and Adsorption Affinity of Metal Ions. *Environ. Sci. Technol.* **30**. 1996. pp. 1198 – 1204.

Tan. K. *Principles of Soil Chemistry*. Marcel Dekker. New York. 1992.

Taskayev, A. I., Ovchenko, V., Ya., Aleksahkin, R. M. and Shuktomova, I. I. Uptake of Radium-226 into Plants and Changes in its State in the Soil-Aboveground Mass-Litterfall System. *Soviet Soil Science*. **1**. 1977. pp. 79 – 85.

Taskayev, A.I., Ovchenkov, V.Ya. and Aleksahkin, R.M. Forms of ^{226}Ra in the Horizons of Soil with a High Concentration of this Isotope. *Pochvovedeniye*. **2**. 1978. pp. 18 – 24.

Titaeva, N.A. On the Character of Radium and Uranium Bonding in Peat. *Geokhimiya*. **12**. 1967. pp. 1493 - 1495.

Titaeva, N.A. and Veksler, T.I. The State of Radioactive Disequilibrium in the Uranium and Thorium Series as an Indicator of Migration of Radioactive Elements and Active Interaction Between Phases Under Natural Conditions. *Geochemistry International*. **14**. 1977. pp. 99 – 107.

Tyuryukanova, E.B. and Kalugina, V.A. The Behaviour of Thorium in Soils. *Soviet Journal of Ecology*. **2**. 1971. pp. 467 - 469.

Vauclin, M., Vieria, S.R., Vachaud, G. and Nielsen, D.R. The Use of Co-kriging with Limited Field Soil Observations. *Soil. Sci. Sco. Am. J.* **47**. 1981. pp. 175 – 184.

Verkovskaja, I.N., Vavilov, P.P and Maslov, V.I. "The Migration of Natural Radioactive Elements under Natural Conditions and their Distribution According to Biotic and Abiotic Environmental Components" in *Radiological Concentration Processes*, Proc. of Intl. Symp., Stockholm, April 1966, Aberg, B., Hungate, F.P. (Ed's), Pergamon, Oxford 1967. pp. 313-328.

Von Gunten, H.R., Surbeck, H. and Rossler, E. Uranium Series Disequilibrium and High Thorium and Radium Enrichments in Karst Formations. *Environ. Sci. Technol*. **30**. 1996. pp. 1268 – 1274.

Wang, X. J. and Qi, F. The Effects of Sampling Design on Spatial Structure of Contaminated Soil. *Science of the Total Environment*, **224**. 1998. pp. 29 – 41.

Walker, G. P. L. and Leedal, G. P. The Barnesmore granite complex, County Donegal. Sci. Proc. R. Dublin. Soc. 26. 1954. pp. 207 - 243.
Wilson, M.R. Uranium Enrichment in European Peat Bogs. in. *Surficial Uranium Deposits*. I.A.E.A. Technical Document No.322. Vienna. 1984. pp. 197 - 200.

Yost, R.S., Uehara, G. and Fox, R.L. Geostatistical Analysis of Soil Chemical Properties of Large Land Areas. I. Variograms. *Soil. Sci. Soc. Am. J.* **46**. 1982. Pp. 1028 – 1032.

Yakobenchuk, V. F. Radioactivity and Chemical Properties of Sod-Podzolic Soils in the Ukrainian Western Polesie, Visn. *Sil's 'kogospod. Nauki*. **11**. 1968. pp. 45 - 50.

Yucel, H., Cetiner, M. A. and Demirel, H. Use of the 1001 keV Peak of Pa^{234m} Daughter of U^{238} in Measurement of Uranium Concentration by HPGe Gamma-Ray spectrometry. *Nucl. Instr. And Meth. In Phys. Res.* Sec. **A. 413.** 1998. pp. 74 – 82.

Zielinski, R.A., Bush, C.A. and Rosholt, J.N. Uranium Series Disequilibrium in a Young Surficial Uranium Deposit, North-eastern Washington, USA. *Applied Geochemistry*. **1**. 1986. pp. 503 – 511.

Zielinski, R.A., Meier, A.L. The Association of Uranium with Organic Matter in Holocene Peat: an Experimental Leaching Study. *Applied Geochemistry*. **3**. 1988. pp. 631 - 643.

Zielinski, R.A., Otton, J.K., Wanty, R.B. and Pierson, C.T. The Aqueous Geochemistry of Uranium in a Drainage Containing Uraniferous Organic-rich Sediments, Lake Tahoe Area, Nevada, U.S.A. *Uranium*. **4**. 1988. pp. 281 – 305.

Zikovsky, L. and Blagoeva, R. Determination of Thorium-232 in Canadian Soils by Gamma-Ray Spectrometry via Lead-212 and Actinium-228, Interference from Uranium. *Radioactivity and Radiochemistry*. **5**. 1994. pp. 23 – 25.

APPENDIX 1.

No.	Easting.	Northing.	^{228}Ra.	^{226}Ra.	^{238}U.	^{40}K.	^{137}Cs.
1	750	3770	16.0	25.3	18.0	468.8	5.7
2	270	2820	12.4	18.74	10.4	440.5	21.6
3	950	2780	31.0	75.0	23.0	636.5	150.6
4	1050	2800	31.0	72.0	34.0	675.0	3.6
5	1580	2770	35.0	43.0	38.1	700.1	3.1
6	570	2160	28.0	111.0	95.0	990.0	3.0
7	50	1870	34.2	226.0	87.9	824.3	6.9
8	800	2080	30.6	238.0	110.1	752.5	31.6
9	1190	1870	22.6	421.5	75.9	434.2	21.7
10	1040	1390	46.0	258.0	152.0	1012.0	<0.5
11	1240	650	38.75	279.0	132.7	932.5	7.5
12	1310	390	41.0	243.0	118.4	899.7	8.7
13	830	140	36.9	262.0	136.8	1015.1	13.0
14	920	340	52.4	399.8	153.6	868.2	5.5
15	1130	3830	35.4	72.0	21.0	644.7	69.3
16	2390	3660	25.2	32.4	24.5	480.3	3.9
17	1500	3850	32.5	34.6	23.8	593.7	4.5
18	1270	1520	80.1	353.6	746.0	470.9	11.9
19	2710	3770	3.2	12.1	5.0	83.0	8.5
20	2170	3620	30.4	36.4	29.0	639.0	6.0
21	3090	1140	47.4	25.2	34.5	1088.1	1.9
22	2780	2960	39.0	52.9	29.0	889.0	29.5
23	2300	2380	24.7	47.0	25.6	521.6	9.7
24	3000	2300	41.2	43.0	58.7	960.3	55.5
25	1690	1740	39.0	373.0	132.3	364.1	61.4
26	2380	1490	60.4	295.0	135.0	432.5	3.7
27	3840	1670	135.0	145.5	103.0	696.0	9.0
28	3360	1660	95.0	84.0	29.0	100.2	9.0
29	2400	330	33.2	13.7	25.0	416.6	20.1
30	2950	250	29.7	19.9	19.8	217.5	13.8
31	3590	3700	25.7	29.9	30.1	427.2	4.2
32	3810	3680	24.6	24.4	30.0	611.2	1.1
33	3600	3510	33.9	44.0	30.0	633.9	50.2
34	3180	3200	19.4	22.0	16.6	564.2	40.3
35	3300	2730	3.5	7.0	5.4	33.9	7.6
36	3450	2100	30.7	21.0	36.2	288.1	5.2
37	3380	2410	9.2	14.0	11.1	8.1	8.5
38	3850	2190	5.3	4.0	2.7	156.9	0.7
39	4840	3110	25.6	29.0	20.1	562.0	21.8
40	4030	960	56.3	132.0	91.8	597.0	9.9
41	3400	960	92.0	393.0	546.0	90.1	2.5
42	3200	560	30.4	58.8	35.7	648.9	3.9
43	4770	3930	28.3	44.0	19.1	580.4	1.98
44	2540	1940	25.3	50.4	28.7	540.6	12.5

45	4730	3750	27.7	52.2	21.4	516.7	1.3
46	4600	3600	28.4	47.0	18.0	566.3	178.7
47	4180	2080	14.2	15.2	20.4	368.2	7.4
48	4780	950	21.7	46.5	34.6	705.1	9.6
49	4310	1440	5.1	8.4	3.6	29.9	6.0
50	4780	1620	35.5	48.0	27.5	632.0	1.9
51	4150	1130	49.4	65.0	46.7	783.0	11.1
52	4390	500	19.6	25.8	17.0	302.1	18.2
53	4630	430	43.4	70.80	96.9	325.2	8.7
54	1850	1550	117.3	479.0	788.1	162.0	7.3
55	650	3500	26.8	81.1	57.0	385.3	8.9
56	800	2560	24.0	48.5	33.0	459.0	67.9
57	2140	1700	8.3	12.5	9.2	86.8	22.4
58	150	3570	14.5	20.4	18.9	446.0	26.3
59	390	2640	9.7	11.9	7.7	100.6	5.2
60	2650	3380	45.5	54.9	31.83	739.5	1.4

Table i. Spatial co-ordinates and radionuclide values for soil samples of Survey 1. Shaded cells denote samples taken from the granite region of the Cronamuck valley during Survey 1 (on-pluton). Co-ordinate values in meters, radionuclide values in Bq/kg dry weight.

Win. No.	^{228}Ra	S.D.	^{226}Ra	S.D.	^{238}U	S.D.	^{40}K	S.D.	^{226}Ra/^{238}U	S.D.
1	50.83	27.79	329.4	87.27	252.3	272.5	698.3	309.0	2.24	1.40
2	48.00	28.27	282.4	145.4	217.0	261.3	591.2	334.4	1.99	1.37
3	45.14	29.23	233.1	168.4	196.9	271.4	497.4	303.0	1.85	1.38
4	52.55	34.51	164.0	181.2	162.1	259.0	377.0	304.3	1.48	0.86
5	55.67	39.77	109.8	131.8	96.59	162.9	431.7	325.1	1.13	0.73
6	53.20	39.11	91.64	109.4	86.89	155.2	463.0	339.1	1.53	0.65
7	47.08	38.97	82.03	102.8	76.15	144.2	461.8	339.7	1.62	0.61
8	48.51	30.7	304.2	112.9	257.7	288.9	660.2	309.2	2.13	1.52
9	45.07	30.87	260.6	150.4	218.3	275.1	559.9	320.5	2.00	1.37
10	46.26	32.33	256.8	165.8	222.5	291.7	495.7	291.4	2.04	1.42
11	47.76	34.13	145.8	171.2	143.8	240.7	407.0	340.6	1.47	0.81
12	39.16	30.12	87.33	123.7	79.37	150.9	410.1	355.8	1.43	0.69
13	43.74	37.61	72.35	98.53	71.01	134.5	443.8	345.6	1.38	0.64
14	46.99	39.28	78.82	104.6	75.75	144.4	416.9	343.5	1.47	0.64
15	34.85	28.04	187.5	169.4	128.9	213.1	566.9	295.9	1.99	1.28
16	37.94	28.38	195.6	169.4	134.2	211.9	539.9	286.7	1.94	1.28
17	41.71	28.60	188.6	178.7	222.6	554.8	307.6	1.95	1.35	0.64
18	41.14	31.99	110.5	153.0	97.21	202.9	441.1	358.9	1.50	0.76
19	40.38	38.24	61.65	79.96	39.08	39.08	446.3	372.9	1.49	0.64
20	38.48	38.55	41.20	40.01	31.46	27.33	457.1	390.0	1.42	0.67
21	39.12	42.02	39.75	43.60	29.10	28.57	380.4	366.6	1.44	0.69
22	34.85	28.04	187.5	169.4	128.9	213.1	566.9	295.9	1.99	1.28
23	35.90	28.82	186.6	174.4	134.1	222.2	549.6	298.8	1.92	1.34
24	39.45	27.95	166.1	179.5	124.1	224.9	572.9	305.6	1.91	1.35
25	37.36	31.86	92.63	144.2	88.25	203.8	417.9	316.2	1.51	0.71
26	36.32	38.02	42.41	38.61	29.44	26.67	421.3	328.8	1.50	0.57
27	37.98	41.09	41.73	42.05	30.98	28.57	418.6	336.7	1.39	0.64
28	37.34	43.29	38.97	44.22	27.20	28.62	340.9	260.3	1.42	0.62
29	22.95	9.83	53.44	67.24	29.76	29.7	517.0	183.6	1.68	0.69
30	27.27	6.20	61.85	61.19	36.06	27.03	564.4	113.0	1.66	0.65
31	30.21	10.88	42.14	15.47	28.22	13.58	614.3	238.9	1.71	0.76
32	25.35	12.92	31.80	15.14	25.42	14.49	491.7	306.9	1.4	0.48
33	23.43	12.76	29.21	15.81	24.09	14.41	461.9	294.5	1.36	0.48
34	21.95	13.80	25.96	16.27	23.28	15.51	435.0	313.4	1.28	0.52
35	19.69	10.88	25.62	16.45	18.82	10.90	368.0	238.8	1.51	0.69

Table ii. Summary statistics for moving windows analysis.

No.	Actual Value.	Kriging.	Triangulation.	Polygonal.	Inv.Dist.^{2}.
1	25.3	70.0	45.1	81.1	66.2
2	18.7	29.3	4.9	11.9	27.4
3	75.0	62.7	17.6	72.7	65.5
4	72.0	76.6	73.2	75.0	69.7
5	43.0	103.0	60.3	72.7	69.3
6	111.0	172.3	177.7	283.3	170.2
7	226.0	131.3	131.6	111.0	111.5
8	238.0	194.7	131.6	111.0	75.9
9	421.0	281.6	131.6	353.6	315.0
10	258.0	337.7	304.4	353.6	360.0
11	279.0	288.7	313.8	243.0	292.3
12	243.0	276.4	293.7	279.0	310.4
13	262.0	251.0	n/a	399.8	365.5
14	399.8	260.5	239.1	262.0	260.2
15	72.0	35.1	49.4	81.1	36.9
16	32.4	32.8	48.6	36.4	35.3
17	34.6	58.0	n/a	72.0	60.7
18	353.6	356.6	403.7	258.0	336.2
19	12.1	37.3	n/a	32.4	39.1
20	36.4	36.2	41.8	32.4	33.1
21	25.2	250.9	199.2	393.0	314.9
22	52.9	38.7	38.4	54.8	32.9
23	47.0	50.5	48.7	8.9	24.6
24	43.0	34.4	28.9	14.2	22.6
25	373.0	362.1	414.5	479.0	372.9
26	295.0	64.2	29.8	12.5	138.2
27	145.5	60.0	45.1	84.0	29.0
28	84.0	108.8	148.6	21.4	63.5
29	13.7	117.7	112.5	19.9	146.0
30	19.9	44.4	n/a	58.8	81.4
31	29.9	33.1	n/a	44.0	35.5
32	24.4	36.5	37.1	29.9	20.9
33	44.0	26.8	33.5	29.9	27.9
34	22.0	35.8	48.5	52.9	39.5
35	7.0	23.5	39.5	14.2	27.0
36	21.0	40.4	38.1	14.2	28.3
37	14.0	14.3	12.3	21.4	19.9
38	4.0	32.6	15.4	15.2	37.1
39	29.0	25.3	24.9	44.0	32.5
40	132.0	115.8	131.7	65.9	105.9
41	393.0	64.3	65.1	25.2	38.9
42	58.8	152.8	44.3	19.9	121.0
43	44.0	48.8	n/a	52.2	50.3
44	50.4	76.5	24.9	292.0	104.9

45	52.2	45.3	n/a	44.4	45.0
46	47.0	46.0	48.7	52.2	48.5
47	15.2	35.0	77.2	4.6	39.4
48	46.5	50.1	n/a	70.9	40.9
49	8.4	66.5	95.3	65.9	71.8
50	48.0	20.6	n/a	8.4	25.5
51	65.0	94.0	116.6	132.6	113.6
52	25.8	84.2	75.6	70.9	74.4
53	70.80	32.3	n/a	25.8	38.5
54	479.0	257.6	271.8	373.0	256.9
55	81.1	32.7	35.2	25.3	30.4
56	48.5	94.2	36.8	75.0	32.5
57	12.5	307.9	326.3	479.0	311.0
58	20.4	41.6	n/a	81.1	53.4
59	11.9	46.4	71.4	18.7	40.5
60	54.9	33.5	36.0	32.4	31.5

Table iii. ^{226}Ra estimates produced by each of the four point estimation procedures. Values in Bq/kg dry weight.

No.	Actual Value	Kriging.	Triangulation.	Polygonal.	Inv Dist ^{2}.
1	16.0	30.9	26.9	26.8	28.6
2	12.4	16.5	8.8	9.7	14.0
3	31.0	28.3	28.5	31.0	29.1
4	31.0	33.9	32.2	31.0	30.0
5	35.0	26.9	28.9	31.0	30.5
6	28.0	29.9	29.7	30.6	22.4
7	34.2	20.4	31.6	28.0	24.2
8	30.6	25.7	31.9	28.0	28.9
9	22.6	30.5	83.1	80.1	55.2
10	46.0	63.9	62.5	80.1	63.7
11	38.75	46.9	52.4	41.0	43.7
12	41.0	48.6	45.7	38.7	42.6
13	36.9	49.6	n/a	52.4	49.9
14	52.4	39.3	38.0	36.9	38.3
15	35.4	24.3	28.8	26.8	23.7
16	25.2	20.9	40.1	30.4	23.7
17	32.5	39.7	n/a	35.4	31.0
18	80.1	75.0	26.8	46.0	45.0
19	3.2	23.4	n/a	25.2	31.9
20	30.4	34.2	35.5	25.2	26.3
21	47.4	75.8	55.2	42.0	82.9
22	39.0	17.5	27.7	45.5	27.7
23	24.7	43.6	30.8	4.6	27.2
24	41.2	23.6	21.8	9.2	23.3
25	39.0	42.3	77.5	117.3	81.0
26	60.4	67.8	21.7	8.3	36.9
27	135.0	63.0	49.0	95.1	31.1
28	95.0	94.0	93.7	30.7	63.0
29	33.2	33.9	34.1	29.7	34.6
30	29.7	40.2	n/a	30.4	39.8
31	25.7	24.0	n/a	33.9	29.6
32	24.6	26.8	28.9	25.7	17.9
33	33.9	24.1	33.5	25.7	24.9
34	19.4	34.0	36.2	39.0	30.0
35	3.5	25.5	34.6	9.2	21.7
36	30.7	27.2	39.9	9.2	27.7
37	9.2	28.3	11.1	30.7	21.9
38	5.3	16.1	14.1	14.2	36.8
39	25.6	17.6	14.6	33.9	27.4
40	56.3	61.5	52.8	49.4	38.4
41	92.0	53.6	46.4	34.5	42.3
42	30.4	47.9	38.4	29.7	63.4
43	28.3	26.7	n/a	27.7	27.6
44	25.3	31.9	23.6	60.3	32.4

45	27.7	28.4	n/a	28.3	28.2
46	28.4	26.6	27.6	27.7	27.6
47	14.2	26.4	66.9	5.3	35.1
48	21.7	38.8	n/a	43.4	27.5
49	5.1	57.6	80.0	49.4	35.1
50	35.5	35.0	n/a	5.1	27.5
51	49.4	42.2	67.7	56.3	45.7
52	19.6	40.8	43.1	43.4	18.8
53	43.4	22.5	n/a	19.6	45.3
54	117.3	53.6	60.0	39.0	42.8
55	26.8	15.3	18.9	16.0	18.1
56	24.0	22.6	12.1	31.0	15.9
57	8.3	58.3	78.5	117.3	66.7
58	14.5	18.9	n/a	26.8	22.1
59	9.7	20.9	16.8	12.4	18.2
60	45.5	23.0	26.2	25.2	22.7

Table iv. ^{228}Ra estimates produced by each of the four point estimation procedures. Values in Bq/kg dry weight.

No.	Actual Value.	Kriging.	Triangulation.	Polygonal.	Inv.Dist.^{2}.
1	468.8	452.9	600.3	385.1	497.1
2	440.5	195.1	172.3	100.6	240.4
3	636.5	587.6	632.0	675.0	618.4
4	675.0	634.6	662.3	636.5	609.5
5	700.1	547.6	662.5	675.0	659.2
6	990.0	489.3	686.1	752.5	583.5
7	824.3	623.4	686.1	990.0	673.2
8	752.5	789.5	793.7	990.0	668.7
9	434.2	597.6	570.0	470.9	754.0
10	1012.0	560.0	638.5	470.9	488.4
11	932.5	821.6	793.2	899.7	940.3
12	899.7	858.4	776.4	932.5	928.9
13	1015.1	873.5	n/a	868.2	877.4
14	868.2	975.1	1000.3	1015.0	972.8
15	644.7	572.6	308.2	644.7	495.9
16	480.3	541.3	739.9	639.0	444.9
17	593.7	601.4	n/a	644.7	592.2
18	470.9	670.3	454.3	1012.0	688.3
19	83.0	633.4	n/a	480.3	579.7
20	639.0	570.4	323.3	480.3	469.4
21	1088.1	363.3	377.7	90.1	300.1
22	889.0	734.4	469.9	739.5	562.1
23	521.6	523.9	653.9	20.1	380.9
24	960.3	341.9	288.6	8.1	102.9
25	364.1	305.5	286.4	162.0	228.1
26	432.5	393.7	367.1	86.8	111.7
27	696.0	285.4	129.9	100.0	216.7
28	100.2	531.6	532.8	288.1	501.6
29	416.6	571.7	422.4	217.5	732.1
30	217.5	620.3	n/a	648.9	586.8
31	427.2	604.7	n/a	633.9	492.7
32	611.2	490.5	523.0	427.2	323.3
33	633.9	466.4	604.0	427.2	492.8
34	564.2	351.4	775.1	889.0	577.9
35	33.9	300.48	789.7	8.1	446.9
36	288.1	94.8	66.1	8.1	244.1
37	8.1	220.7	236.6	288.1	341.5
38	156.9	498.6	217.9	368.2	329.8
39	562.0	494.3	270.3	633.9	573.4
40	597.0	743.9	525.5	783.0	382.2
41	90.1	598.4	843.7	1088.0	878.3
42	648.9	403.1	455.2	217.5	415.7
43	580.4	520.4	n/a	516.7	524.5
44	540.6	481.9	474.3	432.5	438.1

45	516.7	574.0	n/a	580.4	574.3
46	566.3	521.7	526.4	516.7	535.2
47	368.2	201.9	451.3	156.9	304.4
48	705.1	460.6	n/a	325.0	378.8
49	29.9	651.3	685.6	783.0	701.6
50	632.0	442.4	n/a	209.0	388.0
51	783.0	383.1	344.9	597.0	499.9
52	302.1	437.6	323.1	325.0	440.0
53	325.2	426.0	n/a	362.0	454.6
54	162.0	320.2	389.4	364.1	299.7
55	385.3	465.6	500.8	46.8	485.9
56	459.0	644.0	204.0	636.5	283.6
57	86.8	372.0	329.9	162.0	275.0
58	446.0	574.0	n/a	459.0	320.6
59	100.6	509.6	516.2	440.5	526.8
60	739.5	454.3	552.9	480.3	475.6

Table v. ^{40}K estimates produced by each of the four point estimation procedures. Values in Bq/kg dry weight.

Sample	^{238}U	^{226}Ra	^{228}Ra	^{40}K	$^{226}Ra/^{238}U$	$^{228}Ra/^{238}U$	$^{226}Ra/^{228}Ra$
E 0-15	92.3	418.0	20.0	339.7	4.50	0.22	20.90
E 15-30	109.6	523.5	44.2	470.4	4.77	0.40	11.84
E 30-45	499.3	515.2	66.6	381.3	1.60	0.13	7.74
E 45-60	884.0	692.4	107.7	478.4	0.78	0.12	6.43
E 60-75	737.8	847.9	142.1	367.7	1.14	0.19	5.97
A 0-15	53.8	334.9	30.5	361.5	6.22	0.57	10.97
A 15-30	59.5	354.1	36.3	397.2	5.95	0.61	9.75
A 30-45	50.2	457.1	33.0	360.9	9.10	0.66	13.85
A 45-60	73.7	411.0	31.4	405.8	5.57	0.43	13.09
A 60-75	109.6	255.0	41.9	517.8	2.32	0.29	6.09
E 1	53.1	320.4	18.6	660.2	6.04	0.39	17.23
E 4	476.0	540.0	123.5	318.0	1.13	0.19	4.37
E 5	115.3	421.6	38.8	339.0	3.65	0.34	11.78
E6	83.6	444.8	32.2	275.0	5.32	0.39	13.81
9*	75.9	421.5	22.6	434.2	5.55	0.30	18.63
54*	788.0	479.0	117.3	162.0	0.61	0.15	4.08
41*	546.2	393.0	30.4	89.3	0.93	0.06	12.93
F 0-15	25.0	34.0	2.1	293.5	13.70	0.08	16.19
F 15-30	7.0	39.9	2.7	204.1	5.70	0.39	14.78
F 30-45	154.0	71.3	66.3	75.7	0.46	0.43	1.08
C10-15	14.1	19.1	5.9	134.4	1.35	0.42	3.23
C15-30	38.3	55.5	21.2	362.0	1.43	0.55	2.62
C 30-45	44.5	51.6	44.5	788.0	1.15	1.00	1.16
F 2	20.8	49.8	25.6	76.1	2.38	1.23	1.99
F 3	206.9	218.3	46.8	68.0	1.05	0.23	4.66

Table vii. Radiological properties of samples taken in Survey 2. Values in Bq/kg. * denotes samples taken in Survey 1 but included for data analysis with those of Survey2.

Sample	^{238}U E.C.	%^{238}UE.C.	^{238}UE.O.	%^{238}UE.O.	^{238}UFe	%^{238}UFe
E 0-15	5.9	6.4	7.9	8.5	55.9	60.5
E 15-30	6.3	5.8	6.0	5.4	99.8	91.0
E 30-45	4.9	1.0	49.5	9.9	350.9	70.2
E 45-60	1.3	0.2	167.8	19.0	542.9	61.4
E 60-75	11.9	1.4	110.4	12.5	522.3	70.8
A 0-15	3.8	7.2	1.2	2.2	40.1	74.5
A 15-30	2.7	4.6	6.7	11.3	49.8	83.6
A 30-45	1.9	3.7	5.1	10.1	30.9	41.9
A 45-60	11.4	15.6	40.2	54.4	28.2	38.2
A 60-75	3.8	3.5	58.5	53.3	46.1	42.0
E 1	2.0	3.8	19.9	37.6	31.0	58.3
E 4	10.6	2.2	114.0	23.9	320.0	67.2
E 5	17.5	15.2	54.0	46.8	40.1	34.7
E6	3.5	4.2	4.1	4.8	1.1	1.3
9*	7.5	10.0	36.6	48.2	21.1	27.8
54*	17.0	2.2	85.9	10.9	451.2	57.2
41*	8.2	1.5	74.9	13.8	283.0	51.8

Table viii. Speciation of ^{238}U for samples of Survey 2. Values in Bq/kg where applicable. * denotes samples taken in Survey 1 but included for data analysis with those of Survey2. E.C. - exchangeable cations, E.O. - easily oxidisable organic matter, Fe - amorphous iron oxides.

Sample	Ra^{226} E.C.	$\%Ra^{226}$E.C.	Ra^{226}E.O.	$\%Ra^{226}$E.O.	Ra^{226}Fe	$\%R^{a226}$Fe
E 0-15	4.8	1.15	2.3	0.6	26.5	6.3
E 15-30	5.3	1.02	2.1	0.4	26.1	4.9
E 30-45	8.19	1.59	0.3	0.1	36.2	7.0
E 45-60	15.9	2.30	5.4	0.8	67.7	9.7
E 60-75	18.7	2.20	6.6	1.0	63.3	7.4
A 0-15	5.3	1.57	1.3	0.4	3.4	1.0
A 15-30	3.4	0.95	0.6	0.2	27.8	7.8
A 30-45	1.5	0.33	2.1	0.5	84.1	18.4
A 45-60	4.7	1.15	1.4	0.3	84.5	20.5
A 60-75	10.2	4.03	2.8	1.1	53.3	20.9
E 1	1.6	0.50	2.5	0.8	76.0	23.7
E 4	23.8	4.42	11.6	2.1	3.9	0.7
E 5	37.5	8.90	9.6	2.3	17.7	4.2
E6	2.9	0.67	1.1	0.3	2.2	0.5
9*	1.1	0.26	1.2	0.3	13.0	3.1
54*	8.0	1.67	2.4	0.5	31.5	6.6
41*	14.0	3.56	1.4	0.4	19.0	4.8

Table ix. Speciation of ^{226}Ra for samples of Survey 2. Values in Bq/kg where applicable. * denotes samples taken in Survey 1 but included for data analysis with those of Survey2. E.C. - exchangeable cations, E.O. - easily oxidisable organic matter, Fe - amorphous iron oxides.

Sample	Ra^{228} E.C.	$\%Ra^{228}$E.C.	Ra^{228}E.O.	$\%Ra^{228}$E.O.	Ra^{228}Fe	$\%R^{a228}$Fe
E 0-15	2.1	10.4	5.5	27.5	3.7	18.5
E 15-30	3.2	7.1	8.3	11.9	3.5	7.9
E 30-45	6.1	9.1	1.7	2.5	9.7	14.5
E 45-60	7.6	7.1	4.5	4.2	21.7	20.1
E 60-75	9.0	6.3	3.4	0.3	26.0	18.3
A 0-15	2.3	7.5	4.1	13.4	3.4	11.3
A 15-30	1.4	3.8	0.5	1.5	8.5	23.4
A 30-45	3.8	11.5	0.9	2.8	14.3	43.3
A 45-60	5.0	16.0	8.0	25.5	9.0	28.7
A 60-75	5.8	13.7	1.1	2.5	10.3	24.6
E 1	4.7	25.1	2.1	11.1	9.7	52.3
E 4	14.2	11.5	4.1	3.3	8.1	6.6
E 5	3.9	10.8	3.8	9.9	2.3	6.0
E6	4.7	14.5	1.7	5.2	2.8	8.6
9*	4.7	20.6	0.5	2.2	2.2	10.1
54*	4.1	3.5	2.4	0.5	14.9	12.7
41*	8.6	28.4	6.1	20.1	8.7	28.6

Table x. Speciation of ^{228}Ra for samples of Survey 2. Values in Bq/kg where applicable. * denotes samples taken in Survey 1 but included for data analysis with those of Survey2. E.C. - exchangeable cations, E.O. - easily oxidisable organic matter, Fe - amorphous iron oxides.

Sample	% Org.Mat.	% H_2O	pH	Eh	CEC	Hum.Acid %	NonHum%
E 0-15	32.8	74.3	4.6	220.0	39.8	16.1	16.7
E 15-30	19.2	63.1	4.5	190.0	29.9	9.8	9.4
E 30-45	29.9	76.5	4.3	190.0	49.8	15.9	14.0
E 45-60	38.7	78.5	4.6	300.0	79.2	34.7	4.0
E 60-75	36.7	78.6	4.8	165.0	58.3	13.1	23.6
A 0-15	28.9	61.4	3.8	421.0	37.2	14.8	14.1
A 15-30	22.6	56.2	4.2	496.0	38.3	10.9	12.0
A 30-45	14.1	55.9	4.3	504.0	42.8	7.8	6.3
A 45-60	15.6	56.5	5.7	19.0	129.9	7.2	8.4
A 60-75	19.8	58.1	5.7	-55.0	15.3	14.1	5.7
E 1	11.5	51.1	4.0	287.0	58.2	7.6	3.9
E 4	41.6	78.0	5.7	182.0	68.9	37.1	4.5
E 5	45.4	77.8	5.8	136.0	56.7	17.2	28.2
E6	38.5	68.4	5.4	n/a	40.6	19.2	19.3
9*	19.7	43.9	4.9	n/a	3.7	8.4	11.3
54*	49.7	81.8	5.1	n/a	68.7	18.4	31.3
41*	40.8	80.7	5.4	n/a	46.1	20.6	20.2
F 0-15	96.5	82.1	3.8	308.0	136.9	40.2	56.3
F 15-30	96.9	83.6	3.8	264.0	131.9	39.2	57.7
F 30-45	87.9	83.4	3.9	191.0	92.4	20.8	67.1
C10-15	84.1	88.0	3.7	213.0	60.3	15.0	69.1
C15-30	38.3	84.9	3.9	192.0	54.0	13.3	25.0
C 30-45	40.4	67.3	3.9	182.0	37.1	12.1	28.3
F 2	90.9	85.2	3.8	334.0	82.9	32.5	58.4
F 3	85.1	83.3	4.1	330.0	91.8	34.6	50.5

Table xi. Chemical properties of samples of Survey 2. * denotes samples taken in Survey 1 but included for data analysis with those of Survey2. %Org.Mat-%age organic material w/w, %H_2O-%age moisture w/w, Eh-mV, CEC-cation exchange capacity meq/100 g, %HumAcid-%age humic acid w/w, %NonHum-%age non humic material w/w.

Sample	Iron	Sol. Iron	Manganese	Sol.mang.	Potassium	Sol. Potass.
E 0-15	106900	<0.3	34550	445	153	37
E 15-30	104900	< 0.3	39250	212	100	11
E 30-45	88550	< 0.3	30200	255	159	16
E 45-60	39750	< 0.3	6570	50	268	1
E 60-75	45080	< 0.3	3060	37	169	1
A 0-15	110600	< 0.3	16700	320	147	32
A 15-30	117700	< 0.3	29400	200	156	6
A 30-45	2150	< 0.3	43600	128	109	0
A 45-60	143200	< 0.3	21090	160	125	0
A 60-75	97900	4.7	6450	8	68	2
E 1	72580	< 0.3	25400	260	75	7
E 4	54370	5.9	1570	40	185	2
E 5	63340	21.4	11000	238	72	6
E6	3850	< 0.2	130	< 2	116	16
9*	90000	< 0.3	43600	54	110	1
54*	66500	< 0.3	6950	23	63	5
41*	147300	< 0.3	14650	70	139	0
F 0-15	1620	< 0.3	260	< 1	177	58
F 15-30	2770	< 0.3	28	< 3	105	23
F 30-45	580	< 0.3	70	< 3	74	6
C10-15	2490	14.2	60	< 4	260	202
C15-30	17580	< 0.3	55	< 2	63	17
C 30-45	1260	< 0.3	135	< 5	61	3
F 2	810	< 0.3	30	< 3	44	4
F 3	1690	< 0.3	30	< 4	79	12

Table xii. Chemical properties of samples of Survey 2. * denotes samples taken in Survey 1 but included for data analysis with those of Survey2. All values in ppm. Sol.Iron-soluble iron, Sol.mang-soluble manganese, Sol.potass- soluble potassium.

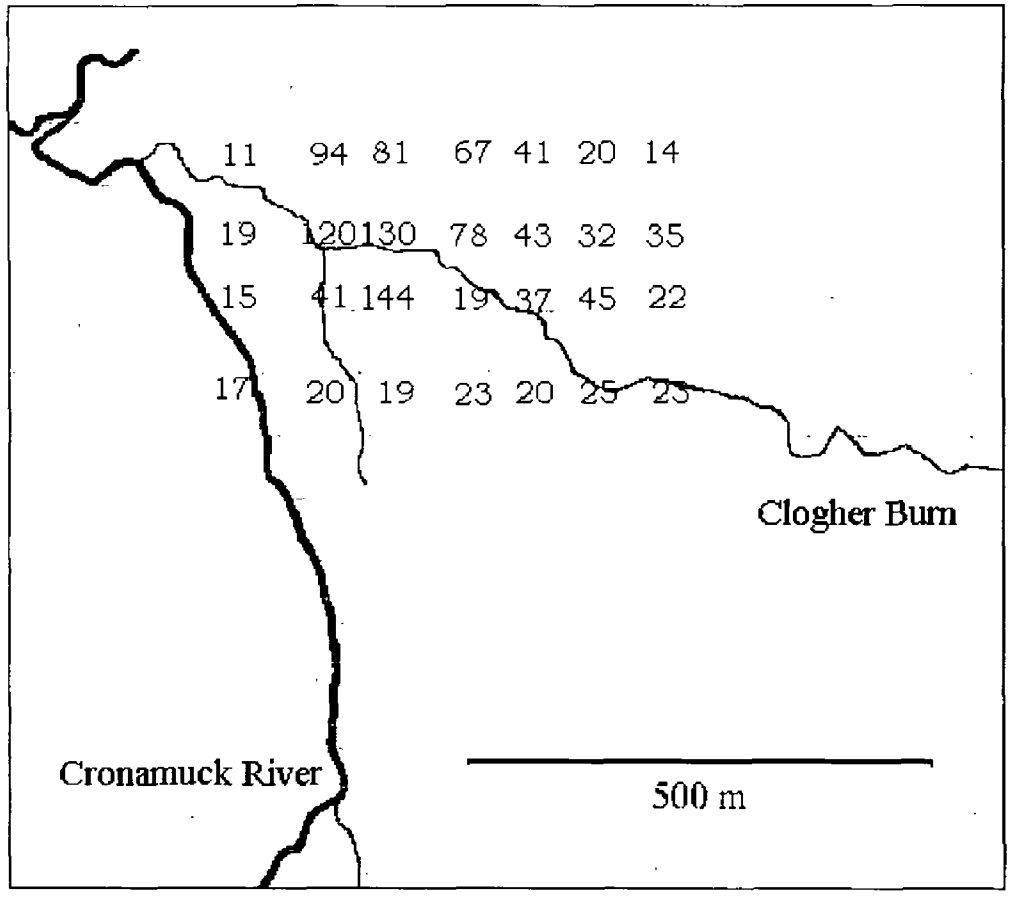

Figure i. Raw data for portable gamma spectrometer survey of location X. Values in counts per second.

Sample	pH	Eh mV	Cond. µS	Tds ppm	Fe ppm	U ppb
1	n/a	33	75.8	n/a	0.05	7.7
2	6.4	45	N/a	116	0.053	3.1
3	n/a	68	N/a	462	0.282	5.1
4	n/a	71	N/a	50	***0.005***	4.7
5	6.91	61	86.9	66	0.23	0.5
6	7.05	76	43.2	48	0.43	1.0
7	6.61	82	104	92	0.104	1.5
8	7.2	100	66.5	n/a	0.51	1.0
9	7.21	109	68.1	90	***0.005***	19.3
10	6.62	104	68	68	0.23	1.7
11	6.69	148	55.1	80	***0.01***	6.7
12	6.5	152	62.1	40	***0.01***	1.8
13	7.04	152	62.2	70	***0.01***	n/a
14	n/a	155	46.7	46	***0.01***	n/a
15	n/a	155	20.2	56	***0.01***	1.1
16	5.56	160	87	126	0.23	3.7
17	4.3	133	69.2	102	n/a	1.8
18	6.01	137	91	112	0.35	2.0
19	5.3	122	79	96	0.2	54.5
20	7.14	138	84	112	0.05	3.9

Table xii. Chemical properties of water samples taken during Survey 2. Cond. – conductivity, Tds. – total dissolve solids, ppm.

APPENDIX 2.

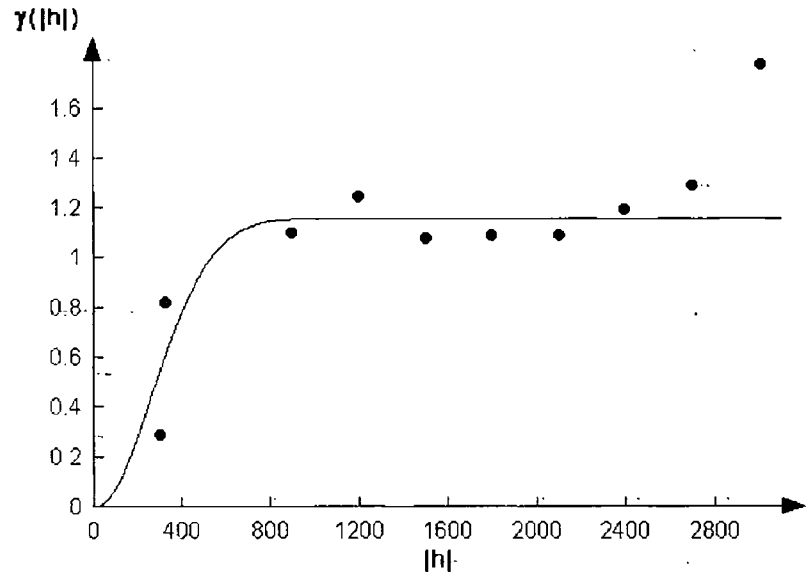

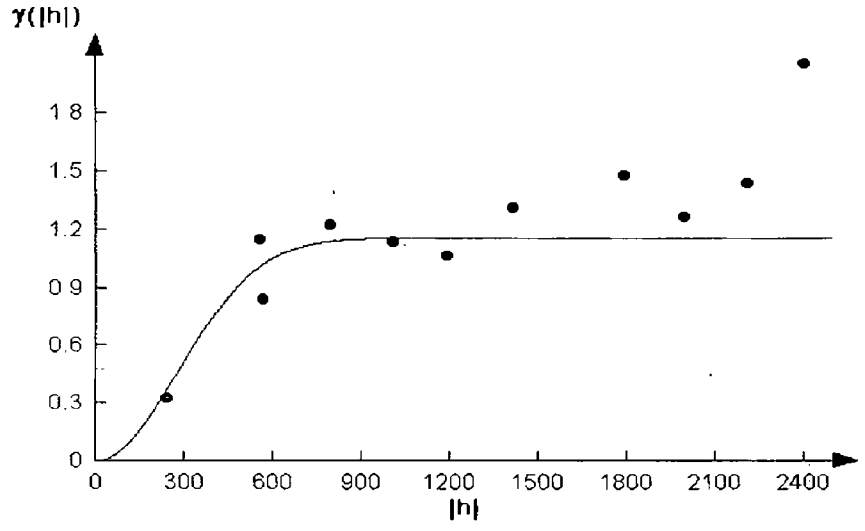

Figure i. Directional semi-variograms for $\ln^{238}U$. Top - 0^0, bottom - 45^0.

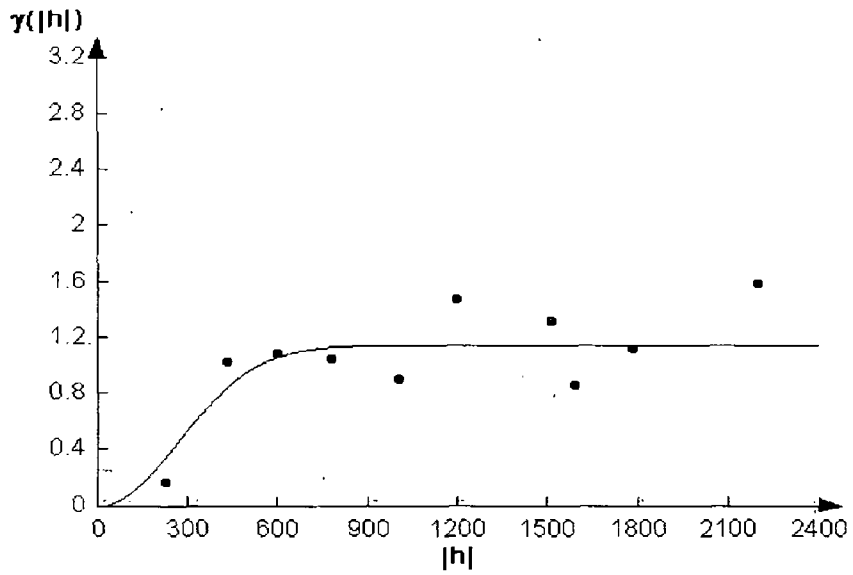

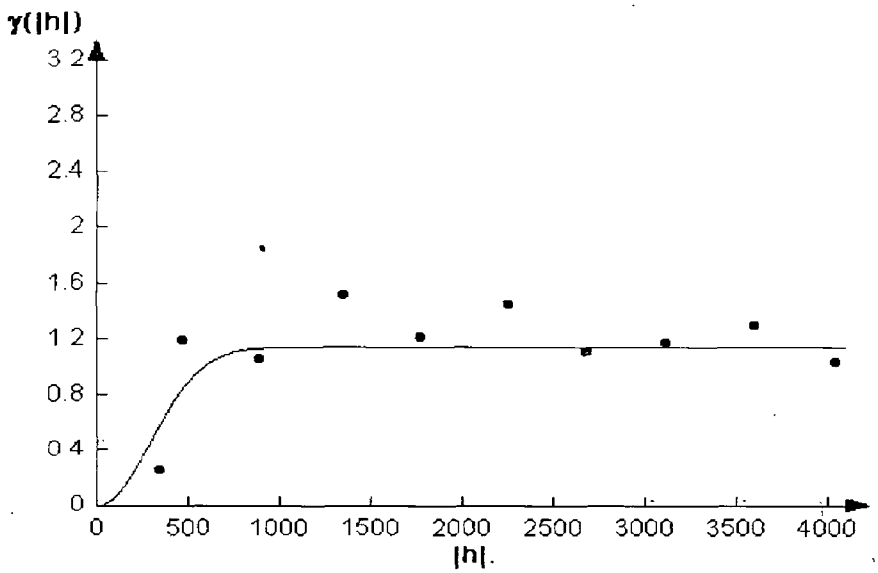

Figure ii. Directional semi-variograms for $\ln^{238}U$. Top - 90^0, bottom - 135^0.

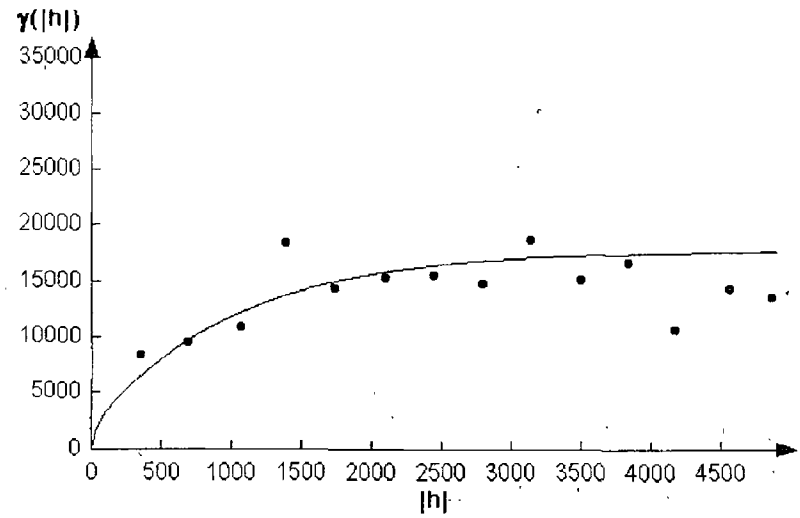

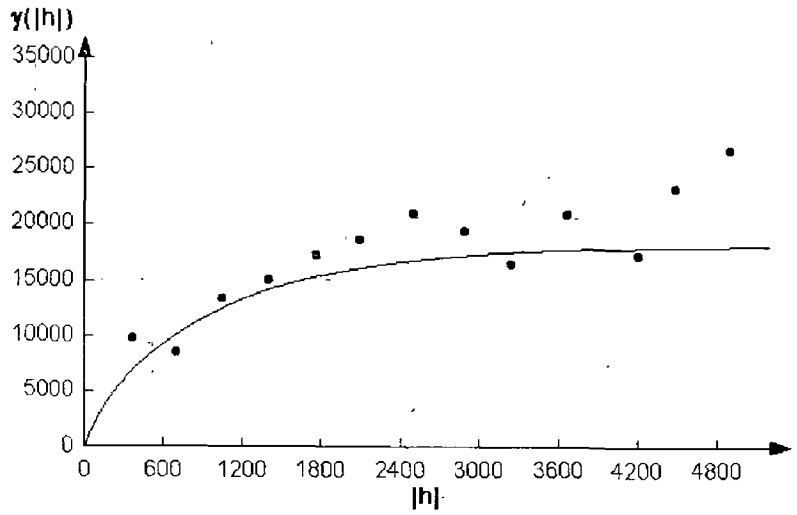

Figure iii. Directional semi-variograms for ^{226}Ra. Top - 0^0, bottom - 45^0.

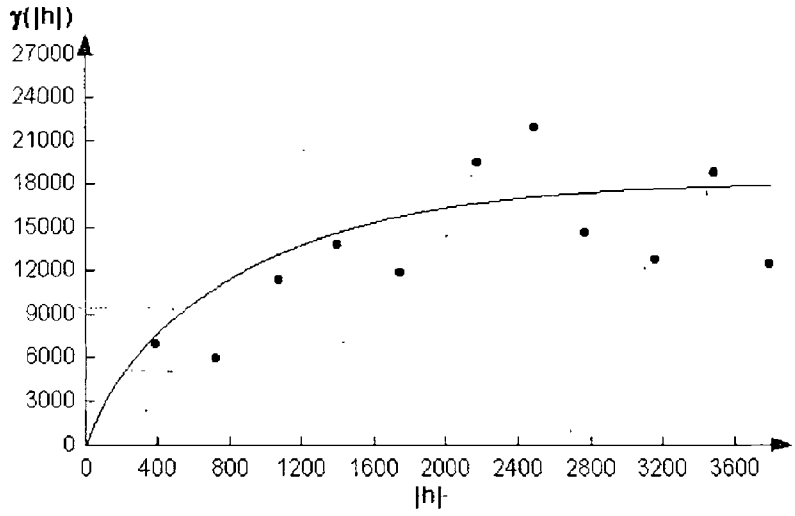

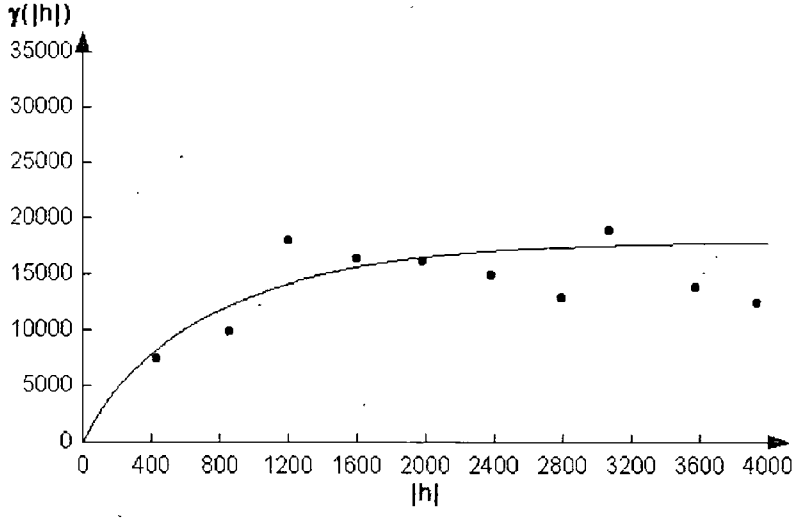

Figure iv. Directional semi-variograms for ^{226}Ra. Top - 90^0, bottom - 135^0.

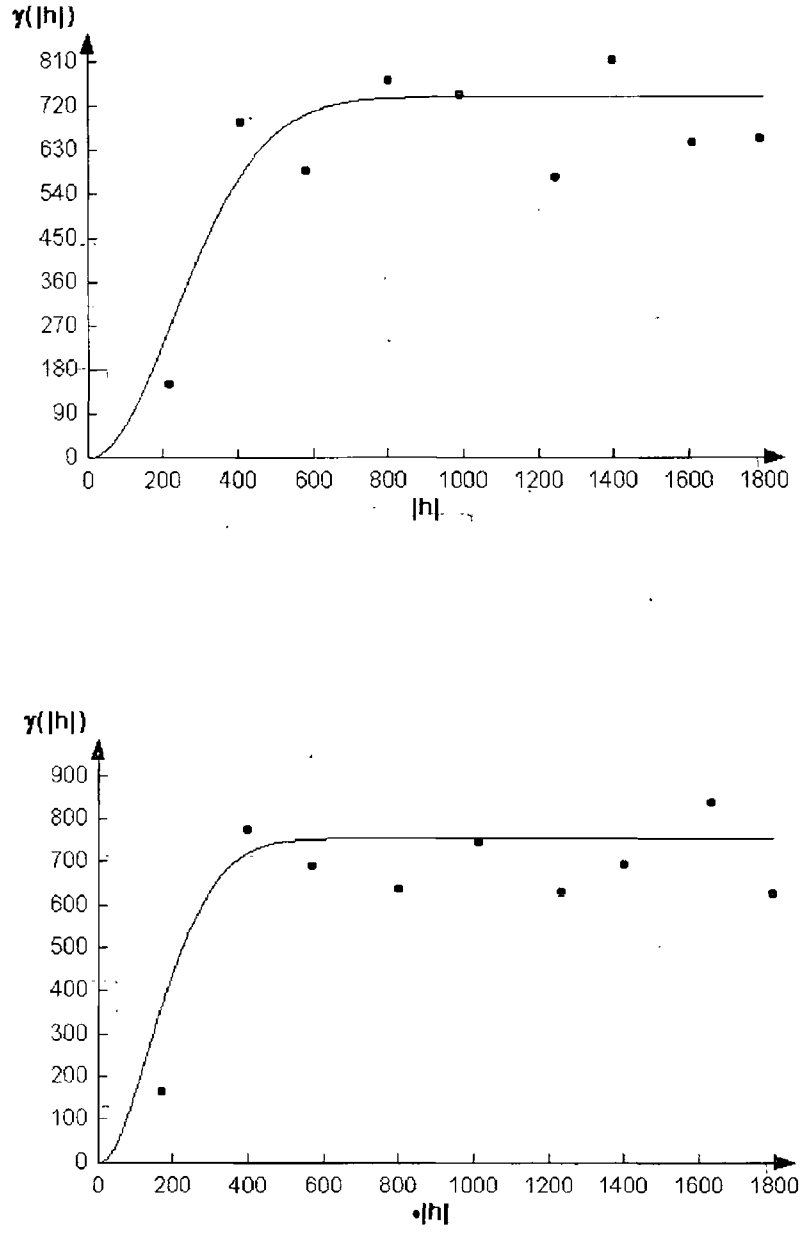

Figure v. Directional semi-variograms for ^{228}Ra. Top - 0^0, bottom - 45^0.

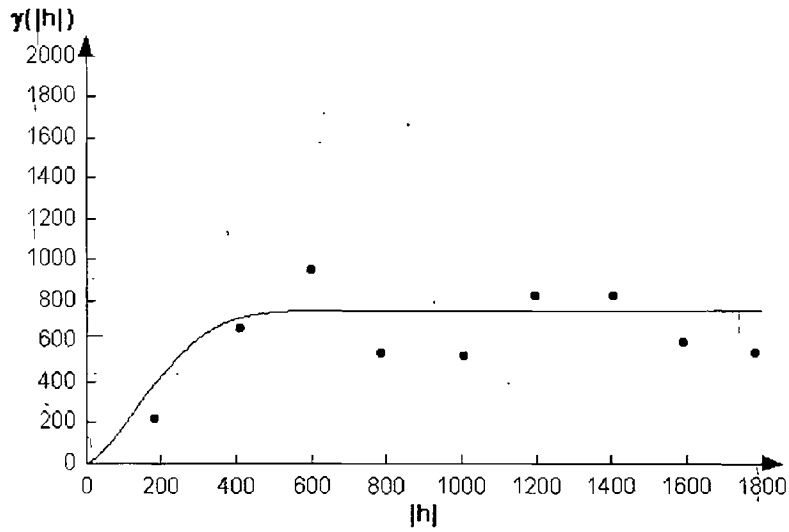

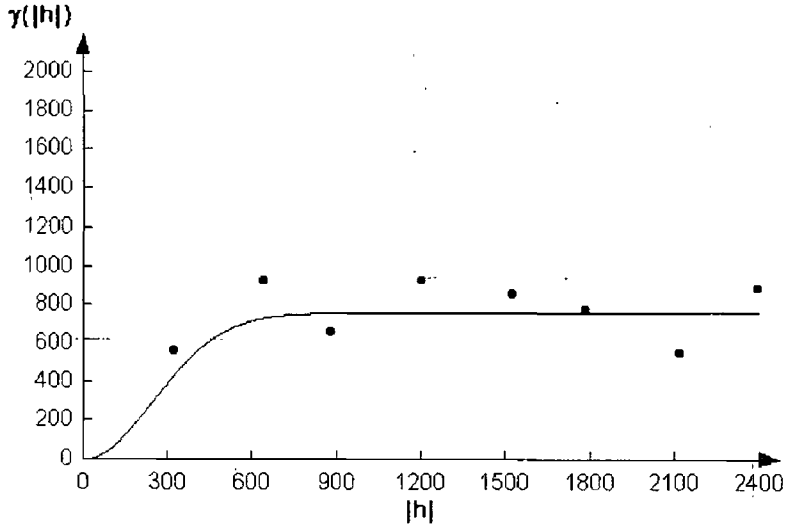

Figure vi. Directional semi-variograms for ^{228}Ra.. Top - 90^0, bottom - 135^0.

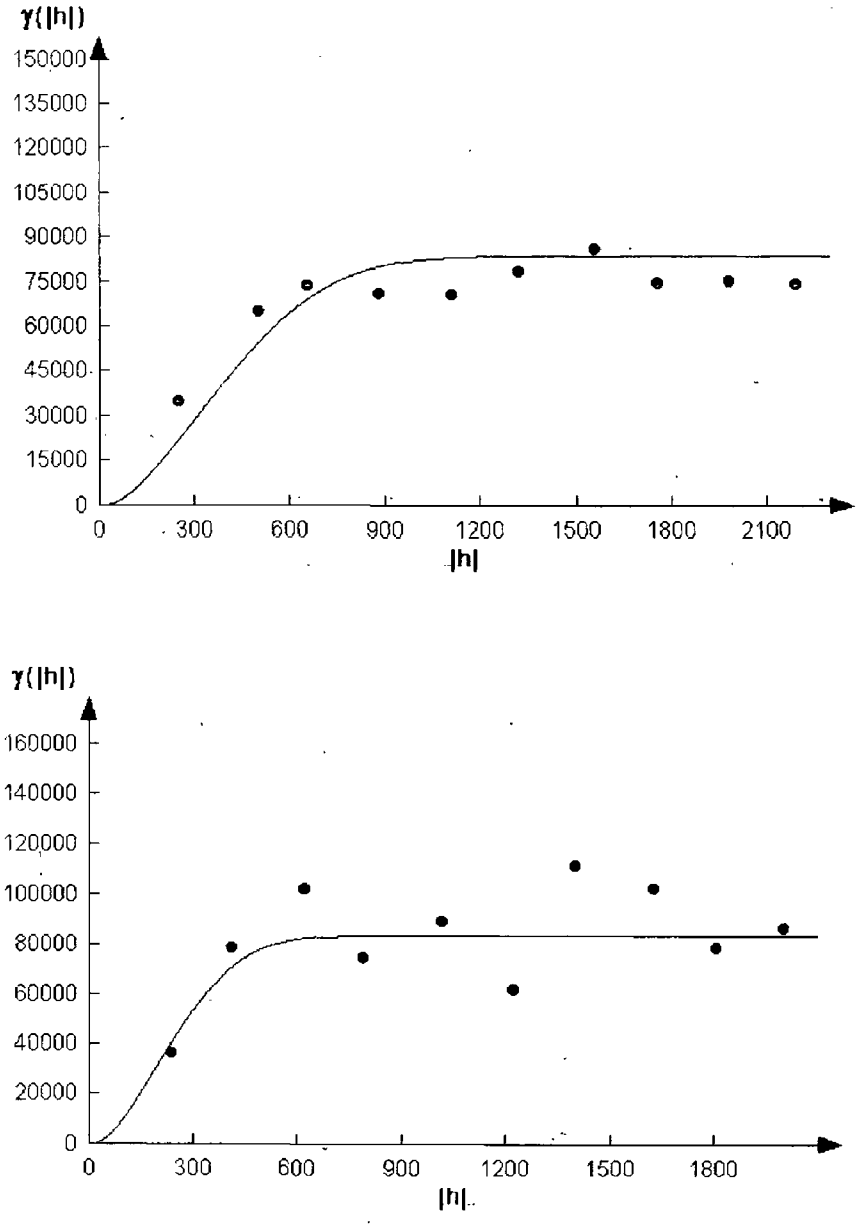

Figure vii. Directional semi-variograms for ^{40}K. Top - 0^0, bottom - 45^0.

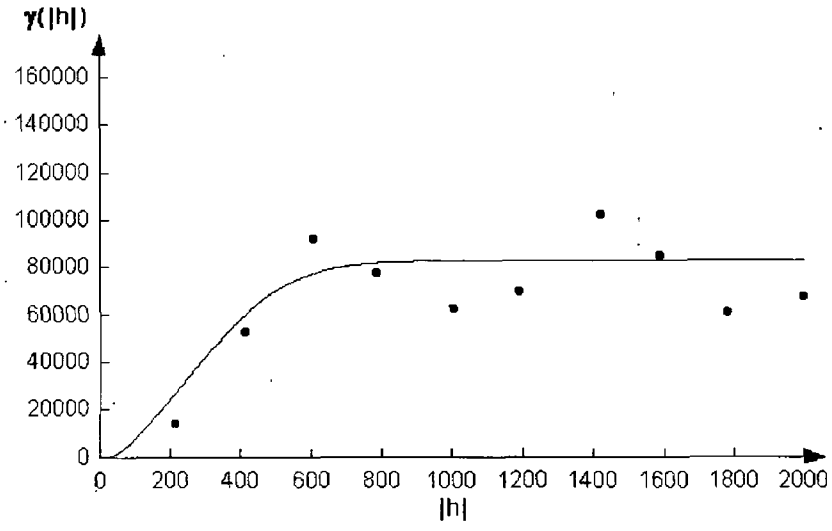

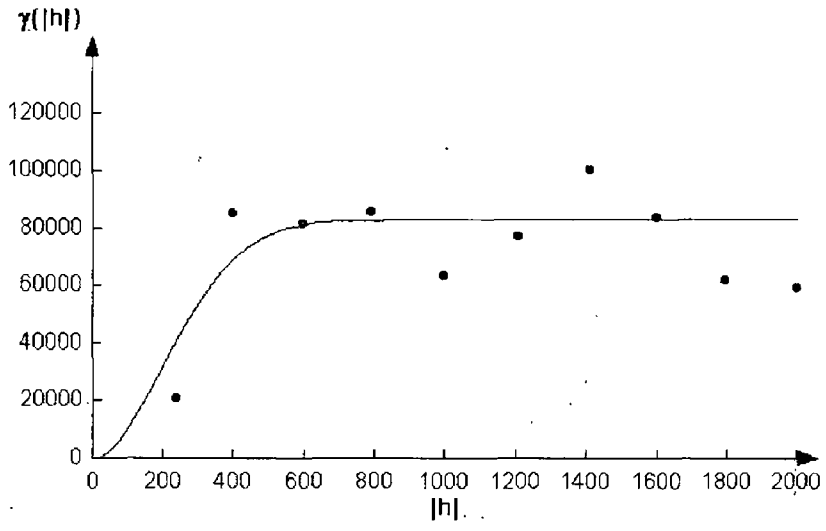

Figure viii. Directional semi-variograms for ^{40}K. Top - 90^0, bottom - 135^0

APPENDIX 3.

Correlation Matrix for ^{238}U.

^{238}U	^{226}Ra C.C. 0.71** Sig. 0.000 N 25	^{228}Ra C.C. 0.78** Sig. 0.000 N 25	$^{226}Ra/^{238}U$ C.C. -0.67** Sig. 0.000 N 25
$^{228}Ra/^{238}U$ C.C. –0.64** Sig. 0.001 N 25	$^{226}Ra/^{228}Ra$ C.C. –0.14 Sig. 0.504 N 25	^{238}U Ex. Cation. C.C. 0.44 Sig. 0.077 N 17	^{226}Ra Ex. Cation. C.C. 0.78** Sig. 0.000 N 17
^{228}Ra Ex. Cation. C.C. 0.58 Sig. 0.14 N 17	^{238}U Eas. Ox. Org C.C. 0.81** Sig. 0.000 N 17	^{226}Ra Eas. Ox. Org. C.C. 0.40 Sig. 0.111 N 17	^{228}Ra Eas. Ox. Org. C.C. 0.32 Sig. 0.200 N 17
^{238}U Fe Oxides C.C. 0.81** Sig. 000 N 17	^{226}Ra Fe Oxides C.C. –0.43 Sig. 0.870 N 17	^{228}Ra Fe Oxides C.C. 0.36 Sig. 0.15 N 17	Moisture C.C. –0.52 Sig. 0.80 N 25
pH C.C. 0.66** Sig. 0.000 N 25	Eh C.C. –0.36 Sig. 0.105 N 21	Cation Ex. Cap. C.C. –0.03 Sig. 0.868 N 25	Humic acids C.C. 0.16 Sig. 0.525 N 25
Non humic acids C.C. –0.29 Sig. 0.156 N 25	Organic material C.C. –0.64 Sig. 0.762 N 25	Iron C.C. 0.31 Sig. 0.125 N 25	Manganese C.C. 0.23 Sig. 0.265 N 25
Total Lab. ^{238}U C.C. 0.92** Sig. 0.000 N 17	Total Lab. ^{226}Ra C.C. 0.22 Sig. 0.392 N 17	Total Lab. ^{228}Ra C.C. 0.57 Sig. 0.017 N 17	

Table xiii. Correlation matrix for ^{238}U. C.C. - Correlation coefficient (Spearmans), Sig. - Significance (2 tailed), N - number of data points. Asterisks denote significant correlation at the 0.01 level (2 tailed).

Correlation Matrix for ^{226}Ra

^{238}U C.C. 0.71** Sig. 0.000 N 25	^{226}Ra	^{228}Ra C.C. 0.68** Sig. 0.000 N 25	$^{226}Ra/^{238}U$ C.C. −0.23 Sig. 0.265 N 25
$^{228}Ra/^{238}U$ C.C. −0.40 Sig. 0.045 N 25	$^{226}Ra/^{228}Ra$ C.C. 0.15 Sig. 0.465 N 25	^{238}U Ex. Cation. C.C. 0.26 Sig. 0.302 N 17	^{226}Ra Ex.Cation. C.C. 0.39 Sig. 0.114 N 17
^{228}Ra Ex.Cation. C.C. 0.36 Sig. 0.145 N 17	^{238}U Eas.Ox.Org C.C. 0.45 Sig. 0.067 N 17	^{226}Ra Eas.Ox.Org. C.C. 0.33 Sig. 0.189 N 17	^{228}Ra Eas.Ox.Org. C.C. 0.35 Sig. 0.216 N 17
^{238}U Fe Oxides. C.C. 0.82** Sig. 0.000 N 17	^{226}Ra Fe Oxides C.C. 0.02 Sig. 0.913 N 17	^{228}Ra Fe Oxides. C.C. 0.68** Sig. .002 N 17	Moisture C.C. −0.38 Sig. 0.189 N 25
pH C.C. 0.70** Sig. 0.000 N 25	Eh C.C. −0.24 Sig. 0.151 N 21	Cation Ex. Cap. C.C. −0.268 Sig. 0.269 N 25	Humic acids C.C. −0.157 Sig. 0.450 N 25
Non humic acids C.C. −0.58 Sig. 0.002 N 25	Organic material C.C. −0.41 Sig. 0.037 N 25	Iron C.C. 0.40 Sig. 0.045 N 25	Manganese C.C. 0.54 Sig. 0.005 N 25
Total Lab. ^{238}U C.C. 0.63 Sig. 0.006 N 17	Total Lab. ^{226}Ra C.C. 0.22 Sig. 0.382 N 17	Total Lab. ^{228}Ra C.C. 0.49 Sig. 0.045 N 17	

Table xiv. Correlation matrix for ^{226}Ra. C.C. - Correlation coefficient (Spearmans), Sig. - Significance (2 tailed), N - number of data points. Asterisks denote significant correlation at the 0.01 level (2 tailed).

Correlation Matrix for ^{228}Ra

^{238}U C.C. 0.78** Sig. 0.000 N 25	^{226}Ra C.C. 0.68** Sig. 0.000 N 25	^{228}Ra	$^{226}Ra/^{238}U$ C.C. –0.62** Sig. 0.001 N 25
$^{228}Ra/^{238}U$ C.C. –0.18 Sig. 0.384 N 25	$^{226}Ra/^{228}Ra$ C.C. –0.509** Sig. 0.009 N 25	^{238}U Ex. Cation. C.C. 0.27 Sig. 0.290 N 17	^{226}Ra Ex.Cation. C.C. –0.65** Sig. 0.004 N 17
^{228}Ra Ex.Cation. C.C. 0.41 Sig. 0.095 N 17	^{238}U Eas.Ox.Org C.C. 0.58 Sig. 0.013 N 17	^{226}Ra Eas.Ox.Org. C.C. 0.41 Sig. 0.096 N 17	^{228}Ra Eas.Ox.Org. C.C. 0.02 Sig. 0.922 N 17
^{238}U Fe Oxides C.C. 0.69** Sig. 0.002 N 17	^{226}Ra Fe Oxides C.C. 0.10 Sig. 0.69 N 17	^{228}Ra Fe.Oxides C.C. 0.47 Sig. 0.055 N 17	Moisture C.C. –0.05 Sig. 0.790 N 25
pH C.C. 0.45 Sig. 0.023 N 25	Eh C.C. –0.37 Sig. 0.094 N 21	Cation Ex. Cap. C.C. –0.03 Sig. 0.861 N 25	Humic acids C.C. 0.05 Sig. 0.810 N 25
Non humic acids C.C. –0.21 Sig. 0.308 N 25	Organic material C.C. –0.38 Sig. 0.858 N 25	Iron C.C. –0.13 Sig. 0.951 N 25	Manganese C.C. 0.04 Sig. 0.841 N 25
Total Lab. ^{238}U C.C. 0.75** Sig. 0.001 N 17	Total Lab. ^{226}Ra C.C. 0.30 Sig. 0.228 N 17	Total Lab. ^{228}Ra C.C. 0.55 Sig. 0.020 N 17	

Table xv. Correlation matrix for ^{228}Ra. C.C. - Correlation coefficient (Spearmans), Sig. - Significance (2 tailed), N - number of data points. Asterisks denote significant correlation at the 0.01 level (2 tailed).

Correlation Matrix for $^{226}Ra/^{238}U$

^{238}U C.C.-0.67** Sig. 0.000 N 25	^{226}Ra C.C. −0.23 Sig. 0.265 N 25	^{228}Ra C.C. −0.62** Sig. 0.001 N 25	$^{226}Ra/^{238}U$
$^{228}Ra/^{238}U$ C.C. 0.36 Sig. 0.070 N 25	$^{226}Ra/^{228}Ra$ C.C. 0.67** Sig. 0.000 N 25	^{238}U Ex. Cation. C.C. −0.43 Sig. 0.083 N 17	^{226}Ra Ex.Cation. C.C. −0.73** Sig. 0.001 N 17
^{228}Ra Ex.Cation. C.C. −0.59 Sig. 0.011 N 17	^{238}U Eas.Ox.Org C.C. −0.81** Sig. 0.000 N 17	^{226}Ra Eas.Ox.Org. C.C. −0.34 Sig. 0.177 N 17	^{228}Ra Eas.Ox.Org. C.C. −0.28 Sig. 0.272 N 17
^{238}U Fe Oxides C.C. −0.73** Sig. 0.000 N 17	^{226}Ra Fe Oxides C.C. 0.06 Sig. 0.815 N 17	^{228}Ra Fe Oxides C.C. −0.34 Sig. 0.176 N 17	Moisture C.C. −0.49 Sig. 0.011 N 25
pH C.C. −0.21 Sig. 0.292 N 25	Eh C.C. 0.40 Sig. 0.072 N 21	Cation Ex. Cap. C.C. −0.17 Sig. 0.402 N 25	Humic acids C.C. −0.36 Sig. 0.073 N 25
Non humic acids C.C. −0.23 Sig. 0.253 N 25	Organic material C.C. −0.39 Sig. 0.052 N 25	Iron C.C. 0.15 Sig. 0.470 N 25	Manganese C.C. 0.32 Sig. 0.119 N 25
Total Lab. ^{238}U C.C. −0.86** Sig. 0.000 N 17	Total Lab. ^{226}Ra C.C. −0.17 Sig. 0.504 N 17	Total Lab. ^{228}Ra C.C.-0.55 Sig. 0.022 N 17	

Table xvi. Correlation matrix for $^{226}Ra/^{238}U$. C.C. - Correlation coefficient (Spearmans), Sig. - Significance (2 tailed), N - number of data points. Asterisks denote significant correlation at the 0.01 level (2 tailed).

Correlation Matrix for $^{228}Ra/^{238}U$

^{238}U C.C. −0.64** Sig. 0.001 N 25	^{226}Ra C.C. −0.40 Sig. 0.045 N 25	^{228}Ra C.C. −0.18 Sig. 0.384 N 25	$^{226}Ra/^{238}U$ C.C. 0.36 Sig. 0.070 N 25
$^{228}Ra/^{238}U$	$^{226}Ra/^{228}Ra$ C.C. −0.28 Sig. 0.167 N 25	^{238}U Ex. Cation C.C. −0.32 Sig. 0.209 N 17	^{226}Ra Ex.Cation C.C. −0.55 Sig. 0.020 N 17
^{228}Ra Ex.Cation C.C. 0.60** Sig. 0.009 N 17	^{238}U Eas.Ox.Org C.C. −0.75** Sig. 0.000 N 17	^{226}Ra Eas.Ox.Org. C.C. −0.27 Sig. 0.279 N 17	^{228}Ra Eas.Ox.Org. C.C. −0.25 Sig. 0.325 N 17
^{238}U Fe Oxides C.C. −0.68** Sig. 0.002 N 17	^{226}Ra Fe Oxides C.C. 0.02 Sig. 0.926 N 17	^{228}Ra Fe Oxides C.C. −0.29 Sig. 0.249 N 17	Moisture C.C. −0.15 Sig. 0.474 N 25
pH C.C. −0.38 Sig. 0.054 N 25	Eh C.C. 0.22 Sig. 0.337 N 21	Cation Ex. Cap. C.C. −0.20 Sig. 0.325 N 25	Humic acids C.C. −0.424 Sig. 0.035 N 25
Non humic acids C.C. 0.10 Sig. 0.622 N 25	Organic material C.C. −0.17 Sig. 0.392 N 25	Iron C.C. −0.22 Sig. 0.282 N 25	Manganese C.C. −0.12 Sig. 0.564 N 25
Total Lab. ^{238}U C.C. −0.75** Sig. 0.000 N 17	Total Lab. ^{226}Ra C.C. −0.17 Sig. 0.492 N 17	Total Lab. ^{228}Ra C.C. −0.47 Sig. 0.052 N 17	

Table xvii. Correlation matrix for $^{228}Ra/^{238}U$. C.C. - Correlation coefficient (Spearmans), Sig. - Significance (2 tailed), N - number of data points. Asterisks denote significant correlation at the 0.01 level (2 tailed).

Correlation Matrix for $^{226}Ra/^{228}Ra$

^{238}U C.C. −0.14 Sig. 0.504 N 25	^{226}Ra C.C. 0.15 Sig. 0.465 N 25	^{228}Ra C.C. −0.509** Sig. 0.009 N 25	$^{226}Ra/^{238}U$ C.C. 0.67** Sig. 0.000 N 25
$^{228}Ra/^{238}U$ C.C. −0.28 Sig. 0.167 N 25	$^{226}Ra/^{228}Ra$	^{238}U Ex. Cation. C.C. −0.27 Sig. 0.290 N 17	^{226}Ra Ex.Cation. C.C. −0.71** Sig. 0.001 N 17
^{228}Ra Ex.Cation. C.C. −0.41 Sig. 0.095 N 17	^{238}U Eas.Ox.Org C.C. −0.63** Sig. 0.007 N 17	^{226}Ra Eas.Ox.Org. C.C. −0.37 Sig. 0.133 N 17	^{228}Ra Eas.Ox.Org. C.C. −0.01 Sig. 0.963 N 17
^{238}U Fe.Oxides C.C. −0.71** Sig. 0.001 N 17	^{226}Ra Fe Oxides. C.C. −0.02 Sig. 0.911 N 17	^{228}Ra Fe Oxides. C.C. −0.47 Sig. 0.051 N 17	Moisture C.C. −0.53** Sig. 0.006 N 25
pH C.C. 0.20 Sig. 0.321 N 25	Eh C.C. 0.20 Sig. 0.384 N 21	Cation Ex. Cap. C.C. −0.17 Sig. 0.391 N 25	Humic acids C.C. −0.19 Sig. 0.355 N 25
Non humic acids C.C. −0.40 Sig. 0.045 N 25	Organic material C.C. −0.41 Sig. 0.040 N 25	Iron C.C. 0.44 Sig. 0.027 N 25	Manganese C.C. 0.57** Sig. 0.003 N 25
Total Lab. ^{238}U C.C. −0.69** Sig. 0.002 N 17	Total Lab. ^{226}Ra C.C. −0.23 Sig. 0.390 N 17	Total Lab. ^{228}Ra C.C. −0.52 Sig. 0.030 N 17	

Table xviii. Correlation matrix for $^{226}Ra/^{228}Ra$. C.C. - Correlation coefficient (Spearmans), Sig. - Significance (2 tailed), N - number of data points. Asterisks denote significant correlation at the 0.01 level (2 tailed).

Correlation Matrix for ^{238}U: Exchangeable Cations

^{238}U C.C. 0.44 Sig. 0.077 N 17	^{226}Ra C.C. 0.26 Sig. 0.302 N 17	^{228}Ra C.C. 0.27 Sig. 0.290 N 17	$^{226}Ra/^{238}U$ C.C. −0.32 Sig. 0.209 N 17
$^{228}Ra/^{238}U$ C.C. −0.32 Sig. 0.209 N 17	$^{226}Ra/^{228}Ra$ C.C. −0.27 Sig. 0.290 N 17	^{238}U Ex. Cation.	^{226}Ra Ex.Cation. C.C. 0.47 Sig. 0.056 N17
^{228}Ra Ex.Cation. C.C. 0.22 Sig. 0.391 N 17	^{238}U Eas.Ox.Org C.C. 0.41 Sig. 0.097 N 17	^{226}Ra Eas.Ox.Org. C.C. 0.29 Sig. 0.251 N 17	^{228}Ra Eas.Ox.Org. C.C. 0.34 Sig. 0.176 N 17
^{238}U Fe Oxides C.C. 0.19 Sig. 0.463 N 17	^{226}Ra Fe Oxides C.C. −0.23 Sig. 0.389 N 17	^{228}Ra Fe Oxides C.C. −0.16 Sig. 0.535 N 17	Moisture C.C. 0.47 Sig. 0.051 N 17
pH C.C. 0.62** Sig. 0.008 N 17	Eh C.C. −0.73** Sig. 0.004 N 13	Cation Ex. Cap. C.C.0.262 Sig. 0.309 N 17	Humic acids C.C. 0.14 Sig. 0.570 N 17
Non humic acids C.C. 0.59 Sig. 0.12 N 17	Organic material C.C. 0.47 Sig. 0.055 N 17	Iron C.C. 0.173 Sig. 0.507 N 17	Manganese C.C. −0.19 Sig. 0.448 N 17
Total Lab. ^{238}U C.C. 0.46 Sig. 0.059 N 17	Total Lab. ^{226}Ra C.C. 0.04 Sig. 0.874 N 17	Total Lab. ^{228}Ra C.C. 0.16 Sig. 0.522 N 17	

Table xix. Correlation matrix for ^{238}U: Exchangeable Cations. C.C. - Correlation coefficient (Spearmans), Sig. - Significance (2 tailed), N - number of data points. Asterisks denote significant correlation at the 0.01 level (2 tailed).

Correlation Matrix for ^{226}Ra: Exchangeable Cations.

^{238}U C.C. 0.78** Sig. 0.000 N 17	^{226}Ra C.C. 0.39 Sig. 0.114 N 17	^{228}Ra C.C. −0.65** Sig. 0.004 N 17	$^{226}Ra/^{238}U$ C.C. −0.55 Sig. 0.020 N 17
$^{228}Ra/^{238}U$ C.C. −0.55 Sig. 0.020 N 17	$^{226}Ra/^{228}Ra$ C.C. −0.71** Sig. 0.001 N 17	^{238}U Ex. Cation C.C. 0.47 Sig. 0.056 N17	^{226}Ra Ex.Cation.
^{228}Ra Ex.Cation. C.C. 0.52 Sig. 0.032 N 17	^{238}U Eas.Ox.Org C.C. 0.73** Sig. 0.001 N 17	^{226}Ra Eas.Ox.Org. C.C. 0.61** Sig. 0.008 N 17	^{228}Ra Eas.Ox.Org. C.C. 0.42 Sig. 0.092 N 17
^{238}U Fe Oxides C.C. 0.70** Sig. 0.002 N 17	^{226}Ra Fe Oxides C.C. −0.11 Sig. 0.670 N 17	^{228}Ra Fe Oxides C.C. 0.20 Sig. 0.430 N 17	Moisture C.C. 0.79** Sig. 0.000 N 17
pH C.C. 0.45 Sig. 0.064 N 17	Eh C.C. −0.57 Sig. 0.040 N 13	Cation Ex. Cap. C.C. 0.41 Sig. 0.097 N 17	Humic acids C.C. 0.64** Sig. 0.005 N 17
Non humic acids C.C. 0.23 Sig. 0.358 N 17	Organic material C.C. 0.71** Sig. 0.001 N 17	Iron C.C. −0.10 Sig. 0.680 N 17	Manganese C.C. −0.60** Sig. 0.006 N 17
Total Lab. ^{238}U C.C. 0.78** Sig. 0.000 N 17	Total Lab. ^{226}Ra C.C. 0.29 Sig. 0.254 N 17	Total Lab. ^{228}Ra C.C. 0.52 Sig. 0.030 N 17	

Table xx. Correlation matrix for ^{226}Ra: Exchangeable Cations. C.C. - Correlation coefficient (Spearmans), Sig. - Significance (2 tailed), N - number of data points. Asterisks denote significant correlation at the 0.01 level (2 tailed).

Correlation Matrix for ^{228}Ra: Exchangeable Cations.

^{238}U C.C. 0.58 Sig. 0.14 N 17	^{226}Ra C.C. 0.36 Sig. 0.145 N 17	^{228}Ra C.C. 0.41 Sig. 0.095 N 17	$^{226}Ra/^{238}U$ C.C. −0.59 Sig. 0.011 N 17
$^{228}Ra/^{238}U$ C.C. 0.60** Sig. 0.009 N 17	$^{226}Ra/^{228}Ra$ C.C. −0.41 Sig. 0.095 N 17	^{238}U Ex. Cation. C.C. 0.22 Sig. 0.391 N 17	^{226}Ra Ex.Cation. C.C. 0.52 Sig. 0.032 N 17
^{228}Ra Ex.Cation.	^{238}U Eas.Ox.Org C.C. 0.0.75** Sig. 0.000 N 17	^{226}Ra Eas.Ox.Org. C.C. 0.35 Sig. 0.165 N 17	^{228}Ra Eas.Ox.Org. C.C. 0.13 Sig. 0.611 N 17
^{238}U Fe Oxides C.C. 0.38 Sig. 0.125 N 17	^{226}Ra Fe Oxides C.C.0.15 Sig. 0.566 N 17	^{228}Ra Fe Oxides C.C. 0.41 Sig. 0.102 N 17	Moisture C.C. 0.44 Sig. 0.074 N 17
pH C.C. 0.45 Sig. 0.065 N 17	Eh C.C. −0.50 Sig. .081 N 13	Cation Ex. Cap. C.C. 0.51 Sig. 0.033 N 17	Humic acids C.C. 0.35 Sig. 0.167 N 17
Non humic acids C.C. −0.17 Sig. 0.497 N 17	Organic material C.C. 0.30 Sig. 0.242 N 17	Iron C.C. −0.25 Sig. 0.317 N 17	Manganese C.C. −0.55 Sig. 0.021 N 17
Total Lab. ^{238}U C.C. 0.60** Sig. 0.010 N 17	Total Lab. ^{226}Ra C.C.0.45 Sig. 0.070 N 17	Total Lab. ^{228}Ra C.C. 0.69** Sig.0.002 N 17	

Table xxi. Correlation matrix for ^{228}Ra: Exchangeable Cations. C.C. - Correlation coefficient (Spearmans), Sig. - Significance (2 tailed), N - number of data points. Asterisks denote significant correlation at the 0.01 level (2 tailed).

Correlation Matrix ^{238}U: Easily Oxidisable Organic.

^{238}U C.C. 0.81** Sig. 0.000 N 17	^{226}Ra C.C. 0.45 Sig. 0.067 N 17	^{228}Ra C.C. 0.58 Sig. 0.013 N 17	$^{226}Ra/^{238}U$ C.C. −0.81** Sig. 0.000 N 17
$^{228}Ra/^{238}U$ C.C. −0.75** Sig. 0.000 N 17	$^{226}Ra/^{228}Ra$ C.C. −0.63** Sig. 0.007 N 17	^{238}U Ex. Cation. C.C. 0.41 Sig. 0.097 N 17	^{226}Ra Ex.Cation. C.C. 0.73** Sig. 0.001 N 17
^{228}Ra Ex.Cation. C.C. 0.0.75** Sig. 0.000 N 17		^{226}Ra Eas.Ox.Org. C.C. 0.62** Sig. 0.008 N 17	^{228}Ra Eas.Ox.Org. C.C. 0.19 Sig.0.456. N 17
^{238}U Fe Oxides C.C. 0.68** Sig. 0.002 N 17	^{226}Ra Fe Oxides C.C. 0.23 Sig. 0.374 N 17	^{228}Ra Fe Oxides C.C. 0.51 Sig. 0.036 N 17	Moisture C.C. 0.65** Sig. 0.004 N 17
pH C.C. 0.50 Sig. 0.037 N 17	Eh C.C. −0.58 Sig. 0.047 N 13	Cation Ex. Cap. C.C. 0.60** Sig. 0.10 N 17	Humic acids C.C. 0.47 Sig. 0.054 N 17
Non humic acids C.C. −0.10 Sig. 0.970 N 17	Organic material C.C. 0.56 Sig. 0.18 N 17	Iron C.C. −0.18 Sig. 0.468 N 17	Manganese C.C. −0.50 Sig. 0.039 N 17
Total Lab. ^{238}U C.C. 0.88** Sig. 0.000 N 17	Total Lab. ^{226}Ra C.C. 0.53 Sig. 0.026 N 17	Total Lab. ^{228}Ra C.C. 0.74** Sig. 0.001 N 17	

Table xxii. Correlation matrix for ^{238}U: Easily Oxidisable Organic. C.C. - Correlation coefficient (Spearmans), Sig. - Significance (2 tailed), N - number of data points. Asterisks denote significant correlation at the 0.01 level (2 tailed).

Correlation Matrix for ^{226}Ra: Easily Oxidisable Organic.

^{238}U C.C. 0.40 Sig. 0.111 N 17	^{226}Ra C.C. 0.33 Sig. 0.189 N 17	^{228}Ra C.C. 0.41 Sig. 0.096 N 17	$^{226}Ra/^{238}U$ C.C. –0.34 Sig. 0.177 N 17
$^{228}Ra/^{238}U$ C.C. –0.27 Sig. 0.279 N 17	$^{226}Ra/^{228}Ra$ C.C. –0.37 Sig. 0.133 N 17	^{238}U Ex. Cation. C.C. 0.29 Sig. 0.251 N 17	^{226}Ra Ex. Cation. C.C. 0.61** Sig. 0.008 N 17
^{228}Ra Ex. Cation. C.C. 0.35 Sig. 0.165 N 17	^{238}U Eas. Ox. Org C.C. 0.62** Sig. 0.008 N 17	^{226}Ra Eas. Ox. Org.	^{228}Ra Eas. Ox. Org. C.C. 0.29 Sig. 0.252 N 17
^{238}U Fe Oxides C.C. 0.38 Sig. 0.130 N 17	^{226}Ra Fe Oxides C.C. 0.18 Sig. 0.485 N 17	^{228}Ra Fe Oxides C.C. 0.32 Sig. 0.210 N 17	Moisture C.C. 0.39 Sig. 0.117 N 17
pH C.C. 0.40 Sig. 0.103 N 17	Eh C.C. –0.42 Sig. 0.153 N 13	Cation Ex. Cap. C.C. 0.45 Sig. 0.068 N 17	Humic acids C.C. 0.27 Sig. 0.290 N 17
Non humic acids C.C. –0.14 Sig. 0.573 N 17	Organic material C.C. 0.34 Sig. 0.182 N 17	Iron C.C. –0.41 Sig. 0.100 N 17	Manganese C.C. –0.47 Sig. 0.056 N 17
Total Lab. ^{238}U C.C. 0.50 Sig. 0.040 N 17	Total Lab. ^{226}Ra C.C. 0.52 Sig. 0.029 N 17	Total Lab. ^{228}Ra C.C. 0.49 Sig. 0.046 N 17	

Table xxiii. Correlation matrix for ^{226}Ra: Easily Oxidisable Organic. C.C. - Correlation coefficient (Spearmans), Sig. - Significance (2 tailed), N - number of data points. Asterisks denote significant correlation at the 0.01 level (2 tailed).

Correlation Matrix for ^{228}Ra: Easily Oxidisable Organic.

^{238}U C.C. 0.32 Sig. 0.200 N 17	^{226}Ra C.C. 0.35 Sig. 0.216 N 17	^{228}Ra C.C. 0.02 Sig. 0.922 N 17	$^{226}Ra/^{238}U$ C.C. –0.28 Sig. 0.272 N 17
$^{228}Ra/^{238}U$ C.C. –0.25 Sig. 0.325 N 17	$^{226}Ra/^{228}Ra$ C.C. –0.01 Sig. 0.963 N 17	^{238}U Ex. Cation. C.C. 0.34 Sig. 0.176 N 17	^{226}Ra Ex.Cation. C.C. 0.42 Sig. 0.092 N 17
^{228}Ra Ex.Cation. C.C. 0.13 Sig. 0.611 N 17	^{238}U Eas.Ox.Org C.C. 0.19 Sig. 0.456. N 17	^{226}Ra Eas.Ox.Org. C.C. 0.29 Sig. 0.252 N 17	^{228}Ra Eas.Ox.Org.
^{238}U Fe Oxides C.C. 0.32 Sig. 0.21 N 17	^{226}Ra Fe Oxides C.C. –0.02 Sig. 0.918 N 17	^{228}Ra Fe Oxides C.C. –0.04 Sig. 0.868 N 17	Moisture C.C. 0.45 Sig. 0.065 N 17
pH C.C. 0.19 Sig. 0.457 N 17	Eh C.C. –0.26 Sig. 0.388 N 13	Cation Ex. Cap. C.C. 0.36 Sig. 0.149 N 17	Humic acids C.C. 0.24 Sig. 0.347 N 17
Non humic acids C.C. 0.05 Sig. 0.822 N 17	Organic material C.C. 0.21 Sig. 0.405 N 17	Iron C.C. 0.32 Sig. 0.210 N 17	Manganese C.C. –0.11 Sig. 0.652 N 17
Total Lab. ^{238}U C.C. 0.39 Sig. 0.119 N 17	Total Lab. ^{226}Ra C.C. 0.15 Sig. 0.566 N 17	Total Lab. ^{228}Ra C.C. 0.36 Sig. 0.152 N 17	

Table xxiv. Correlation matrix for ^{228}Ra: Easily Oxidisable Organic. C.C. - Correlation coefficient (Spearmans), Sig. - Significance (2 tailed), N - number of data points. Asterisks denote significant correlation at the 0.01 level (2 tailed).

Correlation Matrix for ^{238}U: Iron Oxides.

^{238}U C.C. 0.81** Sig. 000 N 17	^{226}Ra C.C. 0.82** Sig. 0.000 N 17	^{228}Ra C.C. 0.69** Sig. 0.002 N 17	$^{226}Ra/^{238}U$ C.C. −0.73** Sig. 0.000 N 17
$^{228}Ra/^{238}U$ C.C. −0.68** Sig. 0.002 N 17	$^{226}Ra/^{228}Ra$ C.C. −0.71** Sig. 0.001 N 17	^{238}U Ex. Cation. C.C. 0.19 Sig. 0.463 N 17	^{226}Ra Ex.Cation. C.C. 0.70** Sig. 0.002 N 17
^{228}Ra Ex.Cation. C.C. 0.38 Sig. 0.125 N 17	^{238}U Eas.Ox.Org C.C. 0.68** Sig. 0.002 N 17	^{226}Ra Eas.Ox.Org. C.C. 0.38 Sig. 0.130 N 17	^{228}Ra Eas.Ox.Org. C.C. 0.32 Sig. 0.21 N 17
^{238}U Fe Oxides	^{226}Ra Fe.Oxides C.C. 0.15 Sig. 0.557 N 17	^{228}Ra Fe.Oxides C.C. 0.56 Sig. 0.018 N 17	Moisture C.C. 0.77** Sig. 0.000 N 17
pH C.C. −0.05 Sig. 0.836 N 17	Eh C.C. −0.03 Sig. 0.900 N 13	Cation Ex. Cap. C.C. 0.39 Sig. 0.121 N 17	Humic acids C.C.0.51 Sig. 0.035 N 17
Non humic acids C.C. 0.13 Sig. 0.596 N 17.	Organic material C.C. 0.53 Sig. 0.026 N 17	Iron C.C. −0.08 Sig. 0.757 N 17	Manganese C.C. −0.28 Sig. 0.264 N 17.
Total Lab. ^{238}U C.C. 0.26 Sig. 0.302 N 17	Total Lab. ^{226}Ra C.C. 0.86** Sig. 0.000 N 17	Total Lab. ^{228}Ra C.C. 0.67** Sig. 0.003 N 17	

Table xxv. Correlation matrix for ^{238}U: Iron Oxides. C.C. - Correlation coefficient (Spearmans), Sig. - Significance (2 tailed), N - number of data points. Asterisks denote significant correlation at the 0.01 level (2 tailed).

Correlation Matrix for ^{226}Ra: Iron Oxides.

^{238}U C.C. –0.43 Sig. 0.870 N 17	^{226}Ra C.C. 0.02 Sig. 0.913 N 17	^{228}Ra C.C. 0.10 Sig. 0.69 N 17	$^{226}Ra/^{238}U$ C.C. 0.06 Sig. 0.815 N 17
$^{228}Ra/^{238}U$ C.C. 0.02 Sig. 0.926 N 17	$^{226}Ra/^{228}Ra$ C.C. 0.02 Sig. 0.926 N 17	^{238}U Ex. Cation. C.C. –0.23 Sig. 0.389 N 17	^{226}Ra Ex. Cation. C.C. –0.11 Sig. 0.670 N 17
^{228}Ra Ex. Cation. C.C. 0.15 Sig. 0.566 N 17	^{238}U Eas. Ox. Org C.C. 0.23 Sig. 0.374 N 17	^{226}Ra Eas. Ox. Org. C.C. 0.18 Sig. 0.485 N 17	^{228}Ra Eas. Ox. Org. C.C. –0.02 Sig. 0.918 N 17
^{238}U Fe Oxides C.C. 0.15 Sig. 0.557 N 17	^{226}Ra Fe Oxides	^{228}Ra Fe Oxides C.C. 0.79** Sig. 0.000 N 17	Moisture C.C. –0.16 Sig. 0.535 N 17
pH C.C. –0.17 Sig. 0.508 N 17	Eh C.C. 0.008 Sig. 0.979 N 13	Cation Ex. Cap. C.C. 0.42 Sig. 0.088 N 17	Humic acids C.C. –0.50 Sig. 0.040 N 17
Non humic acids C.C. –0.40 Sig. 0.112 N 17	Organic material C.C. 0.45 Sig. 0.068 N 17	Iron C.C. –0.08 Sig. 0.751 N 17	Manganese C.C. 0.18 Sig. 0.480 N 17
Total Lab. ^{238}U C.C. 0.17 Sig. 0.504 N 17	Total Lab. ^{226}Ra C.C. 0.86** Sig. 0.000 N 17	Total Lab. ^{228}Ra C.C. 0.55 Sig. 0.021 N 17	

Table xxvi. Correlation matrix for ^{226}Ra: Iron Oxides. C.C. - Correlation coefficient (Spearmans), Sig. - Significance (2 tailed), N - number of data points. Asterisks denote significant correlation at the 0.01 level (2 tailed).

Correlation Matrix for ^{228}Ra: Iron Oxides.

^{238}U C.C. 0.36 Sig. 0.15 N 17	^{226}Ra C.C. 0.68** Sig. .002 N 17	^{228}Ra C.C. 0.47 Sig. 0.055 N 17	$^{226}Ra/^{238}U$ C.C. –0.34 Sig. 0.176 N 17
$^{228}Ra/^{238}U$ C.C. –0.29 Sig. 0.249 N 17	$^{226}Ra/^{228}Ra$ C.C. –0.47 Sig. 0.051 N 17	^{238}U Ex. Cation. C.C. –0.16 Sig. 0.535 N 17	^{226}Ra Ex.Cation. C.C. 0.20 Sig. 0.430 N 17
^{228}Ra Ex.Cation. C.C. 0.41 Sig. 0.102 N 17	^{238}U Eas.Ox.Org C.C. 0.51 Sig. 0.036 N 17	^{226}Ra Eas.Ox.Org. C.C. 0.32 Sig. 0.210 N 17	^{228}Ra Eas.Ox.Org. C.C. –0.04 Sig. 0.868 N 17
^{238}U Fe.Oxides C.C. 0.56 Sig. 0.018 N 17	^{226}Ra Fe Oxides C.C.0.79** Sig. 0.000 N 17	^{228}Ra Fe.Oxides	Moisture. C.C. 0.30 Sig. 0.237 N 17
pH C.C. –0.13 Sig. 0.609 N 17	Eh C.C. 0.04 Sig. 0.897 N 13	Cation Ex. Cap. C.C. 0.51 Sig. 0.036 N 17	Humic acids C.C. –0.03 Sig. 0.896 N 17
Non humic acids C.C. –0.19 Sig. 0.465 N 17	Organic material C.C. –0.01 Sig. 0.970 N 17	Iron C.C. –0.27 Sig. 0.279 N 17	Manganese C.C. –0.22 Sig. 0.379 N 17
Total Lab. ^{238}U C.C. 0.48 Sig. 0.050 N 17	Total Lab. ^{226}Ra C.C. 0.74** Sig. 0.001 N 17	Total Lab. ^{228}Ra C.C. 0.79** Sig. 0.000 N 17	

Table xxvii. Correlation matrix for ^{228}Ra: Iron Oxides. C.C. - Correlation coefficient (Spearmans), Sig. - Significance (2 tailed), N - number of data points. Asterisks denote significant correlation at the 0.01 level (2 tailed).

Correlation Matrix for Moisture.

^{238}U C.C. −0.52 Sig. 0.80 N 25	^{226}Ra C.C. −0.38 Sig. 0.189 N 25	^{228}Ra C.C. −0.05 Sig. 0.790 N 25	$^{226}Ra/^{238}U$ C.C. −0.49 Sig. 0.011 N 25
$^{228}Ra/^{238}U$ C.C. −0.15 Sig. 0.474 N 25	$^{226}Ra/^{228}Ra$ C.C. −0.53** Sig. 0.006 N 25	^{238}U Ex. Cation. C.C. 0.47 Sig. 0.051 N 17	^{226}Ra Ex.Cation. C.C. 0.79** Sig. 0.000 N 17
^{228}Ra Ex.Cation. C.C. 0.44 Sig. 0.074 N 17	^{238}U Eas.Ox.Org C.C. 0.65** Sig. 0.004 N 17	^{226}Ra Eas.Ox.Org. C.C. 0.39 Sig. 0.117 N 17	^{228}Ra Eas.Ox.Org. C.C. 0.45 Sig. 0.065 N 17
^{238}U Fe.Oxides C.C. 0.77** Sig. 0.000 N 17	^{226}Ra Fe Oxides. C.C. −0.16 Sig. 0.535 N 17	^{228}Ra Fe Oxides C.C. 0.30 Sig. 0.237 N 17	Moisture
pH C.C. −0.40 Sig. 0.043 N 25	Eh C.C.0.01 Sig. 0.949 N 21	Cation Ex. Cap. C.C. 0.63** Sig. 0.001 N 25	Humic acids C.C. 0.70** Sig. 0.000 N 25
Non humic acids C.C. 0.77** Sig. 0.000 N 25	Organic material C.C. 0.86** Sig. 0.000 N 25	Iron C.C. −0.56** Sig. 0.004 N 25	Manganese C.C. −0.79** Sig. 0.000 N 25
Total Lab. ^{238}U C.C. 0.77** Sig. 0.000 N 17	Total Lab. ^{226}Ra C.C. 0.12 Sig. 0.639 N 17	Total Lab. ^{228}Ra C.C. 0.55 Sig. 0.020 N 17	

Table xxviii. Correlation matrix for Moisture. C.C. - Correlation coefficient (Spearmans), Sig. - Significance (2 tailed), N - number of data points. Asterisks denote significant correlation at the 0.01 level (2 tailed).

Correlation Matrix for pH.

^{238}U C.C. 0.66** Sig. 0.000 N 25	^{226}Ra C.C. 0.70** Sig. 0.000 N 25	^{228}Ra C.C. 0.70** Sig. 0.000 N 25	$^{226}Ra/^{238}U$ C.C. −0.21 Sig. 0.292 N 25
$^{228}Ra/^{238}U$ C.C. −0.38 Sig. 0.054 N 25	$^{226}Ra/^{228}Ra$ C.C. 0.20 Sig. 0.321 N 25	^{238}U Ex. Cation. C.C. 0.62** Sig. 0.008 N 17	^{226}Ra Ex. Cation. C.C. 0.45 Sig. 0.064 N 17
^{228}Ra Ex. Cation. C.C. 0.45 Sig. 0.065 N 17	^{238}U Eas. Ox. Org C.C. 0.50 Sig. 0.037 N 17	^{226}Ra Eas. Ox. Org. C.C. 0.40 Sig. 0.103 N 17	^{228}Ra Eas. Ox. Org. C.C. 0.19 Sig. 0.457 N 17
^{238}U Fe Oxides C.C. −0.05 Sig. 0.836 N 17	^{226}Ra Fe Oxides C.C. −0.17 Sig. 0.508 N 17	^{228}Ra Fe Oxides C.C. −0.13 Sig. 0.609 N 17	Moisture C.C. −0.40 Sig. 0.043 N 25
pH	Eh C.C.-0.57** Sig. 0.006 N 21	Cation Ex. Cap. C.C. −0.23 Sig. 0.252 N 25	Humic acids C.C. −0.13 Sig. 0.509 N 25
Non humic acids C.C. −0.52** Sig. 0.007 N 25	Organic material C.C. −0.34 Sig. 0.096 N 25	Iron C.C. 0.51** Sig. 0.009 N 25	Manganese C.C. 0.39 Sig. 0.050 N25
Total Lab. ^{238}U C.C. 0.31 Sig. 0.214 N 17	Total Lab. ^{226}Ra C.C. 0.17 Sig. 0.496 N 17	Total Lab. ^{228}Ra C.C. 0.18 Sig. 0.469 N 17	

Table xxix. Correlation matrix for pH. C.C. - Correlation coefficient (Spearmans), Sig. - Significance (2 tailed), N - number of data points. Asterisks denote significant correlation at the 0.01 level (2 tailed).

Correlation Matrix for Eh.

^{238}U C.C. −0.36 Sig. 0.105 N 21	^{226}Ra C.C. −0.24 Sig. 0.151 N 21	^{228}Ra C.C. −0.37 Sig. 0.094 N 21	$^{226}Ra/^{238}U$ C.C. 0.40 Sig. 0.072 N 21
$^{228}Ra/^{238}U$ C.C. 0.22 Sig. 0.337 N 21	$^{226}Ra/^{228}Ra$ C.C. 0.20 Sig. 0.384 N 21	^{238}U Ex. Cation. C.C. −0.73** Sig. 0.004 N 13	^{226}Ra Ex.Cation. C.C. −0.57 Sig. 0.040 N 13
^{228}Ra Ex.Cation. C.C. −0.50 Sig. .081 N 13	^{238}U Eas.Ox.Org C.C. −0.58 Sig. 0.047 N 13	^{226}Ra Eas.Ox.Org. C.C. −0.42 Sig. 0.153 N 13	^{228}Ra Eas.Ox.Org. C.C. −0.26 Sig. 0.388 N 13
^{238}U Fe.Oxides C.C. −0.03 Sig. 0.900 N 13	^{226}Ra Fe Oxides C.C. 0.008 Sig. 0.979 N 13	^{228}Ra Fe.Oxides. C.C. 0.04 Sig. 0.897 N 13	Moisture C.C.0.01 Sig. 0.949 N 21
pH C.C.-0.57** Sig. 0.006 N 21	Eh	Cation Ex. Cap. C.C. 0.11 Sig. 0.628 N 21	Humic acids C.C. 0.14 Sig. 0.523 N 21
Non humic acids C.C. 0.09 Sig. 0.670 N 21	Organic material C.C. 0.08 Sig. 0.726 N 21	Iron C.C. −0.21 Sig. 0.355 N 21	Manganese C.C. 0.00 Sig. 0.978 N 21
Total Lab. ^{238}U C.C. −0.48 Sig. 0.096 N 13	Total Lab. ^{226}Ra C.C. −0.31 Sig. 0.301 N 13	Total Lab. ^{228}Ra C.C. −0.23 Sig. 0.442 N 13	

Table xxx. Correlation matrix for Eh. C.C. - Correlation coefficient (Spearmans), Sig. - Significance (2 tailed), N - number of data points. Asterisks denote significant correlation at the 0.01 level (2 tailed).

Correlation Matrix for Cation Exchange Capacity.

^{238}U C.C. −0.03 Sig. 0.868 N 25	^{226}Ra C.C. −0.268 Sig. 0.269 N 25	^{228}Ra C.C. −0.03 Sig. 0.861 N 25	$^{226}Ra/^{238}U$ C.C. −0.17 Sig. 0.402 N 25
$^{228}Ra/^{238}U$ C.C. −0.20 Sig. 0.325 N 25	$^{226}Ra/^{228}Ra$ C.C. −0.17 Sig. 0.391 N 25	^{238}U Ex. Cation. C.C. 0.262 Sig. 0.309 N 17	^{226}Ra Ex. Cation. C.C. 0.41 Sig. 0.097 N 17
^{228}Ra Ex. Cation. C.C. 0.51 Sig. 0.033 N 17	^{238}U Eas. Ox. Org C.C. 0.60** Sig. 0.10 N 17	^{226}Ra Eas. Ox. Org. C.C. 0.45 Sig. 0.068 N 17	^{228}Ra Eas. Ox. Org. C.C. 0.36 Sig. 0.149 N 17
^{238}U Fe Oxides. C.C. 0.39 Sig. 0.121 N 17	^{226}Ra Fe Oxides. C.C. 0.42 Sig. 0.088 N 17	^{228}Ra Fe Oxides C.C. 0.51 Sig. 0.036 N 17	Moisture C.C. 0.63** Sig. 0.001 N 25
pH C.C. −0.23 Sig. 0.252 N 25	Eh C.C. 0.11 Sig. 0.628 N 21	Cation Ex. Cap.	Humic acids C.C. 0.57** Sig. 0.003 N 25
Non humic acids C.C. 0.41 Sig. 0.038 N 25	Organic material C.C. 0.63** Sig. 0.001 N 25	Iron C.C. −0.47 Sig. 0.018 N 25	Manganese C.C. −0.56** Sig. 0.003 N 25
Total Lab. ^{238}U C.C. 0.52 Sig. 0.031 N 17	Total Lab. ^{226}Ra C.C. 0.67** Sig. 0.003 N 17	Total Lab. ^{228}Ra C.C. 0.72** Sig. 0.001 N 17	

Table xxxi. Correlation matrix for Cation Exchange Capacity. C.C. - Correlation coefficient (Spearmans), Sig. - Significance (2 tailed), N - number of data points. Asterisks denote significant correlation at the 0.01 level (2 tailed).

Correlation Matrix for Humic Acids.

^{238}U C.C. 0.16 Sig. 0.525 N 25	^{226}Ra C.C.-0.15 Sig. 0.450 N 25	^{228}Ra C.C.0.05 Sig. 0.810 N 25	$^{226}Ra/^{238}U$ C.C.-0.36 Sig. 0.073 N 25
$^{228}Ra/^{238}U$ C.C.-0.42 Sig. 0.035 N 25	$^{226}Ra/^{228}Ra$ C.C.-0.19 Sig. 0.355 N 25	^{238}U Ex. Cation. C.C.0.14 Sig. 0.570 N 17	^{226}Ra Ex.Cation. C.C. 0.64** Sig. 0.005 N 17
^{228}Ra Ex.Cation. C.C. 0.35 Sig. 0.167 N 17	^{238}U Eas.Ox.Org C.C.0.47 Sig. 0.054 N 17	^{226}Ra Eas.Ox.Org. C.C. 0.27 Sig. 0.290 N 17	^{228}Ra Eas.Ox.Org. C.C. 0.24 Sig. 0.347 N 17
^{238}U Fe Oxides C.C. 0.51 Sig. 0.035 N 17	^{226}Ra Fe Oxides. C.C.-0.50 Sig. 0.040 N 17	^{228}Ra Fe Oxides C.C.-0.03 Sig. 0.896 N 17	Moisture C.C.0.70** Sig. 0.000 N 25
pH C.C.-0.13 Sig. 0.509 N 25	Eh C.C.0.14 Sig. 0.523 N 21	Cation Ex. Cap. C.C.0.57** Sig. 0.003 N 25	Humic acids
Non humic acids C.C. 0.46 Sig. 0.02 N 25	Organic material C.C. 0.85** Sig. 0.000 N 25	Iron C.C.-0.42 Sig. 0.034 N 25	Manganese C.C. –0.61** Sig. 0.001 N 25
Total Lab. ^{238}U C.C. 0.46 Sig. 0.058 N 17	Total Lab. ^{226}Ra C.C. –0.211 Sig. 0.417 N 17	Total Lab. ^{228}Ra C.C. 0.22 Sig. 0.390 N 17	

Table xxxii. Correlation matrix for Humic Acids. C.C. - Correlation coefficient (Spearmans), Sig. - Significance (2 tailed), N - number of data points. Asterisks denote significant correlation at the 0.01 level (2-tailed).

Correlation Matrix for Non Humic Acids.

^{238}U C.C.-0.29 Sig. 0.156 N 25	^{226}Ra C.C.-0.58 Sig. 0.002 N 25	^{228}Ra C.C.-0.21 Sig. 0.308 N 25	$^{226}Ra/^{238}U$ C.C.-0.23 Sig. 0.253 N 25
$^{228}Ra/^{238}U$ C.C. 0.10 Sig. 0.622 N 25	$^{226}Ra/^{228}Ra$ C.C.-0.40 Sig. 0.045 N 25	^{238}U Ex. Cation. C.C. 0.59 Sig. 0.12 N 17	^{226}Ra Ex.Cation. C.C. 0.23 Sig. 0.358 N 17
^{228}Ra Ex.Cation. C.C. –0.17 Sig. 0.497 N 17	^{238}U Eas.Ox.Org C.C. –0.10 Sig. 0.970 N 17	^{226}Ra Eas.Ox.Org. C.C.-0.14 Sig. 0.573 N 17	^{228}Ra Eas.Ox.Org. C.C. 0.05 Sig. 0.822 N 17
^{238}U Fe.Oxides C.C. 0.13 Sig. 0.596 N 17	^{226}Ra Fe.Oxides C.C.-0.40 Sig. 0.112 N 17	^{228}Ra Fe Oxides. C.C. –0.19 Sig. 0.465 N 17	Moisture. C.C.0.77** Sig. 0.000 N 25
pH C.C.-0.52** Sig. 0.007 N 25	Eh C.C.0.09 Sig. 0.670 N 21	Cation Ex. Cap. C.C.0.41 Sig. 0.038 N 25	Humic acids C.C. 0.46 Sig. 0.020 N 25
Non humic acids	Organic material C.C. 0.81** Sig. 0.000 N 25	Iron C.C. 0.58** Sig. 0.002 N 25	Manganese C.C. –0.67** Sig. 0.000 N 25
Total Lab. ^{238}U C.C. 0.12 Sig. 0.639 N 17	Total Lab. ^{226}Ra C.C. –0.32 Sig. 0.198 N 17	Total Lab. ^{228}Ra C.C. 0.22 Sig. 0.390 N 17	

Table xxxiii. Correlation matrix for Non Humic Acids. C.C. - Correlation coefficient (Spearmans), Sig. - Significance (2 tailed), N - number of data points. Asterisks denote significant correlation at the 0.01 level (2 tailed).

Correlation Matrix for Organic Matter.

^{238}U C.C.-0.64 Sig. 0.762 N 25	^{226}Ra C.C.-0.41 Sig. 0.037 N 25	^{228}Ra C.C. −0.38 Sig. 0.858 N 25	$^{226}Ra/^{238}U$ C.C. −0.39 Sig. 0.052 N 25
$^{228}Ra/^{238}U$ C.C.-0.17 Sig. 0.392 N 25	$^{226}Ra/^{228}Ra$ C.C.-0.41 Sig. 0.040 N 25	^{238}U Ex. Cation. C.C. 0.47 Sig. 0.055 N 17	^{226}Ra Ex.Cation. C.C. 0.71** Sig. 0.001 N 17
^{228}Ra Ex.Cation. C.C.0.30 Sig. 0.242 N 17	^{238}U Eas.Ox.Org C.C.0.56 Sig. 0.18 N 17	^{226}Ra Eas.Ox.Org. C.C.0.34 Sig. 0.182 N 17	^{228}Ra Eas.Ox.Org. C.C.0.21 Sig. 0.405 N 17
^{238}U Fe.Oxides C.C. 0.53 Sig. 0.026 N 17	^{226}Ra Fe Oxides C.C. 0.45 Sig. 0.068 N 17	^{228}Ra Fe Oxides C.C. −0.01 Sig. 0.970 N 17	Moisture C.C.0.86** Sig. 0.000 N 25
pH C.C.-0.34 Sig. 0.096 N 25	Eh C.C.0.08 Sig. 0.726 N 21	Cation Ex. Cap. C.C.0.63** Sig. 0.001 N 25	Humic acids C.C. 0.85** Sig. 0.000 N 25
Non humic acids C.C. 0.81** Sig. 0.000 N 25	Organic material	Iron C.C. −0.62** Sig. 0.001 N 25	Manganese C.C. −0.78** Sig. 0.000 N 25
Total Lab. ^{238}U C.C. 0.56 Sig. 0.018 N 17	Total Lab. ^{226}Ra C.C. −0.12 Sig. 0.626 N 17	Total Lab. ^{228}Ra C.C. 0.23 Sig. 0.36 N 17	

Table xxxiv. Correlation matrix for Organic Material. C.C. - Correlation coefficient (Spearmans), Sig. - Significance (2 tailed), N - number of data points. Asterisks denote significant correlation at the 0.01 level (2 tailed).

Correlation Matrix for Iron.

^{238}U C.C. 0.31 Sig.0.125 N 25	^{226}Ra C.C. 0.40 Sig. 0.045 N 25	^{228}Ra C.C. –0.13 Sig. 0.951 N 25	$^{226}Ra/^{238}U$ C.C. 0.15 Sig. 0.470 N 25
$^{228}Ra/^{238}U$ C.C. –0.22 Sig. 0.282 N 25	$^{226}Ra/^{228}Ra$ C.C. 0.44 Sig. 0.027 N 25	^{238}U Ex. Cation. C.C. 0.173 Sig. 0.507 N 17	^{226}Ra Ex.Cation. C.C. –0.10 Sig. 0.680 N 17
^{228}Ra Ex.Cation. C.C.-0.25 Sig. 0.317 N 17	^{238}U Eas.Ox.Org C.C. –0.18 Sig. 0.468 N 17	^{226}Ra Eas.Ox.Org. C.C.-0.41 Sig. 0.100 N 17	^{228}Ra Eas.Ox.Org. C.C.0.32 Sig. 0.210 N 17
^{238}U Fe Oxides C.C.-0.08 Sig. 0.757 N 17	^{226}Ra Fe.Oxides C.C.-0.08 Sig. 0.751 N 17	^{228}Ra Fe.Oxides. C.C.-0.27 Sig. 0.279 N 17	Moisture C.C.-0.56** Sig. 0.004 N 25
pH C.C.0.51** Sig. 0.009 N 25	Eh C.C.-0.21 Sig. 0.355 N 21	Cation Ex. Cap. C.C. –0.47 Sig. 0.018 N 25	Humic acids C.C. –0.42 Sig. 0.034 N 25
Non humic acids C.C. –0.58** Sig. 0.002 N 25	Organic material C.C. –0.62** Sig. 0.001 N 25	Iron	Manganese C.C. 0.69** Sig. 0.000 N 25
Total Lab. ^{238}U C.C. 0.34 Sig. 0.174 N 17	Total Lab. ^{226}Ra C.C.0.28 Sig. 0.265 N 17	Total Lab. ^{228}Ra C.C. –0.18 Sig. 0.480 N 17	

Table xxxv. Correlation matrix for Iron. C.C. - Correlation coefficient (Spearmans), Sig. - Significance (2 tailed), N - number of data points. Asterisks denote significant correlation at the 0.01 level (2 tailed).

Correlation Matrix for Manganese.

^{238}U C.C. 0.23 Sig. 0.265 N 25	^{226}Ra C.C.0.54 Sig. 0.005 N 25	^{228}Ra C.C.0.04 Sig. 0.841 N 25	$^{226}Ra/^{238}U$ C.C.0.32 Sig. 0.119 N 25
$^{228}Ra/^{238}U$ C.C.-0.12 Sig. 0.564 N 25	$^{226}Ra/^{228}Ra$ C.C.0.57** Sig. 0.003 N 25	^{238}U Ex. Cation. C.C.-0.19 Sig. 0.448 N 17	^{226}Ra Ex.Cation. C.C.-0.60** Sig. 0.006 N 17
^{228}Ra Ex.Cation. C.C.-0.55 Sig. 0.021 N 17	^{238}U Eas.Ox.Org C.C.-0.50 Sig. 0.039 N 17	^{226}Ra Eas.Ox.Org. C.C.-0.47 Sig. 0.056 N 17	^{228}Ra Eas.Ox.Org. C.C.-0.11 Sig. 0.652 N 17
^{238}U Fe Oxides C.C.-0.28 Sig. 0.264 N 17	^{226}Ra Fe Oxides C.C.0.18 Sig. 0.480 N 17	^{228}Ra Fe Oxides C.C.-0.22 Sig. 0.379 N 17	Moisture C.C.-0.79** Sig. 0.000 N 25
pH C.C.0.39 Sig. 0.050 N 25	Eh C.C.0.00 Sig. 0.978 N 21	Cation Ex. Cap. C.C.-0.56** Sig. 0.003 N 25	Humic acids C.C. –0.61** Sig. 0.001 N 25
Non humic acids C.C.-0.67** Sig. 0.000 N 25	Organic material C.C.-0.78** Sig. 0.000 N 25	Iron C.C. 0.69** Sig. 0.000 N 25	Manganese
Total Lab. ^{238}U C.C. –0.35 Sig. 0.158 N 17	Total Lab. ^{226}Ra C.C. –0.14 Sig. 0.593 N 17	Total Lab. ^{228}Ra C.C. –0.365 Sig. 0.149 N 17	

Table xxxvi. Correlation matrix for Manganese. C.C. - Correlation coefficient (Spearmans), Sig. - Significance (2 tailed), N - number of data points. Asterisks denote significant correlation at the 0.01 level (2 tailed).

Correlation Matrix for Total Labile ^{238}U.

^{238}U C.C. 0.92** Sig. 0.000 N 17	^{226}Ra C.C.0.63 Sig. 0.006 N 17	^{228}Ra C.C.0.75** Sig. 0.001 N 17	$^{226}Ra/^{238}U$ C.C.-0.86** Sig. 0.000 N 17
$^{228}Ra/^{238}U$ C.C.-0.75** Sig. 0.000 N 17	$^{226}Ra/^{228}Ra$ C.C.-0.69** Sig. 0.002 N 17	^{238}U Ex. Cation. C.C.0.46 Sig. 0.059 N 17	^{226}Ra Ex.Cation. C.C.0.78** Sig. 0.000 N 17
^{228}Ra Ex.Cation. C.C.0.60** Sig. 0.010 N 17	^{238}U Eas.Ox.Org C.C. 0.88** Sig. 0.000 N 17	^{226}Ra Eas.Ox.Org. C.C.0.50 Sig. 0.040 N 17	^{228}Ra Eas.Ox.Org. C.C.0.39 Sig. 0.119 N 17
^{238}U Fe Oxides C.C.0.26 Sig. 0.302 N 17	^{226}Ra Fe Oxides C.C.0.17 Sig. 0.504 N 17	^{228}Ra Fe Oxides C.C.0.48 Sig. 0.050 N 17	Moisture C.C. 0.77** Sig. 0.000 N 17
pH C.C.0.31 Sig. 0.214 N 17	Eh C.C.-0.48 Sig. 0.096 N 13	Cation Ex. Cap. C.C.0.52 Sig. 0.031 N 17	Humic acids C.C.0.46 Sig. 0.058 N 17
Non humic acids C.C. 0.12 Sig. 0.639 N 17	Organic material C.C. 0.56 Sig. 0.018 N 17	Iron C.C. 0.34 Sig. 0.174 N 17	Manganese C.C. –0.35 Sig. 0.188 N 17
Total Lab. ^{238}U	Total Lab. ^{226}Ra C.C.0.42 Sig. 0.092 N 17	Total Lab. ^{228}Ra C.C. 0.72** Sig. 0.001 N 17	

Table xxxvii. Correlation matrix for Total Labile ^{238}U. C.C. - Correlation coefficient (Spearmans), Sig. - Significance (2 tailed), N - number of data points. Asterisks denote significant correlation at the 0.01 level (2 tailed).

Correlation Matrix for Total Labile ^{226}Ra.

^{238}U C.C. 0.22 Sig. 0.392 N 17	^{226}Ra C.C. 0.22 Sig. 0.382 N 17	^{228}Ra C.C.0.30 Sig. 0.228 N 17	$^{226}Ra/^{238}U$ C.C.-0.17 Sig. 0.504 N 17
$^{228}Ra/^{238}U$ C.C.-0.17 Sig. 0.492 N 17	$^{226}Ra/^{228}Ra$ C.C. –0.23 Sig. 0.390 N 17	^{238}U Ex. Cation. C.C.0.04 Sig. 0.874 N 17	^{226}Ra Ex.Cation. C.C.0.29 Sig. 0.254 N 17
^{228}Ra Ex.Cation. C.C.0.45 Sig. 0.070 N 17	^{238}U Eas.Ox.Org C.C.0.53 Sig. 0.026 N 17	^{226}Ra Eas.Ox.Org. C.C.0.52 Sig. 0.029 N 17	^{228}Ra Eas.Ox.Org. C.C. 0.15 Sig. 0.566 N 17
^{238}U Fe Oxides C.C.0.86** Sig. 0.000 N 17	^{226}Ra Fe Oxides C.C.0.86** Sig. 0.000 N 17	^{228}Ra Fe Oxides C.C.0.74** Sig. 0.001 N 17	Moisture. C.C.0.12 Sig. 0.639 N 17
pH C.C.0.17 Sig. 0.496 N 17	Eh C.C.-0.31 Sig. 0.301 N 13	Cation Ex. Cap. C.C. 0.67** Sig. 0.003 N 17	Humic acids C.C.-0.21 Sig. 0.417 N 17
Non humic acids C.C.-0.32 Sig. 0.198 N 17	Organic material C.C.0.12 Sig. 0.626 N 17	Iron C.C.0.28 Sig. 0.265 N 17	Manganese C.C. –0.14 Sig. 0.593 N 17
Total Lab. ^{238}U C.C.0.42 Sig. 0.092 N 17	Total Lab. ^{226}Ra	Total Lab. ^{228}Ra C.C. 0.71** Sig. 0.001 N 17	

Table xxxviii. Correlation matrix for Total Labile ^{226}Ra. C.C. - Correlation coefficient (Spearmans), Sig. - Significance (2 tailed), N - number of data points. Asterisks denote significant correlation at the 0.01 level (2 tailed).

Correlation Matrix for Total Labile ^{228}Ra.

^{238}U C.C. 0.57 Sig. 0.017 N 17	^{226}Ra C.C. 0.49 Sig. 0.045 N 17	^{228}Ra C.C.0.55 Sig. 0.020 N 17	$^{226}Ra/^{238}U$ C.C.-0.55 Sig. 0.022 N 17
$^{228}Ra/^{238}U$ C.C.-0.47 Sig. 0.052 N 17	$^{226}Ra/^{228}Ra$ C.C.-0.52 Sig. 0.030 N 17	^{238}U Ex. Cation. C.C.0.16 Sig. 0.522 N 17	^{226}Ra Ex.Cation. C.C. 0.52 Sig. 0.030 N 17
^{228}Ra Ex.Cation. C.C. 0.69** Sig. 0.002 N 17	^{238}U Eas.Ox.Org C.C.0.74** Sig. 0.001 N 17	^{226}Ra Eas.Ox.Org. C.C.0.49 Sig. 0.046 N 17	^{228}Ra Eas.Ox.Org. C.C.0.36 Sig. 0.152 N 17
^{238}U Fe Oxides C.C.0.67** Sig. 0.003 N 17	^{226}Ra Fe.Oxides C.C.0.55 Sig. 0.021 N 17	^{228}Ra Fe. Oxides C.C. 0.79** Sig. 0.000 N 17	Moisture C.C.0.55 Sig. 0.020 N 17
pH C.C.0.18 Sig. 0.469 N 17	Eh C.C.-0.23 Sig. 0.442 N 13	Cation Ex. Cap. C.C.0.72* Sig. 0.001 N 17	Humic acids C.C.0.22 Sig. 0.39 N 17
Non humic acids C.C.0.22 Sig. 0.39 N 17	Organic material C.C.0.23 Sig. 0.363 N 17	Iron C.C.-0.18 Sig. 0.480 N 17	Manganese C.C.-0.36 Sig. 0.149 N 17
Total Lab. ^{238}U C.C. −0.72** Sig. 0.001 N 17	Total Lab. ^{226}Ra C.C.0.71** Sig. 0.001 N 17	Total Lab. ^{228}Ra	

Table xxxix. Correlation matrix for Total Labile ^{228}Ra. C.C. - Correlation coefficient (Spearmans), Sig. - Significance (2 tailed), N - number of data points. Asterisks denote significant correlation at the 0.01 level (2 tailed).

APPENDIX 4.

Amersham International plc
Amersham Laboratories

0344/1494/5440 00

NAMAS
CALIBRATION
No. 0146

[redacted]

iption

Principal radionuclide: Radium-226

Product code: RAY.24

Solution number: R9/50/151

rement

Reference time:	1200 GMT on 2 January 1991	
Radioactive concentration of radium-226:	4.499	kilobecquerels per gram of solution
which is equivalent to:	121.6	nanocuries per gram of solution
Mass of solution:	5.0676	grams
Total activity of radium-226:	22.80	kilobecquerels
which is equivalent to:	616	nanocuries
Recommended half life:	1600	years

Method of measurement:
The activity of the solution was measured in a high pressure re-entrant ionisation chamber calibrated with a large number of absolutely standardized solutions.

racy

Overall uncertainty in the radioactive concentration quoted above: ± 3.7 %

Random uncertainty: ± 0.7 % Systematic uncertainty: ± 3.0 %

The limits of overall uncertainty were taken as the arithmetic sum of the uncertainty due to random variations, calculated at the 99.7% confidence level, and the estimated systematic uncertainties in the measurement.

ionuclidic
ity

The estimated activities of any radioactive impurities found by high-resolution gamma ray spectrometry, or in any other examination of the solution, are listed below expressed as percentages of the activity of the principal radionuclide at the reference time.

mical
position

Carrier free in 0.5M HCl

arks

At the reference date radium-226 was shown to be in radioactive equilibrium with its daughter nuclides down the decay chain to polonium-214 and thallium-210, the precursors of lead-210. The ionisation chamber was calibrated using a standard supplied by the National Bureau of Standards, Washington DC, USA.

This product meets the quality assurance requirements of NRC Regulatory Guide 4.15 for achieving implicit NIST traceability as defined in NCRP 58 (1985).

proved
gnatory

G.D.M.Parker

Amersham

INTERNATIONAL ATOMIC ENERGY AGENCY
AGENCE INTERNATIONALE DE L'ENERGIE ATOMIQUE
МЕЖДУНАРОДНОЕ АГЕНТСТВО ПО АТОМНОЙ ЭНЕРГИИ
ORGANISMO INTERNACIONAL DE ENERGIA ATOMICA

WAGRAMERSTRASSE 5, P.O. BOX 100, A-1400 VIENNA, AUSTRIA
TELEX: 1-12645, CABLE: INATOM VIENNA, FACSIMILE: 43 222 230184, TELEPHONE: (222) 2360

IN REPLY PLEASE REFER TO:
DE RAPPELER LA REFERENCE:
352-G4.12

DIAL DIRECTLY TO EXTENSION:
COMPOSER DIRECTEMENT LE NUMERO DE POSTE:
November 1988

REFERENCE SHEET

IAEA-152 Milk Powder
for
Radionuclides

A. Description and preparation of the material

A bulk samples of approximately 500 kg (20 sacks of about 25 kg each) of milk powder with elevated radioactivity was collected from a processing plant. These twenty sacks were all from the same batch process. Thus, they were assumed to be as homogeneous as possible. Nevertheless, a preliminary homogeneity testing of every two sacks for ^{134}Cs and ^{137}Cs was performed before bottling in approximate portions of 250 grams. In order to assure long-term stability of the material, all bottles were sterilized by gamma-ray irradiation of about 2.5×10^4 Gy using a ^{60}Co source.

The final homogeneity testing (after bottling) was performed on 12 bottles from different sacks as follows:

bottles A and B - six measurements each of 250 grams
bottles C and D - three measurements each of 250 grams
bottles E to L - one measurement each of 250 grams

Considering the results of ^{134}Cs and ^{137}Cs from the above and employing the Student's t-test it was found that they did not differ by more than 3% of the mean value and thus this material can be considered homogeneous for these components for a sample size of greater or equal to 250 grams.

B. Criteria for recommended values and confidence intervals*

The overall mean values (excluding data that was detected and rejected as outliers) were considered as the recommended values when

1) more than ten laboratory means were available
2) the percentage of outliers was less than 20% and
3) the results of the A and B intercomparisons are mutually consistent (i.e. the mean value for A falls within the confidence interval for B and vice versa).

C. Recommended values and confidence intervals for radionuclides in IAEA-152 (Milk Powder)

Radionuclide	Recommended Value (Bq/kg)	Confidence Interval** (Bq/kg)
^{134}Cs	764	722 - 802
^{137}Cs	2129	2053 - 2209
^{40}K	539	510 - 574
^{90}Sr	7.7	7.0 - 8.3

** Based on the outermost confidence intervals of the A and B intercomparison for a significance level 0.05

Reference date: 31 August 1987.

D. Important Note

The analysts using the Reference Material IAEA-152 are kindly requested to communicate their meaningful analytical results on this material to:

International Atomic Energy Agency
Laboratory Seibersdorf
Analytical Quality Control Services
P.O.Box 100, A-1400 Vienna, Austria

These results may be used in the future for an updating of the recommended values which are the best estimates as of September 1988.

Finally, a detailed description of results of the intercomparison and of the criteria used for their qualification has been published in IAEA/AL/009. This report is free of charge upon request.

* Please note that these criteria are designed especially for this report and do not apply in general.

ISSARIAT À L'ÉNERGIE ATOMIQUE

DAMRI
DIRECTION DES TECHNOLOGIES AVANCÉES

ETALON MELANGE MULTIGAMMA

SOLUTION ETALON : 9ML01-ELMA60 N°: 4980
DATE DE REFERENCE: 01-10-96 à 12 H T.U.(3)
DESTINATAIRE :
COMMANDE N° :

RADIONUCLEIDE	ACTIVITE MASSIQUE Bq g-1 (1)	INCERT. GLOBALE en%(8)
^{241}Am	3.971E+04	4
^{109}Cd	2.070E+05	5
^{57}Co	1.028E+04	4
^{139}Ce	9.634E+03	4
^{51}Cr	3.920E+05	4
^{113}Sn	6.042E+04	4.5
^{85}Sr	3.952E+04	4
^{137}Cs	5.878E+04	4
^{60}Co	5.860E+04	4
^{88}Y	5.845E+04	4

()renvois voir note jointe

DAMRI/LMRI BP 52 - 91193 GIF-SUR-YVETTE CEDEX FRANCE
TEL : 33 (1) 69.08.25.13 - FAX : 33 (1) 69.08.26.19

AMMISSARIAT A L'ÉNERGIE ATOMIQUE

DAMRI
DIRECTION DES TECHNOLOGIES AVANCÉES

ETALON MELANGE MULTIGAMMA

SOLUTION ETALON : 9ML01-ELMA60 N°: 4980
DATE DE REFERENCE: 01-10-96 à 12 H T.U.(3)
DESTINATAIRE :
COMMANDE N° :

RADIONUCLEIDE	ENERGIE en (keV)	INTENSITE ABSOLUE % k=1	FLUX MASSIQUE PHOTONIQUE 4PI sr.s-1g-1	INCERT. GLOBALE en%(8) k=3
^{241}Am	59.537 ± 0.001	35.9 ± 0.4	1.426E+04	3
^{109}Cd	88.034 ± 0.002	3.65 ± 0.06	7.556E+03	4
^{57}Co	122.0614 ± 0.001	85.68 ± 0.13	8.808E+03	3
^{57}Co	136.4743 ± 0.001	10.67 ± 0.13	1.097E+03	3
^{139}Ce	165.857 ± 0.006	79.87 ± 0.06	7.694E+03	3
^{51}Cr	320.0842 ± 0.001	9.85 ± 0.09	3.861E+04	3
^{113}Sn	391.702 ± 0.004	64.89 ± 0.17	3.921E+04	3.5
^{85}Sr	514.009 ± 0.012	99.29 ± 0.04	3.924E+04	3
^{137}Cs	661.660 ± 0.003	85.2 ± 0.2	5.008E+04	3
^{88}Y	898.042 ± 0.004	94.1 ± 0.5	5.500E+04	3
^{60}Co	1173.240 ± 0.004	99.89 ± 0.02	5.854E+04	3
^{60}Co	1332.500 ± 0.005	99.983 ± 0.001	5.859E+04	3
^{88}Y	1836.060 ± 0.013	99.36 ± 0.05	5.808E+04	3

()renvois voir note jointe

SACLAY le 01-10-96

le chef du DAMRI

J.L BOUTAINE

po le chef du LMRI

A.PROMENTIN

DAMRI/LMRI BP 52 - 91193 GIF-SUR-YVETTE CEDEX FRANCE
TEL : 33 (1) 69.08.25.13 - FAX : 33 (1) 69.08.26.19

APPENDIX 5.

$^{226}Ra/^{238}U$ disequilibrium in an upland organic soil exhibiting elevated natural radioactivity.

Mark Dowdall and John O'Dea
Institute of Technology, Sligo,
Ballinode, Sligo, Ireland.

Submitted for publication to:
Journal of Environmental Radioactivity
February 2000.

$^{226}Ra/^{238}U$ disequilibrium in an upland organic soil exhibiting elevated natural radioactivity.

Mark Dowdall and John O'Dea.
Dept. of Applied Science, Institute of Technology, Sligo, Ballinode, Sligo, Ireland.

Abstract
This paper presents the results of a study into the anomalous $^{226}Ra/^{238}U$ disequilibrium ($^{226}Ra/^{238}U$ of 0.5 - 9) exhibited by an upland organic soil in Co. Donegal, Ireland. Radiochemical speciation of ^{226}Ra, ^{238}U and ^{228}Ra indicates that in this organic soil the high $^{226}Ra/^{238}U$ ratio is due to loss of ^{238}U relative to ^{226}Ra via oxidation and mobilisation of ^{238}U in the upper layers of the soil and subsequent loss in solution. At the lower, more reducing depths of the soil profile, ^{238}U and ^{226}Ra are essentially in equilibrium. Loss of ^{238}U appears to occur primarily from the easily oxidised organic and iron oxide fractions of the soil, samples exhibiting high $^{226}Ra/^{238}U$ ratios displaying significantly lower ^{238}U levels in these fractions than samples whose ratio is below the average value for the soil of the valley. Selective enrichment of ^{226}Ra by plants or preferential leaching of ^{226}Ra from the underlying rock is not supported by the results of this study.

Keywords: Radionuclides; Redox; Disequilibrium; Soil; Ireland

1. Introduction

Although identified as a region of anomalous natural radioactivity in the past (Irish Base Metals, 1979), the Cronamuck Valley in the Barnesmore Mountains, Co. Donegal, Ireland has been shown to contain regions of anomalous $^{226}Ra/^{238}U$ disequilibrium (O'Dea & Dowdall,

1999), soil samples in these regions exhibiting ratios of between 0.5 - 9.0. This paper outlines the results of a study into the nature and causes of this disequilibrium and presents a likely mechanism to account for the ratios observed in samples drawn from the areas.

Previous work into the nature and cause of ^{238}U series disequilibrium has resulted in the identification of a number of processes by which the radionuclides of the ^{238}U series may be brought into disequilibrium. Ivanovich (1994) highlights four processes that may produce disequilibrium in the surfical environment: precipitation/dissolution, alpha recoil, diffusion and the Szilard-Chalmers effect. Practical investigations of $^{226}Ra/^{238}U$ disequilibrium typically highlight precipitation and dissolution as the primary cause. Uranium is mobile under oxidising conditions whereas radium and thorium are essentially immobile in the surfical environment (Landstrom & Sundblad, 1986). The differing mobility's of these radionuclides has previously been identified as causing disequilibrium in young organic uranium deposits (Zielinski, et al,1986, Levinson et al, 1984). Megumi (1979) supports this hypothesis by asserting that disequilibrium in the ^{238}U decay series (prior to ^{222}Rn) is due primarily to the immobility of ^{230}Th. Greeman and Rose (1990) studied radioactive disequilibrium in the ^{238}U series for a number of soils and concluded that in the surface horizons of some soils, ^{226}Ra excess could be attributed to the cycling of ^{226}Ra by plants, leading to an increase in the isotope relative to ^{238}U. Von Gunten et al (1996) observed ^{226}Ra activities a factor of 20 above the activity of ^{238}U in a karst region of Switzerland and proposed that, following continuous weathering of calcite particles, uranium was lost from the soil as the soluble carbonate complex, ^{226}Ra being retained within the soil. de Jong et al (1993) hypothesised that the $^{226}Ra/^{238}U$ disequilibrium in a Saskatchewan soil was probably due to the mode of deposition of the parent material rather than subsequent selective leaching of members of

the series. Titaeva and Veksler (1977) discuss the possibility of ^{226}Ra excess being due to the deposition of ^{226}Ra from water onto the surface of weathered particles but offer no conclusive proof. Ivanovich and Harmon (1992) state categorically that in soils subject to leaching, the primary cause of radioactive disequilibrium is the removal of uranium relative to thorium and immobile daughters.

The areas of anomalous $^{226}Ra/^{238}U$ disequilibrium within the Cronamuck Valley as reported by O'Dea and Dowdall (1999), consist of localised areas (< 100 m diameter) lying at the bottom of the valley. They are typically found at the confluence of watercourses within the valley and exhibit concomitant elevated levels of natural radionuclides. The aim of the study whose results are reported in this paper was the characterisation of the disequilibrium condition of one such area and the investigation of possible causes for the $^{226}Ra/^{238}U$ ratios exhibited by samples of soil from the area. In order to fully elucidate the distribution of ^{226}Ra, ^{238}U and ^{228}Ra at the site a number of depth sections were taken and subjected to a sequential chemical extraction procedure. A range of chemical parameters of the soil were also analysed. The primary radioanalytical method was High Resolution Gamma Ray spectrometry.

2. Methods

Results were obtained for two depth sections taken from a selected region of elevated natural radioactivity. Two sample sites were selected from within the region, the sites being denoted as A and B. The sections were sampled by depth rather than horizon as little or no horizon development was evident within the peat. Sections were obtained by excavating a pit to the bedrock (< 1m in both cases) and sampling one wall of the pit at incremental depths of 15 cm. Samples

consisting of 10 -15 kg (wet weight) were bagged and removed to the laboratory. A number of random samples were also taken in order to obtain information on the disequilibrium condition at different points within the general area (Fig.1a.). These samples were all drawn from the basal layers of the peat, at the rock - soil interface.

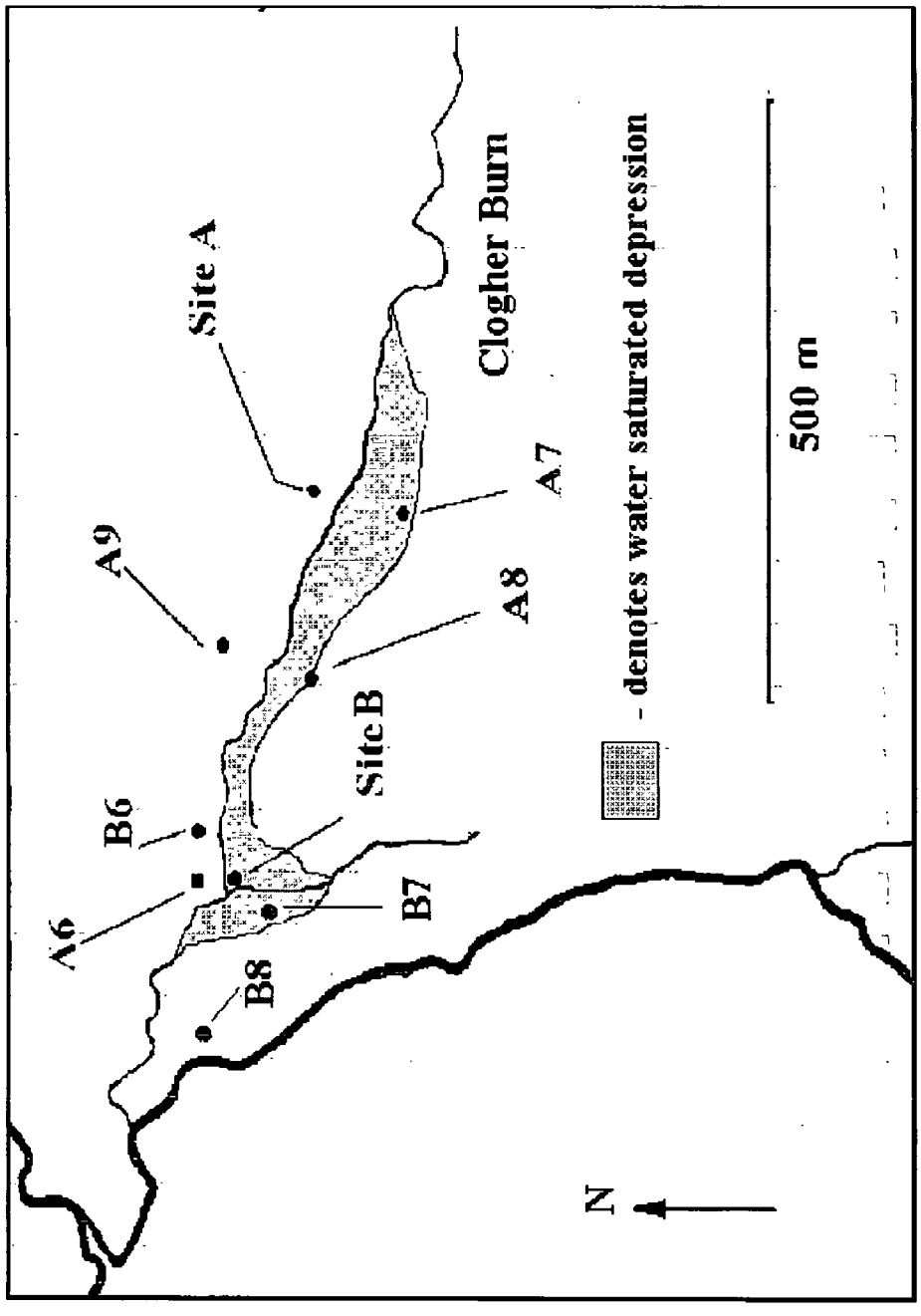

Figure 1a. Location of sampling points. Site A and Site B denote depth sections. Numbered locations denote individual samples.

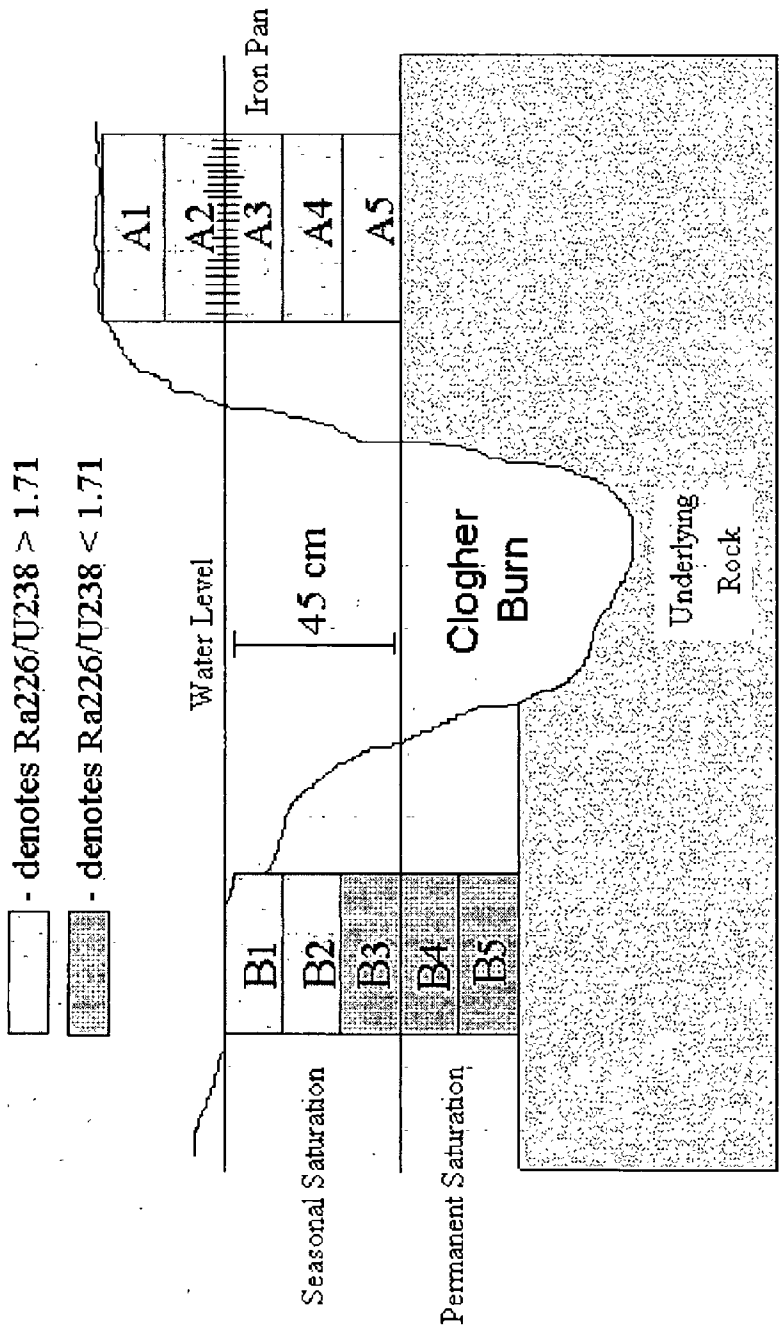

Figure 1b. Vertical orientation of sampling sites relative to Clogher Burn stream

Radiological Analysis

Samples were dried at 101^0 C to a constant mass, dissaggregated using a rubber stopper and sieved through a 2 mm mesh sieve. The samples were then packed into 1l Marinelli re-entrant beakers for gamma analysis. The liquid extracts produced during the chemical speciation of the radionuclides were reduced, where necessary, to 1 l by evaporation and placed in 1 l Marinelli re-entrant beakers. These beakers were sealed with thick polyethylene tape and stored for a period in excess of 30 days to allow for radon ingrowth. Samples were counted on a high purity germanium detector linked to a 8 k multichannel analyzer incorporating the Genie-PC software suite from Canberra. The system was calibrated with a NIST traceable mixed radionuclide standard solution (Commissariat a L'Energie Atomique, 9ML01-ELMA60) and errors due to differing matrix densities were avoided using the calibration procedures described by Nemeth and Parsa (1992). Calibrations were checked using IAEA Reference Material 152. Count times were long enough to ensure a 2σ counting error of less than 10%. The peaks utilized for analysis of soil samples were the 63 keV and 92 keV peaks of the daughter ^{234}Th for ^{238}U and the 911 keV and 969 keV peaks of ^{228}Ac for ^{228}Ra activity. ^{226}Ra was determined via the 186 keV peak of ^{235}U and ^{226}Ra having corrected for the ^{235}U contribution as follows:

$$\text{Counts due to } ^{235}\text{U} = A^{235U} C_T R_U E_{186} W$$

A^{235U} is the activity of ^{235}U (equal to the specific activity of ^{238}U divided by 21.4), C_T is the count time in seconds, R_U is the emission probability of ^{235}U at 186 keV, E_{186} is the counting efficiency of the detector system at 186 keV and W is the sample mass in grams.

Analysis of the liquid extracts differed in that equilibrium of ^{234}Th with ^{238}U could not be assured. The samples were sealed for a period long enough to ensure equilibrium between ^{226}Ra, ^{222}Rn and its gamma emitting daughters (>30 days). The activity of ^{226}Ra was then determined via the emissions of ^{214}Bi (295 keV, 609 keV and 1120 keV) and ^{214}Pb (242 keV). The peak at 186 keV was then corrected in a similar manner to above to determine ^{235}U and hence ^{238}U. The ability of the Marinelli beakers to retain radon under the analytical conditions employed was confirmed using a NIST traceable ^{226}Ra standard solution (R9/50/151 from Amersham International plc).

Sequential Extractions

The methods used by Greeman and Rose (1990) were adapted to cater for large samples and employed to determine the chemical nature of the radionuclides within the peat. The samples used for the sequential extractions were 100 g portions of the soil mass used for gamma analysis. The entire soil mass was riffled to obtain a random portion, this being crushed to a fine powder in a stainless steel mill. The three fractions were extracted as follows:

100 g of finely ground soil was placed in a 1l acid washed plastic bottle with 600 ml of extraction solution. The bottle was shaken for 1hr and the mixture was then centrifuged at 10 k rpm for 600 s. The supernatant was stored and the solid material was resuspended in 300 ml of distilled water and shaken for 1200 s before being centrifuged at 10 k rpm for 600 s. Supernatants were bulked, filtered through a 0.45 µm filter, made up to one liter and sealed for gamma analysis. All extractions were done at 20^{0}C except for Fe oxides which were performed at 80^{0}C. The extracting solutions were as follows:

Exchangeable cations

1 M magnesium chloride, pH 6 with HNO_3

Easily oxidisable organic matter

5% sodium hypochlorite, pH 6 with HNO_3

Fe oxides

50 g/l of sodium dithionite in a 0.3 M sodium citrate/ 0.2 M sodium bicarbonate buffer.

Chemical Analysis

A number of chemical parameters for each sample were determined. The samples for analysis (with the exception of those for pH and Eh) were extracted from the riffled soil mass used for gamma analysis.

pH.

pH values for the soils were determined in situ. A small hole was made in the soil into which the electrode was inserted. In cases where a good contact between the electrode and the soil water was not made, a small amount of distilled water was added. The reading was taken after a 10 minute equilibration period.

Eh.

A portable Eh meter was utilized to determine the Eh status of the soil in a similar manner to the pH determination, the electrode being left for up to 10 minutes in the soil to allow equilibrium to occur.

Total iron and manganese

Approximately 1 g of finely ground soil was digested with 5 ml of a 3:1 HCl/HNO_3 mixture and boiled for 1 hr. The mixture was filtered through glass fiber filter paper before being filtered with a 0.45 µm

filter. The solution was then made up to 100 ml. Both metals were analyzed by AAS.

Cation exchange capacity (CEC)

4-6 g of soil was mixed with 33 ml of 1 N NaOAc and shaken for 300 s. The supernatant was removed after centrifuging at 10 k rpm for 600 s. The cycle was repeated three times. The soil was then mixed with 33 ml of propan–2-ol, this cycle being repeated three times. The soil was then mixed with 33 ml of NH_4OAc, this cycle also being repeated three times, the three NH_4OAc supernatants were filtered (0.45 µm), combined, and then brought up to 100 ml. The Na content of this solution was measured by flame photometry.

Organic matter content

Organic matter was determined as the loss on ignition at 500^0 C for 4 hr.

Humic acid content

Approximately 1 g of ground soil was mixed with 50 ml of 0.5 M NaOH and shaken for 600 s. The mixture was centrifuged at 10 k rpm for 600 s, the supernatant being discarded. The procedure was repeated on the solid material until three consecutive supernatants ran clear (typically 7 to 8 times). The material was washed with three 30 ml aliquots of distilled water, and dried at 101^0 C. Humic acid content was calculated from loss of mass from the soil.

Quality Control

Chemical analyses were conducted subject to the regular quality control procedures implemented in the laboratory. Reproducibility of results was assessed using replicates (three) of

homogenized samples. The coefficients of variation were typically less than 20% (2σ). The accuracy of the analytical methods was checked using traceable reference standards, spikes and blanks at a typical loading of 5 per 50 analytical samples.

2. Results

Sample	pH	Eh	Fe	Mn	C.E.C.	Humic Acid	Organic-Matter	Moisture Content
A1	3.8	421.0	110600	16700	58.3	13.1	28.9	78.6
A2	4.2	496.0	117700	29400	37.2	14.8	22.6	61.4
A3	4.3	504.0	2110*	43600	38.3	10.9	14.1	56.2
A4	5.7	19.0	143200	21100	42.8	7.8	15.6	55.9
A5	5.7	-55.0	97900	6450	129.9	7.2	19.8	56.5
A6	4.9	n/a	90000	43600	3.7	8.4	19.7	43.9
A7	5.1	n/a	66500	6950	68.7	18.4	49.7	81.8
A8	5.4	n/a	147300	14650	46.1	20.6	40.8	80.7
A9	5.4	n/a	3850	132	40.6	19.2	38.5	68.4

Table 1. Chemical properties of samples taken from site A. Units are: Eh - mV, Fe - ppm, Mn - ppm, Cation Exchange Capacity (C.E.C.) - meq / 100 g, Humic Acid - % , Moisture Content - % and Organic matter - %. The Fe value at for sample A3 (denoted by an asterisks) is after removal of concreted iron pan from the analytical sample, total Fe being estimated at 35% w/w.

Sample	pH	Eh	Fe	Mn	C.E.C	Humic Acid	Organic Matter	Moisture Content
B1	4.6	220.0	106900	34550	39.8	16.1	32.8	74.3
B2	4.5	190.0	104900	39200	29.9	9.8	19.2	63.1
B3	4.3	190.0	88500	30200	49.8	15.9	29.9	76.5
B4	4.6	300.0	39700	6600	79.2	34.7	38.7	78.5
B5	4.8	165.0	45100	3060	58.3	13.1	36.7	78.6
B6	4.0	287	72600	25400	58.2	7.6	11.5	51.1
B7	5.7	182	54400	1570	68.9	37.1	41.6	78.0
B8	5.8	136	63300	11000	56.7	17.2	45.4	77.8

Table 2. Chemical properties of samples taken from site B. Units are: Eh - mV, Fe - ppm, Mn - ppm, Cation Exchange Capacity (C.E.C.) - meq / 100 g, Humic Acid - %, Moisture Content - % and Organic matter - %.

Sample	U^{238}	Ra^{226}	Ra^{228}
1 (A)	124.0	201.6	84.68
2 (A)	132.1	188.3	79.5
3 (A)	140.3	175.6	81.0
4 (A)	110.5	198.7	75.8
1 (B)	462.2	271.3	192.4
2 (B)	390.5	241.8	175.9
3 (B)	420.1	220.3	180.0
4 (B)	378.9	205.7	160.2

Table 3. Radionuclide activities for vegetation samples from Site's A and B. Values in Bq/kg ash weight.

Sample	U^{238}	Ra^{226}	Ra^{228}
1 (A)	134.6	145.4	86.1
2 (A)	168.0	150.6	98.2
3 (A)	157.4	132.9	79.2
4 (A)	146.2	128.7	74.6
1 (B)	143.2	164.5	98.6
2 (B)	174.1	152.9	106.7
3 (B)	156.2	148.9	101.0
4 (B)	159.8	127.0	96.2

Table 4. Radionuclide activities for rock samples drawn from Site's A and B. Values in Bq/kg.

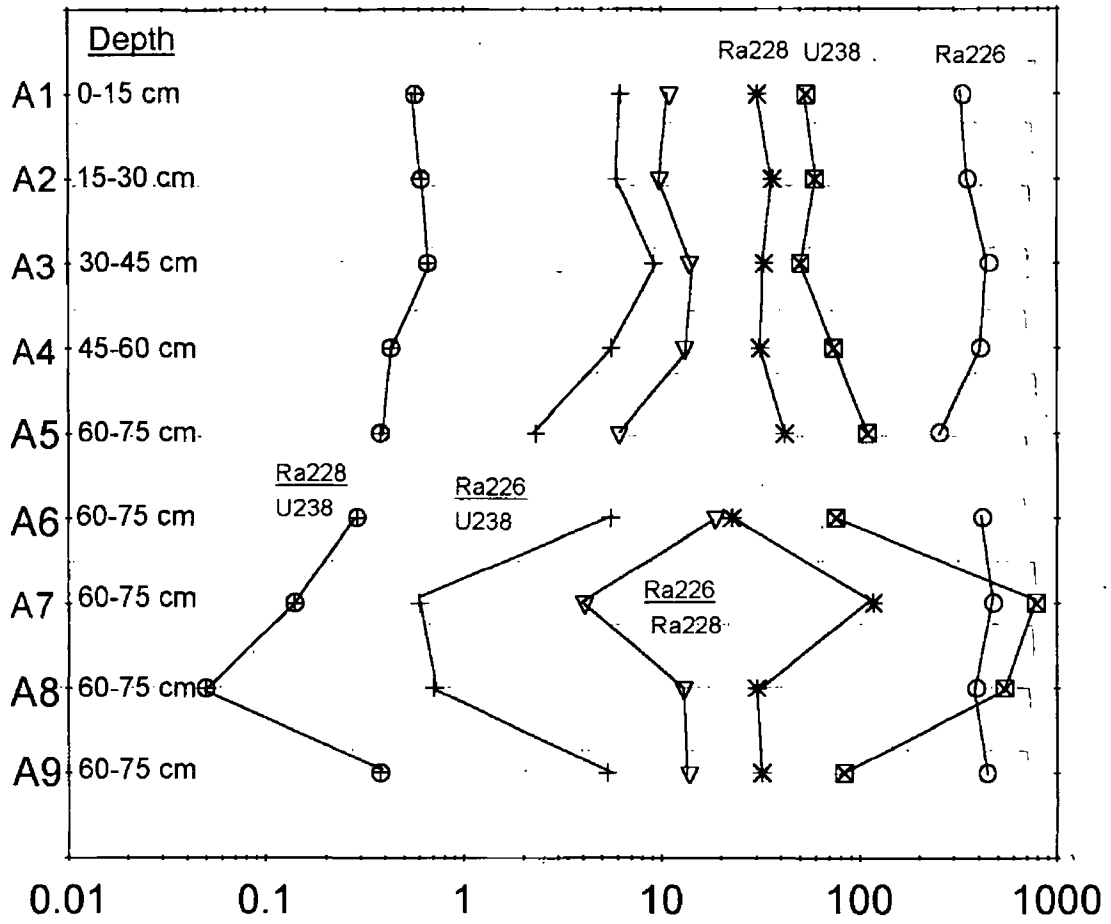

Figure 2. Radiological properties of Site A depth section and individual samples. Values where applicable in Bq/kg (dry weight). Note log axis.

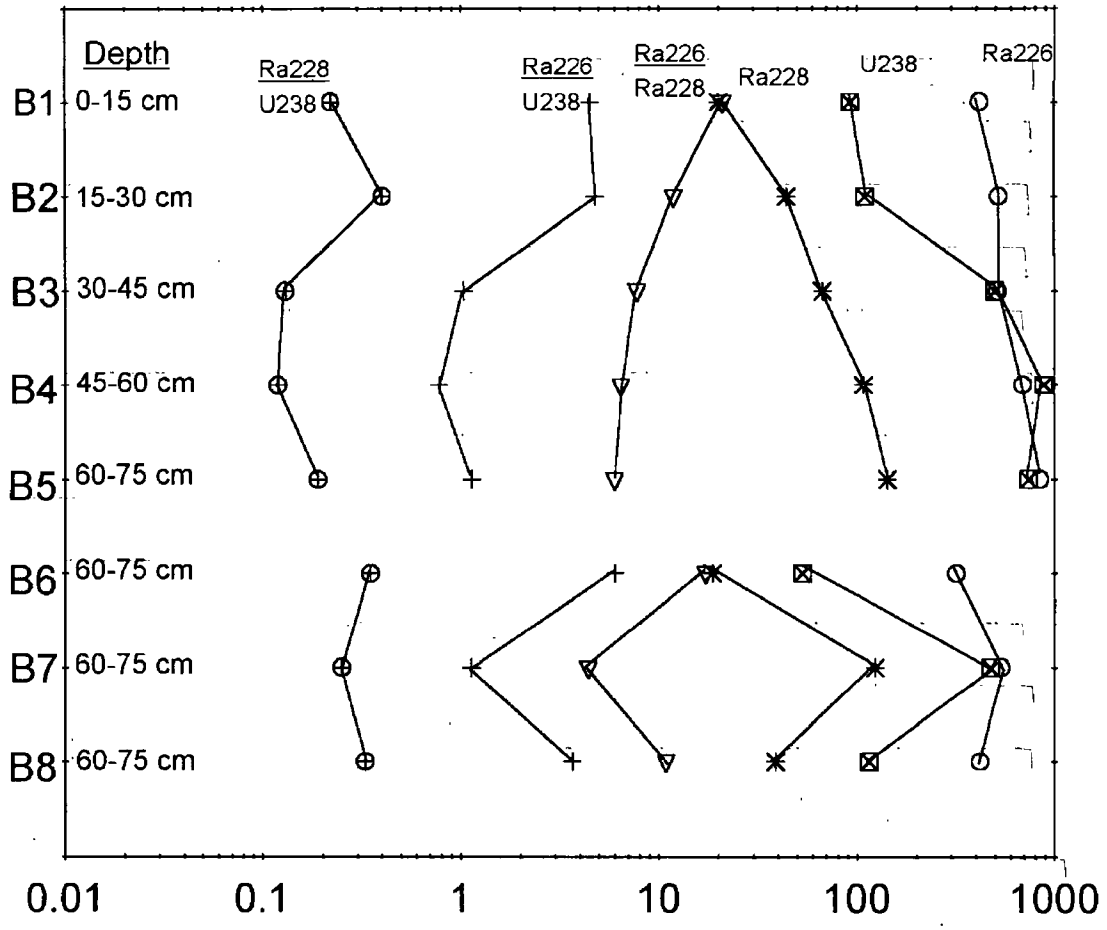

Figure 3. Radiological properties of Site B depth section and individual samples. Values where applicable in Bq/kg (dry weight). Note log axis.

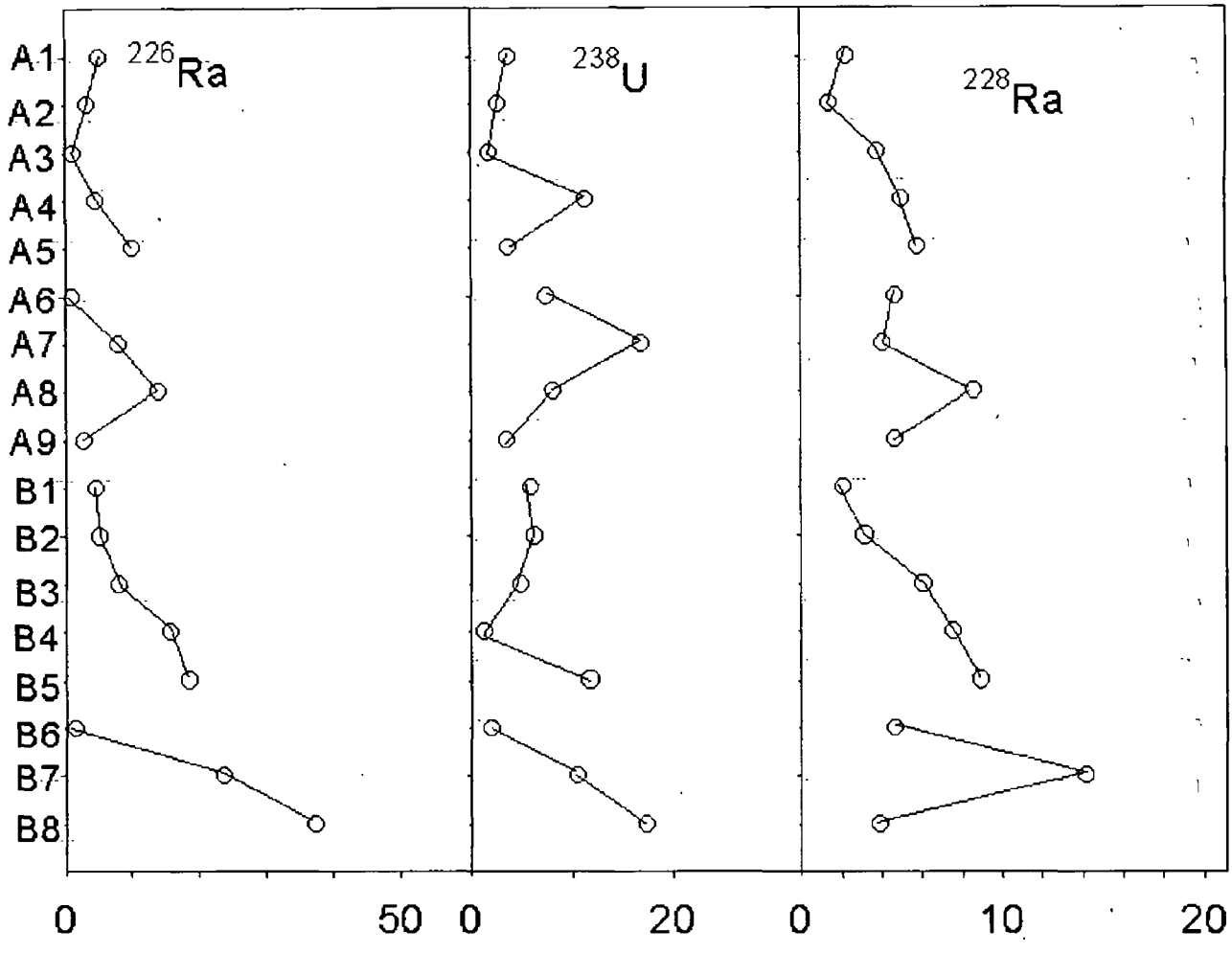

Figure 4. Radionuclide levels present in association with the exchangeable cation fraction. Values in Bq/kg (dry weight).

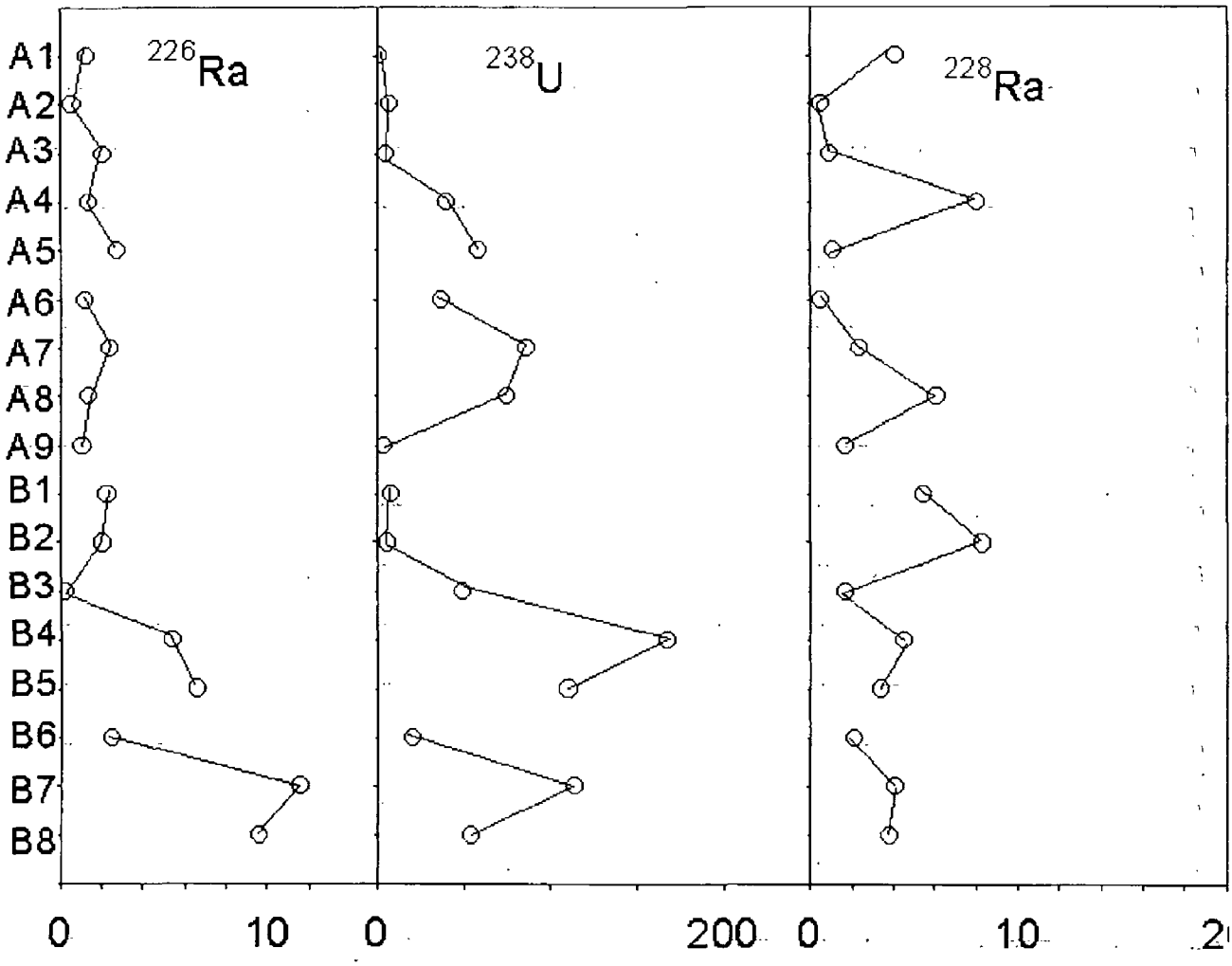

Figure 5. Radionuclide levels present in association with the easily oxidisable organic fraction. Values in Bq/kg (dry weight).

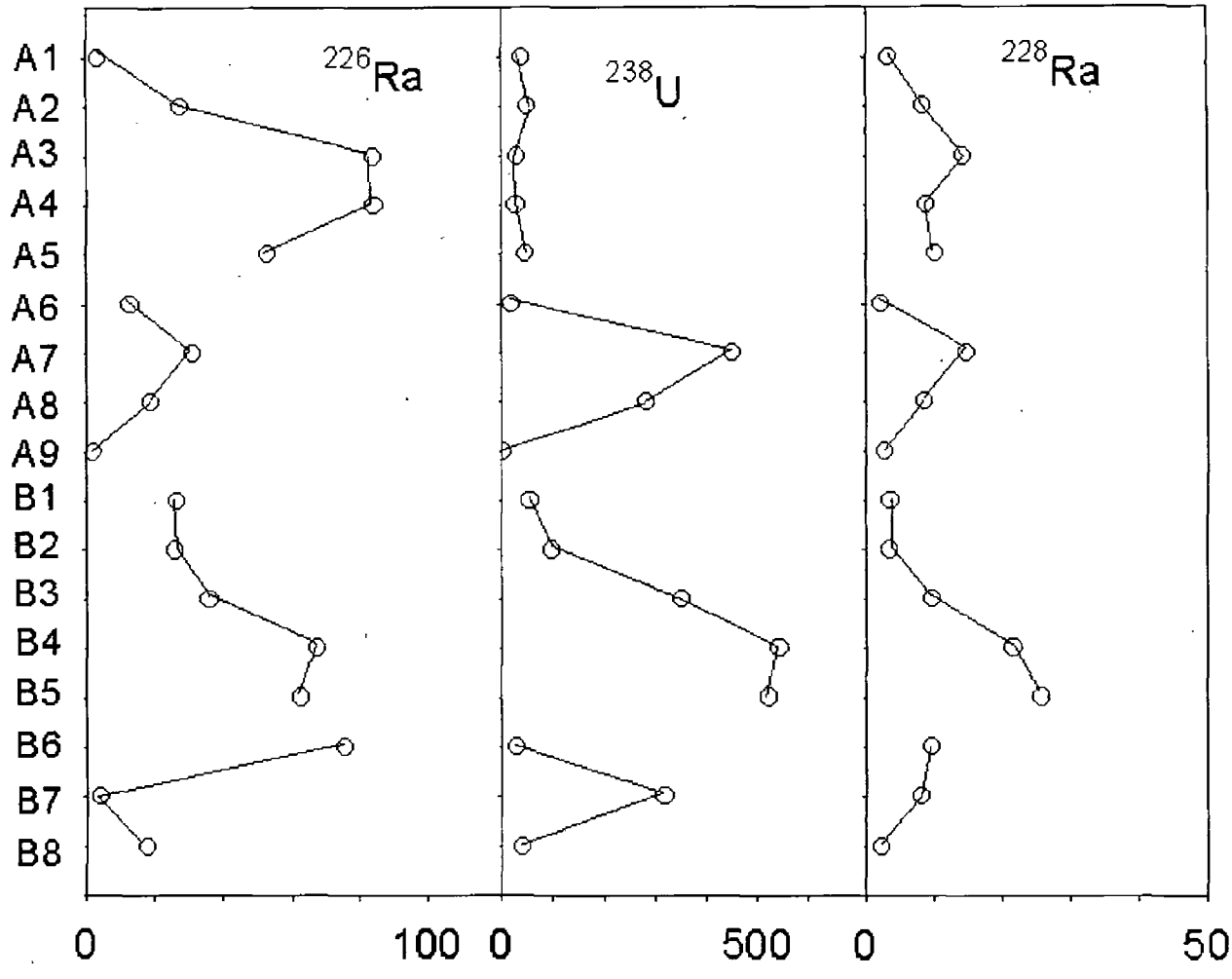

Figure 6. Radionuclide levels present in association with the iron oxides fraction. Values in Bq/kg (dry weight).

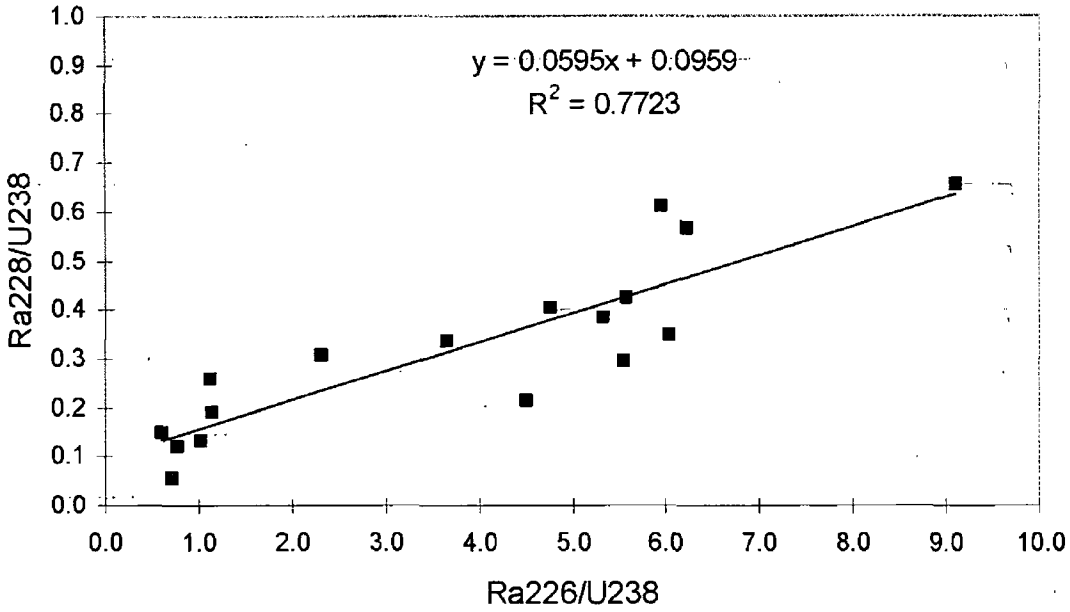

Figure 7. Plot of $^{226}Ra/^{238}U$ against $^{228}Ra/^{238}U$.

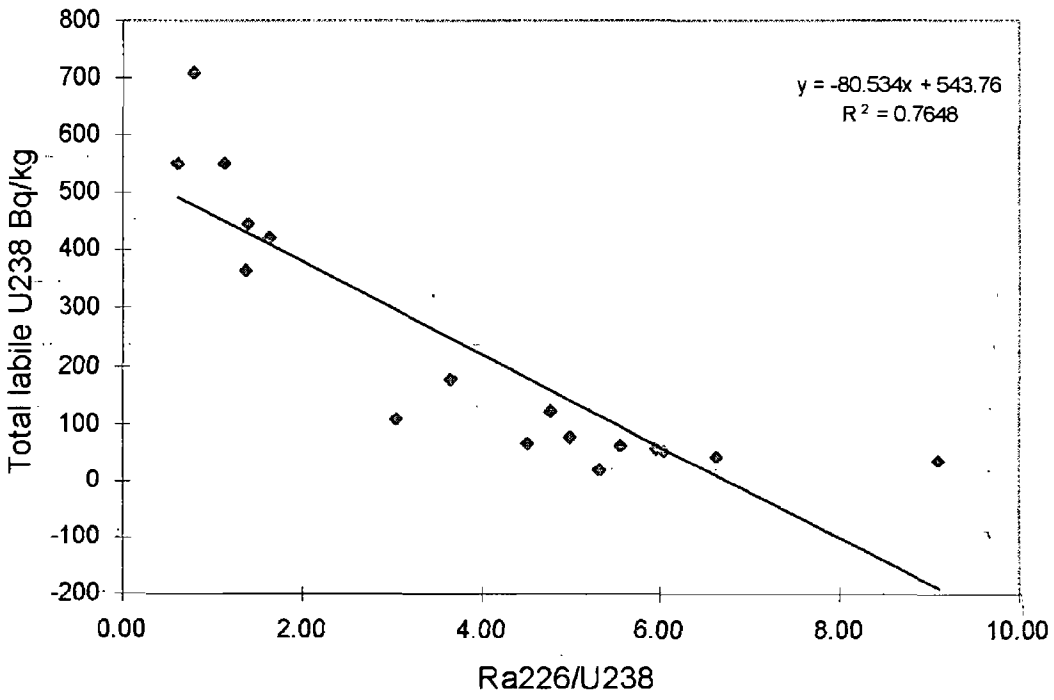

Figure 8. Plot of total labile ^{238}U against $^{226}Ra/^{238}U$.

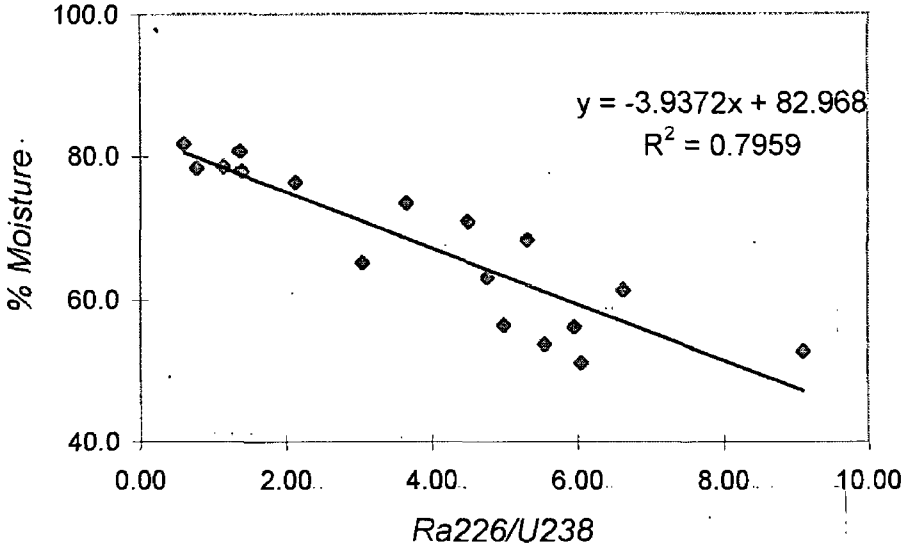

Figure 9. Plot of $^{226}Ra/^{238}U$ against moisture content (%).

3. Discussion

The site selected for this study is typical of the sites within the Cronamuck Valley that exhibit elevated natural radioactivity. The site consists of a shallow depression lying at one of the lowest parts of the valley at the confluence of Clogher Burn river and a small stream. The north eastern bank of the Clogher Burn river, upon which site A is located, is elevated some 30 - 40 cm with respect to the opposite bank. As a result of this, the lower depths of Site A are only saturated for parts of the year when the level of water in the depression rises. The lower depths of Site B remain saturated for most of the year (Fig. 1b.). A distinct, concreted, iron pan is present at an approximate depth of 30 - 45 cm at Site A, indicating the maximum level of stream water within the soil profile at this location. This pan is not present at Site B although amorphous iron levels are at a maximum at a depth corresponding with the location of the pan at Site A.

$^{226}Ra/^{238}U$ ratios range from 9.10 to 2.32 at Site A and 4.50 to 0.78 at Site B. The $^{226}Ra/^{238}U$ ratio at both Site's A and B appears to reach a maximum towards the upper levels of the depth sections. The largest value occurs at the level of Site A at which iron pan formation is evident. As the activity of ^{226}Ra is less variable with depth at both sites and given the generally accepted concept that radium is less mobile than uranium in the surfical environment (Sheppard, 1980), it would initially appear that uranium mobilization and loss relative to radium is the cause of the disequilibrium exhibited at these sites. This hypothesis is also supported by the relationship between the ratios $^{228}Ra/^{238}U$ and $^{226}Ra/^{238}U$. Although no statistically significant correlation exists between the two ratios, a scatterplot of the ratios provides some evidence for a positive relationship between the two parameters (Fig.7.).

Using ^{228}Ra as an indicator for ^{232}Th, which may be considered very immobile (Landstrom and Sundblad, 1986), it is possible to conclude that uranium is similarly depleted relative to thorium. Samples displaying low $^{226}Ra/^{238}U$ ratios all contain significant amounts of labile ^{238}U, the highest disequilibrium values being associated with low levels of labile ^{238}U (Fig.8.), a fact which also supports the depletion of ^{238}U in samples with high $^{226}Ra/^{238}U$ ratios.

Adopting an average $^{226}Ra/^{238}U$ ratio of 1.71 for the soil of the Cronamuck Valley (O'Dea & Dowdall, 1999) allows for division of the data set on the basis of the samples $^{226}Ra/^{238}U$ ratios being above or below average for the soil of the valley. None of the chemical parameters measured for the soil samples, except moisture content, show any significant difference between the two groups on the basis of a Mann Whitney Rank Sum Test. The amount of ^{226}Ra is not significantly different for either the easily oxidisable organic fraction (p=0.315) or

the iron oxides (p=0.802) of the two groups of samples. In samples displaying above average $^{226}Ra/^{238}U$ ratios, ^{238}U occurrence in the aforementioned two fractions has a significantly lower occurrence (p=0.002 and p=0.001 respectively) than for samples exhibiting lower than average $^{226}Ra/^{238}U$ ratios indicating the probable loss of ^{238}U from samples exhibiting greater than average $^{226}Ra/^{238}U$ ratios.

The apparent loss of ^{238}U relative to ^{226}Ra in these samples appears related to the positions of the samples relative to the water level, samples that remain saturated for much of the year exhibiting the higher $^{226}Ra/^{238}U$ ratios. The most oxidising layers, based on the measured Eh values, are found above the iron pan at Site A and in the surface layers at Site B. Although there is no statistical relationship between Eh or pe+pH values and the disequilibrium status of the samples, a marked transition in $^{226}Ra/^{238}U$ values may be observed on traversing the iron pan at Site A. Samples taken from above the pan (Eh values >400 mV) exhibit the highest ratios, samples taken from the more reducing lower layers (Eh < 20 mV) having ratios closer to the average for the valley (Fig's.2 & 3.). Given the seasonal fluctuation of water levels in the depression, the Eh values taken in this study are not indicative of the redox status of the soil throughout the year. It is obvious however that the samples moisture content is related to its disequilibrium status (Fig.9.), the two variables having a negative correlation.

This fact provides further evidence that the better drained / less saturated, and hence, more oxidising soil levels, exhibit greater depletion of ^{238}U relative to ^{226}Ra. This view is supported by the disequilibrium values of the series of random samples taken from the vicinity of Sites A and B (Tables 1 & 2, Fig's.2 & 3.). Samples A8, A7

and B7, taken from the lower layers within the water saturated depression, all display $^{226}Ra/^{238}U$ ratios of less than 1.71 (0.60 - 1.13), and moisture contents of 78 - 82%, in accordance with the hypothesis that ^{238}U depletion is less severe for samples taken from water logged, reducing areas. The remainder of the random samples were all taken from relatively well drained locations, with lower moisture contents (43 - 77%) and $^{226}Ra/^{238}U$ ratios in the range 3 to 5.5.

Considering the distribution of ^{238}U within the soil phases of Sites A and B and the fact that a relatively small proportion of Site A's ^{238}U resides in the organic fraction, it appears that ^{238}U loss is primarily from the easily oxidised organic material of the soil. This observation is supported by the evidence provided by both profiles as the proportion of U^{238} present in this fraction, tends to increase on going down the profile, as conditions become increasingly reducing.

Greeman and Rose's (1990) assertion that selective plant uptake may be responsible for $^{226}Ra/^{238}U$ disequilibrium by enriching ^{226}Ra in the surface layers of soil is not supported by the results of this study. There is no evidence of ^{226}Ra enrichment in the upper layers of either section, ^{226}Ra activities being greater with depth by up to a factor of 2. The average $^{226}Ra/^{238}U$ ratio in plant ash from Site B is 0.56 and 1.49 for Site A indicating preferential uptake of uranium by vegetation growing on peat containing excess ^{226}Ra. It would appear unlikely therefore that preferential uptake and cycling of ^{226}Ra by vegetation has given rise to the exhibited disequilibrium ratios. Analysis of the underlying rock yields no indication of preferential leaching of ^{226}Ra (Table 4.) which may have accounted for the enrichment of the overlying peat with ^{226}Ra. Average $^{226}Ra/^{238}U$ ratios for rock samples drawn from Site's B and A are 0.943 and 0.925 respectively.

The conclusion that elevated $^{226}Ra/^{238}U$ ratios (due to leaching of uranium) at this site are a result of pertaining redox conditions is in agreement with Kochenov et al (1965), Zielinski et al (1987) and Boyle (1984). The loss of ^{238}U from this fraction as a result of soil redox status is of concern given the proportions of ^{238}U bound in this manner at Site B. Given the fact that a large number of such sites have been reported in the Cronamuck Valley (Irish Base Metals, 1979) it would appear that a significant amount of U^{238} is therefore vulnerable to release from the soil should a change in the redox status of the peat occur.

Acknowledgments

The authors wish to acknowledge the following persons for their contribution to this study: P. Maughan, R. Courtney, C. Duffy and J.J. McGloin.

References

Boyle, D. R. (1984) The genesis of surfical uranium deposits, in Surfical uranium deposits. IAEA-TECDOC-322.

deJong, E., Acton, D. F. & Kozak, L. M. (1993). Naturally occurring gamma-emitting isotopes, radon release and properties of parent materials of Saskatchewan Soils. *Canadian Journal of Soil Science, 74*, 47-53.

Greeman, D. J. The geochemistry of uranium, thorium and radium in soils of the eastern United States. Ph.D. Thesis. University Microfilms International, Ann Arbor, M. I.

Greeman, D. J. & Rose, A. W. (1990). Form and behaviour of radium, uranium and thorium in central Pennsylvania soils derived from Dolomite. *Geophysical Research Letters, 17/6*, 833 - 836.

Irish Base Metals Ltd. (1979). Research into the occurrence of radioactive raw materials in Ireland. Final Report, 33 - 34..

Ivanovich, M. (1994). Uranium series disequilibrium: concepts and applications. *Radiochimica Acta, 64*, 81 - 94.

Ivanovich, M. & Harmon, R. S. (1992). Uranium series disequilibrium: applications to earth, marine and environmental sciences. Oxford, Clarendon Press.

Kochenov, A. V., Zinev'yev, V. V. & Lovaleva, S.A. (1965) Some features of the accumulation of uranium in peat bogs. *Geokhimiya, 1*, 97 - 103.

Landstrom, O. & Sundblad, B. (1986). Migration of thorium, uranium, radium and ^{137}Cs in till soils and their uptake in organic matter and peat. Studsvik Energiteknik AB. Report No. SKB - TR - 86 - 24. 2 - 15.

Levinson, A. A. , Bland, C. J. & Dean, J. R. (1984). Uranium series disequilibrium in young surfical uranium deposits in southern British Columbia. *Can. J. Earth Sci., 21*, 559 - 566.

Megumi, K. (1979). Radioactive disequilibrium of uranium and actinium series nuclides in soil. *Journal of Geophysical Research, 84*, 3677 - 3682.

Nemeth, W. K. & Parsa, B. (1992). Density correction of gamma ray detection efficiency in environmental samples. *Radioactivity and Radiochemistry. 3(3)*, 32 – 39.

O'Dea, J. & Dowdall, M. (1999). Spatial analysis of natural radionuclides in peat overlying a lithological contact in Co. Donegal, Ireland. *Journal of Environmental Radioactivity. 44*, 107 - 117.

Sheppard, M. I. (1980) The environmental behavior of radium. AECL-6796. Whiteshell Nuclear Research Establishment, Manitoba, Canada. 7 - 9.

Titaeva, N. A. & Veksler, T. I. (1977). The state of radioactive disequilibrium in the uranium and thorium series as an indicator of migration of radioactive elements and active interaction between phases under natural conditions. *Geochemistry International, 14*, 99 – 107.

Von Gunten, H.R., Surbeck, H. & Rossler, E. (1996). Uranium series disequilibrium and high thorium and radium enrichments in karst formations. *Environ. Sci. Technol, 30*, 1268 – 1274.

Zielinski, R. A., Bush, C. A. & Rosholt, J. N. (1986). Uranium series disequilibrium in a young surfical uranium deposit, northeasten Washington, U.S.A. *Applied Geochemistry. 1*, 503 - 511.

Zielinski, R. A., Otton, J. K., Wanty, R. B. & Pierson, C. T. (1987). The geochemistry of water near a surfical organic-rich uranium deposit, northeastern Washington state, U.S.A. *Chemical Geology, 62*, 263-289.

Speciation of ^{226}Ra, ^{238}U and ^{228}Ra in an Upland Organic Soil Overlying a Uraniferous Granite.

Mark Dowdall and John O'Dea
Institute of Technology, Sligo,
Ballinode, Sligo, Ireland.

Radiochimica Acta. **87**. 1999. pp. 109-114.

Radiochim. Acta 87, 109–114 (1999)

Speciation of ^{226}Ra, ^{238}U and ^{228}Ra in an Upland Organic Soil Overlying a Uraniferous Granite

By Mark Dowdall* and John O'Dea

Research Laboratory, Department of Applied Science, Institute of Technology, Ballinode, Sligo, Ireland

(Received May 12, 1999; accepted in revised form October 15, 1999)

Peat / Radionuclides / Speciation / Redox / Ireland

Summary

A sequential chemical extraction procedure was implemented in order to ascertain the chemical speciation of ^{226}Ra, ^{238}U and ^{228}Ra within fractions of an upland organic soil. A number of samples and depth cores were taken from a region where the soil contains elevated levels of these radionuclides. Sequential chemical extractions were employed to identify within which of the three soil phases, namely exchangeable cations, easily oxidisable organic matter or iron oxides, the radionuclides were incorporated. The primary analytical technique was high-resolution gamma ray spectrometry. A number of other chemical parameters likely to affect the mode of occurrence of the radionuclides were also analysed. These included humic acid content, iron and manganese content and cation exchange capacity. Results indicate that the average amount of radionuclides bound as exchangeable cations, expressed as a percentage of the specific activities of each radionuclide, are: ^{226}Ra – 2.13% (S.D. 2.15), ^{238}U – 5.2% (S.D. 4.6) and ^{228}Ra – 12.2% (S.D. 7.0). For easily oxidisable organic matter, the average percentages are: ^{226}Ra – 3.2% (S.D. 3.2), ^{238}U – 21.9% (S.D. 18.4), and ^{228}Ra – 8.5% (S.D. 8.7). Percentages for iron oxides are ^{226}Ra – 8.7% (S.D. 7.5), ^{238}U –54.8% (S.D. 22.2) and ^{228}Ra – 19.7% (S.D. 12.9). N equals 17 in all cases. The results indicate that the primary factor controlling U^{238} accumulation, and to a lesser extent ^{226}Ra and ^{228}Ra, is the redox condition of the peat. Release of radionuclides from the peat could possibly occur via changes in the redox status as a result of activities such as forestry or drainage of the peat.

Introduction

The aim of the study was to ascertain the chemical form of natural radionuclides in an upland organic soil exhibiting elevated levels of these radionuclides. The procedure adopted was the sequential chemical extraction of radionuclides bound to three distinct chemical fractions of the soil, namely as exchangeable cations, easily oxidisable organic matter and bound as iron oxides. Such procedures have previously been adopted for the speciation of radionuclides in soil. Bunzl *et al.* [1] used the Tessier *et al.* [2] procedure to determine the speciation of radionuclides in the vicinity of a uranium mine. Greeman and Rose [3] modified the Tessier *et al.* procedure for the speciation of radionuclides in soils of the eastern U.S. Other examples of sequential chemical extractions as applied to the analysis of radionuclides in soils include Voss *et al.* [4], and Lima and Penna-Franca [5].

* Author for correspondence
(E-mail: dowdallm@students.itsligo.ie).

The chemical form of radionuclides in peats and organic soils has been the subject of work by researchers in the past. Szalay [6] concluded that the insoluble (in 0.5 M NaOH) humic acid fraction of peat was mainly responsible for the enrichment of uranium in peat by a cation exchange process. Although this hypothesis has been supported by Titaeva [7], Doi *et al.* [8] found that peat whose humic acid component had been removed tended to adsorb more uranium from solution than peat whose humic acids remained intact. Idiz *et al.* [9] concur with Szalay, finding that uranium is the only metal whose enrichment in peat bogs is controlled by the organic component. Halbach *et al.* [10] investigated the role of humic and fulvic acids in the mobilization and fixation of uranium in a peat bog and concluded that uranium is primarily removed from the granite bedrock as a uranyl fulvate complex but is fixed in the peat as a uranyl humate complex.

A significant number of researchers conclude that, at least in some soils, soil iron oxides are the major component responsible for uranium enrichment. Lowson *et al.* [11] reported that up to 80% of the uranium in a soil derived from granite bedrock was associated with Fe oxides. Megumi [12], using ammonium oxalate as the extracting agent, found that up to 50% of uranium in soil was associated with Fe oxides, no trend in the proportion being observed with sample depth. All researchers conclude that little uranium is held as exchangeable cations, Lowson *et al.* [11] finding less than 1% whilst Megumi [12] observed values less than 0.8%.

Although radium shows little tendency to form complexes Schubert *et al.* [13] and Granger *et al.* [14] showed that it may be expected to replace other divalent cations in replacement reactions. Arnold and Crouse [15] obtained a correlation between radium adsorption and cation exchange capacity, the leaching studies of Havlik *et al.* [16] supporting the view that cation exchange is an important mechanism for radium adsorption. Megumi [12] established that, unlike uranium or thorium, radium may have a significant occurrence as an exchangeable ion. Nathwani and Phillips [17] showed that organic matter was the component of soil responsible for radium adsorption and that soils with a low cation exchange capacity exhibited reduced ability for adsorption. Titaeva [7] studied the nature of radium bonding in peat and concluded that radium is

100 g of finely ground soil was placed in a 1l acid washed plastic bottle with 600 ml of extraction solution. The bottle was shaken for 1 hr then the mixture was centrifuged at 10 k rpm for 600 s. The supernatant was stored and the solid material was resuspended in 300 ml of distilled water and shaken for 1200 s before being centrifuged at 10 k rpm for 600 s. Supernatants were bulked, filtered through a 0.45 μm filter, made up to one litre and sealed for gamma analysis. All extractions were done at 20°C except for Fe oxides which was performed at 80°C. The extracting solutions were as follows:

Exchangeable cations

1 M magnesium chloride, pH 6 with HNO_3.

Easily oxidized organic matter

5% sodium hypochlorite, pH 6 with HNO_3.

Fe oxides

50 g/l of sodium dithioite in a 0.3 M sodium citrate/ 0.2 M sodium bicarbonate buffer.

Chemical Analysis

A number of chemical parameters for each sample were also determined. The samples for analysis (with the exception of pH and Eh) were extracted from the riffled soil mass used for gamma ray analysis.

pH

pH values for the soils were determined in situ. A small hole was made in the soil into which the electrode was inserted. In cases where a good contact between the electrode and the soil water was not made, a small amount of distilled water was added.

Eh

A portable Eh meter was utilized to determine the Eh status of the soil in a similar manner to the pH determination, the electrode being left for up to 10 minutes in the soil to allow equilibrium to occur.

Total Iron and Manganese

Approximately 1 g of finely ground soil was digested with 5 ml of a 3:1 HCl/HNO_3 mixture and boiled for 1 hr. The mixture was filtered through glass fiber filter paper before being filtered with a 0.45 μm filter. The solution was then made up to 100 ml. Both metals were analyzed by AAS.

Cation exchange capacity (CEC)

4–6 g of soil was mixed with 33 ml of 1 N NaOAc and shaken for 300 s. The supernatant was removed after centrifuging at 10 k rpm for 600 s. The cycle was repeated three times. The soil was then mixed with 33 ml of propan–2-ol, this cycle being repeated three times. The soil was then mixed with 33 ml of NH_4OAC, this cycle also being repeated three times, the three NH_4OAC supernatants being filtered (0.45 μm) and combined, then brought up to 100 ml. The Na content of this solution was measured by flame photometry.

Organic matter content

Organic matter was determined as the loss on ignition at 500°C for 4 hours.

Humic acid content

Approximately 1 g of ground soil was mixed with 50 ml of 0.5 M NaOH and shaken for 600 s. The mixture was centrifuged at 10 k rpm for 600 s, the supernatant being discarded. The procedure was repeated on the solid material until three consecutive supernatants ran clear (typically 7 to 8 times). The material was washed with three 30 ml aliquots of distilled water, and dried at 101°C. Humic acid content was calculated from loss of mass from the soil.

Quality control

Chemical analyses were conducted subject to the regular quality control procedures implemented in the laboratory. Reproducibility of results was assessed using replicates (three) of homogenized samples. The coefficients of variation were typically less than 20% (2σ). The accuracy of the analytical methods was checked using traceable reference standards, spikes and blanks at a typical loading of 5 per 50 analytical samples.

Results

Table 1. Radionuclide activities (Bq/kg) for site E. Depth given in cm.

Sample	Depth	^{226}Ra	^{238}U	^{228}Ra
E 1	0–15	418.0	92.3	20.0
E 2	15–30	523.5	109.6	44.2
E 3	30–45	515.2	499.3	66.6
E 4	45–60	692.4	884.0	107.7
E 5	60–75	847.9	737.8	142.1
E 6	60–75	320.4	53.1	18.6
E 7	60–75	540.0	476.0	123.5
E 8	60–75	421.6	115.3	38.8

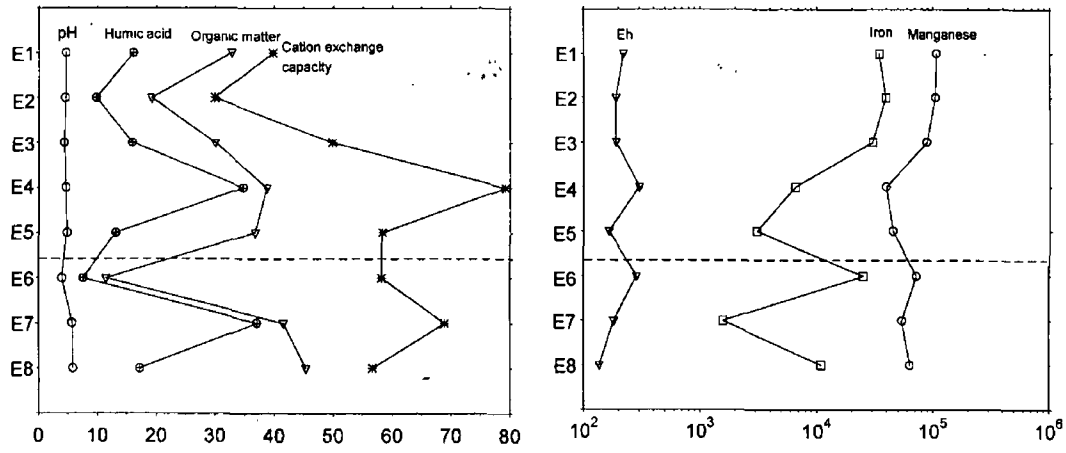

Fig. 1. Chemical properties of samples from site E. Units are as follows: Eh – mV, iron – ppm, manganese – ppm, cation exchange capacity – meq/100 g, organic matter – % (w/w), humic acid – % (w/w). Horizontal dashed line denotes division of depth core and individual samples.

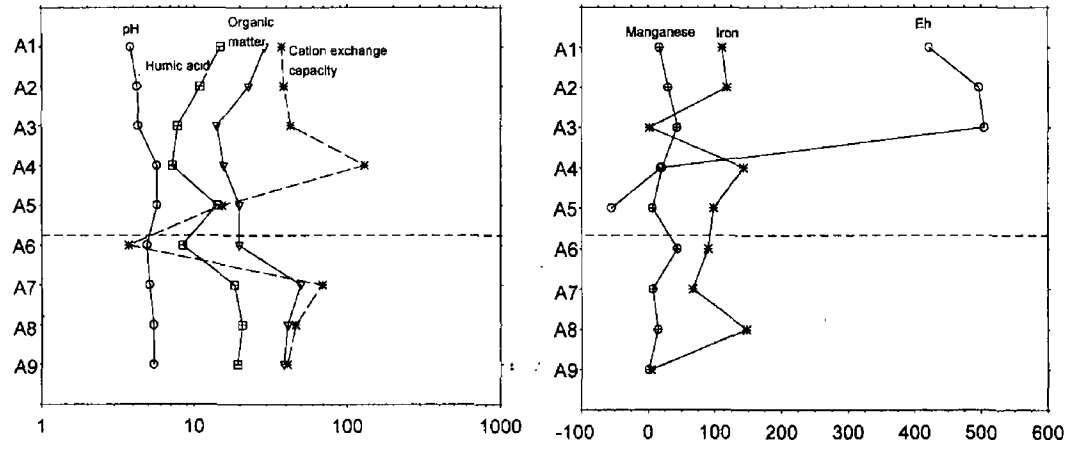

Fig. 2. Chemical properties of samples from site A. Units are as follows: Eh – mV, iron – ppm$\times 10^{-3}$, manganese – ppm, cation exchange capacity – meq/100 g, organic matter – % (w/w), humic acid – % (w/w). Horizontal dashed line denotes division of depth core and individual samples.

^{228}Ra has a significant and comparable occurrence as an exchangeable cation at both sites, the occurrence in the easily oxidized fraction being less than that of the exchangeable cations for almost all samples. Similar to the previous two nuclides, ^{228}Ra has its major mode of occurrence in the Fe oxide fraction. Assuming that, given its short half life relative to soil processes, ^{228}Ra can be used to infer ^{232}Th levels, it appears that ^{232}Th is bound chiefly to the organic material (exchangeable cations + easily oxidisable fractions) and Fe oxides.

Averaging the total labile (exchangeable cations + easily oxidisable organic + Fe oxides) radionuclide content for the 17 samples yields values of 12.01% for ^{226}Ra, 81.3% for ^{238}U and 41.2% for ^{228}Ra. These figures appear to confirm the generally accepted hypothesis that Ra is relatively immobile in soil and U is mobile. ^{226}Ra levels do not exhibit the same amount of variation throughout the soil columns as U and Th indicating a lower level of vertical migration than either U or Th. The apparent disparity between the behaviours of ^{228}Ra and ^{226}Ra is probably due to the different behaviour of the parent nuclides, ^{232}Th and ^{238}U respectively.

The controlling factor for U accumulation would appear to be the redox condition of the soils. U is relatively immobile in reducing conditions (+4 valency) compared with its mobility in oxidizing conditions (+6 valency). The majority of samples from site E exhibit Eh values lower than 200 mV, indicating reducing conditions, the soils of site A having Eh values of up to 500 mV. The depth section of site E has an average ^{238}U activity nearly 5 times greater than that of site A. Further evidence is provided by the fact that ^{238}U activity increases by a factor of two on going from the oxidized upper layers to the more reducing lower levels of the peat. Both sites exhibit similar levels of organic matter and humic acid, cation exchange capacities for both soils also being comparable. It would appear that in this region, redox potential of the soil is a major factor controlling either the enrichment or depletion of U within the peat. Activities

Comparison of Point Estimation Techniques in the Spatial Analysis of Radium-226, Radium-228 and Potassium-40 in Soil.

Mark Dowdall and John O'Dea
Institute of Technology, Sligo,
Ballinode, Sligo, Ireland

Environmental Monitoring and Assessment. **59**. 1999.
pp. 191-209.

COMPARISON OF POINT ESTIMATION TECHNIQUES IN THE SPATIAL ANALYSIS OF RADIUM-226, RADIUM-228 AND POTASSIUM-40 IN SOIL

MARK DOWDALL* and JOHN O'DEA
Institute of Technology Sligo, Sligo, Ireland
(author for correspondence, e-mail: dowdallm@students.itsligo.ie)*

(Received 8 May 1998; accepted 3 August 1998)

Abstract. Many environmental surveys require the implementation of estimation techniques to determine the spatial distribution of the variable being investigated. Traditional methods of interpolation and estimation, for example, inverse distance squared and triangulation often ignore features of the data set such as anisotropy which may have a significant impact on the quality of the estimates produced. Geostatistical techniques may offer an improved method of estimation by modelling the spatial continuity of the variable using semi-variogram analysis. The theoretical model fitted to the semi-variogram is then used in the assignation of weighting factors to the samples surrounding the location to be estimated. This paper outlines the results of a comparison between three common estimation methods, polygonal, triangulation and inverse distance squared and a geostatistical method, in the estimation of soil radionuclide activities. The geostatistical estimation method known as kriging performed best over a range of parameters used to test the performance of the methods. Kriging exhibited the best correlation between actual and estimated values, the narrowest error distribution and the lowest overall estimation error. Polygonal estimation was best at reproducing the data set distribution. Conditional bias was evident in all the methods, low values being over-estimated and high values being under-estimated.

Keywords: estimation, geostatistics, interpolation, radionuclides, soil

1. Introduction

By necessity, many enironmental surveys are limited to relatively small data sets. Such data sets often require the implementation of estimation methods to provide a clearer picture than that provided by mere visual inspection of the survey results. In many cases estimation methods are applied with little or no regard as to the quality of the estimates produced or how they relate to the actual data values. To assess how well an estimation procedure has performed in relation to the known data set, it is possible to use a jack-knifing procedure involving the elimination of a single data value from the data set and then producing an estimate of this value using the remaining data points and the chosen method. The data point is then replaced and the procedure repeated until all data points have been estimated and a set of estimated values and their estimation errors have been produced. Certain features of both the set of estimates and the distribution of the associated errors can be used

Environmental Monitoring and Assessment **59:** 191–209, 1999.

TABLE I

Parameters of theoretical models fitted to the experimental semi-variograms of each radionuclide

	^{228}Ra	^{40}K	^{226}Ra
Fitted model	Gaussian	Gaussian	exponential
Sill	750	83 000	18 000
Nugget	0	0	0
Range (m)	700	750	3 000
North–South	400	600	3 000
East–West	1000	1 100	3 000

to assess the effectiveness of the estimation method in reproducing the original data set.

The data set used in this study consisted of activity values (Bq kg^{-1}) for the natural radionuclides, radium-226 (^{226}Ra), radium-228 (^{228}Ra) and potassium-40 (^{40}K) for a set of sixty soil samples extracted from a 20 km^2 region in County Donegal, Ireland, as part of a radiological survey being conducted by the Institute of Technology, Sligo. Sample locations were identified using a 1:10 560 (six inch) scale map and samples were randomly chosen from within a 300 m radius circumscribed around the location, the random number function of a pocket calculator being used to determine a direction and a distance from the centre of the circle. In cases where the final sample location coincided with rock outcrop or water, the procedure was repeated. The final position of the sample was determined using a compass and a tape measure and the easting–northing co-ordinates were noted. Samples were sealed in polythene bags and removed to the laboratory for analysis by high resolution gamma ray spectrometry. All spectra were corrected for known interferences and laboratory background. A matrix of sample values and co-ordinates was then constructed for subsequent data analysis.

The four estimation techniques chosen were (1) a basic polygonal method, (2) inverse distance squared, (3) triangulation and (4) the methods embodied in the theory of geostatistics. A polygonal estimator can be described as a weighted linear combination which results in all of the weight being assigned to the closest neighbouring data point. Each known sample location is therefore surrounded by a polygon of influence delineated by the perpendicular bisectors of the lines joining the sample point and its adjoining points. A basic polygonal estimation procedure produces a discontinuous set of estimates in which the value of an estimate changes abruptly as the location being estimated moves from one polygon to the next. The triangulation method attempts to remove this discontinuity by mathematically describing the plane that exists between the three samples surrounding the location to

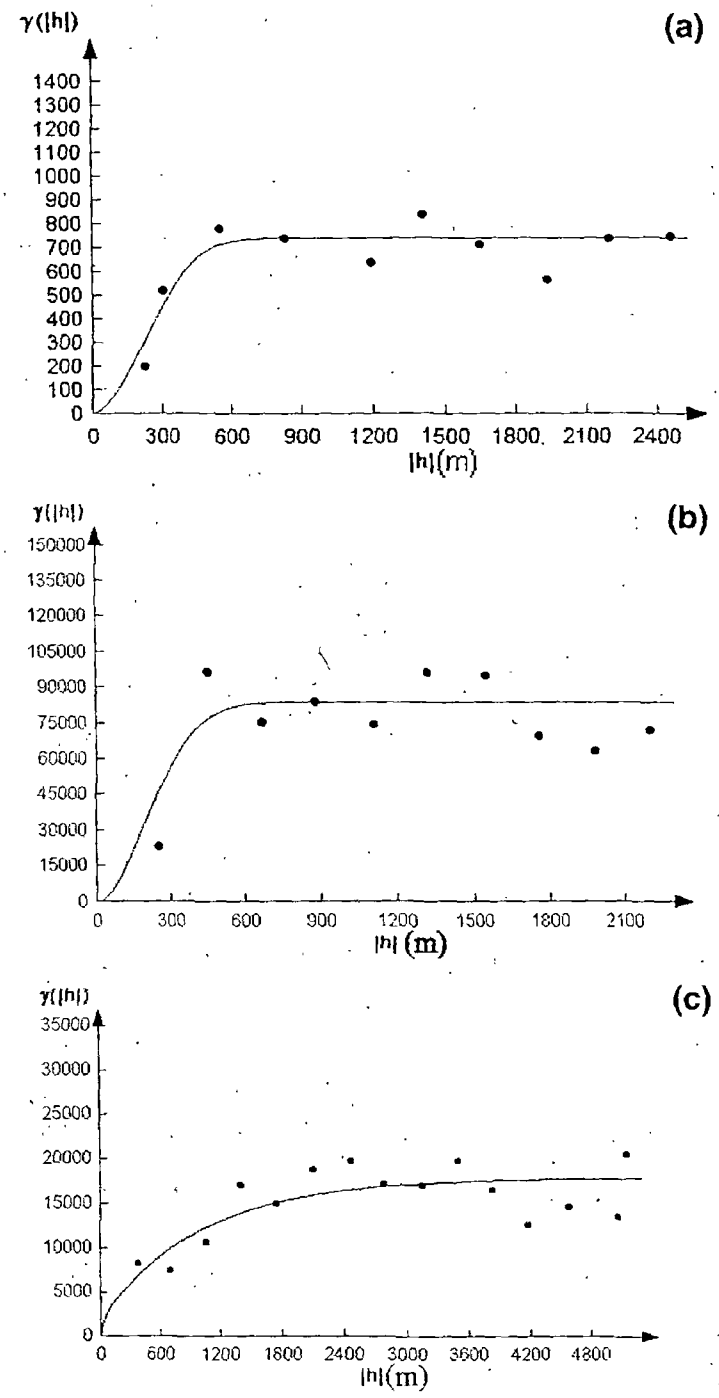

Figure 1. Omni-directional semi-variograms for (a) ^{228}Ra, (b) ^{40}K and (c) ^{226}Ra.

TABLE II

Summary statistics for actual and estimated ^{226}Ra. Values in Bq kg^{-1} (dry weight)

	Actual	Poly.	Inv. Dist.	Kriging	Actual	Triang.
n	60	60	60	60	49	49
Mean	104.7	110.1	104.5	101.5	114.3	107.02
Std. dev	125.5	130.0	108.2	98.1	133.9	117.2
Skew.	1.51	1.49	1.38	1.39	1.29	1.43
Min.	4.6	4.6	19.9	14.3	4.6	4.9
20% tile	20.5	19.9	31.5	33.4	18.7	36.8
40% tile	43.0	44.0	39.4	45.3	43.2	48.75
Median	47.7	56.8	51.8	58.0	48.5	49.4
60% tile	55.0	72.1	69.2	70.0	72.1	131.6
80% tile	226.0	238.3	146.0	172.0	243.3	403.7
Max.	479.0	479.0	372.9	362.1	479	414.5
p. coeff.		0.573	0.451	0.701		0.628
C.V. (%)	119.9	118.0	103.5	96.6	117.1	109.2

TABLE III

Summary statistics for actual and estimated ^{228}Ra. Values in Bq kg^{-1} (dry weight)

	Actual	Poly.	Inv. Dist.	Kriging	Actual	Triang.
n	60	60	60	60	49	49
Mean	35.1	35.2	34.4	36.5	36.7	39.1
Std. Dev.	25.1	23.3	15.0	17.2	27.2	20.4
Skew.	1.93	1.72	1.40	1.10	1.73	0.86
Min.	3.2	4.6	14.0	15.3	3.5	8.8
20% tile	19.4	19.6	23.3	23.0	19.2	26.8
40% tile	27.7	28.0	27.69	26.9	28.0	32.2
Median	47.7	30.6	29.7	30.4	30.7	33.5
60% tile	33.2	31.0	31.9	34.9	34.2	46.4
80% tile	43.4	43.4	42.8	49.6	47.1	83.0
max.	135.0	117.3	82.9	93.9	135.0	93.69
p. coeff.		0.254	0.253	0.604		0.307
C.V. (%)	71.9	66.2	43.5	47.1	74.16	52.19

TABLE IV

Summary statistics for actual and estimated ^{40}K. Values in Bq kg^{-1} (dry weight)

	Actual	Poly.	Inv. Dist.	Kriging	Actual	Triang.
n	60	60	60	60	49	49
Mean	526.4	488.0	498.1	516.3	535	501.9
Std. Dev.	278.1	295.1	195.2	170.8	279.2	208.9
Skew.	–0.061	0.012	0.40	0.14	–0.12	0.05
Min.	8.0	8.16	103.5	94.8	8.0	66.1
20% tile	288.1	162.0	320.6	372.0	30.2	323.3
40% tile	459.0	427.2	446.9	481.7	468.8	500.8
Median	551.3	475.2	492.1	521.1	562.0	516.2
60% tile	597.1	580.3	524.5	560.9	633.9	638.5
80% tile	739.5	739.6	618.4	623.1	783.2	843.7
Max.	1088.0	1088.0	972.5	975.1	1088.0	1000.3
p. coeff.		0.263	0.219	0.338		0.222
C.V. (%)	52.83	60.50	39.10	33.00	51.82	41.62

TABLE V

Summary statistics of estimate errors (actual–estimate) for ^{226}Ra. Values in Bq kg^{-1} (dry weight)

	Polygonal	Inv. dist.^{2}	Kriging	Triang.
n	60	60	60	49
Mean	6.05	0.49	0.48	–7.40
Std. Dev.	118.9	96.2	89.6	106.7
Skew.	0.85	–0.25	0.56	–0.71
Min.	–370.0	–354.6	–295.6	–327.8
Median	5.2	2.9	–0.4	5.4
Max.	470.2	298.6	328.5	313.8
M.S.E.	14022.5	9260.9	7902.6	11128.9
M.A.E.	68.8	59.1	51.8	66.8

be estimated. If a sample's easting and northing co-ordinates are denoted as e and n respectively, and the variable value is g, then the equation of the plane joining three points, in the form $g = ae + bn + c$, can be obtained by solving for a, b and c in the set of equations:

$$ae_1 + bn_1 + c = g_1$$

TABLE VI

Summary statistics of estimate errors (actual–estimate) for ^{228}Ra. Values in Bq kg^{-1} (dry weight)

	Polygonal	Inv. dist.^{2}	Kriging	Triang.
n	60	60	60	49
Mean	0.32	−0.05	1.30	2.30
Std. dev.	29.7	25.9	20.2	28.5
Skew.	0.40	−1.30	−0.93	−0.26
Min.	−70.8	−103.9	−71.9	−86.0
Median	0.0	−0.7	2.9	1.7
Max.	90.8	475.0	52.0	74.9
M.S.E.	884.6	671.8	406.6	823.9
M.A.E.	19.5	17.4	13.7	19.2

$$ae_2 + bn_2 + c = g_2$$

$$ae_3 + bn_3 + c = g_3$$

Substitution of the co-ordinate values for the unknown location into the resulting equation yields the estimate value. The method known as inverse distance squared involves assigning weights to samples based on the relative distances of the samples from the unknown location, using the equation given below:

$$g^* = \sum_{i=1}^{n} \left(\frac{1}{d_i^2}\right) g_i \Big/ \sum_{i=1}^{n} \left(\frac{1}{d_i^2}\right)$$

where g^* is the estimated value, g_i is the known sample value and d is the separation distance.

Geostatistical methods are those embodied in the theory of regionalised variables, empirically described by Krige (1951) as a means of ore estimation and theoretically grounded by Matheron (1970). Geostatistical methods involve two distinct stages, modelling of the spatial correlation of the variable using semi-variogram analysis and the estimation of variable values at unsampled locations using the method known as kriging. The semi-variogram is constructed by plotting the semi-variance, $\gamma(h)$, in relation to the distance between sample points, h. The semi-variance is calculated according to the equation:

$$\gamma(h) = \frac{1}{2n(h)} \sum_{i=1}^{n-h} [z(x_{i+h}) - z(x_i)]^2$$

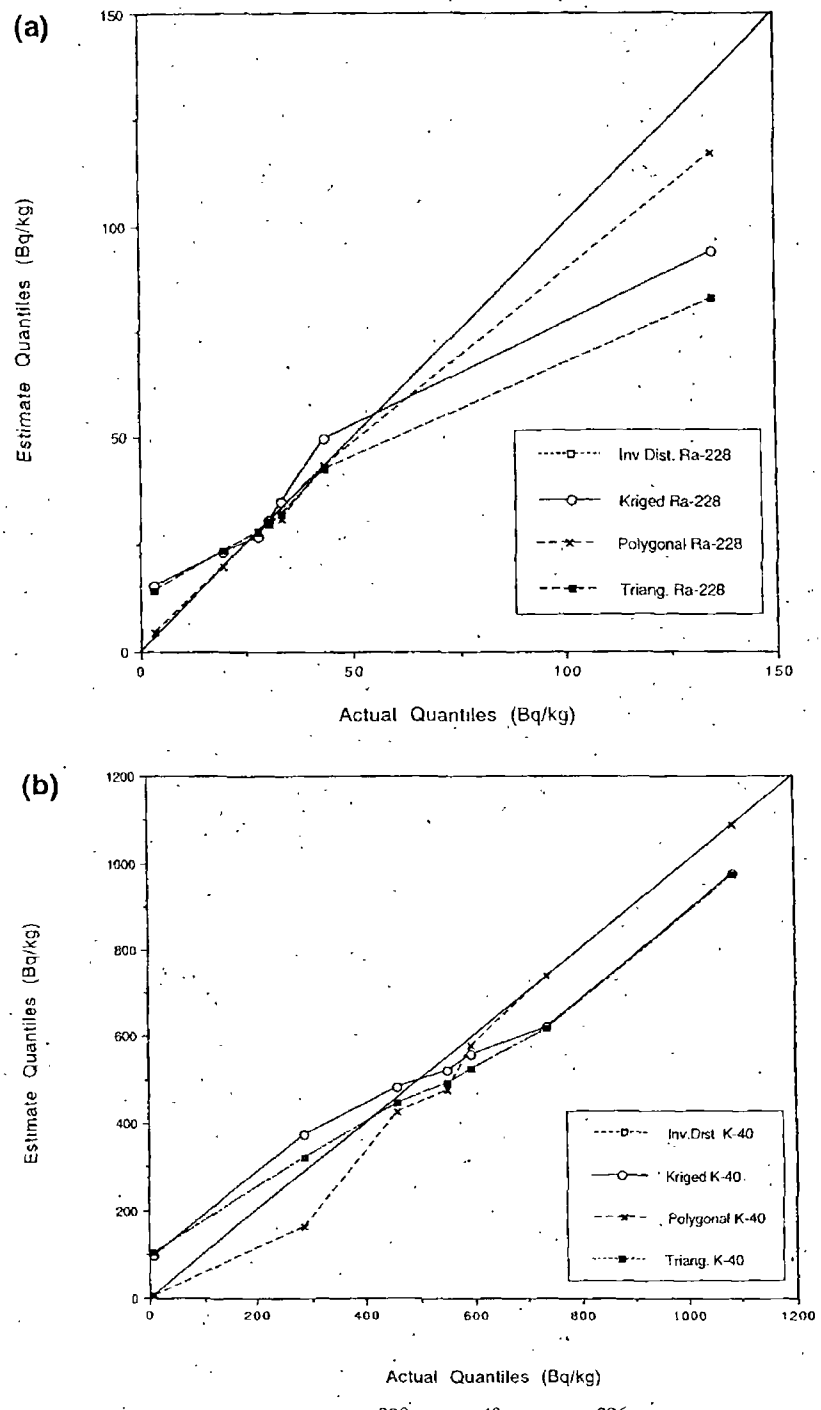

Figure 2a-c. Quantile–quantile plots for (a) ^{228}Ra, (b) ^{40}K and (c) ^{226}Ra. All values in Bq kg^{-1}.

TABLE VII

Summary statistics of estimate errors (actual–estimate) for ^{40}K. Values in Bq kg^{-1} (dry weight)

	Polygonal	Inv. dist.^{2}	Kriging	Triang.
n	60	60	60	49
Mean	–29.7	–19.4	–10.1	–36.5
Std. dev.	347.2	301.2	272.7	309.3
Skew.	–0.13	–0.12	–0.03	0.38
Min.	–1000.0	–857.4	–724.6	–710.3
Median	–25.5	–33.1	–40.8	–30.9
Max.	989.9	788.0	621.4	755.8
M.S.E.	121599.1	91239.4	74477.3	97025.5
M.A.E.	262.1	230.0	211.7	233.49

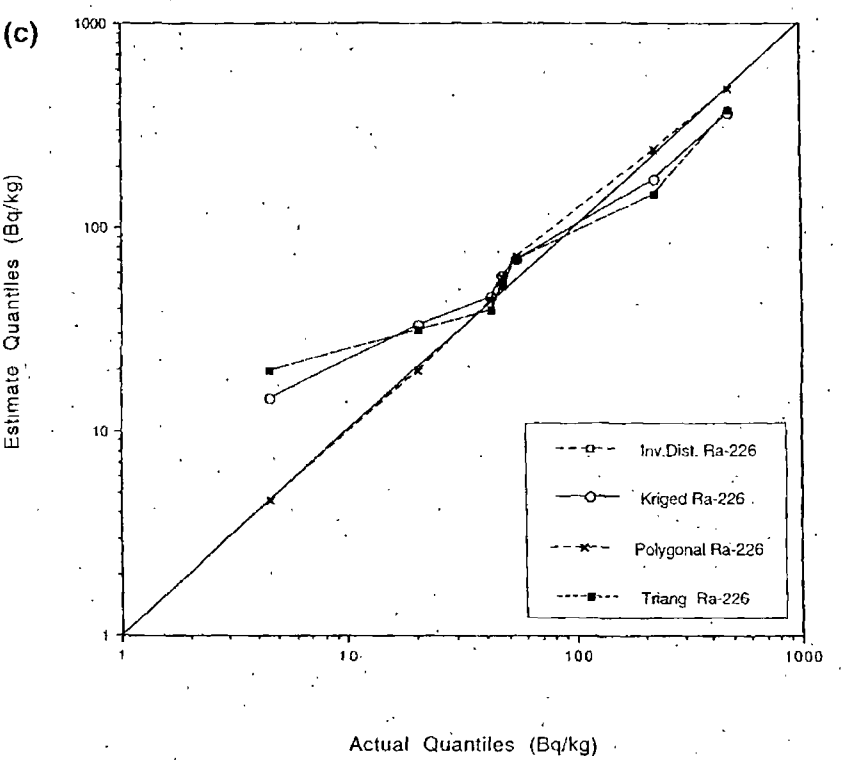

Figure 2c.

where $n(h)$ is the number of sample pairs separated by distance, or lag, h and $[z(x_{i+h}) - z(x_i)]$ is the difference between variable values separated by a distance h.

The resulting plot, termed the semi-variogram, describes the spatial correlation of the data set, the semi-variance typically increasing as the distance between samples increases. To describe the spatial correlation, it is necessary to fit a mathematical model to the experimental semi-variogram, the model usually being a gaussian, exponential or spherical function. The features of most interest in the semi-variogram are the maximum semi-variance value, or sill, and the separation distance at which the sill is reached, termed the range of correlation. Samples separated by a distance more than the range are spatially independant. If the semi-variance is not equal to 0 at $h = 0$, then a random component, termed the nugget, is present.

The second step in a geostatistical study involves the estimation of variable values at unknown locations using a weighted moving average estimation method called kriging. Subject to the conditions that the variance of the difference between sample values is only a function of the separation distance and that the data set approaches a normal distribution, kriging assigns weights to samples according to the information provided by the semi-variogram, in a manner that ensures that the estimate produced is a best linear unbiased estimator. Point kriging can be described by the equation:

$$z^*(x_o) = \sum_{i=1}^{n} [\lambda_i z(x_i)]$$

$z^*(x_o)$ being the kriged estimate, λ_i being the weight assigned to the known sample z at the location (x_i). Sample weights are assigned according to the kriging system:

$$\sum_{j=1}^{n} \lambda_i \gamma(x_i, x_j) + \mu = \gamma(x_i, x_0) , \qquad 1 = 1, 2, 3, \ldots, n$$

(x_i, x_j), (x_i, x_0) are the lag intervals separating the relevant points, x_0 is the location to be estimated, γ is the semi-variogram value for that lag distance, λ_i is the assigned weight and μ is a Lagrange multiplier. In a manner similar to the polygonal and inverse distance squared methods, the weights are normalised to ensure an un-distorted estimate distribution.

Although originally developed as a means of ore estimation, geostatistical methods are increasingly being applied to the spatial analysis of environmental variables. Flatman,Englund and Yfantis (1988), Gilbert (1987) and McBratney and Laslett (1993) detail the general application of such methods to environmental monitoring, specific applications being described by Einax and Soldt (1994), Litaor (1995) and Barns (1980). Detailed mathematical descriptions of the methods involved in geostatistics are contained in Davis (1973) and Journel and Huybregts (1978).

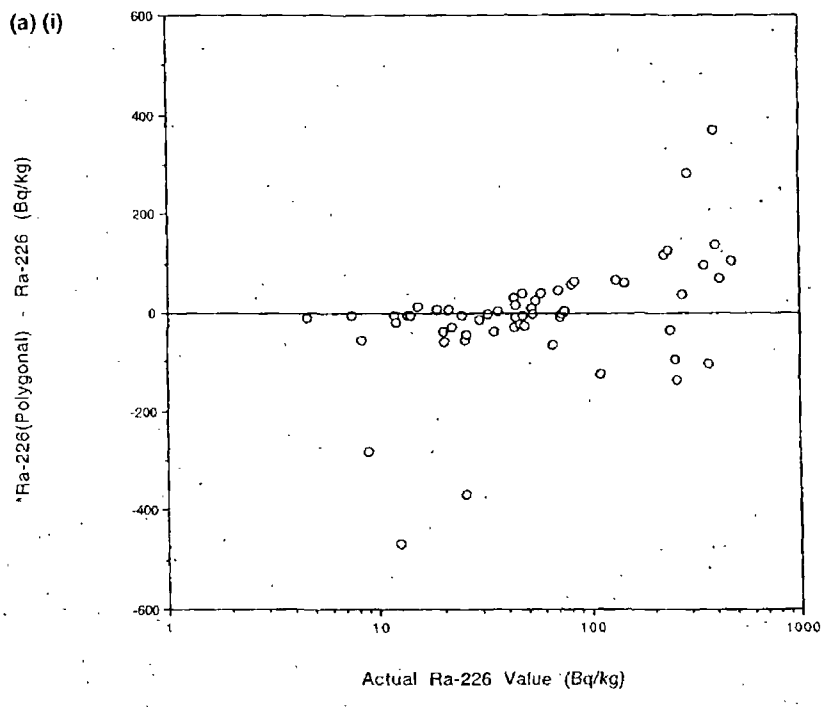

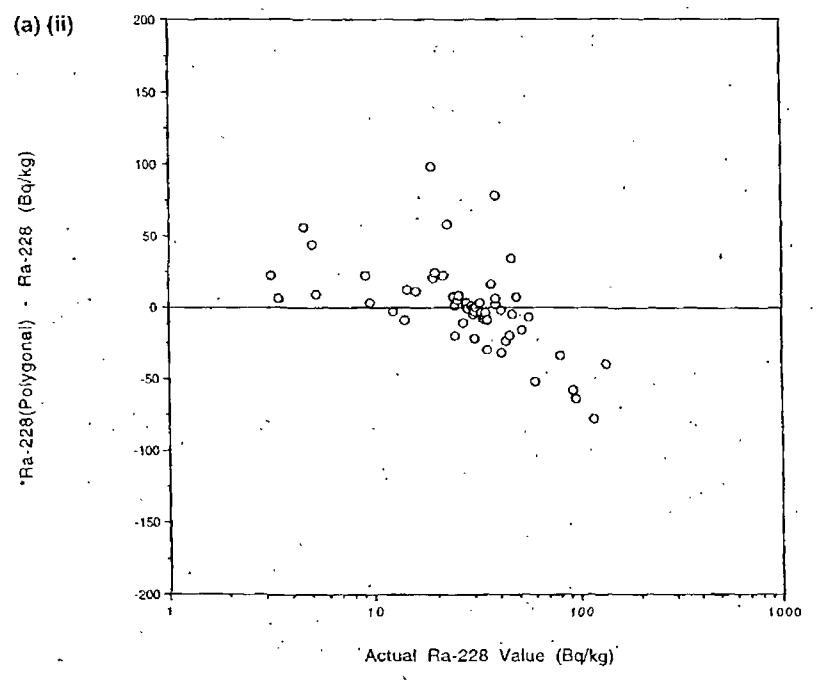

Figure 3a (i)–3d (iii). Residual plots for radionuclides estimated by (a) polygonal method, (b) triangulation, (c) inverse distance squared and (d) kriging. In each case (i) ^{226}Ra, (ii) ^{228}Ra and (iii) ^{40}K. All values in Bq kg^{-1}.

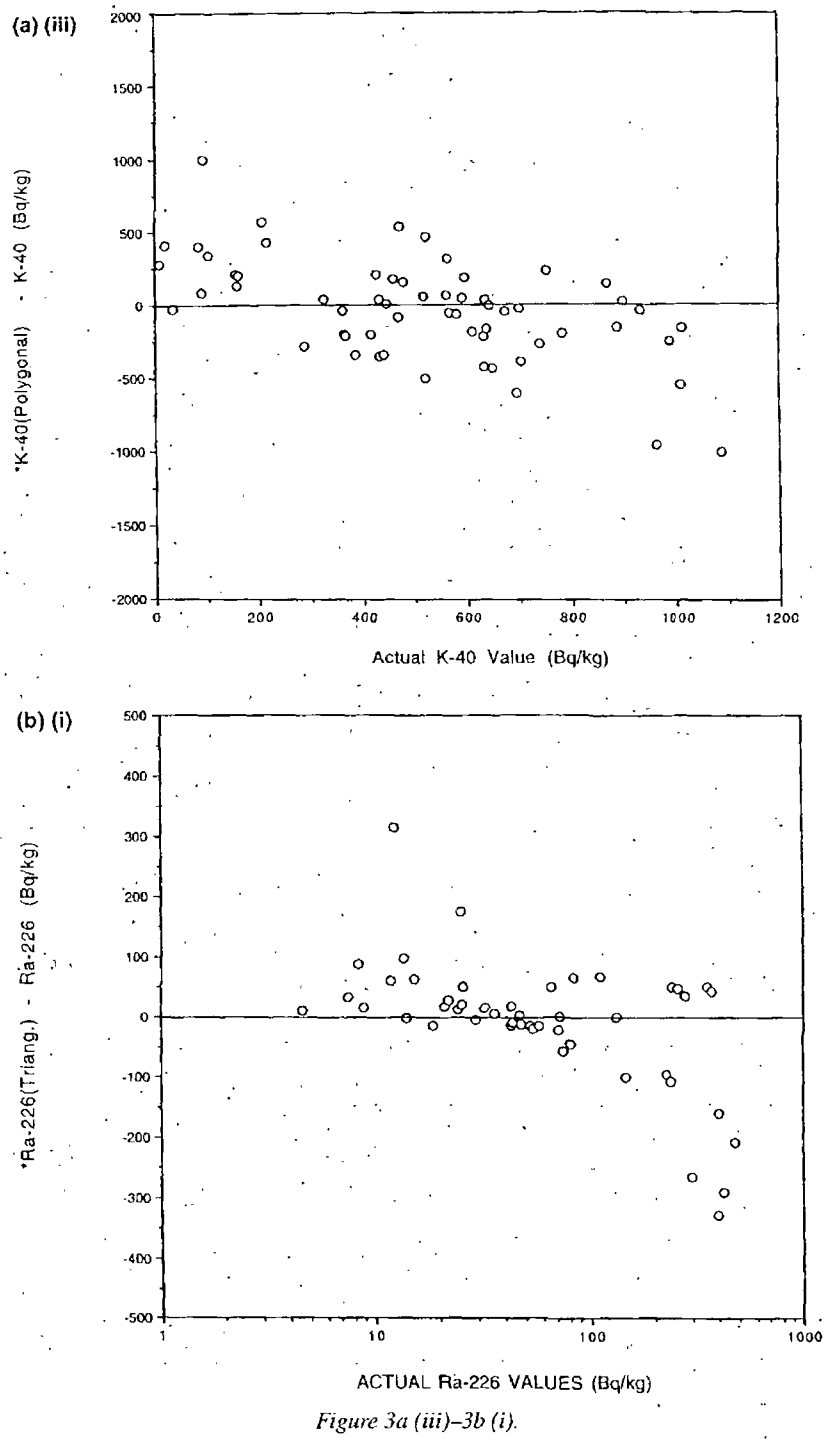

Figure 3a (iii)–3b (i).

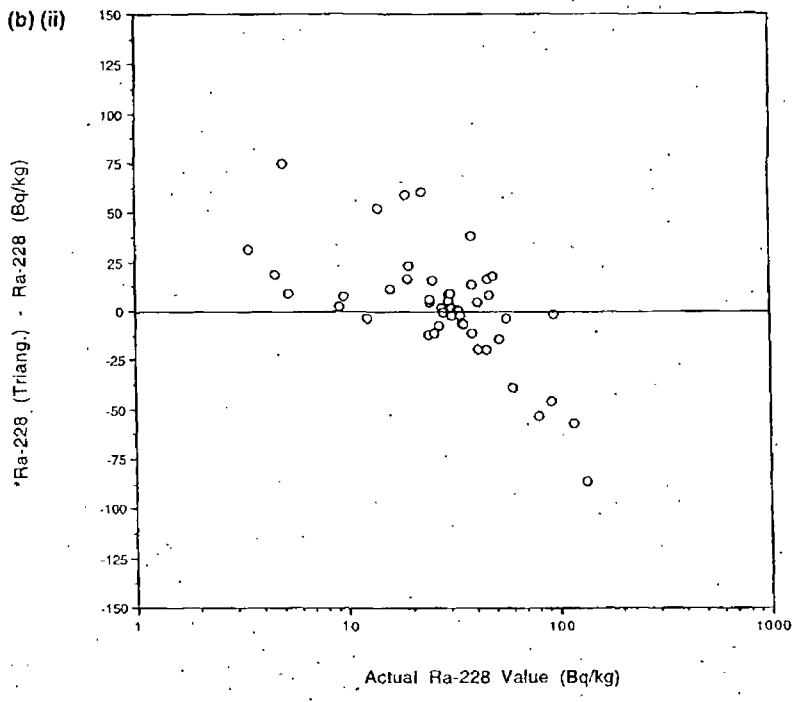

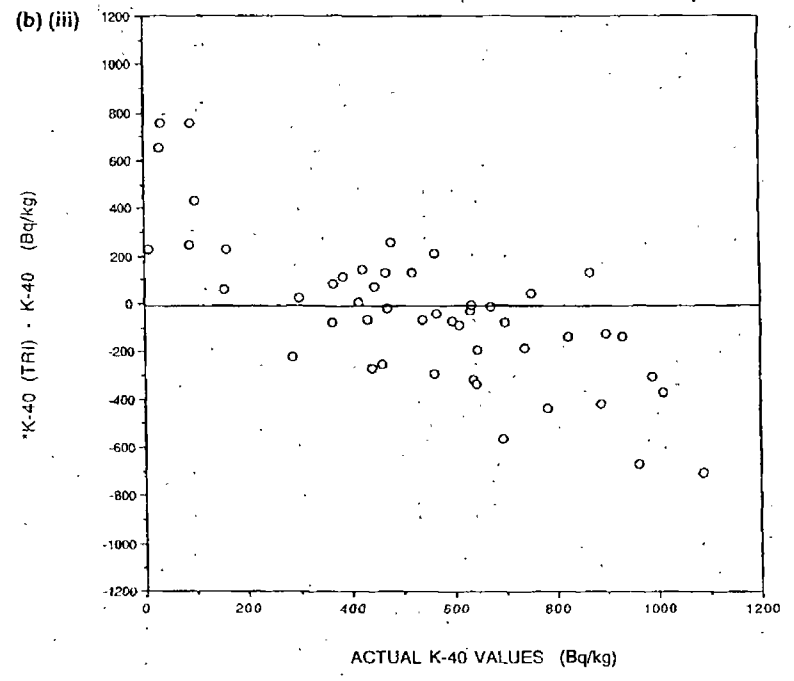

Figure 3b (ii)–3b (iii).

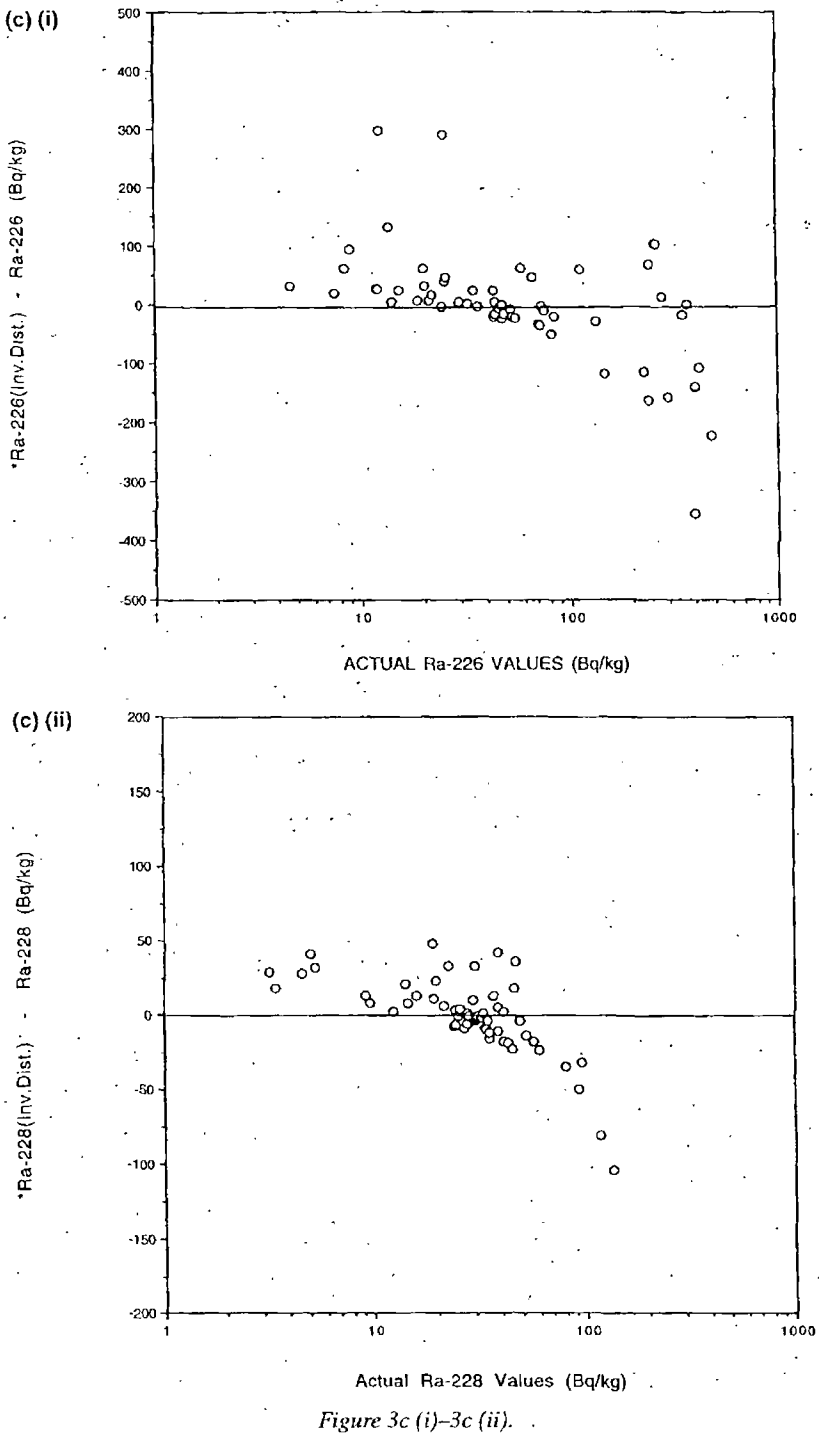

Figure 3c (i)–3c (ii).

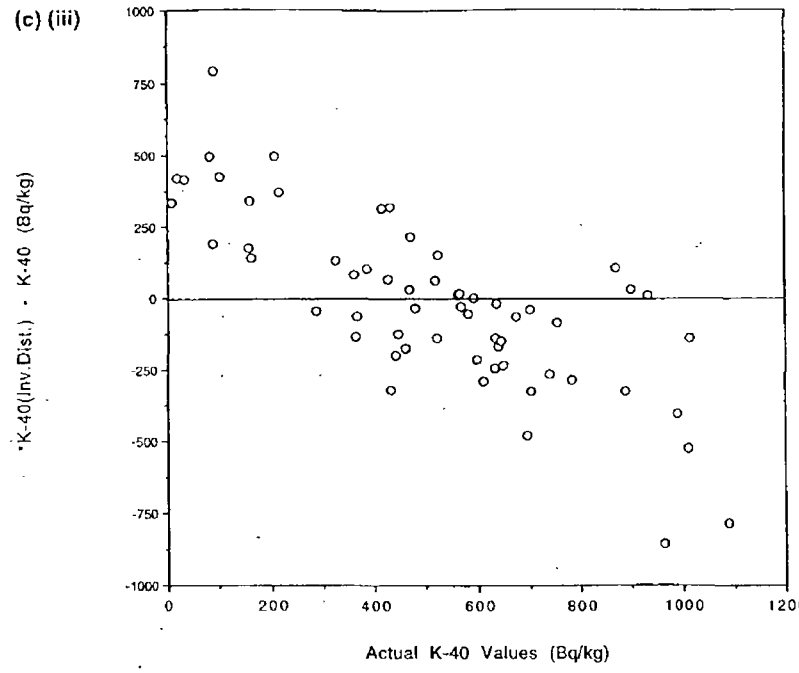

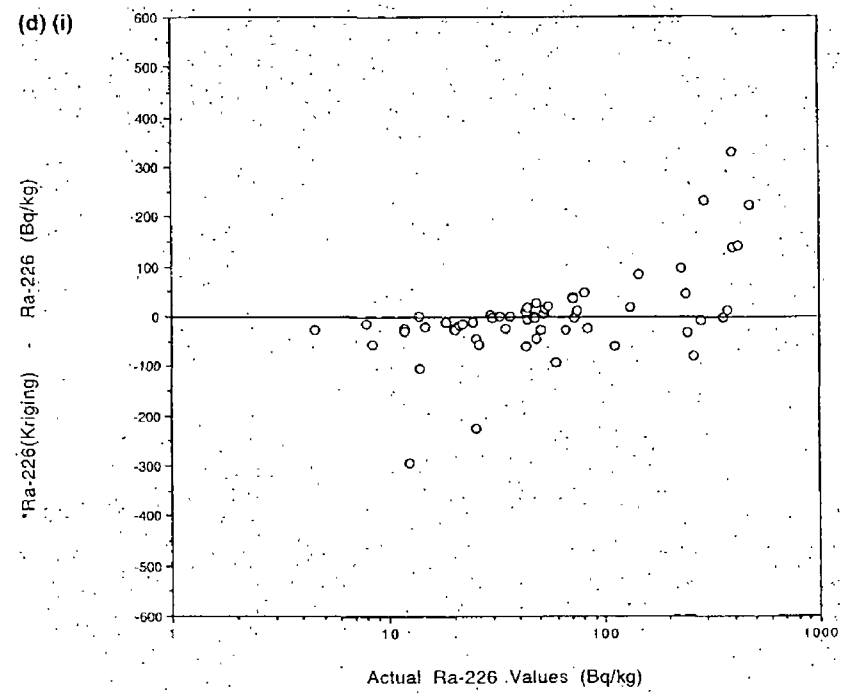

Figure 3c (iii)–3d (i).

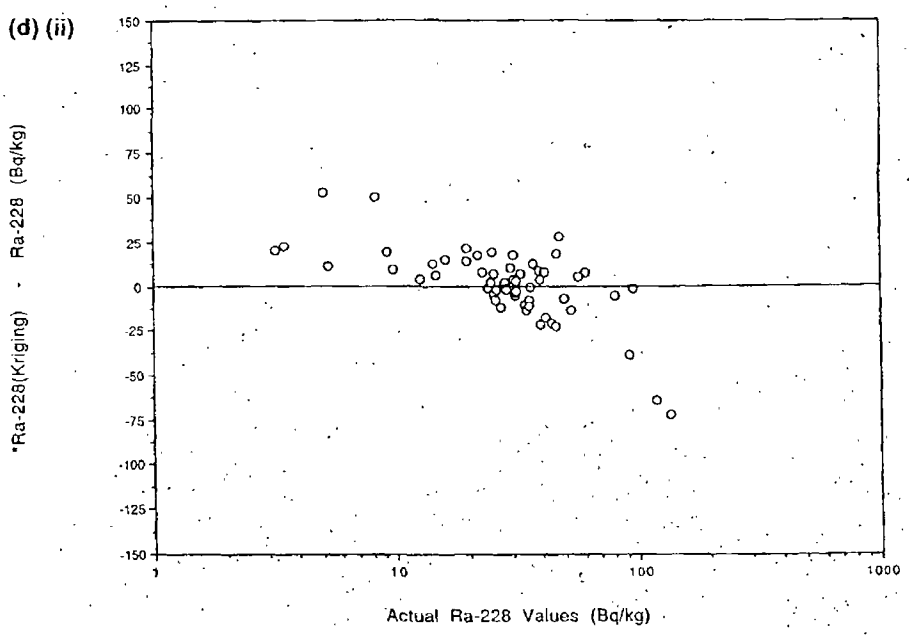

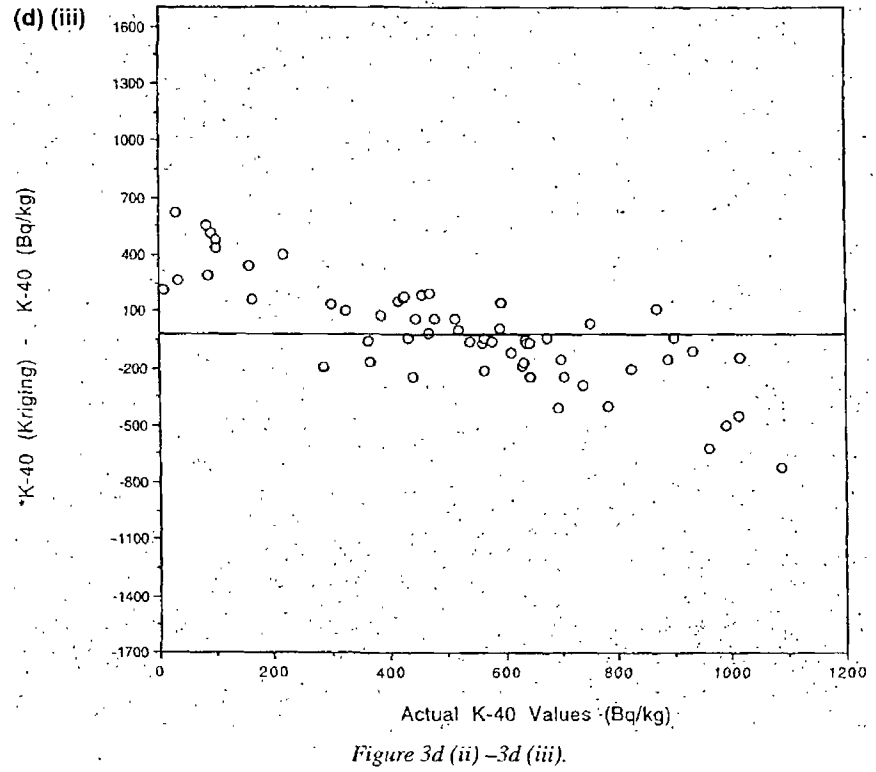

Figure 3d (ii) –3d (iii).

2. Methods

Individual sample points were eliminated from the sample matrix and then estimated using each of the four methods previously described before being replaced in the matrix. The polygonal method estimated a point using the nearest known sample, the triangulation method used the nearest three samples to the unknown location. In cases where a location could not be circumscribed with a triangle it was not estimated, in this study resulting in a decrease from 60 samples to 49 estimates. A computer program was written to solve the nine simultaneous equations associated with each estimate.

Semi-variograms were constructed for each of the radionuclides, Figure 1 depicting the omni-directional semi-variograms, one for each radionuclide.

Directional semi-variograms were then constructed for each radionuclide to determine if the spatial correlation was the same in each direction (isotropy). Both ^{40}K and ^{228}Ra displayed evidence of anisotropy, the range of correlation being significantly longer in the east–west direction than in the north–south direction. Table I gives details of the spatial correlation and fitted theoretical model for each radionuclide.

Points were estimated using the samples contained within a 1200 m search radius, a minimum of 3 points being required for each estimation. Semi-variogram modelling of the radionuclides was conducted using Geostatistical Toolbox software (Froideuaux, 1990) and Variowin 2.2 (Pannatier, 1996), ordinary point kriging being performed using the GEO–EAS software suite (Englund and Sparks, 1988).

The parameters suggested by Srivastava and Isaaks (1989) were used to compare the results of the four methods, these being:

1. the univariate statistics of the estimate – error distributions;
2. the scatterplot of estimate against actual value;
3. the mean absolute error (MAE) and mean squared error (MSE);
4. the ability of the methods to reproduce the actual distribution.

An estimation method that performs well in relation to the original data set should have a mean and median error close to zero, with the error distribution exhibiting a small standard deviation. The MAE and MSE should be low and the scatterplot of the estimates against the actual values should fall close to the ideal, a 45 degree line. Plots of the quantiles of the estimated distribution against the actual distributions' quantiles reflect how well the actual distribution has been reproduced. Scatter plots of the estimate error against the actual value are used to indicate global or conditional bias.

3. Results and Discussion

Tabulated summary statistics for the actual radionuclide values and the statistics for the estimates produced by each method are presented in Tables II to IV. As only 49 estimates could be produced by the triangulation procedure, the statistics for the true values of the 49 points are used for comparison with the triangulation method. Summary statistics for the error distributions of each method are also presented (Tables V to VII).

Examination of the statistics for both the estimates and the estimate errors indicates that the geostatistical procedure performs better than the other procedures for a number of parameters. It produces the lowest MSE and MAE of all the methods and the narrowest error distribution. The mean and median errors for ^{228}Ra and ^{40}K indicate slight global over and under-estimation respectively but the values compare favourably with the other methods. The correlation coefficient for the scatter-plot of actual values against estimates is highest for the kriging method. Quantile plots of estimate quantiles against actual quantiles (Figure 2) indicate that all the methods, with the exception of the polygonal method, produce smoothing of the upper and lower data values. Incorporation of the highest and lowest data values in the polygonal method undoubtedly contributes to it's better reproduction of the data set distribution. The deviation from the ideal 45 degree line is less severe for kriging than for the inverse distance squared and triangulation procedures but highlights the possibility of conditional bias in the estimates.

The extent and type of bias present in the estimates was investigated using residual plots of estimate error against actual values. An unbiased set of estimates produces a uniform cloud of points centred on a zero line, global bias being reflected by groupings above or below the zero line, conditional bias appearing as deviations from the zero line at the upper and lower regions of the distribution. The residual plots for each nuclide (Figure 3) indicate that all the methods produce one or both kinds of bias. The ^{40}K plots indicate that all methods produce conditional bias, the effect being most severe for triangulation and inverse distance squared. The polygonal method shows little evidence of bias, the estimates being relatively poor across the entire range and being equally distributed above and below the zero line, despite having performed well in the quantile–quantile plots. All the methods show positive global bias for ^{228}Ra as well as a slight negative conditional bias towards the higher value region. The effect is least for the kriging estimates. Kriging and the polygonal method exhibit strong positive bias at the higher ^{226}Ra values, the opposite occurring in the inverse distance squared and triangulation procedures. The use of residual plots highlights the fact that although an estimation method may appear to reproduce a sample distribution accurately, based on quantile plots, the overall quality of the estimates may be relatively poor.

The difference in the spatial correlations exhibited by ^{226}Ra and ^{228}Ra may, initially, appear surprising given that both isotopes should behave similarly. However, given the differing behaviour of their progenitors, ^{238}U and ^{232}Th respectively, in a

surfical environment (U being mobile relative to Th), it is unlikely that the two Ra isotopes would exhibit the same spatial characteristics.

For the range of parameters used in this study, kriging appears to perform better than the other methods tried in relation to the data set studied. The incorporation of the anisotropy present in the data set, and the fact that it is an error variance minimisation technique may contribute to the better performance of the geostatistical technique. Assessment of the performance of any estimation method is dependant on what is required from the technique in relation to the data set in hand. It would appear that kriging performs best over a range of parameters for the data set used in this study, offering a better reproduction of the data set, lowest average error and the narrowest error distribution. It did not perform as well as the polygonal method in reproducing the data set distribution due to smoothing of the more extreme values. The results obtained in this study would appear to suggest that geostatistical methods may offer advantages in the determination of spatial distributions using small data sets in environmental studies.

References

Barns, M. G.: 1980, 'The use of Kriging for Estimating the Spatial Distribution of Radionuclides and Other Spatial Phenomena', TRANSTAT (Statistics for Environmental Studies) No. 13. Battelle Memorial Institute, Richland, W.A., pp. 1–22.

Davis, J. C.: 1973, *Statistics and Data Analysis in Geology*, John Wiley & Sons, New York.

Emax, J. and Soldt, U.: 1994, 'Geostatistical Investigations of Polluted Soils', *Fresenius J. Anal. Chem.* **351**, pp. 48–53.

Englund, E. and Sparks, A.: 1988, 'GEO-EAS: Geostatistical Environmental Assessment Software, Users Guide', USEPA Rep. 600/4-88/033. USEPA Las Vegas, N.V.

Flatman, G. T., Englund, E. and Yfantis, A. A.: 1988, 'Geostatistical Approaches to the Design of Sampling Schemes', in L. H. Keith (ed.), *Principles of Environmental Sampling*, American Chemical Society, pp. 73–84.

Froideuaux, R.: 1990, Geostatistical Toolbox Primer, Version. 1.30. FSS International, 10, Chemin de Drize, 1256 Troinex, Switzerland.

Gilbert, R. O.: 1987, *Statistical Methods for Environmental Monitoring*, Van Nostrand Reinhold, New York.

Journel, A. G. and Huybregts, Ch. J.: 1978, 'Mining Geostatistics', Academia Press, London and New York, 1.

Krige, D. G.: 1951, 'A Statistical Approach to some Basic Mine Valuation Problems in the Witwatersrand', *Journal of the Chemical, Metallurgical and Mining Society of South Africa* **52**, 119.

Litaor, M. I.: 1995, 'Spatial Analysis of $^{239+240}$Pu and ^{241}Am in Soils around Rocky Flats, Colorado', *J. Environ. Qual.* **24**, pp. 505–516.

Matheron, G. F.: 1970, 'La Theorie des Variables Regionalisees et ses Applications', Rep. Fascicule 5, Les Cahiers du Centre de Morphologie Mathematique de Fontainbleau, Ecole Superieure des Mines de Paris.

McBratney, A. B. and Laslett, G. M.: 1993, 'Sampling Schemes for Contaminated Soils', in H. Eijsackers and T. Hamers (eds.), *Integrated Soil and Sediment Research: A Basis for Proper Protection*, pp. 435–439.

Pannatier, Y.: 1996, *Variowin 2.2: Software for Spatial Data Analysis in 2D*, Springer-Verlag, New York.

Srivastava, R. M. and Isaaks, E. H.: 1989, *Applied Geostatistics*, Oxford University Press.

Spatial analysis of natural radionuclides in peat overlying a lithological contact in Co. Donegal Ireland.

John O'Dea and Mark Dowdall
Institute of Technology, Sligo,
Ballinode, Sligo, Ireland.

Journal of Environmental Radioactivity. **44**. 1999.
pp. 107-117.

ELSEVIER

Journal of
Environmental Radioactivity 44 (1999) 107–117

JOURNAL OF
ENVIRONMENTAL
RADIOACTIVITY

Spatial analysis of natural radionuclides in peat overlying a lithological contact in Co. Donegal, Ireland

John O'Dea, Mark Dowdall

Institute of Technology, Sligo, Ballinode, Sligo, Ireland

Received 20 December 1997; accepted 9 June 1998

Abstract

The Cronamuck Valley lies on the north-eastern contact of the Barnesmore pluton in Co. Donegal and has been identified as a region with elevated levels of natural radionuclides during a programme of uranium prospecting in the region, conducted in the 1970s. As part of a radiological survey of the area carried out by the Institute of Technology, Sligo the spatial distribution of ^{238}U, ^{226}Ra, ^{228}Ra and ^{40}K in the valley was investigated using geostatistical methods. Radionuclide levels in sixty soil samples were determined using high-resolution gamma-ray spectrometry. ^{238}U levels ranged from 2.7 to 788 Bq kg^{-1} with a mean value of 79 Bq kg^{-1}, ^{226}Ra levels ranged from 4 to 479 Bq kg^{-1}, with a mean value of 104 Bq kg^{-1}, ^{228}Ra levels ranging from 3 to 135 Bq kg^{-1} with a mean of 35 Bq kg^{-1} and ^{40}K activities ranged from 8 to 1088 Bq kg^{-1} with a mean value of 526 Bq kg^{-1}. Standard deviations for the radionuclide distributions were 149.9, 125.5, 25.1 and 278.1 Bq kg^{-1}, respectively. Isopleth maps of the radionuclide activities were constructed using geostatistical techniques. These indicate strong geological control over soil radionuclide levels in the region, the highest activity values occurring in the granite area, and provide evidence of the immobility of natural radionuclides in organic soils.

Keywords: Soil; Radionuclides; Geostatistics; Gamma ray spectrometry

1. Introduction

The Barnesmore pluton forms the Bluestack Mountains, an isolated range in central County Donegal. The pluton, 52 km^2 in area and comprised of three granite types, is an oblong shaped body set in Dalradian metasediments by cauldron subsidence (Pitcher & Berger, 1972). O'Connor et al. (1983) identified the Barnesmore granite as having the highest average levels of uranium and thorium of any of the

0265-931X/99/$ – see front matter
PII: S0265-931X(98)00070-8

Donegal granites, 8.1 and 25.1 ppm, respectively. Radioelement levels in the Dalradian metasediments of the Kilmacrennan succession, into which the pluton was emplaced, are not available but figures for similar lithologies in Donegal indicate uranium levels of 0.8–2.3 ppm and thorium levels of 2.2–17.2 ppm (O'Connor & Long, 1985).

As part of a period of uranium prospecting conducted in the 1970s, Irish Base Metals Ltd. performed widespread stream sediment and soil sampling in the region, preceded by extensive radiometric (ground and airborne) and soil radon surveys. The results of these surveys indicated a high background uranium content in the region, the presence of secondary uranium minerals in the granite (autinite) and a series of widespread uranium enrichments in the soils of the Cronamuck Valley (Irish Base Metals Ltd., 1979). McAuley and Moran (1988), as part of a national survey, identified the Barnesmore region and surrounding area as having soil ^{40}K levels of greater than 600 Bq kg^{-1} and ^{226}Ra levels of 60–100 Bq kg^{-1}. McAuley and Marsh (1992) identified the region as having soil ^{226}Ra levels of 65–100 Bq kg^{-1}.

The purpose of this study was to investigate the spatial distribution of ^{238}U, ^{226}Ra, ^{228}Ra and ^{40}K in the soils of the Cronamuck Valley and to delineate the extent of the region of elevated natural radioactivity reported in the 1970s. Previous studies on the spatial distributions of natural radionuclides in Ireland have been conducted on a nation-wide scale. This study aims to investigate how radionuclides are distributed on a smaller scale in a region of elevated natural radioactivity. This objective was accomplished by utilising geostatistics, a data analysis technique not previously used in this country in the assessment of radioactivity levels. The analytical technique employed in the study was high-resolution gamma-ray spectrometry.

2. Survey region and sampling plan

The Cronamuck Valley lies between Cronamuck Mt. and Clogher Hill, running in a NE–SW direction for approximately 5 km. The Cronamuck River flows along the valley, joining the Owendoo River, flowing from the west, at the north eastern end of the valley (Fig. 1). Soils in the area consist of shallow peat in the higher regions, deepening towards the bottom of the valley. Some man-modified regions exist to the east as a result of forestry and sheep farming. The region is remote and sparsely populated.

A 4 km × 5 km rectangle was set up around the valley and 60 sampling locations were identified using small-scale maps of the area. Circles, with diameters of 300 m, were established around each location and a sample was selected at random within the circle, subject to the condition that flooded, forested or hazardous areas would not be sampled. A regular sampling grid could not be implemented due to the nature of the terrain. The exact location of each sample site was determined using a compass and tape measure and easting and northing co-ordinates were determined.

Samples consisting of 9–12 kg of wet soil were taken from depths of greater than 60 cm to avoid the effects of plant cycling of the radionuclides. In the majority of cases, the shallow nature of the soil meant that samples were taken from the soil immediately

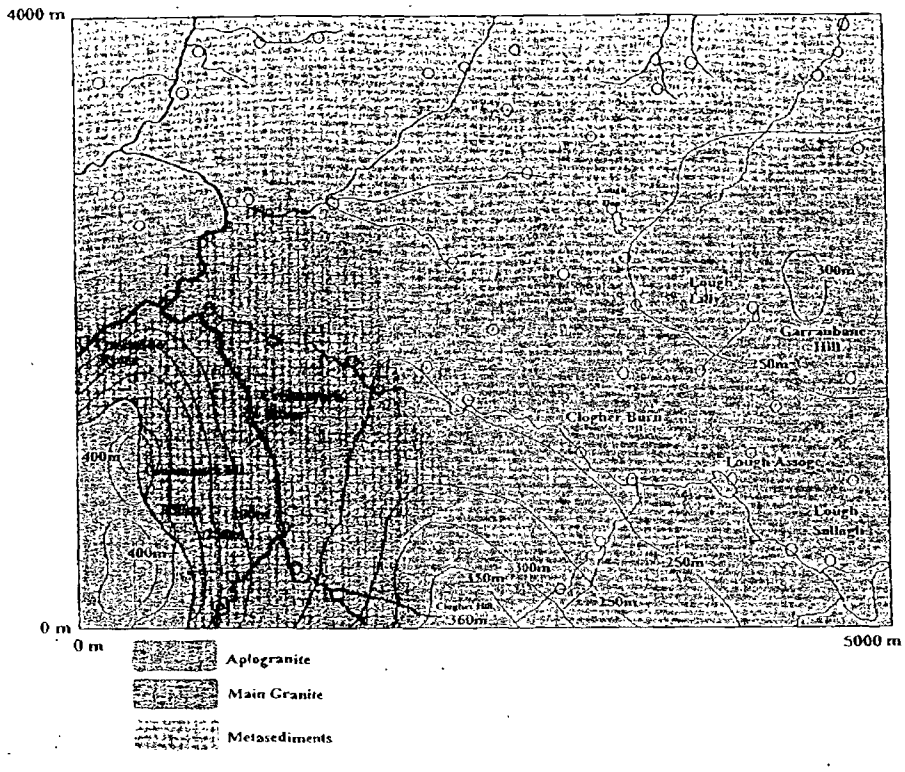

Fig. 1. Outline map of the survey area. Open circles denote sampling sites.

above the bedrock. Samples were sealed in polythene bags and taken to the laboratory for analysis.

3. Methods

Gross samples were oven-dried at 110°C for 48 h. Soil aggregates were crushed with a mallet and the soil was sieved through a 2 mm mesh before being packed into 1 L Marinelli re-entrant beakers for gamma analysis.

Samples were analysed using high-resolution gamma-ray spectrometry incorporating a 4 k multichannel analyser and the Genie-PC suite of analysis software from Canberra. The system was calibrated for energy and efficiency using a traceable mixed radionuclide standard solution. Errors due to density variations between samples were avoided by using the calibration procedures developed by Nemeth and Parsa (1992). ^{238}U was determined via the peaks of its daughter, ^{234}Th, at 63 and 92 keV. ^{226}Ra was determined via its 186 keV peak, having corrected for the ^{235}U interference

in the following manner. The ^{238}U activity for each sample was divided by 21.4 (calculated using the specific activities of ^{235}U and ^{238}U and their relative isotopic abundances) to obtain the ^{235}U activity for each sample. The contribution of ^{235}U to the 186 keV peak was then determined using:

$$^{235}U \text{ counts} = A^{235}U C_T R_U \text{Eff}_{186} W$$

where $A^{235}U$ is the ^{235}U activity, C_T the count time in seconds, R_U the emission probability of ^{235}U @ 186 keV, Eff_{186} the counting efficiency @ 186 keV and W the sample mass (kg). The ^{235}U contribution was then subtracted from the total counts at 186 keV and the ^{226}Ra activity determined.

^{228}Ra was determined via the ^{228}Ac photopeaks at 911 and 969 keV. The 1460 keV peak was employed for ^{40}K analysis. All samples were counted for a period sufficient to ensure a 2 sigma counting error of less than 10% (15% for ^{226}Ra), resulting in counts ranging from 1 day to 1 week. All samples were corrected for laboratory background.

4. Data analysis

Radionuclide activities and spatial co-ordinates were entered into a matrix for data analysis. Experimental semi-variograms and theoretical models were constructed for each radionuclide using Geostatistical Toolbox (Froideuaux, 1990). Geostatistical estimation methods perform best when the data set is normally distributed (Rendu, 1978) and in order to better approximate a normal distribution, the ^{238}U data were transformed using the natural logarithm of the data. Transformation of the ^{238}U data also served to smooth the experimental semi-variogram and simplified the fitting of the theoretical model. The distributions of ^{226}Ra, ^{228}Ra and ^{40}K did not require transformation. Ordinary block kriging, cross validation analysis and contouring of estimates were conducted using the GEO-EAS software suite (Englund & Sparks, 1988). The search radius employed was 1200 m, an unsampled location requiring a maximum of 14 and a minimum of three known data points within the search radius for estimation to take place. The block size was 250 m × 250 m with 16 points per block, resulting in a grid of 320 estimates. Cross validation analysis was performed to optimise search conditions, those search conditions that resulted in the narrowest distribution of errors, lowest mean absolute error (MAE) and smoothest error map being deemed best. Kriging was performed on the natural logarithms of the ^{238}U data, the final estimates being back transformed to the original units using the equation given by Litaor (1995).

5. Results and discussion

Summary statistics for each radionuclide are presented in Table 1 and details of the experimental semi-variograms and theoretical models in Table 2. Fig. 2 depicts isopleth maps for the kriged estimates for each radionuclide. Fig. 3 displays the frequency distributions of the radionuclides and the ratio $^{226}Ra/^{238}U$.

Table 1
Summary statistics for ^{238}U, ^{226}Ra, ^{228}Ra and ^{40}K. Values in Bq kg^{-1} dry weight

	^{238}U	^{226}Ra	^{228}Ra	^{40}K
n	60	60	60	60
Mean	79.3	104.7	35.8	526.4
Std. dev.	149.9	125.5	25.1	278.1
Coeff. var.	189.0	119.9	71.5	52.8
Skewness	3.78	1.50	1.93	−0.06
Minimum	2.7	4.0	3.0	8.0
Median	29.5	47.7	30.5	551.3
Maximum	788	479.0	135.0	1088.0

Table 2
Semi-variogram and theoretical model parameters

	$ln^{238}U$	^{226}Ra	^{228}Ra	^{40}K
Model	Gaussian	Exponential	Gaussian	Gaussian
Sill value	1.150	18000	750	83000
Nugget	0.0	0.0	0.0	0.0
Range (m)	600	3000	700	750
N–S (m)	650	3000	400	600
E–W (m)	700	3000	1000	1100

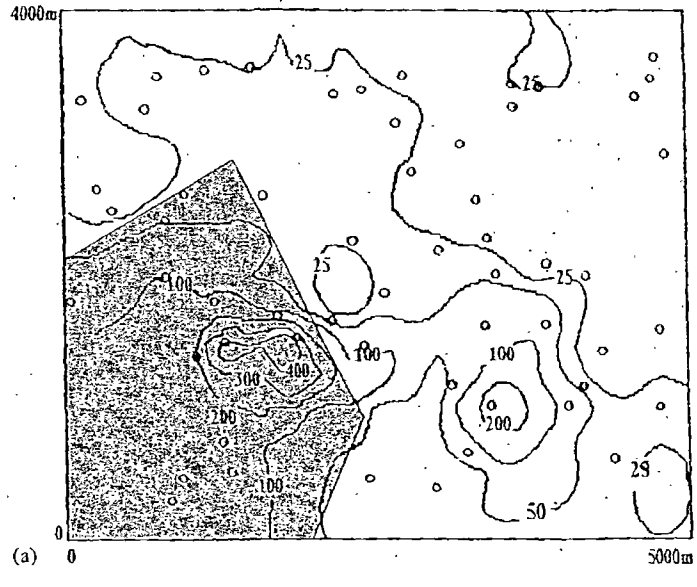

Fig. 2. Isopleth maps of kriged radionuclide estimates, (a) ^{238}U, (b) ^{226}Ra, (c) ^{228}Ra, and (d) ^{40}K. Values in Ba kg^{-1} dry weight. Shaded area denotes granite region. Open circles denote sampling sites.

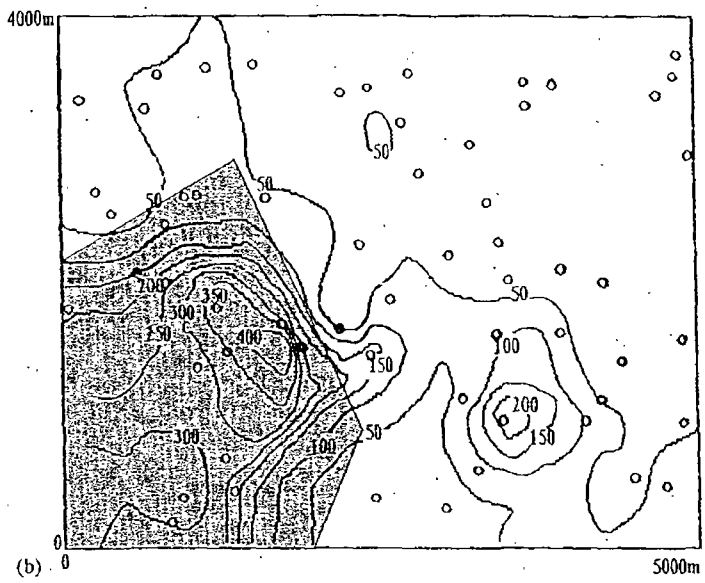

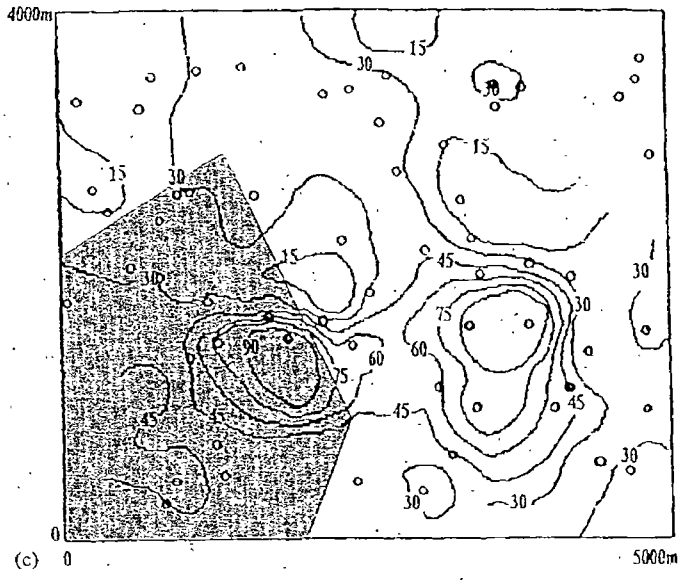

Fig. 2. continued

All of the radionuclides exhibited strong spatial correlation, the range of correlation being approximately 650 m for ^{236}U, 3000 m for ^{226}Ra and 750 m for ^{228}Ra and ^{40}K. Significant geometric anisotropies were present for ^{228}Ra and ^{40}K, the ranges being approximately 1000 m in the E–W direction and 500 m in the N–S direction.

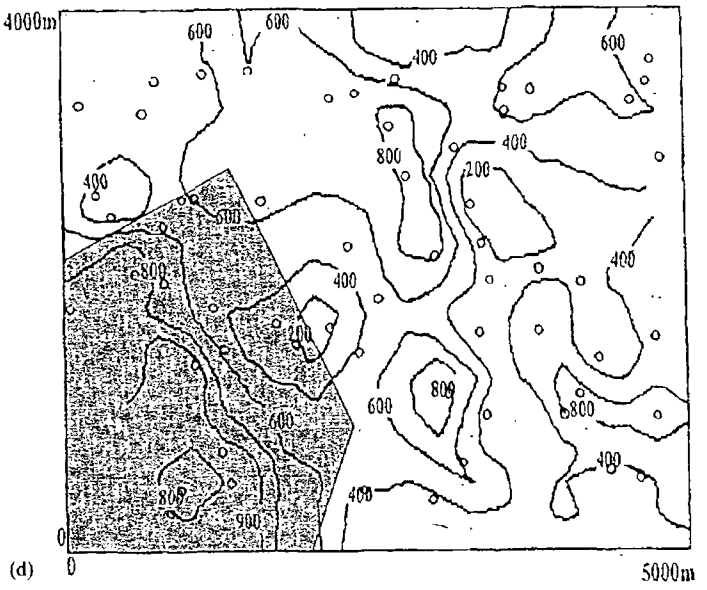

Fig. 2. continued

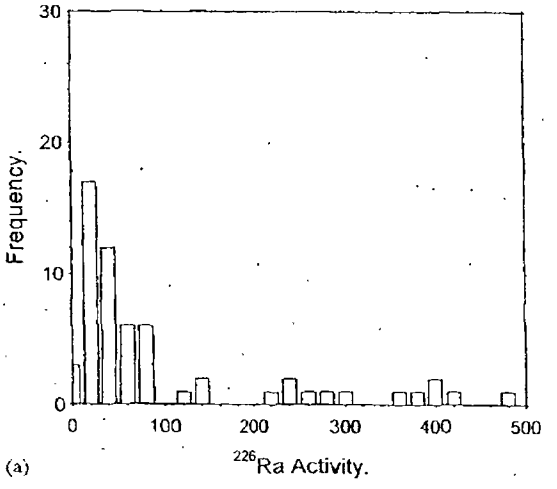

Fig. 3. Frequency distributions of (a) ^{226}Ra, (b) ^{228}Ra, (c) ^{238}U, (d) ^{40}K and (e) $^{226}Ra/^{238}U$. Radionuclide activities in Bq kg^{-1}.

Inspection of the isopleth maps indicates that the soils showing elevated levels of ^{238}U, ^{226}Ra and ^{228}Ra correspond well with area underlain by the granite bedrock. Activities of these radionuclides in the soils overlying the metasediments are lower than those in the granite area by up to an order of magnitude in some cases. ^{40}K

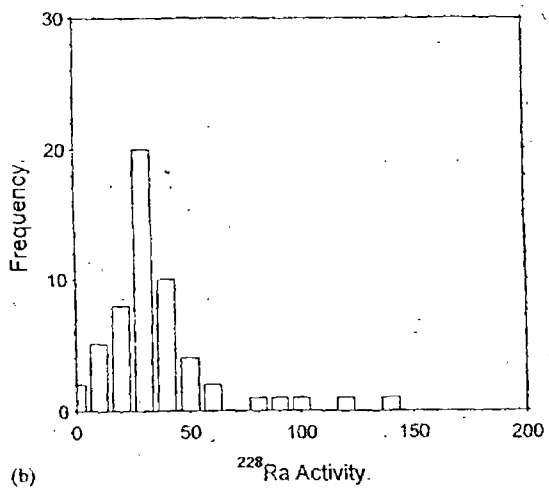

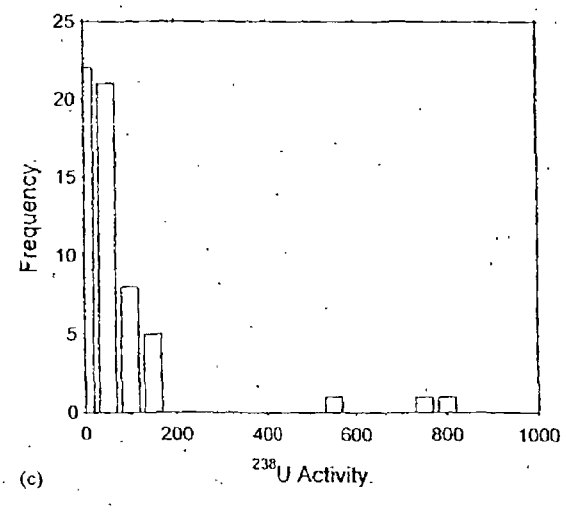

Fig. 3. Continued

activities are more widely distributed throughout the survey area, the difference in ^{40}K soil values between the two regions being less pronounced than for the other radionuclides. This finding is supported by the fact that %K values for the granite and metasediments are quite similar and do not differ by the same amount as either uranium or thorium. Reported values are 3.3%K for the metasediments (O'Connor & Long, 1985) and 3.6 to 5.1%K for the Barnesmore granite (O'Connor et al., 1983). A region of elevated radionuclide levels is also indicated slightly to the east of the contact, in an area underlain by the metasediments. The reason for the high levels of radioactivity in this portion of the study region are unknown at present. A sharp

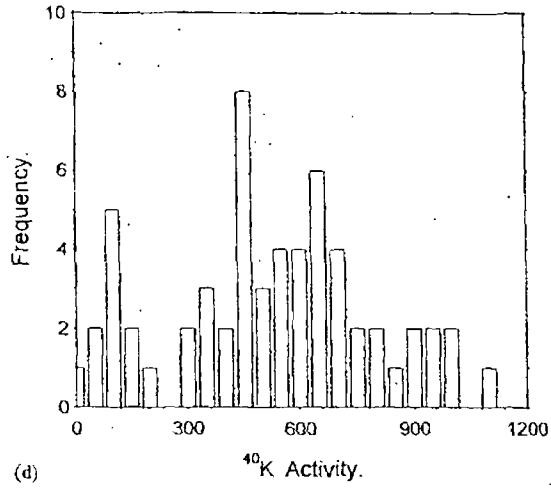

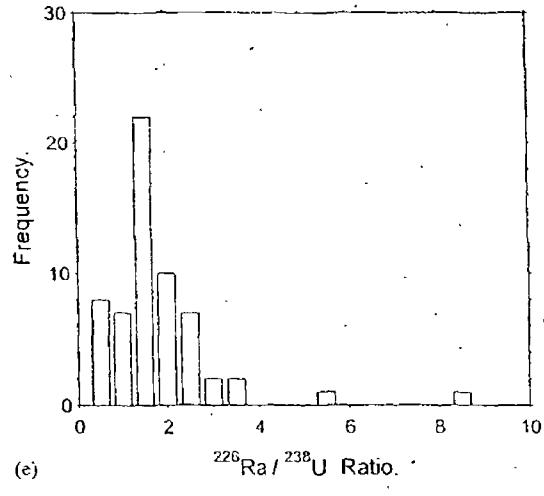

Fig. 3. Continued

reduction in radionuclide levels over a relatively short distance occurs in the northern end of the valley, the drop corresponding well with the contact of the granite and the metasediments. This reduction is not surprising given the sharp contact of the two lithologies (Pitcher & Berger, 1972) and the immobility of the radionuclides in organic soils and peat (Sheppard, 1980).

A surprising observation was that both regions of elevated activity displayed marked ^{226}Ra/^{238}U disequilibrium, ^{226}Ra activities being over five time greater than ^{238}U activity for some samples. The area to the north contained samples with ^{226}Ra/^{238}U ratios of 0.5 in close proximity with samples exhibiting ratios of 5.0–9.0.

Although a national average for this parameter is unavailable, McAuley and Marsh (1992) suggest that the majority of soils in Ireland exhibit $^{226}Ra/^{238}U$ ratios in the range 0.5–2.0. Ivanovich (1994) identifies four mechanisms as being responsible for fractionation of decay chain radionuclides in natural systems: solution and precipitation, alpha recoil, diffusion and susceptibility to leaching due to the Szilard–Chalmers effect. Osburn (1965) indicates that in an oxidised environment, sharp disequilibrium may exist due to the increased solubility of uranium above its daughters. All the sites displaying high $^{226}Ra/^{238}U$ ratios occurred in an area of shallow overburden on a relatively sharp incline. The area was well drained in comparison to the rest of the study region. It is therefore possible that the disequilibrium is a consequence of U being lost by dissolution in soil water and subsequently being carried away with the flow of water down the slope. Further elucidation of this phenomenon requires an in-depth study of the radiological, physical and chemical conditions prevailing at the site.

None of the samples displayed evidence of having being drawn from one of the numerous uranium anomalies (soil U levels of up to 1000 ppm) reported by Irish Base Metals Ltd. (1979). Given that the majority of these anomalies consist of areas less than 10 m in diameter and the number of samples taken in this study, the probability of encountering such levels would appear to be low.

Acknowledgements

The authors wish to thank the following for assistance with aspects of this study: the staff of the Geological Survey of Ireland, the Radiological Protection Institute of Ireland, Dr. B. Crocock (Institute of Technology, Waterford) and E. Grennan, P. Maughan (Institute of Technology, Sligo).

References

Englund, E., & Sparks, A. (1988). *GEO-EAS, geostatistical environmental assessment software, users guide. USEPA* Report 600/4–88/033, Las Vegas, NV.

Froideuaux, R. (1990). Geostatistical toolbox printer, version 1.3. FSS International, Chemin de Drize 10, 1256 Troinex, Switzerland.

Irish Base Metals Ltd. (1979). Research into the occurrence of radioactive raw materials in Ireland. Final Report (pp. 33–34).

Ivanovich, M. (1994). Uranium series disequilibrium: concepts and applications. *Radiochimica Acta, 64*, 81–94.

Litaor, M. I. (1995). Spatial analysis of $^{239+240}Pu$ and ^{241}Am in soils around Rocky Flats, Colorado *Journal of Environmental Quality, 24*, 506–516.

McAuley, I. R., & Marsh, D. (1992). ^{226}Ra concentrations in soil in the Republic of Ireland. *Radiation Protection Dosimetry, 45*(1/4), 265–267.

McAuley, I. R., & Moran, D. (1988). Natural radioactivity in soil in the Republic of Ireland. *Radiation Protection Dosimetry, 24*(1/4), 47–49.

Nemeth, W. K., & Parasa, B. (1992). Density correction of gamma ray detection efficiency in environmental samples. *Radioactivity and Radiochemistry, 3*(3), 32–39.

O'Connor, P. J., & Long, C. B. (1985). Radioelement abundance data for some Dalradian Rocks from Co. Donegal, Ireland. *Mineralogical Magazine, 49*, 643–648.

O'Connor, P. J., & Long, Hennessey, J. (1983). Radioelement geochemistry of Irish newer caledonian granites. Geological Survey of Ireland Bulletin *3*, 125–140.

Osburn, W. S. (1965) Primordial radionuclides: their distribution, movement, and possible effects within terrestrial ecosystems. *Health Physics, 11*, 1275–1295.

Pitcher, W. S., & Berger, A. R. (1972). *The geology of Donegal*. New York: Wiley Interscience.

Rendu, J. M. M. (1978). Geostatistics, a powerful tool in the evaluation of energy resources. In *Proceedings of Fifth Annual UMR-DNR Conference and Exposition on Energy*, University of Missouri-Rolla.

Sheppard, M. I. (1980). The environmental behaviour of uranium and thorium. Atomic Energy of Canada Ltd, AECL-6795.

APPENDIX 6.

^{137}Cs in the Cronamuck Valley

Although this study was not designed to investigate the occurrence of ^{137}Cs in the soils of the Cronamuck Valley, the levels of this anthropogenic radionuclide in the soil samples were measured as a matter of course. The sampling rationale and methodology of the study were not optimized for obtaining information on this radionuclide as the majority of soil samples were extracted from the bottom of the peat beds, where levels of this radionuclide are typically at their lowest due to the nature of the deposition of this radionuclide.

	^{137}Cs Bq/kg
N	60
Mean	19.2
Std. Deviation	31.9
Minimum	0.5
Median	8.6
Maximum	178.7

Table xxxx. Summary statistics for ^{137}Cs values of the 60 samples of Survey 1.

Construction of a histogram for the ^{137}Cs values indicates a skewed distribution that is strongly affected by the presence of two values in excess of 100 Bq/kg. The majority of samples display values less than 50 Bq/kg. A scatterplot of the samples values does not indicate any obvious clustering of high ^{137}Cs values, the two samples exhibiting the highest levels being separated by a distance of over 1 km. The scatterplot does not provide any evidence that ^{137}Cs soil levels are any greater over elevated portions of the study region, most notably the south – western corner of the valley.

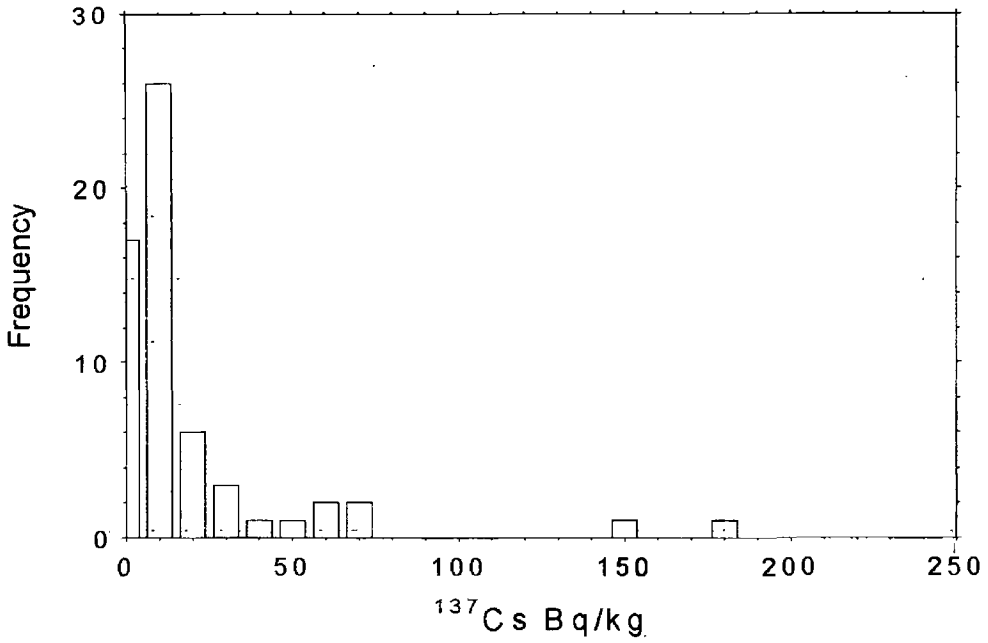

Figure ix. Histogram of ^{137}Cs values for the 60 samples taken as part of Survey 1.

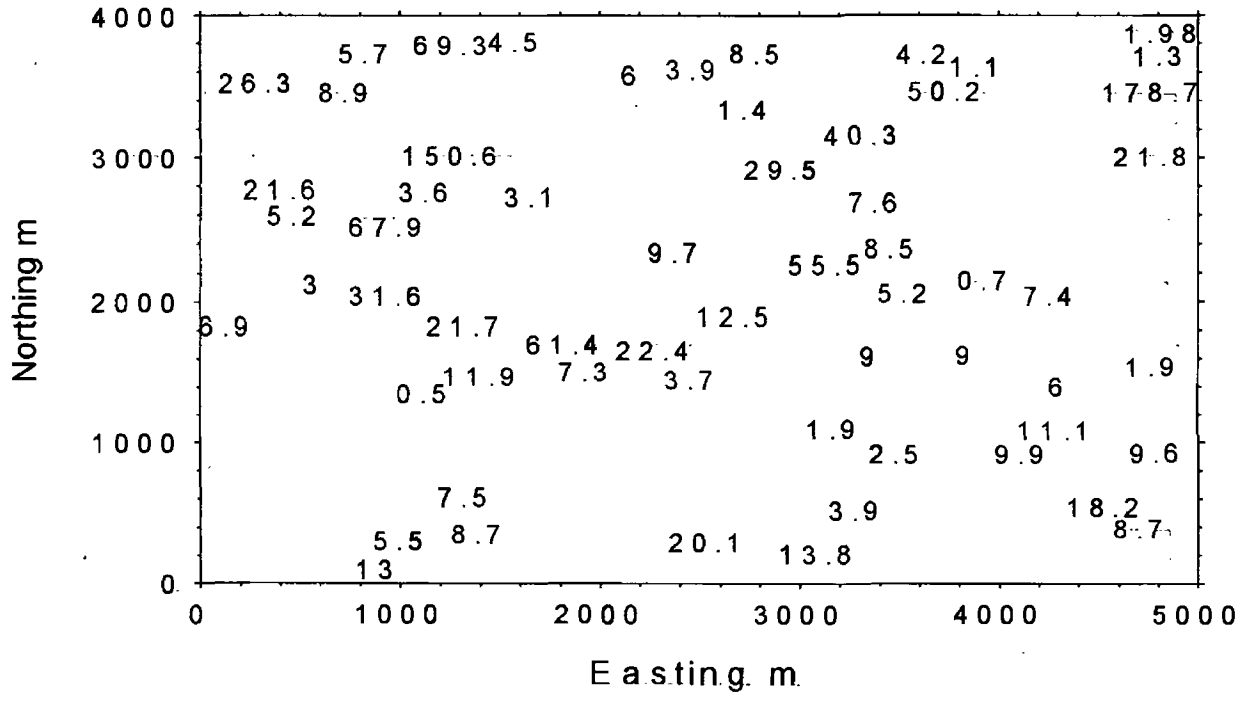

Figure x. Scatterplot of ^{137}Cs values for the 60 samples of Survey 1.

Sample	^{137}Cs	^{137}CsEx	%^{137}CsEx	^{137}CsOrg	%^{137}CsOrg	^{137}CsFeO	%CsFeO
E 0-15	191.2	8.6	4.5	<0.5	<0.3	<0.9	<0.5
E 15-30	55.1	<1.2	<2.2	<1.1	<1.9	<1.1	<1.9
E 30-45	44.9	<1.4	<3.2	2.3	5.2	1.7	3.7
E 45-60	9.9	<1.3	<13.1	<1.1	<11.5	<3.9	<39.3
E 60-75	2.7	1.1	38.8	<1.5	<54.4	<1.2	<45.9
A 0-15	186.4	<2.2	<1.2	<1.2	<0.6	<1.4	<0.8
A 15-30	30.7	<1.2	<3.8	<1.5	<4.8	<1.4	<4.5
A 30-45	22.9	<1.5	<6.6	<1.2	<5.2	<1.4	<6.2
A 45-60	2.8	1.4	49.4	1.7	59.4	<1.2	<43.9
A 60-75	1.4	0.7	51.8	<1.6	<100.0	1.2	88.7
E 1	46.7	<1.6	<3.4	<1.2	<2.6	<1.4	<2.9
E 4	3.6	1.1	30.0	<2.0	<54.7	<1.6	44.4
E 5	14.5	2.7	19.0	0.1	0.7	<1.8	<12.2
E6	67.9	<1.2	<1.8	2.1	3.0	<0.9	<1.3
9	21.7	<1.7	<7.7	<0.9	<4.1	<1.2	<5.0
54	7.3	<1.3	<18.9	<1.4	<19.3	<1.4	<19.5
41	1.3	<0.5	<37.8	<1.4	<100.0	<1.5	<100.0

Table xxxxi. ^{137}Cs levels in each of the three fractions studied during Survey 2. Ex – exchangeable cations, Org – easily oxidisable organic matter, FeO – iron oxides. Values in Bq/kg.

The ^{137}Cs levels for the depth cores at A and E indicate the preponderance of ^{137}Cs in the upper levels of the peat and the fact that little or none of this radionuclide has moved downwards in the soil column. It is interesting to note that at depth at both sites, a large percentage of the ^{137}Cs present is associated with the exchangeable cation fraction, possibly indicating that downward transport of the radionuclide is via percolating water. The fact that very little ^{137}Cs exists in any of the three fractions would appear to suggest that the radionuclide is largely associated with the residual organic matter component of the soil, a fact that is in accordance with the relatively recent deposition of this radionuclide. As most of the fractions displayed ^{137}Cs levels below the detection limit of the analytical technique (under the parameters employed) little useful information regarding correlations with any other soil parameter could be obtained.